UNIVERSITA' DEGLI STUDI DI SIENA

Dipartimento di Biotecnologie, Chimica e Farmacia

DOTTORATO DI RICERCA IN

CHEMICAL AND PHARMACEUTICAL SCIENCES

CICLO **XXXIV**

COORDINATORE
Prof. Maurizio Taddei

TITOLO DELLA TESI

Amphiphilic self-assembly polymers with improved environmental profile for home and personal care products

MARIE SKŁODOWSKA-CURIE ACTIONS

Call: H2020-MSCA-ITN-2018

"SAMCAPS"

SETTORE SCIENTIFICO-DISCIPLINARE: CHIM/03

Aleksandra Zawadka

Signed 26/04/2022

DOTTORANDO

Aleksandra Zawadka

TUTOR

Prof.ssa Agnese Magnani

ANNO ACCADEMICO: 2021-2022

ABSTRACT

Graft copolymers constitute an important class of copolymers since it is possible to tune their characteristics opportunely designing their macromolecular structure. There is a growing interest for the design and synthesis of graft copolymers with desired composition and functionality to be used in a wide range of applications. Free radical polymerization techniques offer the straightforward synthesis of amphiphilic graft copolymers materials thanks also to the vast choice of available monomers with different functional groups. Amphiphilic graft copolymers, or polymer containing both hydrophilic and hydrophobic parts in their structure, possess unique properties due to the distinct chemical nature of building blocks and can self-assembly to various morphologies to render the favorable interactions. Characteristics of graft copolymers can be adjusted through the variations of composition (type of the grafted chains, grafting densities) and architecture (length of backbone and grafted chains etc.). Therefore, understanding the relation between the macromolecular architecture, composition and characteristics is crucial to tailor polymers for specific applications. This thesis covers the synthesis, characterization, and applications of amphiphilic graft copolymers, to reveal the effects of their chemical structure on capsules formation, encapsulation of fragrance molecules, and biodegradability rate. A wide range of applications can be defined for the use of amphiphilic copolymers. This work focuses on the self-assembly properties of amphiphilic copolymers, with improved environmental profile, for potential use in perfume sustainable encapsulation technology in liquid home- and personal-care products.

To achieve the synthesis of copolymers with self-assembled structures, hydrophilic poly (ethylene glycols) (PEGs) of different molecular weights, hydrophilic and hydrophobic monomers like thermo-responsive N-vinyl caprolactam (VCL) and/or vinyl acetate (VAc), have been used. Amphiphilic copolymers were obtained through a radical polymerization method using peroxide as an initiator. Different molecular weights (lengths of the chain), grafting densities as well as various chemical moieties have been investigated. Synthetized materials were characterized by FT-IR, 1D NMR, 2D NMR, DSC, TGA, GPC, ToF-Sims. Biodegradability of copolymers was measured by OECD 301b test and capsules formation properties were

investigated using fluorescence microscopy. The studies reported in this work demonstrated that the capsules formation by synthetized copolymers in liquid detergent formulations strongly depend on the molecular weight of hydrophobic content and the degree of grafting of hydrophobic graft chains. Among all synthetized copolymers and commercial copolymer Soluplus only copolymer S2, which has the highest molecular weight of hydrophobic PVAc-*co*-PVCL part and higher grafting degree, showed capsules formation and encapsulation of perfume and PRMs in both SLFE liquid detergent formulations and water matrix. All synthesized copolymers are 4 -5 folds more biodegradable than commercial Soluplus.

DEDICATION

This thesis is dedicated to my adorable parents, for all their love, support, patience and encouragement to achieve my goals; and to my fiancé Sergio for always loving, listening, having an understanding, and teaching me the patience for life.

Without their courage and love, this work could not be accomplished.

ACKNOLEDGEMENTS

I owe my sincere gratitude to those who have contributed to this thesis and helped me to survive this process.

First and foremost, I want to thank my academic supervisors Prof. Agnese Magnani, Dr. Gemma Leone and Dr. Marco Consumi for their patience, tolerance and precious advices. They always supported me and shared their time and experiences generously.

I would like to present my special thanks to my supervisor from P&G Susana FernandezPrieto for her contributions, guidnes, valuable comments and direction leading me to the better.

I want to express my thanks to the present and past members of SAMCAPS group, specially to Claudio Resta who taught to me everything related to polymer synthesis and helped me any time I needed.

I would like to thank Yiping Sun and his group, Ghafoor Misbah for many stimulating discussions and critical suggestions related to polymer characterization.

I also want to thank to my friend from SAMCAPS project, Constantina Sofroniou. This would be a boring and ordinary journey without you. I am grateful for your help any times of need and support beside the unforgettable memories.

Finally, I wish to express my deep appreciation to my family. They have always been a strong source of motivation with their support and love. They were great role models and never stopped believing in me. I am thankful for their trust and support.

TABLE OF CONTENTS

ABSTRACT.....i

DEDICATION..... iii

ACKNOWLEDGMENTS..... iv

CHAPTERS

1. INTRODUCTION.....1

1.1 The role of synthetic polymers with improved environmental footprint for encapsulation of volatile compounds.....1

1.2 Research objectives……..…….…....3

2. LITERATURE REVIEW…….…..4

2.1 Graft copolymers.....4

2.1.1 Amphiphilic graft copolymers...……....6

2.1.2 Self-assembly…….……... 7

2.1.3 Self-assembly of amphiphilic graft copolymers…….……9

2.1.4 Stimuli responsive amphiphilic copolymers…….....11

2.1.5 Synthetic methods of graft copolymers……....……...14

2.1.6 Free radical polymerization method…….……18

2.1.7 Industrial methods of radical polymerization…….…..21

2.1.8 Typical Features of Radical Polymerization……..……...22

2.1.9 Polymer Grafting by Free-Radical Polymerization.....24

2.1.10 Factors Affecting the Grafting……27

2.1.11 New properties of graft copolymers……...…30

2.1.12 Applications of amphiphilic graft copolymers……..……31

2.2 Biodegradability……...…...…..35

2.2.1 General information about biodegradable materials…….....35

2.2.2 Group of biodegradable materials based on the origin……..35

2.2.3 Understanding the bio-based and biodegradable terms……..…..... 36

2.2.4 Biodegradation mechanism……...….. 37

2.2.5 Factors affecting biodegradation rate……...……38

2.2.6 Biodegradability assessment techniques……...……...38

3. MATERIALS, METHODS, AND INSTRUMENTATION…….40
3.1 Materials…….40
3.1.1 Backbone……. 40
3.1.2 Monomers……40
3.1.3 Initiator…… 40
3.1.4 Solvents……41
3.1.5 Fluorescence dye for copolymer labelling……41
3.1.6 Structural reference……..41
3.1.7 Single fragrance molecules……..42
3.1.8 Microencapsulation matrix……..42
3.2 Synthesis method……....43
3.2.1 Synthetic procedure……..43
3.2.2 Purification of S1 (PEG_{6000} -PVCL), S2 (PEG_{6000} -PVAc-PVCL), S3 (PEG_{6000} -PVAc-PVCL), S4 (PEG_{1000} -PVCL), S6 (PEG_{20000} -PVCL) graft(ss)-copolymers……...47
3.3 S1 (PEG_{6000} -PVCL), S2 (PEG_{6000} -PVAc-PVCL), S3 (PEG_{6000} -PVAc-PVCL), S4 (PEG_{1000} -PVCL), S6 (PEG_{20000} -PVCL) graft(ss)- copolymers and Soluplus® labelling procedure……49
3.4 Synthesis procedure of self-assembly microcapsules of S1 (PEG_{6000} -PVCL), S2 (PEG_{6000} -PVAc-PVCL), S3 (PEG_{6000} -PVAc-PVCL), S4 (PEG_{1000} -PVCL), S6 (PEG_{20000} -PVCL) graft(ss)- copolymers and Soluplus®……..50
3.5 Characterization methods of synthetized copolymers and supramolecular self-assembly microcapsules……..50
3.5.1 Fourier transform infrared spectroscopy (FTIR)……..50
3.5.2 Nuclear magnetic resonance spectroscopy (NMR)……51
3.5.3 Diffusion ordered spectroscopy (DOSY)……51
3.5.4 Gel Permeation Chromatography (GPC) ……51
3.5.5 Matrix-assisted laser desorption/ionization-time of flight (MALDI-TOF) mass spectrometry (MS)……...52
3.5.6 Differential scanning calorimetry (DSC)……52
3.5.7 Thermogravimetric analysis (TGA)……53
3.5.8 Thermo-responsive properties - cloud point study (C_{TP})……53
3.5.9 Optical and fluorescence Electron Microscopy……53
3.1 OECD 301B biodegradability carbon dioxide evolution test……..54

3.6.1 Description of the standard methodology of the laboratory……..54
3.6.2 Definitions……...56

4. RESULTS AND DISCUSSION…….57
4.1 Synthesis of PEG-g-(PVAc-*co*-PVCL) and PEG-g-PVCL graft copolymers…….57
4.1.1 Morphological observation of PEG-g-(PVAc-*co*-PVCL) and PEG-g-PVCL graft copolymers……...57
4.2 Chemical structure and characteristics of PEG-g-(PVAc-*co*-PVCL) and PEG-g-PVCL graft copolymers……..58
4.2.1 FTIR investigation.....58
4.2.2 NMR investigation……..66
4.2.3 Grafting investigation by diffusion ordered spectroscopy (DOSY 2D NMR)……76
4.2.4 Molecular weight investigation by GPC.....82
4.2.5 Composition investigation by MALDI-TOF mass spectroscopy…….88
4.2.6 Thermal properties investigation by TGA and DSC.....90
4.2.7 Thermo-Responsive Properties - Cloud Point Study.....98
4.3 Application of copolymers S1 (PEG_{6000}-PVCL), S2 (PEG_{6000}-PVAc-PVCL), S3 (PEG_{6000}-PVAc-PVCL), S4 (PEG_{1000}-PVCL), S6 (PEG_{20000}-PVCL) as perfume carriers - microscope observation.....102
4.3.1 Effect of the different polymer architecture and properties on capsules formation process and encapsulation of volatile compounds…….....102
4.4 OECD 301b biodegradability test…….....110
4.4.1 Possible relationship between the structure, architecture, composition of copolymer and biodegradability rate.....114
5. CONCLUTIONS ……116

REFERENCES……120

APPENDICES……139
APPENDIX A. UV-Vis of 0.5 % solution of filtrated copolymer S2.
APPENDIX B. First 50 ml of filtrated copolymer S2 solution passed through membrane, 1st collected batch.

APPENDIX C. UV-Vis of collected 43rd batch (last) of filtrated copolymer S2 solution after one month of ultrafiltration.
APPENDIX D. Microscope images of (A) 0.5% copolymer S2A before microfiltration and (B) 0.5% copolymer S2A after microfiltration with Methyl anthranilate in water.
APPENDIX E. FTIR spectra of the first 50 ml of copolymer solution passed through the membrane during ultrafiltration (green) and copolymer S2 before ultrafiltration (red).

LIST OF FIGURES

Figure Page

1. Monomer and polymers (UNSW Science)……..1
2. Monomer, polymer, polymeric material, and the resulting material application (Institute for Technical Chemistry and Polymer Chemistry) ……..……..1
3. Schematic representation of graft copolymer……..4
4. Graft Copolymers (1) random graft copolymer (identical branches randomly distributed along the backbone); (2) regular graft copolymer (identical branches equally spaced along the backbone); (3) simple graft copolymer (3-miktoarm star copolymer); and (4) graft copolymer with two trifunctional branch points…….5
5. Chemical structure of Soluplus® (polyvinyl caprolactam-polyvinyl acetate-polyethylene glycol graft copolymer (PCL-PVAc-PEG)……7
6. Classification of self-assemblies based on the size/nature (atomic, molecular, and colloidal) of building units and on the system where the self-assembly occurs (biological and interfacial); the length scale is also of building units……..8
7. Types of polymers based on their source and their end-of-life options. (European bioplastics, 2020)……..36
8. Polyethylene glycol, PEG……40
9. N-Vinylcaprolactam, VCL (left) and Vinyl acetate, VAc (right)……..40
10. Initiator Tert-Butylperoxy 2-Ethylhexyl carbonate**,** Luperox TBEC……40
11. Structure of Rhodamine-B isothiocyanate (mixed isomers)……..41
12. Structure of Soluplus® (PEG-*g*-(PVAc-*co*-PVCL)), BASF product……42
13. Structure of Methyl anthranilate (left) and L-carvone (right). ……..42
14. Reaction reactor……44
15. An example of the final architecture of synthetized PEG-g-(PVAc-co-PVCL) copolymers ……...47
16. Ultrafiltration equipment connected with collective batch……48
17. Copolymer S2 labelled with rhodamine B isothiocyanate (left) and copolymer S2 before labelling procedure ……50
18. OECD 301b experimental design scheme……55

19. Morphology of synthetized copolymers S1, S2A, S2B, S3, S4, S6……...58
20. FTIR spectra of (a) VCL, (b) VAc, and (c) PEG-6000……..62
21. FTIR spectra of copolymer S1 PEG-g-PVCL……...62
22. FTIR spectra of copolymer S4 PEG-g-PVCL……...63
23. FTIR spectra of copolymer (a) S2A and (b) S2B……...64
24. FTIR spectra of copolymer S3……..64
25. FTIR spectra of copolymer S6……..65
26. FTIR spectra of Soluplus®……65
27. Structure of a) PEG-g-PVCL graft copolymer S1 and S4 and b) PEG-g-(PVAc-co-PVCL) graft copolymer S2, S2C, S3, S6 and Soluplus® with assigned protons.....67
28. The ^{1}H-NMR Spectrum of PEG-g-PVCL; S1……..70
29. The ^{1}H-NMR Spectrum of PEG-g-(PVAc-co-PVCL); S2A……71
30. The ^{1}H-NMR Spectrum of PEG-g-(PVAc-co-PVCL); S2B……..71
31. The ^{1}H-NMR Spectrum of PEG-g-(PVAc-co-PVCL); S3……72
32. The ^{1}H-NMR Spectrum of PEG-g-PVCL; S4……...72
33. The ^{1}H-NMR Spectrum of PEG-g-(PVAc-co-PVCL); S6……73
34. The ^{1}H-NMR Spectrum of Soluplus®……...73
35. ^{1}H-^{1}H NOESY map of copolymer S2A……74
36. ^{1}H-^{1}HCOSY map of copolymer S2A ……...……74
37. Structure of a) PEG-g-PVCL graft copolymer S1 and S4 and b) PEG-g-(PVAc-co-PVCL) graft copolymer S2, S2C, S3, S6 and Soluplus® with assigned protons.....78
38. Representative DOSY NMR spectra of copolymer S1 in $CDCl_3$. The horizontal axis represents chemical shifts, whereas the vertical axis is the diffusion coefficient……78
39. Representative DOSY NMR spectra of copolymer S2A in $CDCl_3$. The horizontal axis represents chemical shifts, whereas the vertical axis is the diffusion coefficient……79
40. Representative DOSY NMR spectra of copolymer S2B in $CDCl_3$. The horizontal axis represents chemical shifts, whereas the vertical axis is the diffusion coefficient……79

41. Representative DOSY NMR spectra of copolymer S3 in $CDCl_3$. The horizontal axis represents chemical shifts, whereas the vertical axis is the diffusion coefficient……80
42. Representative DOSY NMR spectra of copolymer S4 in $CDCl_3$. The horizontal axis represents chemical shifts, whereas the vertical axis is the diffusion coefficient……80
43. Representative DOSY NMR spectra of copolymer S6 in $CDCl_3$. The horizontal axis represents chemical shifts, whereas the vertical axis is the diffusion coefficient……81
44. Representative DOSY NMR spectra of copolymer Soluplus® in $CDCl_3$. The horizontal axis represents chemical shifts, whereas the vertical axis is the diffusion coefficient……81
45. Light scattering and reflective index chromatogram of copolymer S1……..84
46. Light scattering and reflective index chromatogram of copolymer S2A……...84
47. Light scattering and reflective index chromatogram of copolymer S2B……85
48. Light scattering and reflective index chromatogram of copolymer S3……..85
49. Light scattering and reflective index chromatogram of copolymer S4……..86
50. Light scattering and reflective index chromatogram of copolymer S6……..86
51. Light scattering and reflective index chromatogram of copolymer Soluplus®……87
52. Light scattering and Refractive index chromatograms of Polystyrene Standards……..87
53. Light Scattering Chromatogram of blank sample, PEG 6000, copolymer S1, S2, S3, S4……88
54. Refractive Index Chromatogram with PEG 6000 Standard, blank sample, copolymer S1, S2, S3, S4……..88
55. MALDI-TOF mass spectra of copolymer S2A filtrate……..89
56. MALDI-TOF mass spectra of copolymer S2B filtrate……..90
57. MALDI-TOF mass spectra of Soluplus® filtrate……..90
58. TGA thermogram of PEG 6000……92
59. TGA thermogram of PEG 1000……92
60. TGA thermogram of VCL……92
61. TGA thermogram of PVAc……...93
62. TGA thermogram of copolymer S1….....93

63. TGA thermogram of S2A……..93
64. TGA thermogram of S2B……..94
65. TGA thermogram of copolymer S3……...94
66. TGA thermogram of S4……94
67. TGA thermogram of S6…… 95
68. TGA thermogram of Soluplus®……95
69. DSC thermogram of PEG 6000, PEG 1000, VCL and PVAc……97
70. DSC thermogram of copolymer S1, S3, S6……..97
71. DSC thermogram of copolymer S2A, S2B, S4, and Soluplus®…….. 98
72. Cloud point……... 99
73. (a) 1% wt aqueous solutions of copolymer (a) S1, (b) S2A, (c) S2B, (d) S3, (e) S4, (f) S6 and (g) Soluplus® at 15 °C……..102
73. (b) 1% wt aqueous solutions of copolymer (a) S1, (b) S2A, (c) S2B, (d) S3, (e) S4, (f) S6 and (g) Soluplus® at 23 °C…….. 102
74. Microscope images of 0.5% copolymerr (A) S1, (B) S2A, (C) S2B, (D) S3, (E) S4, (F) S6, (G) Soluplus®, and 0.5 Carvone in water. Left: Tracking of polymer by optical microscope and Right: Tracking of the labelled polymer using the appropriate filters as mentioned in the main text……106
75. Microscope images of 0.5% copolymer (A) S1, (B) S2A, (C) S2B, (D) S3, S4, S6, Soluplus®, and 0.5 % Methyl anthranilate in water. Left: Tracking of polymer by optical microscope, Middle: Tracking of the labelled polymer and Right: Tracking of Methyl anthranilate using the appropriate filters as mentioned in the main text……..107
76. Microscope images of 0.5% copolymer (A) S1, S3, S4, S6, Soluplus®, and 0.5 Carvone in LSFE. Left: Tracking of polymer by optical microscope and Right: Tracking of the labelled polymer using the appropriate filters as mentioned in the main text. Microscope images of 0.5% copolymer (B) S2A, S2B, and 0.5 Carvone in LFE. Tracking of the labelled polymer using the appropriate filters as mentioned in the main text……108
77. Microscope images of 0.5% copolymer (A) S1, S4, (B) S3, (C) S6, (D) S2A, (E) S2B and 0.5 Methyl anthranilate in LFE. Left: Tracking of the labelled polymer and Right: Tracking of Methyl anthranilate using the appropriate filters as mentioned in the main text……...109

78. Fluorescence microscope image of copolymer S2 in LFE in presence of commercial perfume BZ……109
79. OECD 301B test results of reference substance (sodium acetate)……...111
80. OECD 301B toxicity test results of the copolymer S2Bfor 60 days……111
81. OECD 301B toxicity test results of the copolymer S4 for 60 days……..112
82. OECD 301B test results of the copolymer S2A for 60 days……....113
83. OECD 301B test results of the copolymer S2B for 60 days……113
84. OECD 301B test results of the copolymer S4 for 60 days……...……113

LIST OF TABLES

Table Page

1. Advantages and disadvantages of graft copolymers synthetic methods……15
2. Synthesis procedure of the PEG-g-PVCL; (S1) copolymer……...44
3. Synthesis procedure of the PEG-g-(PVAc-co-PVCL); (S2) copolymer……44
4. Synthesis procedure of the PEG-g-(PVAc-co-PVCL); (S3) copolymer……....45
5. Synthesis procedure of the PEG-g-PVCL; (S4) copolymer……...45
6. Synthesis procedure of the PEG-g-(PVAc-co-PVCL); (S6) copolymer……46
7. FTIR wavenumbers (cm^{-1}) characteristic for components, PEG. Vac, VCL and copolymer S1 and S4……60
8. FTIR wavenumbers (cm^{-1}) characteristic for copolymer S2A, S2B, S3, S6 and Soluplus®……61
9. Assignment of corresponding ^{1}H-NMR spectra for copolymer S1, S2, S3, S4, S6 and Soluplus®……...75
10. Composition and degree of grafting of copolymer S1, S2, S3, S4, S6, Soluplus……76
11. Diffusion coefficient values of assigned protons of copolymer S1, S2, S2C, S3, S4, S6 and Soluplus® components……...82
12. Non-Aqueous GPC Results Using dn/dc value……83
13. Thermal properties of the PEG 6000, PEG 1000, VCL, PVAc, copolymer S1, S2A, S2B, S3, S4, S6 and Soluplus®……....98
14. Cloud point temperatures T_{CP} for copolymer S1, S2A, S2B, S3, S4, S6 and Soluplus® aqueous solutions, their compositions and molecular weights…….101
15. Summary of biodegradation and the main different physico-chemical properties of copolymer S2A, S2B and S4……...114

LIST OF SCHEMS

Scheme Page

1. Methods used for graft copolymer synthesis…….15
2. Reactions induced by an initiating radical generated from the initiator A…….19
3. Formation of radicals by decomposition of 2,2'-ao-bis-isobutyrylnitrile AIBN, benzoyl peroxide initiator…….24
4. Synthetic Route to PEG-g-(PVAc-co-PVCL); (S2); (S3); (S6) amphiphilic graft copolymer via Free Radical Polymerization…….46
5. Synthetic Route to PEG-g-PVCL; (S1); (S4) amphiphilic graft copolymer via Free Radical Polymerization…….47
6. Labeling procedure of copolymer S1, S2, S3, S4, S6 and Soluplus® with rhodamine B isothiocyanate……..49

LIST OF EQUATIONS

Equation Page

1. The degradation rate……..……55
2. CO_2Th, theoretical carbon dioxide……56

LIST OF SYMBOLS AND ABBREVIATIONS

EOs	Essential oils
CARG	Compound annual growth rate
p	Packing parameter
PPO	pullulan-graft-poly(propylene oxide)
PVCL-g-PTHF	Poly(N-vinylcaprolactam)-graft-Polytetrahydrofuran
LCST	Lower critical solution temperature
UCST	Upper critical solution temperature
PNIPAAM	Poly(N-isopropylacrylamide)
DEAM	N,N-diethylacrylamide
MVE	Methylvinylether
VCL	N-vinylcaprolactam
AAm	Acrylamide
AAc	Acrylic acid
Luperox TBEC	Initiator Tert-Butylperoxy 2-Ethylhexyl carbonate
PEG	Poly(ethylene glycol)
PVAc	Poly(vinyl acetate)
PVA	Poly(vinyl alcohol)
Ra*	Unpaired electrons /free radicals
(*)	Active centre with a free
RP	Radical polymerization
FRP	Free-radical polymerization
RDRP	Reversible deactivation radical polymerizations

REX	Reactive extrusion
ATRP	Atom transfer radical polymerization
NMP	Nitroxide mediated polymerization
RAFT	Reversible addition-fragmentation chain transfer
G%	Grafting percentage
HEMA	(Hydroxyethyl)methacrylate
EPR	Enhanced permeability and retention
SLFE	Simplified liquid fabric enhancer
Mw	Molecular weight
BPO	Benzoyl peroxide
AIBN	2,2'-azo-bis-isobutyrylnitrile
PRMs	Single components of perfume composition
TLC	Thin-layer chromatography
FTIR	Fourier transform infrared spectroscopy
NMR	Nuclear magnetic resonance spectroscopy
^{1}H-NMR	Proton nuclear magnetic resonance
COSY	Correlation spectroscopy
NOESY	Nuclear Overhauser effect spectroscopy
DOSY	Diffusion ordered spectroscopy
GPC	Gel Permeation Chromatography
dRI	Differential refractive index detector
RI	Refractive index
MALDI-TOF-MS	Matrix-assisted laser desorption/ionization-time of flight mass spectrometry

DSC	Differential scanning calorimetry
TGA	Thermogravimetric analysis
C_{TP}	Cloud point study
CO_2Th	Theoretical carbon dioxide
% degradation	Degradation rate
PDI	Polydispersity index
LS	Light scattering
Da	Dalton
T_m	Melting temperature
T_g	Glass transition temperature
LLPS	Liquid-liquid phase separation
CA	Carvone
MA	Methyl anthranilate

CHAPTER ONE

1. INTRODUCTION

Polymers are materials which are formed by long chains consisting of repeating units. These materials have unique properties dependent on both types of molecules bonded and how they are bonded.

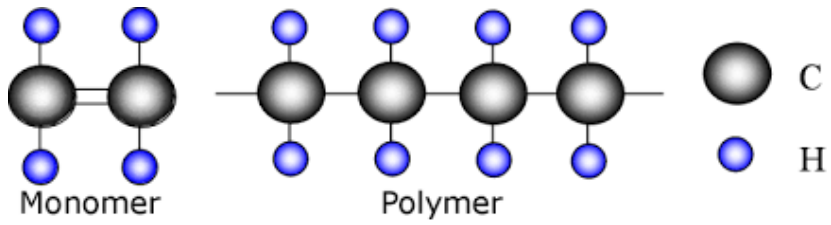

Figure 1. Monomer and polymers (UNSW Science).[1]

Polymers are generally synthesized through a process called polymerization and during this process a high number of monomers are connected with covalent bonds, forming a material with desire properties.[1]

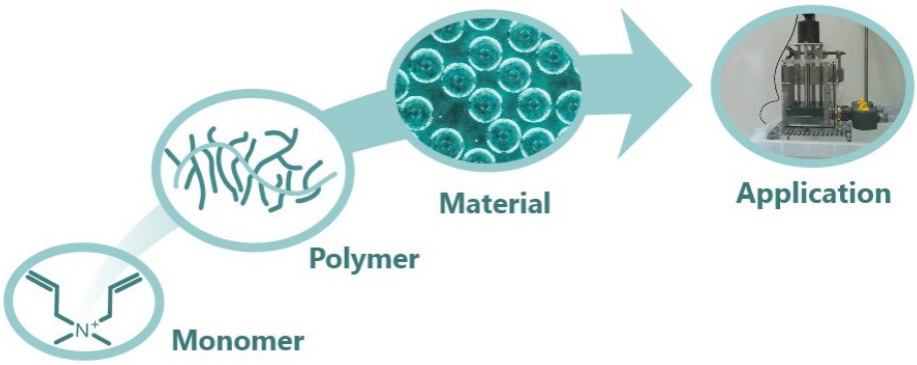

Figure 2. Monomer, polymer, polymeric material, and the resulting material application (Institute for Technical Chemistry and Polymer Chemistry).

Our lifestyle depends upon polymers. Indeed, polymeric materials are used not only to make clothing, houses, cars, aeroplanes but they also find applications in food industry, in medicine, diagnostics and electronics.[2] Moreover, polymers are

commonly present in home and personal care products.[3] Nowadays, the consumers around the world are more focused on health and beauty. The renewed consumer interest in using natural home and personal care products creates the demand for new products or reformulated ones with botanical and functional ingredients. In all these products, such as household detergents, laundry products or cosmetics[4] essential oils (EOs) play a major role as fragrance ingredients. They can optimize product proprieties and preservation, as well as ameliorate the marketing image of the final product. Microencapsulation of EOs can protect and prevent the loss of these volatile aromatic ingredients and improve their controlled release and stability[5]. Sustained release of fragrances is a key performance parameter in many of these personal and household care items, since ensures a longer shelf-life of the products. Very specific wall properties are required to gain a prolonged stability of these microcarriers, encapsulating small and volatile molecules, and the subsequent controlled release.[6] The choice of materials to be used for encapsulation mainly depends on physicochemical behaviour of the active substance. In order to produce the desired encapsulation efficiency, adequate shell or capsule size, optimal surface morphology and functionalities, preformulating studies are mandatory before a new encapsulated product is developed.[7] An ideal material for encapsulation should have the following properties: good rheological properties, the ability to disperse the active material and stabilize the obtained emulsion, non-reactivity with the core material, the ability to completely release the core material under different conditions, solubility in non-toxic solvents and biodegradability. On today market, shell materials suitable for the encapsulation of small-molecular weight molecules are typically polymers such as polyamide, polyurea, polyurethane and urea/ melamine–formaldehyde.[8] Microcapsules found in commercial laundry applications mostly are made of aminoplast-type resins as their capsule wall. The resulting shell wall consists of a densely packed matrix of melamine-linked molecules with a high cross-link density that make the polymeric shell very durable and with a high resistance against temperature, chemicals and hydrolysis.[6,9] Nevertheless, these materials even if provide robust encapsulation, are characterized by an inadequate environmental impact, inefficient biodegradability profile[6,10] and by a limited release of active via pressure.[11] Actually, there is a need for new and different release triggers, especially with dilution[12] and a need of larger deposition of the capsules on the targeted substrates as fabrics and hair.[13]

So, it is duty of present days scientists, educators, and students to develop the possible solutions to minimize the adverse effects on environment and to promote the use of sustainable material to achieve the goals of sustainable development. The key challenge in developing a material is improving the properties of material with respect to its sustainability and economics.

1.1 Research objectives

The global microencapsulation market size is expected to reach USD 19.35 billion by 2025, according to a new report by Grand View Research, Inc.[14], exhibiting a CAGR of 13.7% over the forecast period. Rising demand for microencapsulated fragrances, bleach activators, and anti-bacterial compounds in the home and personal care industry is expected to propel industry growth.[14] The demand from industry and consumers rise steadily and innovation in the field demands to continue to meet regulation and industrial needs.

The main idea of the project is to develop, synthesize and characterize amphiphilic polymeric materials with improved environmental profile for encapsulation technology taking advantage of their self-assembly properties to be used in liquid home- and personal-care products.

CHAPTER TWO

2. LITERATURE REVIEW

2.1 Graft copolymers

Graft copolymers can be defined as macromolecules consisting of two or more different chemical chains in which a chain (named backbone) has multiple branches formed from macromolecular chains with a chemical composition different from that of the backbone. In principle, both the backbone and side chains could be homopolymers or copolymers. A simple graft copolymer can be represented as A_k-graft-B_m or polyA-graft-polyB or poly(A-g-B), where A_k or polyA is the backbone to which the B_m or polyB branches are grafted. The structure of such a copolymer may be represented by **Figure 3**. [15,16]

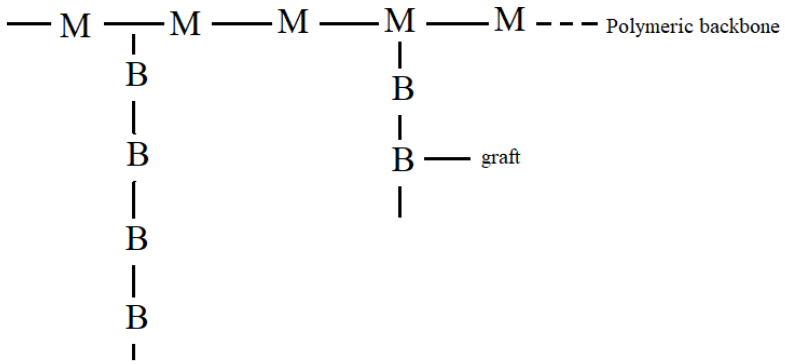

Figure 3. Schematic representation of graft copolymer.

The resulting grafted branches are in most cases distributed randomly along the backbone chain and attached to the trunk polymer by covalent bonds located at the end of the grafted sites. The key parameters of such macromolecules are the chemical structure of the base polymer and grafted branches, as well as the grafting density and distribution of arms along the core (**Fig. 4**) [15-18].[15–18]

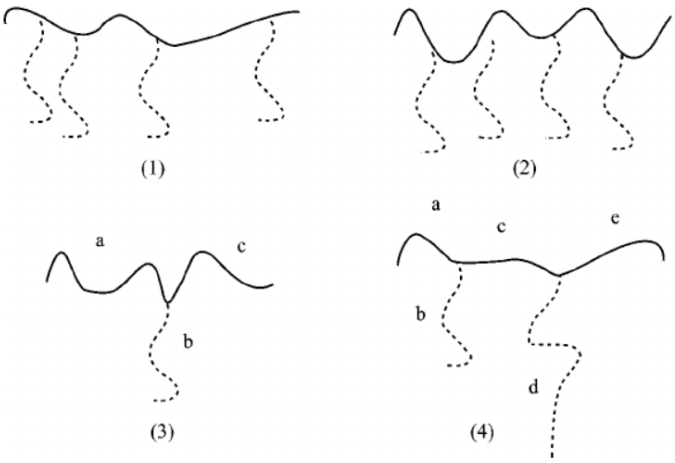

Figure 4. Graft Copolymers (1) random graft copolymer (identical branches randomly distributed along the backbone); (2) regular graft copolymer (identical branches equally spaced along the backbone); (3) simple graft copolymer (3-miktoarm star copolymer); and (4) graft copolymer with two trifunctional branch points.[18]

The preparation of graft copolymers is a domain of polymer chemistry that has received considerable interest in the field of material design and technology. By introducing new reactive sites, the surface morphology of polymers can be tailored to improve certain properties for developing essential products. Graft polymerization is different from random or block copolymerization since it leaves the main polymeric backbone essentially intact. A graft copolymer may combine some of the characteristic properties of each polymer side chains added to the substrate polymer without changing the properties of base polymer or have properties entirely different from those of single components. Grafting conditions are usually chosen to retain the desirable properties and to eliminate the less desirable properties of the individual block or graft components. Hence, such products made of selected polymer combinations can have highly specific properties tailor-made for a particular application.[19,20] Grafting can be an attractive approach to overcome the general problems resulting from different molecular structures as lack of miscibility between different polymers.[21] The grafting of synthetic polymers onto natural polysaccharides assists in overcoming some drawbacks of origin polysaccharides including microbial contamination, uncontrolled hydration, and age-related changes in viscosity.[22] Generally, grafting methods for copolymer synthesis, results in materials that are more thermostable than their homopolymer counterparts.[23]

2.1.1 Amphiphilic graft copolymers

One method of engineering the properties of a new material is by combining two materials with desirable properties into a new material that exhibits the properties of both original materials.[24] The amphiphilic copolymers are very interesting in this regard, as the graft copolymer structure provides integration onto the polymer backbone of considerable functionalities that can be addressed chemically after the assembly process.[25] Amphiphilic polymers are unique group of surface-active agents containing both hydrophilic (water-loving) and hydrophobic (fat-loving) chains. These two blocks with different chemical properties (hydrophilic and hydrophobic) are bonded covalently, creating a resulting macromolecule composed of regions with different affinity to water able to auto-arrange into various morphologies (basic sphere, cylinder, micellar vesicle etc.) through the self-assembly. The interactions and the balance between the hydrophilic and hydrophobic parts determine the interfacial and solution behaviour of amphiphilic copolymers. The thermodynamic incompatibility between the different blocks causes a spatial organization into ordered domains on the nanoscale with the production of novel structural features. The amphiphilic aggregates can be formed via various intermolecular soft interactions such as hydrogen bonds, van der Waals interactions, steric effects, hydrophobic and electrostatic interactions.[26–28] Poly(ethylene glycol) (PEG), also known as poly(ethylene oxide) is frequently utilized for the preparation of amphiphilic polymeric network as hydrophilic agents due to its attractive properties such as water solubility and biocompatibility. It is approved by the FDA to be used in drugs, cosmetics and foods. The hydrophilic character of PEG and its derivatives is interesting and commonly used in many applications, including hydrogels, drug delivery, composite, tissue engineering and absorbents.[29] An example of such an amphiphilic copolymer based on the PEG backbone that have been recently investigated is Soluplus® (polyvinyl caprolactam-polyvinyl acetate-polyethylene glycol graft copolymer (PEG-g-(PVAc-*co*-PVCL)) (**Fig.5**). It is a new pharmaceutical excipient designed originally for preparing solid solutions of poorly water-soluble drugs by hot-melt extrusion technology.[30] Soluplus® is a water-soluble copolymer with molecular weight ranging from 90,000 to 140,000 g/mol, and it is capable of solubilizing poorly water-soluble drugs.[31]

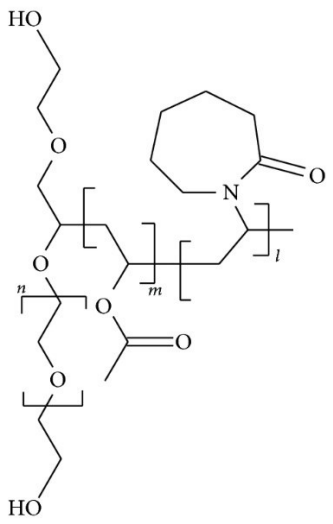

Figure 5. Chemical structure of Soluplus® (polyvinyl caprolactam-polyvinyl acetate-polyethylene glycol graft copolymer (PCL-PVAc-PEG).[31]

2.1.2 Self-assembly

Self-assembly is a nature inspired ubiquitous process which plays numerous important roles in nature in the formation of a wide variety of complex biological structures.[30] Some examples of building blocks used in self-assembled structures in biological systems are phospholipid bilayer of cell membranes, peptides, proteins, ribosome, and DNA complexes.[32] Self-assembly is increasingly important for the fabrication of biomaterials, production of countless cleaning products and cosmetics surfactants. Consequently, over the past decades, scientists extensively studied nature's assembly principles to create artificial materials, with hierarchical structures and tailored properties, for the fabrication of functional devices.[30,33] Recently, molecular self-assembly is becoming increasingly important for the fabrication of advanced composite nanomaterials, transformation and production of energy, new information technologies and microelectronics, pharmacology and medicine, food and personal care products.[34] Self-assembly can be defined as a process in which an organized structure or pattern is assembled as a consequence of specific, local interactions among the components themselves from a disordered system of pre-existing components. Base on the size/nature of constitutive components, we can classify a self-assembly process as atomic, molecular, and colloidal (mesoscopies) and

based on the system where the self-assembly occurs as biological or interfacial self-assembly.[35] The most well-studied subfield of self-assembly is molecular self-assembly by which molecules spontaneously associate into stable, structurally well-defined aggregates through noncovalent or weak covalent interactions (van der Waals, electrostatic, hydrophobic interactions, hydrogen and coordination bonds) under equilibrium state.[36] Amphiphiles self-assemble in selective solvents to minimize unfavourable hydrophobic–hydrophilic interactions and the resulting morphology of the self-assembly is determined by the packing parameter, $p = v/a_o l_c$, where v is the volume of the hydrophobic tail, a_o is the contact area of the hydrophilic head group and l_c is the length of the hydrophobic tail. Spherical micelles are favoured when $p < 1/3$, cylindrical micelles are favoured when $1/3 < p < 1/2$ and vesicles when $1/2 < p < 1$.[37]

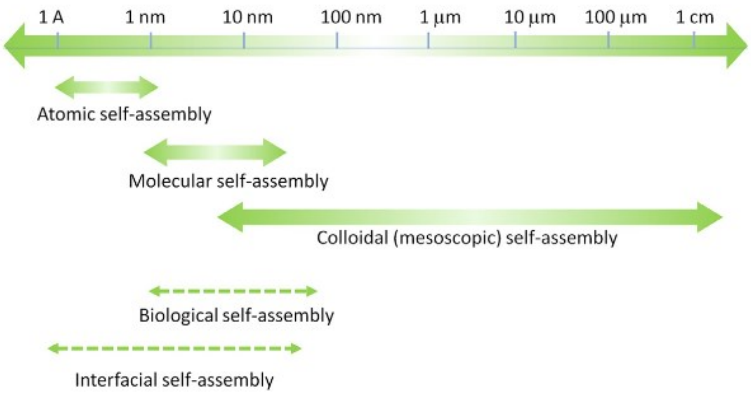

Figure 6. Classification of self-assemblies based on the size/nature (atomic, molecular, and colloidal) of building units and on the system where the self-assembly occurs (biological and interfacial); the length scale is also of building units.[35]

Self-assembly can be classified as either static or dynamic. Static self-assembly involves systems that are at global or local equilibrium and do not dissipate energy. The ordered state occurs when the system is in equilibrium. In static self-assembly, formation of the ordered structure may require energy, but once it is formed, it is stable. Dynamic self-assembly occurs when the formation of an ordered state of equilibrium requires dissipation of energy, thus the interactions responsible for the formation of structures or patterns between components occur only if the system dissipates energy.[38] There are typical attractive and repulsive forces associated with

the self-assembly processes. The main driving forces can be the attainment of equilibrium or minimization of free energy or inter-unit interactions; the inter-unit interactions are mostly non-covalent in nature. The attractive forces include van der Waals, solvation, depletion, bridging, hydrophobic, π-π stacking, hydrogen bond, coordination bond interactions. Electric double layer, solvation, hydration and steric interactions can also be included. [35,39,40]

2.1.3 Self-assembly of Amphiphilic Graft Copolymers

Polymeric nanostructures deriving from amphiphilic block and graft copolymers have had astonishing improvements in drug delivery, nanoreactors, and biomimetics due to their self-assembling and phase separation of hydrophilic and hydrophobic parts in aqueous media.[41] Among the different polymer architectures, graft amphiphilic copolymers have been a rapidly growing field of research in recent years, because of both their unique physical properties in the solid and solution state and simple synthetic routes. Graft copolymers have been found to exhibit distinct self-assembly behavior in comparison to the conventional self-assembly of linear block copolymers.[42] Polymers that possess graft structure of a hydrophobic backbone and hydrophilic side arms are reported to form either unimolecular or multimolecular micelles upon dissolution in a selective solvent. In graft copolymer unimolecular micelles, the hydrophobic backbone collapses and is shielded from unfavourable solvent interactions by the hydrophilic side arms, resulting in a core−shell structure. These graft unimolecular core-shell structures are created even in a good solvent for both the backbone and side arms of graft copolymers. Whether graft copolymers self-assemble into unimolecular or multi-molecular micelles is dependent on grafting density, number of side arms and composition of the side arms and backbone, as these factors determine both the interfacial tension between the hydrophobic backbone and solvated side arms, and repulsive interactions between side arms. In comparison to assemblies composed of linear block copolymers, graft copolymers self-assemble into loose micellar aggregates, where the aggregation number is typically low, as a consequence of the increased number of hydrophilic blocks per hydrophobic block.[33,43] Graft copolymers can self-assemble into unique morphologies such as micelles,[44] nanogels[45] and single-chain polymer particles which cannot be obtained

from the self-assembly of block copolymers. The preparation of particles with a diverse range of morphologies including vesicles, compound micelles and lamellae have also been reported via the self-assembly of graft copolymers with more complex compositions, for example mixed arm systems. Moreover, graft-copolymer self-assembly results not only in the formation of unique nanostructures but is also associated with distinctive self-assembly behaviour. Huang and co-workers found that the self-assembly formation of the vesicles of thermoresponsive pullulan-graft-poly(propylene oxide) (PPO) copolymers is fully reversible upon cooling/heating, and the obtained vesicles have the same size and size distribution even after several cooling/heating cycles, demonstrating that the polymer memorizes the vesicular structure. However, since the molecular structure of graft copolymers is complex, when compared to that of block copolymers, the factors that control the self-assembly process remain unclear, and therefore, molecular design strategies have not yet been established to obtaining specifically sought molecular assemblies.[42,43]

Another class of graft polymers that possess cyclic topology have attracted growing interests because of their unique structural and physical properties respect to the linear analogues.[46] Cyclic grafted copolymer refers to an important class of polymers formed of cyclic backbone and linear grafted side chains. Numerous studies have revealed that in comparison with their linear counterparts, cyclic polymers, due to different topological effects without any terminals, demonstrate unique and prominent physical properties including a smaller hydrodynamic volume, a higher density, a lower intrinsic viscosity, an increased rate of nucleation and crystallization, a higher glass transition temperature, and a higher critical solution temperature.[47] The number of studies focusing on cyclic polymers self-assembly is rather limited. More recently, cyclic polymers have been shown to demonstrate some advantages over linear polymers when considered as potential drug or gene delivery systems.[43] Xu reported that cyclic grafted copolymers with rigid rings, compared with flexible copolymers, provide a larger and loose hydrophobic core and higher structural stability with micelles due to the unique packing way of rigid rings. Therefore, their micelles have a great potential as drug nanocarriers. They possess a better drug loading capacity and disassemble more quickly than flexible counterparts under acidic tumor microenvironment.[48] Meanwhile, Arno demonstrates that self-assemblies comprised

of cyclic-linear graft copolymers are significantly more stable than the equivalent linear-linear graft copolymer assemblies. This difference in stability can be exploited to allow for triggered disassembly by cleavage of just a single bond within the cyclic polymer backbone, via disulfide reduction, in the presence of intracellular levels of L-glutathione.[49]

2.1.4 Stimuli responsive amphiphilic copolymers

Stimuli-responsive polymers also termed 'smart-', 'intelligent-', or 'environmentally sensitive' polymers are intriguing as functional materials for applications in various fields such as medicine, biotechnology, pharmacology, cosmetics, food, environmental, coatings and textiles technology.[50–53] One important feature of this type of materials is reversibility, i.e. the ability of the polymer to return to its initial state upon application of a counter-trigger.[50] They exhibit significant changes in physicochemical properties as a result of a small change in their environment, such as temperature, light, pH, electric potential, magnetic and ionic field, pressure or redox[54]. The stimuli-triggered response in the polymers may result in disintegration, destabilization, isomerization, polymerization or aggregation of micelles, thus releasing drugs.[55] The most important and the most widely investigated stimulus in these studies is temperature. Polymer solutions with stimuli-responsive properties such as fast and reversible conformational or phase change in response to variations in temperature are referred to as thermo-responsive polymers.[54,56] Thermo-responsive polymers in aqueous solutions exhibit a critical solution temperature, where phase separation is induced by a small change in temperature. Temperature-responsive polymers exhibit a volume phase transition at a certain temperature, which causes a sudden change in the solvation state.[57] For the application of thermo-responsive polymers in a particular condition, the phase transition temperature, or cloud point temperature T_{CP}, is one of the most important parameters of a thermo-responsive polymer in solution. T_{CP} refers to the temperature at which the phase transition of a polymer solution at a specific concentration occurs from the soluble state to the collapsed aggregated state, accompanied by clouding of the solution.[58] Different methods have been described to regulate T_{CP}, such as the variation of molecular weights or polymer concentration in aqueous solutions, the introduction of

additives, either low- or high-molecular weight, copolymerisation and crosslinking.[56] It has been shown that the architecture of the (co)polymer, including molecular weight and distribution, the type and number of chain structure such as linear, comb-like, Y-shape, star-like structure, the component of (co)polymer and their hydrophilic-hydrophobic balance, can play an extremely important role in determining its thermo-responsive phase transition behaviour.[51] Verbrugghe, Bernaerts, Du Prez reported that the presence of branching points in amphiphilic poly(N-vinyl caprolactam) graft polytetrahydrofuran copolymers (PVCL-g-PTHF) has a dramatic effect on the phase separation behaviour of such smart materials.[56] Thermo-responsive polymers can be classified into two categories: polymers with a lower critical solution temperature (LCST) below which the polymer is soluble and above which the polymer separate from aqueous solution; and polymers with opposite behaviour with an upper critical solution temperature (UCST) above which polymers become soluble in water.[59] Polymers with LCST behaviour are highly soluble in water. Most commonly, the T_{CP} is reported as the phase separation temperature at a specific concentration, and above this temperature aggregation of the polymer chain results in turbidity. The LCST phase transition is driven by the entropy-loss due to interaction of water molecules with the polymer and upon heating this entropy-loss becomes dominant, eventually leading to dehydration of the polymer and phase separation.[60] UCST polymers are those with positive temperature dependence which exhibits phase separation below cloud point, in other words they are insoluble in solvent, but become soluble with increasing temperature. In many cases, UCST phase transition occurs when solute-solute and solvent-solvent interaction dominates the solute-solvent interaction to generate a positive enthalpy of mixture. Another class of thermo-responsive polymers are polymers with both LCST and UCST behavior. These double thermo-responsive polymers are also attractive because they offer a very good potential to engineer smart materials that can respond only within a specific range of environmental conditions. This type of polymers can either be achieved by copolymerization or modification of an already existing block copolymer like poly(ethylene glycol)-b-poly(acrylamide-co-acrylonitrile) or poly(p-dioxanone)graft-poly(vinyl alchol) copolymers.[54,61,62]

Typical thermo-responsive polymers with a LCST are obtained from Poly(N-isopropylacrylamide) (PNIPAAM), N,N-diethyl acrylamide (DEAM), methylvinylether (MVE), and N-vinyl caprolactam (NVCL) as monomers. Some amphiphilic polymers such as Poloxamers, also exhibit thermo-responsive

behaviour.[63] Poly(N-vinyl caprolactam) (PVCL) and Poly (N-isopropylacrylamide) (PNIAMP) polymers that show cloud point temperatures in the proximity of human body temperature allow self-assembly architectures which are useful for biomedical applications, thus applications in controlled drug delivery have been studied.[64] The polymer itself, PVCL, like PNIPAM, is soluble in cold water but phase separates when the temperature exceeds a critical value, the lower critical solution temperature, LCST. It has been shown that PVCL forms nano-sized aggregates when the solution is heated above the cloud point. It was therefore expected that introduction of amphiphilic grafts on a polymer chain will modify the structure of these heat-induced aggregates.[65] Thermo-responsive polymers with a UCST are based on a combination of acrylamide (AAm) and acrylic acid (AAc). The UCST-type thermo-responsive copolymers, such as poly(ethylene oxide)-b-(protonatedP2VP) potassium persulfate complex and poly(2-oxazoline)-based polymers, and their micellizations have been reported. For the application in drug-controlled release, this type of thermo-responsivity could play an important role, because micelles having UCST can dissolve or dissociate with increasing the temperature, which might lead to the targeted release of encapsulated drugs. [59,63]

In particular, a strong attention has been paid to LCST water-soluble thermo-responsive amphiphilic copolymers, because of the temperature-induced self-assembled capability in aqueous media and the potential applications in many fields. Thermo-responsive amphiphilic copolymers consisting of hydrophobic segments and LCST-type thermosensitive hydrophilic segments can implement a temperature-induced self-assembly above LCST as well as spontaneously form micelles or vesicles below LCST. Owing to their unique self-assembly behaviours and the potential biomedical applications, those kinds of copolymers have attracted more and more attention, especially biodegradable and biocompatible copolymers are extremely important for in vivo biomedical applications.[59] Typical examples of such thermo-responsive amphiphilic polymers are water soluble copolymers contains poly(ethylene glycol) (PEG) segments. PEG-containing monomers have widely been used as building blocks of stimuli-responsive particles or materials because of their water solubility and thermoresponsive behaviour, in addition to their biocompatibility and commercial availability. For example, researchers have investigated micelle-like aggregates of PEG-based polymers, whose morphologies vary according to the temperature and/or pH.[51]

2.1.5 Synthetic methods of graft copolymers

Graft copolymers are polymers with modified physical and chemical properties, generally comprising two polymeric components. The second component consists of randomly distributed branches attached to the first component serving as the backbone. Basically, three general methods have been developed for the synthesis of randomly branched graft copolymers: (1) the "grafting onto", (2) the "grafting from", and (3) the macromonomer method (or "grafting through" method) (8) (**Scheme 1**).[18,66,67] Each of these methods has advantages and disadvantages that affect the final product and that must be analyzed before starting the synthesis (Table 1). The "grafting onto" method involves the use of a backbone chain containing functional groups (X) randomly distributed along the chain and branches having reactive chain ends (Y). The coupling reaction between the functional backbone and the end-reactive branches leads to the formation of graft copolymers. In the "grafting from" method active sites are generated randomly along the backbone. These sites are capable of initiating the polymerization of monomers leading to graft copolymers. The most commonly used method for the synthesis of graft copolymers is the macromonomer method. Macromonomers are oligomeric or polymeric chains bearing a polymerizable one or two end group. Copolymerization of preformed macromonomers with another monomer yields graft copolymers.[18,67]

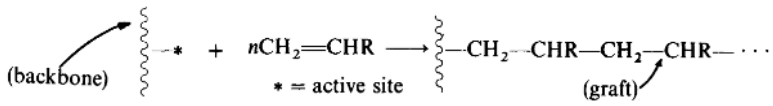

<u>Grafting from</u>: a polymer chain carries active sites which are used to initiate the polymerization of second monomer.

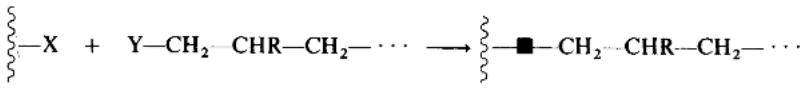

<u>Grafting onto</u>: polymer chain (backbone) carrying randomly distributed reactive functions X, reacts with another molecule carring antogonist functions Y located selectivly at its chain ends.

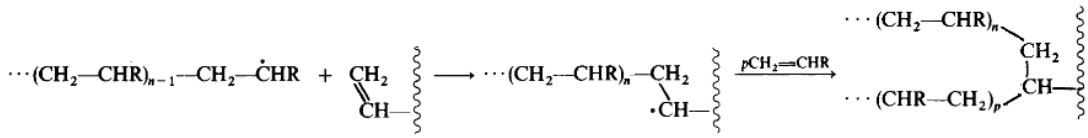

Grafting through a growing polymer chain incorporates a pendant unsaturation belonging to another polymer chain or to a macromonomer.[68]

Scheme 1. Methods used for graft copolymer synthesis.[68]

Table 1. Advantages and disadvantages of graft copolymers synthetic methods.[68]

	Advantages	Disadvantages
Grafting "onto"	Control of the backbone molecular weight with narrow molecular weight distribution Control of the branch molecular weight with narrow molecular weight distribution	Low grafting density. Rather low branch molecular weight Cannot afford polymer brushes
Grafting "from"	Control of the backbone molecular weight with narrow molecular weight distribution High grafting density Can afford polymer brushes	Difficult control of branch molecular weight Broad branch molecular weight distribution Branches cannot be isolated for characterization
Grafting "through"	Control of the branch molecular weight with narrow molecular weight distribution High grafting density Can afford polymer brushes	Low branch molecular weight The backbone cannot be isolated for characterization

The "Grafting From" method

This method is quite general and was used in the 1950s by pioneers of macromolecular synthesis such as Smets et al. and Bamfordeta. In this process, polymer chain can have initiating sites attached to it, or functions capable of generating such sites necessary for initiating the polymerization of a second monomer. The initiating sites can be incorporated by copolymerization, by a post-polymerization reaction, or can already be part of the polymer. [18,69] The polymerization of a second monomer can then be initiated from the backbone chain to yield the grafts, if initiation occurs by addition to

the incoming monomer. The sites created on the backbone can be free radical, anionic, cationic, or Ziegler-Natta type. The number of grafted chains can be controlled by the number of active sites generated along the backbone assuming that each one of them participate to the formation of one branch. Mainly because of kinetic and steric hindrance effects, there may be a difference in the lengths of the produced grafts.[18,66] These methods are generally referred to as "grafting from" processes to stress that the backbone is made first, and the grafts are grown from it in a second polymerization process. Though these methods are quite efficient in a number of cases, no accurate knowledge of the molecular structure of the graft copolymer formed is provided. The number of grafts is not accessible experimentally, and their length may fluctuate very much within the macromolecule. Moreover, these graft copolymers often contain a fair amount of both homopolymers.

"Grafting from" reactions have been conducted starting from polyethylene, polyvinylchloride, and polyisobutylene. Different techniques such as anionic grafting, cationic grafting, atom-transfer radical polymerization, and free-radical polymerization have been used in the synthesis of these "grafting from" copolymers.[70]

The "Grafting Onto" method

In the "grafting onto" method, reaction of pre-formed polymeric chain carrying one reactive site at a chain end, and another polymer with attached antagonist functions distributed at random along its chain, takes place.[18] In most cases the incorporation of functional groups is performed by chemical modification of the backbone.

In these cases, grafting does not involve a chain reaction. However, it does imply that access of the functional chain end to the grafting sites is permitted. This is not obvious, owing to the well-known incompatibility between polymers of different chemical natures. Such reactions are generally carried out in a common solvent for both constituents to provide homogeneity of the reaction medium.[68] "Grafting onto" approach allows the polymer backbone and side arms to be prepared separately and can be characterized individually. Knowing the molecular weight of each of them, and the overall composition of the graft copolymer, it is possible to evaluate the number of grafts per chain, and the average distance between two successive grafts along the

backbone. However, because of steric repulsion between the bulky side arms, grafting density is commonly limited.[66,68] These “grafting onto” reactions have gained interest as the ionic 'living polymerization methods'. A common procedure is the chloro(bromo) methylation of polystyrene, and the subsequent reaction with living polymeric chains. Recently, “grafting onto” has become a more efficient method for the preparation of graft copolymers, with the rise of various "click" chemistries. This approach has been used for the preparation of well-defined star-shaped polymeric structure (Gao et al., 2007) or loosely grafted copolymers (Tsarevsky et al., 2007) have been prepared using this grafting technique.[18,71]

The “grafting through” method (or “macromonomer” method)

“Grafting through” polymerization represents copolymerization of free monomers in solution and polymerizable units bound to a substrate. Free polymer chains are formed initially in solution and can incorporate the surface-bound monomers, and thereby, get covalently bonded to the surface during the polymerization process. As more growing chains attach to the surface bound monomers, an immobilized polymer layer is formed on the surface. Typically, in the grafting through method, also known as the macromonomer method, a monomer of a lower molecular weight is copolymerized with free radicals with an acrylate functionalized macromonomer.[72] The number of branches is determined by the ratio of the macromonomer and comonomer molar concentrations and their copolymerization behaviour. These parameters determine how randomly distributed along the backbone will be branches. Due to the fact, the relative concentrations of the macromonomer and the comonomer change with time during the copolymerization, graft copolymers formed in this process differ in the number of branches. In addition, this copolymerization is not homogeneous throughout the course of the reaction since phase separation may occur. For the above-mentioned reasons, it can be concluded that the graft copolymers prepared by this method are generally characterized by increased compositional and chemical heterogeneity. Macromonomer (grafting through) method can be employed using almost all known polymerization techniques. The major advantages are the living polymerizations which offer special control over the molecular weight, molecular weight distribution, and chain-end functionalization.[68,73]

2.1.6 Free radical polymerization method

Radical polymerization is the most important industrial method for polymer synthesis. Almost 50% of all synthetic polymers we are familiar with in our everyday lives are made using radical processes. Since practically any molecule with a carbon-carbon double bond can be polymerised by radical polymerisation, polymers with a very wide range of properties can be obtained by this method.[74] There are several reasons for the commercial success of radical polymerization, that make a dominant position of radical polymerization (RP) in industry and differentiate it from other polymerization methods. The most important one is the large range of radically polymerizable monomers, their facile copolymerization, a convenient reaction temperature range (from room temperature to 100°C) and very minimal requirements for the purification of monomers, solvents, etc. which need only be deoxygenated. Comparing to ionic or coordination polymerization, RP is not affected by water and protic solvents and trace impurities such as oxygen or monomer stabilizers.[75] Consequently, it can be conducted in polar solvents such as alcohols or, more important, water with monomers that are not rigorously dried or purified. The range of monomers is larger for RP than for any other chain polymerization because radicals are tolerant to many functionalities, including acidic, hydroxyl, and amino groups. Furthermore, many low-priced monomers are available. Thus, from an economical point of view, RP is the technique of choice. For example, the cost to polymerize styrene by anionic polymerization is about 50% higher than for RP. In conventional RP, high molecular weight (MW) polymers are formed at the early stages of the polymerization, and neither long reaction times nor high conversions are required, in sharp contrast to step-growth polymerization.[76] Radical Polymerisation is an example of a 'chain' reaction (Morton, 1973). Chain reaction can be defined as reaction in which one or more reactive intermediates are continuously regenerated, usually through a repetitive cycle of elementary steps (Laidler, 1996; Muller, 1994; Svehla, 1993). In radical polymerisation, the continuously regenerated reaction intermediate is the polymer radical.[74]

The central mechanism of chain formation by free radical polymerization involves few fundamental steps, generation of radicals, (reaction (1)), initiation (reaction (2)),

propagation (reaction (3)), and termination (reactions (4) and (reactions (5) (**Scheme 2**).[77]

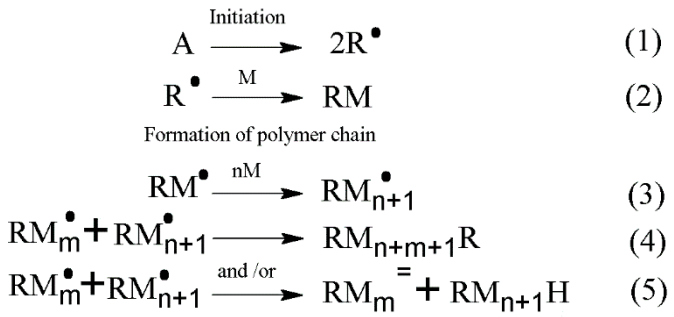

Scheme 2. Reactions induced by an initiating radical generated from the initiator A

The initiation step involves the generation of active species. The free radicals can be produced in several ways, including a direct method like thermal or photochemical decomposition of organic peroxides, hydroperoxides, azo or diazo compounds which result in very reactive unpaired electrons (free radicals Ra*)[78,79] or an indirect method. In the last one radical are formed through redox reaction or high-energy radiation.[80]

Free radicals are typically sp^2 hybridized intermediates with a very short lifetime. They terminate with diffusion-controlled rate through disproportionation and coupling reactions. Radicals show high regioselectivities and add to the less substituted carbon in alkenes. Therefore, polymers formed by RP have head-to-tail structures. Radicals have sufficient chemoselectivity (ratio of rates of propagation to transfer), as evidenced by the formation of high MW polymers.[76]

The two most common initiators of free radicals are benzoyl peroxide (BPO) and 2,2'-azo-bis-isobutyrylnitrile (AIBN). Not all monomers are susceptible to all types of initiators. Radical initiation works best on the carbon–carbon double bond of vinyl monomers and the carbon–oxygen double bond in aldehydes and ketones.[80,81]

The first step of initiation process involves decomposition of initiator into primary radicals. Then, the previously generated from initiator molecule free radicals (Ra*) combines with the monomer molecule to add to the double bond, creating a molecule with an unpaired electron or active centre. The regeneration of the free radical is the hallmark of a chain reaction. The (*) represents the active centre with a free electron

that got transferred from the radical to the ethylene monomer, making the ethylene monomer as the new radical. The initiation stage can be depicted as follows:[78,82]

$$\mathrm{Ra}^* + \mathrm{CH_2} = \mathrm{CH_2} \rightarrow \mathrm{RaCH_2CH_2^*}$$

In propagation step, the chain radical adds successive monomers or repeating units to grow the polymer chain. There may be anywhere from a few to thousands of propagation steps depending on several factors such as radical and chain reactivity, the solvent, and temperature. The process is continuing until there are no more monomers (living polymerization) or until termination occurs.[78,83,84] Using polyethylene polymerization as an example, during this step the reactive species adds to a monomer molecule by opening the π bond to form the free radical building block of ethylene monomer which reacts with other ethylene monomer and each new monomer unit creates an active site for the next attachment.[85] In order to stabilize the active centres, the free radical building block binds with neighbouring monomers extending the length of the chain. The formation of polyethylene chain can be thus constructed by a series of addition reactions between the active centre of the growing chain and available monomers. The reactive group can attach at both end of the growing chain. Process is repeated as many more monomer molecules are successively added to continuously propagate the reactive centre as the following:[78,82,86]

$$\mathrm{RaCH_2CH_2^*} + \mathrm{CH_2} = \mathrm{CH_2} \rightarrow \mathrm{RaCH_2CH_2CH_2CH_2^*}$$

$$\mathrm{RaCH_2CH_2CH_2CH_2^*} + \mathrm{CH_2} = \mathrm{CH_2} \rightarrow \mathrm{RaCH_2CH_2CH_2CH_2CH_2CH_2^*}$$

Termination involves destruction of the radical active centres, thus preventing any further propagation. Chain growing can be terminated on indefinitely until all the monomer is consumed or at any point during the polymerization by combination (coupling) or disproportionation. In the case of combination or coupling, termination occurs when the free electrons from two growing polymer chains react with each other forming a single nonreactive polymer chain.[78,87] Such a mechanism significantly increases molecular mass, if it results in two polymers chain joining.[88] Termination by combination is not the only pathway for termination. In termination by

disproportionation one radical transfers a hydrogen atom to the other, giving an alkene and an alkane. Disproportionation has no effect on molecular mass. [88,89] The third method is chain transfer. The free radical can be transferred to other species. This may be used to control molecular weight (by creating additional polymer molecules for each radical chain initiated). It also leads to the formation of branches, which has a substantial impact on MW distribution and properties. Due the fact that some free radicals combine to form a paired electron covalent bond and a loss of free radical activity, only a small number of free radicals are created to reduce the probability of termination. Chain termination by direct combination could be depicted as:[78,82]

$$\mathrm{Ra}\,(\mathrm{CH_2})_{\mathrm{m}}^{*} + {}^{*}(\mathrm{CH_2})_{\mathrm{n}}\mathrm{Ra} \rightarrow \mathrm{Ra}\,(\mathrm{CH_2})_{\mathrm{m}}(\mathrm{CH_2})_{\mathrm{n}}\,\mathrm{Ra}$$

2.1.7 Industrial methods of radical polymerization

Free radical polymerization can be accomplished in bulk, suspension, solution, or emulsion. Ionic and other nonradical polymerizations are usually confined to solution techniques.[86]

Bulk polymerization, the simplest polymerization reaction without contamination of solvent and other impurities or using especial equipment, contains only initiator and monomer. However, it is usually difficult to control due to the exothermic polymerization reaction.

Suspension polymerization consists in mechanically dispersing monomers in a noncompatible liquid, usually water, monomer soluble initiator and stabilizers, such as polyvinyl alcohol or methyl cellulose (ether), that keep monomer in suspension.

In Solution polymerization, the reaction must be conducted in a solvent easy to be removed at the end of reaction, as carbon dioxide. It requires polar monomers such as acrylates and initiator.

In Emulsion polymerization, the reaction takes place exclusively in micelle. The micelles act as a meeting place for the organic (oil soluble) monomer and the water-soluble initiator. Additional emulsifying agent is also needed.

1.1.8 Typical Features of Radical Polymerization

Copolymerization

Copolymerization of two or more monomers by radical polymerization is commonly used in industry to regulate the properties of commercial polymers. Many industrial polymers are prepared from two, three, or even more monomers. In addition to varying molecular weight, chain length and stereochemistry (trans–cis configurations), copolymers differ in their composition (the relative amounts of each monomer incorporated into the copolymer), sequence distribution (the way in which these monomers are arranged within the chain), and architecture (linear or graft or branched). All of these aspects play important roles in final material properties. With these new parameters, almost unlimited number of polymer types can be produced for better balance of properties for commercial applications. Different monomers lead to different radicals, and the relative rates of propagation depend on the steric and electronic properties of both monomer and radical. Therefore, at any given time, the ratio at which the monomers are incorporated into the polymer is not equal to their ratio in the monomer mixture. Hence, both the composition of the monomer feed and copolymer will change with conversion and, consequently, batch copolymers will in most cases not have homogeneous composition at the molecular level. An advantage of radical polymerization over ionic polymerization is the fact that the reactivities of many monomers are relatively similar, that makes them easy to copolymerize statistically. In case of monomers with opposite polarities, there is a tendency for alternation. Electrophilic radicals (i.e., those with –CN, –C(O)OR, or Cl groups) prefer to react with electron rich monomers (such as styrene, dienes, or vinyl acetate), whereas nucleophilic radicals prefer to react with alkenes containing electron withdrawing substituents.[75,76,89]

Monomers

Many molecules containing unsaturated homo or heteronuclear double bonds, dienes, trienes, strained cyclo aliphatics, exo-methylene-substituted cyclic compounds, or vinyl cyclopropanes can be polymerized by free radical polymerization method. However, the major industrial monomers are compounds (Scheme 1)

containing C=C double bond (s) where X is primarily X=H, (CH_3) and Y=H, Cl, COOH, COOR, $CONH_2$, CN, $OCOCH_3$, C_6H_5, –CH=CH_2), which serve as precursors of the corresponding polymers. Besides the basic monomers that are produced on a very large scale, there is a variety of special monomers that are used to make homopolymers or copolymers with specific properties. Major monomers used in industrial radical polymerization are, Acrylic acid, Acrylamide, Acrylic esters, Acrylonitrile, Methyl-methacrylate, Ethene, Styrene, p-Methyl styrene, N-Vinyl pyrrolidone, Vinyl acetate, Vinyl chloride, Vinyl fluoride, Vinylidene fluoride, Trifluorochloro- and tetrafluoroethene.[75] Monomers which cannot be successfully homopolymerized radically to high MW polymers include simple α-olefins, isobutylene, and those monomers with easily abstractable H atoms (e.g., thiols, allylic derivatives). They have low reactivity and participate in extensive transfer.[76]

Initiators

Ideally, the initiators should be relatively stable at room temperature but should decompose rapidly enough at polymer processing condition to ensure a practical reaction rate. Free radical may be classified into three major types: thermal initiators including peroxides and azo compounds, redox initiators, and photoinitiators (compounds that form radicals under influence of light). Electrons can be used as initiating agent to generate radical ions for chain polymerization.[86] Common molecules that are used as initiators include peroxides (containing a peroxide bond, -O-O-) and azo compounds like 2,2'-azo-bis-isobutyrylnitrile AIBN (containing R-N=N-R'). Examples of common initiators include benzoyl peroxide, which is thermally triggered, and benzophenone, which is UV triggered. For each bond in initiator that is broken, two radicals are formed (**scheme 3**).[90,91] In addition to the type of initiator, its amount is also important. The concentration of the initiator should be lower than the monomer by about 1 wt%.[92] In conclusion, it can be said that selecting an initiator is one of the most important steps that can affect the success of polymer synthesis. The choice of initiator determines the polymerization conditions and monomer type. Selecting a suitable initiator and its proper concentration can yield a polymer with good efficiency and selectivity. The initiator is decomposed by various methods including optical, chemical, electrochemical, thermal, and any procedure that

produces the essential free radicals. The rate and type of destruction of an initiator and the control of radical production depend on the chemical structure of the initiator. The type of destructive energy used in the initial step depends on the type of monomer, template, and initiator. It must ensure that the energy used does not destroy other substances involved in the reaction.[93] For example, some general approaches for selecting initiators for curing unsaturated polyester resins are, initiator half-life, meld temperature, resin viscosity, initiator concentration, promoter levels, and initiator sensitivity to the resin environment.[94]

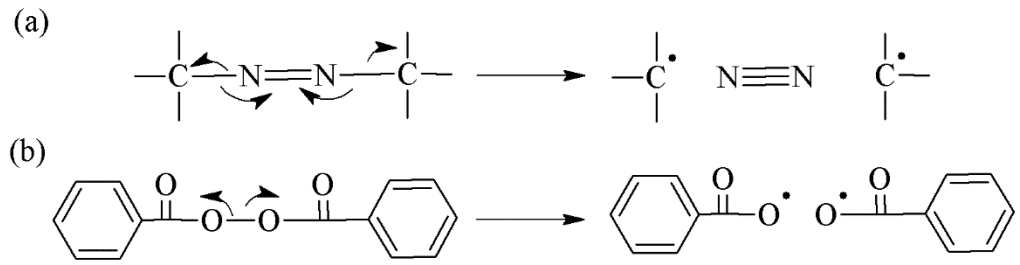

Scheme 3. Formation of radicals by decomposition of 2,2'-ao-bis-isobutyrylnitrile AIBN, benzoyl peroxide initiator.

Additives

Some compounds can affect the rate of RP or the molecular weight (Mw) of the resulting polymers. Some reagents inhibit or retard RP. Oxygen is a classic inhibitor which forms relatively stable and unreactive peroxyl radicals. Other efficient inhibitors include quinones and phenols (in the presence of oxygen), nitro compounds, and some transition metal compounds such as copper(II) chloride or iron(III) bromide. Thiols, disulphides and polyhalogenated compounds do not affect rate but they strongly influence molecular weight via transfer processes.[76]

1.1.9 Polymer Grafting by Free-Radical Polymerization

Grafting is a process where a parent polymer is employed as a backbone onto which branches of a second polymer are connected at different points. In other words, polymer grafting is a method in which monomers are covalently bonded onto the

polymer chain. Polymer grafting aims to improve the functional properties of the polymer.[80]

As previously reported, the "grafting through" and "grafting from" techniques require a polymerization reaction to bind the polymer grafts to the backbone. Among all polymerization methods used for polymer grafting, the most effective ones involve free radical methods (e.g., free-radical polymerization FRP, reversible deactivation radical polymerizations RDRP, and reactive extrusion REX), due to their versatility to work with different chemical groups, and their tolerance to impurities. Previously described FRP, and RDRP, REX polymer grafting reactions can be influence by several factors, including nature of the backbone, monomer, solvent, initiator, additives, and reaction temperature. The synthetic routes and activators used in graft polymerization provide a variety of interesting and versatile routes for this type of polymer modification. The free-radical grafting system usually contains three types of reactants: polymer, unsaturated molecule, such as vinyl monomer, and free radical initiator.[79,95]

Reversible-Deactivation Radical Polymerisation (RDRP) was formerly known as Controlled Radical Polymerisation, even more formerly known as Living Radical Polymerisation. RDRP, is a group of polymerization techniques based on free radical technology that controls the growth of polymer molecules during the polymerization. In RDRP, comparing to conventional radical polymerization, a new reaction is introduced, i.e. reversible deactivation of the chain ends. For RDRP to be effective, this reaction has to occur often on the timescale of propagation. Ideally, a chain will be deactivated and reactivated several times for each propagation reaction. The ability to reversibly deactivate propagating radical species, by effect of controllers that act under some relatively new chemical routes, permits the synthesis of complex polymeric architectures with good control over molecular weight, dispersity and chain-end functionality. The three most common forms of RDRP, Aminoxyl-Mediated Radical Polymerisation, Atom-Transfer Radical Polymerisation, and Reversible-Addition-Fragmentation chain Transfer Polymerisation, correspond to these three possibilities.[95–97]

Atom transfer radical polymerization (ATRP) is a process where free radicals may be generated via a catalysed reaction where an alkyl halide macromolecule reacts with the catalyst, allowing the formation of a radical that propagates until it reacts again with the catalyst, in a reversible way.[98,99]

In Nitroxide mediated polymerization (NMP), the reaction is metal free, and control relies on the reversible capture of the propagating species by nitroxides with formation of dormant chains with alkoxyamine end functionalities. Free radicals may be generated by the spontaneous thermal process (NMP). Whenever this equilibrium is shifted toward the dormant form, the stationary concentration of the active species is low, and the irreversible chain termination is limited. This system provides colourless and odourless polymers with no demanding purification.[99,100]

In Reversible addition-fragmentation chain transfer (RAFT) polymerization, free radicals may be generated reversibly via the degenerative exchange process with dormant species.[98] RAFT can be applied to the widest range of radically polymerizable monomers, using reaction conditions that are similar to those of free radical polymerization. The RAFT process is similar to a conventional free radical polymerization in the presence of a chain transfer agent, where the chain transfer agent is a thiocarbonyl thio compound (so-called RAFT agent). The reversible chain transfer agent captures and releases propagating radicals reversibly, allowing the synthesis of polymers with narrow polydispersity and of predetermined chain length.[101]

Reactive extrusion (REX) is a set of techniques designed to produce and modify polymers, typically carried out in single or twin extruders. Five main types of reactive polymerizations carried out in extruders have been reported: bulk polymerization, polymer grafting, polymer functionalization, controlled degradation, and reactive blending.[102] REX is solvent free melt process.[103] In this radical polymerization method, polymer is modified by standard free-radical polymerization where free radical initiators such as peroxides are used to generate active sites within the backbone or by insertion of active pendant groups that consists of the copolymerization of monomers showing no functional groups with co-monomers possessing pendant groups which make polymer grafting easier to accomplish.[95,104]

2.1.10 Factors Affecting the Grafting

Several factors can affect graft copolymerization, among them an important role is played by additives, backbone nature, initiator role, monomer and temperature.

Additives

Additives are a fundamental factor when studying the grafting mechanism because the amount of graft copolymerization depends on the action of the additives (acids, metal ions and organic-inorganic salts). The presence of additives generally increases the grafting efficiency by promoting the reaction mechanism of monomer/backbone, but sometimes, additives can decrease the grafting efficiency. Zahran and Zohdy (1986) observed that alkali treatment could improve grafting yield and found that the addition of sulfuric acid or alkali controlled grafting yield.[20,105]

Backbone Nature

The backbone nature (viz. physical nature, chemical composition) has its unique role in the graft copolymerization since it includes the covalent bond of a monomer onto the surface of the base polymeric backbone (Ibrahem and Nada 1985).[105] Swelling or dissolution of the backbone like cellulose may take place in the presence of an appropriate solvent, which enhances the mobility of radicals to active sites on the substrate backbone to effect grafting.[79] Ng et al. reported that cellulose is resistant to grafting reactions in water owing to its insolubility, due to the big size of the polymeric chain.[106] It is reported that crystallinity decreases with increasing degree of substitution of cellulose derivatives, affecting the grafting of acrylamide on acetylated wood pulp. As the crystallinity decreases, polymer is less ordered thus facilitating the grafting reaction.[107] The amorphous fraction and solvent can also play role. In the case of styrene grafting to polyethylene, the addition of methanol or methanol-sulfuric acid along with the monomer increases the viscosity in the amorphous region, thus increasing the grafting rate.[79] The presence of many functional groups hydroxyl -OH, tiol -SH, nitro $-NO_2$ groups in the backbone also influences the

grafting. Some of them were reported having positive impact on grafting efficiency like pendant aromatic nitro group present at backbone were find more effective in obtaining a styrene graft cellulose co-polymer. On the contrary, -SH group was associated with a marked decrease in the level of grafting in case of methyl methacrylate grafting on holocellulose (comprising a mixture of a-cellulose plus the hemicelluloses). Taghizadeh and Mehrdad (2006) explained the role of backbone on grafting percentage %G by varying its concentration. The results showed an increase in %G with an increase in starch concentration.[20,79,108]

Initiator Role

All chemical grafting reactions involve the use of initiator, and its concentration, nature, solubility, and function should be considered. According to Gupta et al. (2002) an increase in the concentration of the initiator (in the presence of nitric acid) can efficiently increase the graft copolymerization rate.[20,109] It is apparent from the observations that once a certain initiator concentration is reached, higher levels of initiator do not increase the conversion of grafted monomer.[110] The nature of the initiator has a weighty effect on grafting. For example, AIBN exhibits resonance stabilization. No such resonance stabilization exists with conventional peroxide initiators, and higher grafting yield should be obtained with peroxide initiators than with AIBN. In another example, in the grafting of (Hydroxyethyl)methacrylate (HEMA) on cellulose, AIBN gives poor grafting and potassium persulfate is unsuitable as an initiator since it degrades the cellulose chain. The solubility of the initiator in the grafting medium is another prime factor. Ideally, the initiator should be fully soluble so that it can initiate the grafting reaction through monomers.[79,111]

Monomer

The reactivity of the monomer is also an important factor. The reactivity of monomers depends upon various factors, polar and steric nature, swelling ability of backbone in the presence of the monomers and concentration of monomers.[79] The grafting of hydrophobic monomers such as butadiene, methyl methacrylate, styrene,

and vinyl acetate onto cellulose substrates can improve the adhesion of the grafted materials to hydrophobic fibres.[20] The differences between grafted percentages of different monomers onto the backbone can be explained by their different reactivity to radicals. For example, the grafted vinyl acetate (2.6%) on wool is lower than ethyl acrylate (60.8%), being less reactive to radicals and being reduced in sides reactions.[56] Pandey et al. (2003) also found that the grafting efficiency increases with monomer concentration up to a certain limit and then decreases with further increase in the monomer concentration. Further increase in monomer concentration increases the homopolymerization reaction rather than grafting.[20,79,112]

Effects of solvent

In grafting mechanisms, the solvent is the carrier by which monomers are transported to the vicinity of the backbone. The choice of the solvent depends upon several parameters, including the solubility of monomer in solvent, the swelling properties of the backbone, the miscibility of the solvents if more than one is used, the generation of free radical in the presence of the solvent, etc. The solubility of the monomer depends on the nature of the solvent and the polymer. Swelling of the film caused by the solvents also has great influence on the distribution and average molecular weights of grafted chains.[79,113] Methanol, because of its strong swelling capacity and relatively weak chain transfer capacity, improves the grafting polymerization when its concentration in the mixed solvent with water is low (lower than 20%). When used in high concentration, its chain transfer role surpasses its swelling role and consequently it affects the grafting yield adversely.[114]

Temperature

The temperature is one of the important factors that control the kinetics of graft co-polymerization. In general, increasing polymerization temperature had a positive effect on the grafting efficiency. This can be due to the swell ability of backbone, the solubility and the high diffusion rate of the monomer, and the rate of decomposition of the initiator, which depends on the temperature.[115] However, Joshi & Sinha highlighted that with further increase in temperature, the grafting of acrylic acid onto

carboxymethyl chitosan occurs with poor selectivity, and various hydrogen abstraction and chain-transfer reactions are accelerated, thus, leading to a decrease in grafting. The decrease in grafting efficiency at higher temperature may be attributed to the acceleration of the termination reaction which leads to the formation of more homopolymer.[116]

2.1.11 New properties of graft copolymers

Graft copolymerization is one of the most promising technique used to modify the properties of naturally available polymers with a minimum loss in their native characteristics. With modification of chemical functional groups of polymers, wide range of favourable properties can be imparted to polymer and unfavourable one can be diminished. Many researchers have carried out the grafting onto the different hydrophilic polymers backbone using various vinyl monomers, and using a wide range of initiator, oxidizing agent, monomers, binary vinyl monomeric mixtures, and radiation techniques achieving fruitful results.[117] Graft copolymerization of vinyl monomers onto hydrophilic polymers is the most promising technique given its functionalization of those biopolymers proper to their potential by providing them with desirable properties.[118] Some of the new properties that hydrophilic polymers gain from different monomers grafted onto them include:

- Thermal stability
- Flame resistance
- Dye absorption ability
- Resistance towards acid–base attack and abrasion[118]
- Flexibility and hardness[119]
- Hydrophilic/hydrophobic character[120]
- Thermosensitivity[121]
- High binding metal ion capacities and rapid rate of metal ion extraction[122]
- Absorption of water[123]
- Reduced viscosity[124]
- Swelling abilities[125]
- Antibacterial effect[126]

- Improved biodegradability[127]

Graft copolymers play an important role as reinforcing agents in the preparation of green composites finding extensive applications in diversified fields, i.e. drug delivery devices, controlled release of fungicides, selective water absorption from oil–water emulsions and purification of water.[128]

2.1.12 Applications of amphiphilic graft copolymers

Amphiphilic graft copolymers are emerging in the many fields due to their great potential in terms of stimuli responsiveness, loading capabilities and reversible thermal gelation. Amphiphilicity guarantees self-assembly and thermo-reversibility, while grafting polymers offers the possibility of combining blocks with various properties in one single material.[129] This unique nature of amphiphilic graft copolymers has resulted in several investigations for potential use in polymer alloys, agrochemistry, surface modification, membranes, coatings, pharmaceuticals for drug delivery, tissue engineering, carriers for gene therapy, cell encapsulation, and home & personal care products.[130,131] Amphiphilic polymers are copolymers including both hydrophilic and hydrophobic chains. This specific category of polymers has the unique property of displaying self-assembling behaviour in selective solvents. This behaviour is triggered by hydrophilic-hydrophobic interactions among the polymer chains, which form a variety of microstructures such as a micellar in the nano and micro scale depending on the architectural parameters and the interaction parameter between the graft blocks and solvent.[129,132] The most studied applications of amphiphilic graft copolymer have been listed.

Control drug delivery

Thanks to their amphiphilic nature, amphiphilic graft copolymers enable hydrophobic drugs encapsulation in micelles and their subsequent delivery in aqueous medium. On top of that, these micelles are responsive to external stimuli (temperature, solvents,

solutes concentration, pH), hence they make it possible to accurately tune the on-demand release of the incorporated drug at the target site leading to enhanced drug efficiency and reduction of drug toxicity.[109] Due to the large size of amphiphilic copolymers in aqueous solutions, they can serve as a long-circulating drug carrier significantly improving drug accumulation in solid tumors due to the enhanced permeability and retention (EPR) effect. For diseases like hematological malignancies, where the EPR effect cannot be applied, long-circulating polymer depo of low molecular weight drugs can also be used. Moreover, amphiphilic copolymers can solubilize and deliver potent hydrophobic anticancer molecules whose activity is hindered by their problematic systemic administration. In addition, the conjugation of polymer carrier with highly toxic chemotherapeutics via specific biodegradable spacers guarantees the drug protection during transportation in the blood stream.[133] Randárová et al. demonstrated amphiphilic polymer-based drug delivery systems may significantly improve cancer therapy. Developed amphiphilic poly(ε-caprolactone)-graft-(poly-N-(2-hydroxypropyl) methacrylamide) copolymers (PCL-graft-pHPMA) with tunable amphiphilicity were intended for efficient dual delivery via simultaneous encapsulation of hydrophobic drug, Venetoclax (Bcl-2 inhibitor ABT-199), and pH-sensitive conjugation of other chemotherapeutic, i.e. doxorubicin, to desired sites.[111] Other examples of amphiphilic copolymers as potential candidates for drug delivery are, poly(ε-caprolactone)-graft-poly(N-isopropyl acrylamide) (PCL-*g*-PNIPAAm), poly(ε-caprolactone)-graft-poly(ethylene glycol) methyl ether (PCL-*g*-mPEG), chitosan-graft-poly(N-isopropyl acrylamide (CS-*g*-PNIPAAm), carboxylmethyl chitosan-graft-poly(γ-benzyl- l- glutamate) (*m*-CS-*g*-PBLG)[134], poly(D,L-lactide-co-2-methyl-2-carboxytrimethylene carbonate) (P(LA-*co*-TMCC)-*g*-PEG)[135], (polycaprolactone)-g-(poly glyceryl methacrylate) (PCL-*g*-PDMA).[136]

Injectable hydrogels for biomedical application

Chemical hydrogels typically require an initiator to trigger the chemical reaction, and this may affect the biocompatibility of the hydrogels. Physical hydrogels are advantageous in this respect because no chemical reaction is involved. Among the physical hydrogels, thermosensitive polymer aqueous solutions that are sols at low temperature and become gels at a physiological temperature, are especially attractive.

A delicate balance between hydrophobicity and hydrophilicity is imperative for the temperature-dependent sol–gel transition to occur for polymer aqueous solutions. A too large hydrophilic segment will result in no sol–gel phase transition, and a too large hydrophobic segment will lead to insolubility in aqueous solution at physiologically relevant temperature range.[137] The thermally triggered sol-gel transition of amphiphilic graft copolymers can be tailored to be in the range 25–35°C, making them the ideal cell carrier medium to produce injectable gels undergoing spontaneous physical gelation *in vivo*[129]. Several injectable and thermosensitive hydrogels have been reported included poly(DL-lactic acid-co-glycolic acid)-graft-poly(ethylene glycol) PLGA-*g*-PEG, poly(ε-caprolactone)-graft-poly(ethylene glycol) (PCL-*g*-PEG)[137], poly(ethylene oxide)-poly(propylene oxide)-poly(ethylene oxide)-graft-alginate (PEO-PPO-PEO-*g*-Alg)[138], quaternized alginate-*g*-polytetrahydrofuran (QA-g-PTHF)[139].

Home and personal care products formulations

Polymers are routinely used in many personal care and cosmetic products. The applications take advantage of the various properties of these polymers to impart unique benefits to their formulations[140]. Nowadays, changing trends in the cosmetic market combined with growing awareness of consumers have forced manufacturers to make efforts towards formulating products with high levels of safety-in-use through the selection of skin and environment safe compounds (e.g., alkylpolyglucosides) or the addition of appropriate active substances (e.g., oils, plant extracts).[141] Transdermal delivery of active cosmetic ingredients requires safe and non-toxic means of reaching the target sites without causing any irritation. Many personal care products (for skin, hair, or body care) contain biologically active ingredients such as vitamins and require encapsulation for increased stability of the active materials. As many biologically active substances are not stable and sensitive to temperature, pH, light and oxidation, they require encapsulation to be protected against unwanted degradation and to be released to specific targets.[142] So far, several amphiphilic polymers were identified to achieve the desired loading and release with efficient concentration at a proper time. Odrobińska et al (2019), reported new polymeric systems for delivery in cosmetology applications using self-assembling amphiphilic hydroxyethylmethacrylate (HEMA)-

based and the azido-functionalized PEG graft copolymers [P((HEMA-graft-PEG)-co-MMA)]. The designed amphiphilic graft copolymers P((HEMA-graft-PEG)-co-MMA), showing tendency to micellization in aqueous solution at room temperature, were encapsulated with arbutin (ARB) or vitamin C (VitC) with high efficiencies (>50%). In vitro experiments carried out in the phosphate-buffered saline solution (PBS) at pH 7.4 indicated the maximum release of ARB after at least 20 min and VitC within 10 min. The micellar systems with a short release time (up to 30 min) of the selected antioxidants and skin-lightening agents can be effective in face masks, whereas the other ones delivering bioactive substances over a longer time could be perfect for cream application. PEG graft copolymers seem to be good candidates for potential encapsulation and delivery applications.[143] Odrobińska & Neugebauer (2020), demonstrated that the specific properties of the polymer for encapsulation and delivery can be regulated by a combination of appropriately selected main and side chains polymers as well as their length and degree of grafting. For that reason, the heterograft copolymers of alkyne functionalized 2-hydroxyethyl methacrylate (AlHEMA) and poly(ethylene glycol) methyl ether methacrylate (MPEGMA) with functionalization of poly(ε-caprolactone) (PCL) P(HEMA-graft-PCL)-*co*-MPEGMA), which varied in terms of grafting degree, PEG/PCL side chain ratio and PCL graft length (PCL_{4000} or PCL_{9000}), were designed. All synthesized amphiphilic graft copolymers with varying hydrophilic-hydrophobic balances showed self-assembly ability indicated by critical micelle concentration (CMC) values. The graft copolymers were self-assembled into micellar superstructures with the ability to encapsulate active substances and giving the maximum release levels of active substances after 10–240 min depending on the polymer system.[144]

The encapsulation of poorly water-soluble compounds such as perfumes and fragrances

The high volatility, water-immiscibility, and light/oxygen-sensitivity of most aroma compounds represent a challenge to their incorporation in liquid consumer products. Current encapsulation methods entail the use of petroleum-based materials, initiators, and crosslinkers.[145] Self-assembly processes involving amphiphilic macromolecules provide promising solution for encapsulation of hydrophobic actives.[20] Mamusa et

al. described graft copolymer poly(ethylene glycol)-graft-poly(vinyl acetate) (PEG-*g*-PVAc) as extremely promising candidate for the encapsulation of essential ingredients of fragrance formulation for home care and personal care products. In this study, amphiphilic PEG-*g*-PVAc, due to self-assembly properties, showed ability to successfully encapsulate two fragrances, 2-phenyl ethanol and L-carvone into polymer single-chain nanoparticles. Lower critical solution temperature (LCST) phase behavior, as well as its biodegradable blocks, are additional rock advantages for the use of this polymer as a carrier of hydrophobic compounds like fragrances.[146]

2.2 Biodegradability

2.2.1 General information about biodegradable materials

Since the 1970s biodegradable polymers have undergone extensive investigation. Nowadays, biodegradable materials are used in packaging, agriculture, medicine, hygiene products and other areas. They can be either natural or synthetic and can be derived from either renewable or non-renewable sources. Thanks to their wide-ranging properties, both synthetic and natural polymeric materials perform a vital and ubiquitous role in everyday life. There have been many research achievements in biodegradable and bio-based polymers, such as synthetic polymers based on petroleum, although several bio-based polymers may not be biodegradable.[147,148]

2.2.2 Group of biodegradable materials based on the origin

Synthesized biodegradable polymeric materials (BPMs) have received increasing interest owing to the difficulty in obtaining reproducibility when using natural polymeric materials. Although first introduced in the 1980s, synthetic BPMs have been attracting attention in the last two decades, primarily due to ecological fouling and the realization that our natural resources are finite.[149] Synthetic biodegradable polymers such as poly(lactic acid) (PLA), poly(glycolic acid) (PGA), poly(lactic-*co*-glycolic acid) (PLGA), poly(butylene succinate) (PBA),

polycaprolactone (PCL), poly(ethylene adipate) (PEA), poly(*p*-dioxanone) (PDS), Poly(glycerol sebacate) (PGS), Polyurethanes (PUs), Polyphosphazenes[150] and their copolymers play an imperative role in clinical applications such as nonviral gene delivery vectors, drug-delivery systems, resorbable sutures, biosensors, tissue engineering scaffolds, regenerative medicine including implants, and orthopaedic fixation devices such as pins, rods, and screws.[149,151]

On the other hand, natural polymers, including polysaccharides (starch, alginate, chitosan, hyaluronic acid derivatives) or proteins (soy, collagen, fibrin, gels, silk), and a variety of biofibers , have also been utilized in controlled drug delivery, gene delivery, regenerative medicine, and other biomedical applications.[147,152] Since they are natural materials, they have the advantage of biocompatibility and no toxicity.[153]

2.2.3 Understanding the bio-based and biodegradable terms

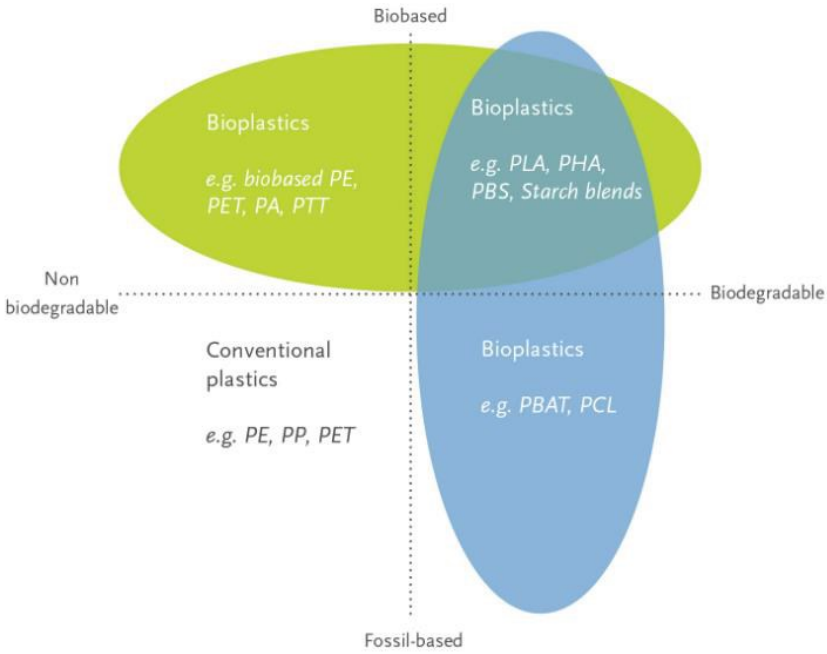

Figure 7. Types of polymers based on their source and their end-of-life options. (European bioplastics, 2020)

The terms biodegradable polymer and biopolymer (or biobased polymers) are sometimes used interchangeably in the literature, but there is a major difference between the two types of polymers.[154] Biodegradable polymers are defined as materials whose chemical and physical characteristics undergo deterioration and

completely degrade when exposed to microorganisms, aerobic, and anaerobic processes.[155]

Biobased is a term focused on the raw materials basis, and it is applied to polymers evolved from renewable sources. Raw materials are defined as renewable if they are replenished by natural procedures at rates comparable or more rapid than their rate of utilization.

Two different criteria underline the definition of a "*biopolymer*": (1) the source of the raw materials, and (2) the biodegradability of the polymer. They can be[156]:

- Biopolymers made from renewable raw materials (biobased), and being biodegradable.
- Biopolymers made from sustainable crude materials (biobased), and not being biodegradable.
- Biopolymers made from fossil fuels and being biodegradable.

2.2.4 Biodegradation mechanism

Biodegradation takes place through the action of enzymes and/or chemical deterioration associated with living organisms. This event occurs in two steps. The first one is the fragmentation of the polymers into lower molecular mass species by means of either abiotic reactions, i.e. oxidation, photodegradation, hydrolysis, or biotic reactions, i.e. degradations by microorganisms into water, carbon dioxide CO_2, and biomass. This is followed by bio-assimilation of the polymer fragments by microorganisms and their mineralisation. Biodegradability depends not only on the origin of the polymer but also on its chemical structure and the environmental degrading conditions.[157,158] In the following phase of biodegradation, the polymeric products of fragmentation are mineralized by microorganisms. This second phase is a necessary step that characterizes this process as biodegradation, because the partially degraded polymers (fragments) are hereby metabolized into end products. The final stage of biodegradation is determined by the mineralization level. Because organic carbon is converted to carbon dioxide in the process of aerobic metabolism, the most widely used method of monitoring this stage is by measuring the amount of carbon dioxide formed in a closed system. To ensure proper results, adequate conditions must

be maintained in the closed system (humidity, temperature, pH, absence of toxic substances) for the existence of the microorganism culture. The method consists of determining the share or amount of carbon in a polymer with known structure and mass. This is followed by precise measurements to establish the amount of carbon that was converted to carbon dioxide during biodegradation. At its core, this process is similar to human metabolism, where food is converted to energy and exhaled as carbon dioxide. Alternatively, biodegradation can also be monitored based on measuring the oxygen consumption (which is converted to carbon dioxide) within the closed system.[159,160]

2.2.5 Factors affecting biodegradation rate

The degradation process of polymers is irreversible; thus, it is important that degradation appears only after they have fulfilled their task. Degradation of polymeric materials can be assessed under specific conditions of temperature, light, dilution, pH, humidity and microbiological environment. There are many factors involved in the process of biodegradation – different combinations of polymer structures, numerous enzymes produced by microorganisms, and variable reaction conditions. In most cases those parameters contribute to weaken the polymeric structure. Indicators of degradation can be determined as a chemical and physical changes of a polymer material, such as changes in molecular weight, chain lengths, chemical structure, brittleness, tensile strength, discoloration and surface structure, depending on the factors causing degradation.[161–165]

2.2.6 Biodegradability assessment techniques

There are several standardized protocols to correctly assess the biodegradation of polymers. The most used procedures are:

- Colour modifications of the polymer surface: estimated by the yellowness index (ASTM D 1925, 1988).

- Tensile tests (strength, elongation at break) are used to investigate mechanical changes during the degradation (ISO 527-3, ASTM D 882, 2002).
- The crystallinity degree: estimated by X-ray diffraction.
- Thermal properties as glass transition, cold crystallisation and/or melting point measured by differential scanning calorimetry (DSC) and thermogravimetric analysis (TGA)
- Molecular weight, chain length of the released polymer fragments: estimated by gel permeation chromatography (GPC) and Size Exclusion Chromatography (SEC)
- Chemical modifications of the polymer structure, roughening of the surface, formation of holes and cracks are regularly revealed by spectroscopic analysis [Fourier transform infra-red (FTIR), fluorescence, nuclear magnetic resonance (NMR)] and spectrometric measurements [mass spectrometry (MS), secondary-ion mass spectrometry (TOF-SIMS)]
- Hydrophilicity of a surface, as well as surface energy: measured by contact angle
- Six methods of OECD test for chemicals decided by the Organisation for Economic Co-operation and Development, permit the screening of chemicals for ready biodegradability in an aerobic aqueous medium.[165–168]

CHAPTER THREE

3. MATERIALS, METHODS, AND INSTRUMENTATION

3.1 Materials

All materials were used without further purification.

3.1.1 Backbone

Polyethylene glycol, PEG Mw 6000 (Gamma Chimica) (**Fig.8**).

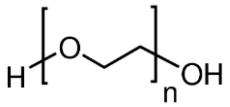

Figure 8. Polyethylene glycol, PEG.

3.1.2 Monomers

Vinyl acetate, VAc (TCI, 98%) and N-Vinyl caprolactam, VCL (Aldrich, ≥90%) (**Fig.9**).

Figure 9. N-Vinyl caprolactam, VCL (left) and Vinyl acetate, VAc (right).

3.1.3 Initiator

Tert-Butylperoxy 2-Ethylhexyl carbonate, Luperox TBEC (Aldrich, 95%), was used as initiator for polymerization of VCL and VAc without further purification. Structure of Luperox TBEC is shown in **Figure 10**.

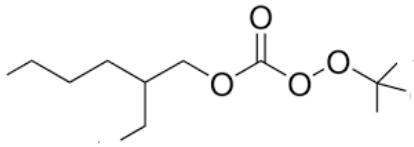

Figure 10. Initiator Tert-Butylperoxy 2-Ethylhexyl carbonate, Luperox TBEC.

3.1.4 Solvents

Ethyl Acetate (Aldrich, anhydrous, 99.8%), deionized water, Hexane (VWR, ≥95%), Chloroform (Aldrich, ≥99.8%) were all reagent grades.

3.1.5 Fluorescence dye for copolymer labelling

Rhodamine-B isothiocyanate (mixed isomers, Sigma-Aldrich, MW 536.08 g mol^{-1}), (**Fig.11**).

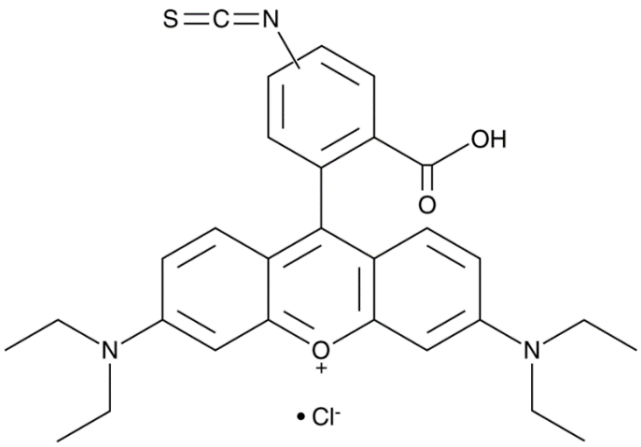

Figure 11. Structure of Rhodamine-B isothiocyanate (mixed isomers).

3.1.6 Structural reference

Soluplus is a (PEG-*g*-(PVAc-*co*-PVCL)) BASF product (**Fig. 12**). The polymer is characterized by a PEG/PVAc/PVCL weight ratio of 13/34/53, range of molecular weight 90 – 140 kDa, (**Fig. 12**).[169]

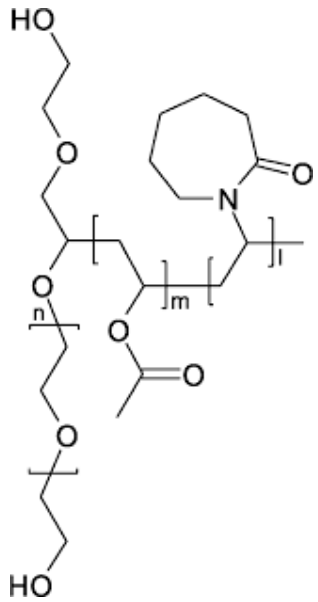

Figure 12. Structure of Soluplus (PEG-*g*-(PVAc-*co*-PVCL)), BASF product.

3.1.7 Single fragrance molecules

Methyl anthranilate (Sigma Aldrich, ≥ 98%, M_w = 151.17 g mol^{-1}); L-carvone (Sigma-Aldrich, ≥ 97%, (FCC, FG), M_W 150.22 g mol^{-1}), (**Fig 13**).

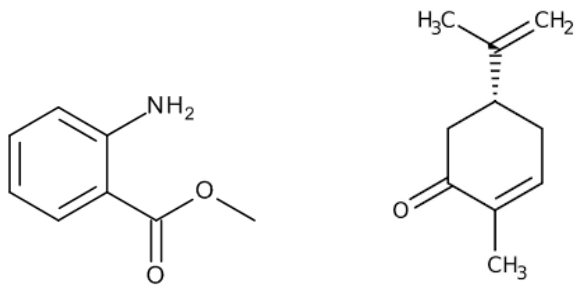

Figure 13. Structure of Methyl anthranilate (left) and L-carvone (right).

3.1.8 Microencapsulation matrix

Simplified liquid fabric enhancer (SLFE) matrix (Procter&Gamble company). The SLFE matrix was used as it is. SLFE matrix is composed of 92.9% water, 7% cationic

surfactant (mixture of distearoylethyl/dipalmitoylethyl dimonium chloride) and <0.1% other minor additives (e.g. hydrochloric acid and formic acid).

3.2 Synthesis method

3.2.1 Synthetic procedure

Amphiphilic PEG-g-(PVAc-co-PVCL) S2 (S2A, S2B), S3, S6 and PEG-g-PVCL S1, S4 graft copolymers were synthesized by free radical polymerization method, using Luperox TBEC as initiator. The polymerization was carried out under nitrogen atmosphere in a cylinder reactor equipped with a mechanical stirrer, a reflux condenser and two dropping funnels. The cylinder reactor was heated in an oil bath with an automatic temperature control system. The amounts of each reagent add to obtain different copolymers are summarized in **Table 2** (S1), **Table 3** (S2), **Table 4** (S3), **Table 5** (S4) and **Table 6** (S6). The reactor was preheated at the targeted temperature performing three nitrogen N_2-charging/vacuuming cycles. PEG was added under nitrogen atmosphere, melted at 85°C and then cooled to reaction temperature, 77°C. When the system has reached the right temperature, initial charge of VAc and initiator were added. The mixtures were stirred for 15 min at 77°C. The feed 1, over the course of 3 hours, and the feed 2, over the course of 3.5 h, were metered into the reactor simultaneously, maintaining a constant flow rate (**Fig. 14**).[170–173] Then, the reaction mixture was stirred at the reaction temperature, 77°C for 67 hours for copolymers S1, S2, S3, S6 and for 20 hours for copolymer S4.

The reaction procedures are depicted in scheme 4 and scheme 5 and example of the final product architecture in **Figure 15.**

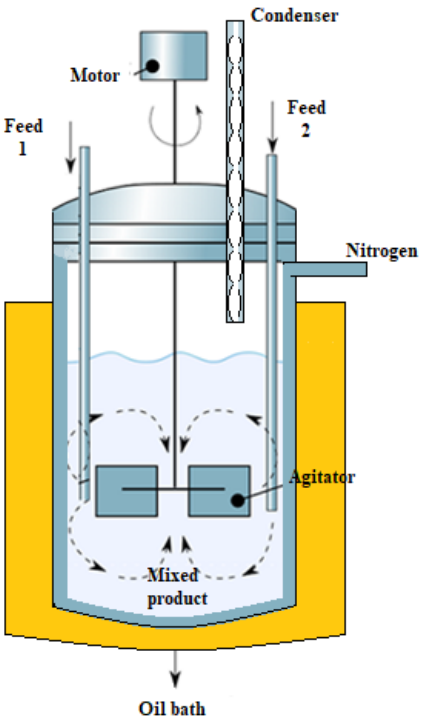

Figure 14. Reaction reactor.

Table 2. Synthesis procedure of the PEG-g-PVCL; (S1) copolymer.

	Synthesis composition by weight
Initial charge	10 g of PEG 6000 2 g of vinyl acetate 1.1 g of feed 2
Feed 1	50 g of vinyl caprolactam 37.5 g of vinyl acetate 10 g of ethyl acetate
Feed 2	tert-Butylperoxy 2-ethylhexyl carbonate 10 g of ethyl acetate

Table 3. Synthesis procedure of the PEG-g-(PVAc-co-PVCL); (S2) copolymer.

	Synthesis composition by weight

Initial charge	10 g of PEG 6000 2 g of vinyl acetate 1.1 g of feed 2
Feed 1	50 g of vinyl caprolactam 37.5 g of vinyl acetate 10 g of ethyl acetate
Feed 2	tert-Butylperoxy 2-ethylhexyl carbonate 10 g of ethyl acetate

Table 4. Synthesis procedure of the PEG-g-(PVAc-co-PVCL); (S3) copolymer.

	Synthesis composition by weight
Initial charge	10 g of PEG 6000 2 g of vinyl acetate 1.1 g of feed 2
Feed 1	50 g of vinyl caprolactam 37.5 g of vinyl acetate 10 g of ethyl acetate
Feed 2	tert-Butylperoxy 2-ethylhexyl carbonate 10 g of ethyl acetate

Table 5. Synthesis procedure of the PEG-g-PVCL; (S4) copolymer.

	Synthesis composition by weight
Initial charge	10 g of PEG 6000 2 g of vinyl acetate 1.1 g of feed 2
Feed 1	50 g of vinyl caprolactam 37.5 g of vinyl acetate 10 g of ethyl acetate
Feed 2	tert-Butylperoxy 2-ethylhexyl carbonate

	10 g of ethyl acetate

Table 6. Synthesis procedure of the PEG-g-(PVAc-co-PVCL); (S6) copolymer.

	Synthesis composition by weight
Initial charge	10 g of PEG 20000 2 g of vinyl acetate 1.1 g of feed 2
Feed 1	50 g of vinyl caprolactam 37.5 g of vinyl acetate 10 g of ethyl acetate
Feed 2	tert-Butylperoxy 2-ethylhexyl carbonate 10 g of ethyl acetate

Scheme 4 and **Scheme 5** show the synthetic route to the PEG-g-(PVAc-co-PVCL) S2 (S2A, S2B), S3, S6 and PEG-g-PVCL S1, S4 graft copolymers by the successive addition of free radical building blocks.

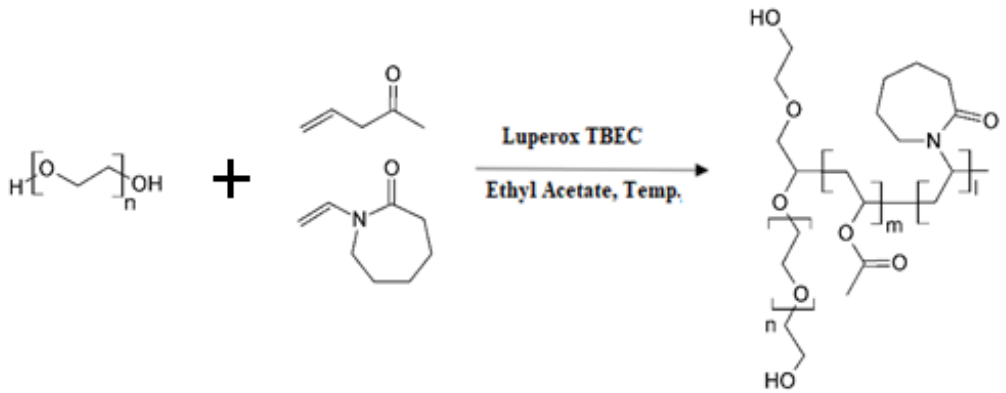

Scheme 4. Synthetic Route to PEG-g-(PVAc-*co*-PVCL); (S2); (S3); (S6) amphiphilic graft copolymer via Free Radical Polymerization.

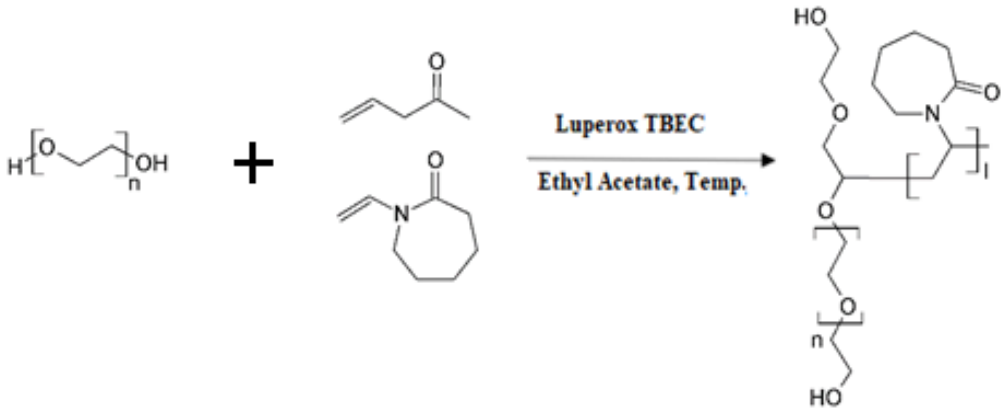

Scheme 5. Synthetic Route to PEG-g-PVCL; (S1); (S4) amphiphilic graft copolymer via Free Radical Polymerization.

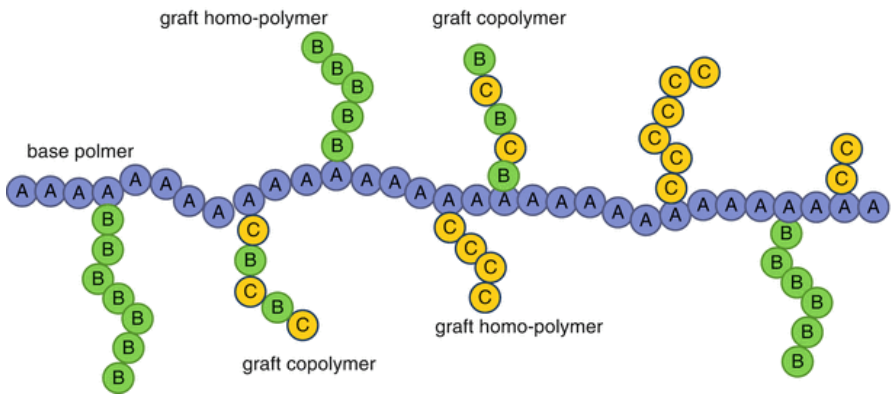

Figure 15. An example of the final architecture of synthetized PEG-g-(PVAc-*co*-PVCL) copolymers (Tauqir A. Sherazi, Graft Polymerization).

3.2.2 Purification of S1 (PEG_{6000}-PVCL), S2 (PEG_{6000}-PVAc-PVCL), S3 (PEG_{6000}-PVAc-PVCL), S4 (PEG_{1000}-PVCL), S6 (PEG_{20000}-PVCL) graft(ss)- copolymers

The polymerization was stopped by cooling the reactor for several hours. Then, the reaction mixture was vacuum distilled at 90 °C for 15 minutes, to remove volatile residuals of Vinyl acetate monomer. Obtained copolymers were washed with 250 mL of deionized water, freeze-dried and lyophilized to remove water content. The copolymers were purified by dissolving them (1g/5mL) in chloroform and

precipitating into hexane. The treatment was repeated for three times. After that, each pure copolymer was filtrated, dried to a constant weight, dried under a vacuum, and ground into a powder.[174] In order to check the purification process, 0.5 % solution of the copolymer S2 in water was subject to ultrafiltration using a cellulose membrane with a cut off of 30000 Da (**Fig. 16**). The water level was constantly topped up and the eluent was regularly collected. The control parameter in this process was the absorbance level which was measured by UV-Vis spectrophotometer in each collected 50 mL of filtrate that passed through the membrane (**APPENDIX A-C**). The microfiltration was terminated when the absorption level of the collected eluent had dropped and was close to zero. This treatment allowed to isolate low molecular weight components present in copolymer structure and thus decreased polydispersity and improved homogeneity of polymer. To further check the purity of copolymers, ^{1}H-NMR spectra were recorded before and after the ultrafiltration. Finally, the microscopic analysis (**APPENDIX D**) of the polymer solution before and after the ultrafiltration treatment showed no difference in capsule forming capacity. Infrared (FTIR) spectra of ultrafiltrated solution and copolymer S2 before treatment were compared (**APPENDIX E**).

Figure 16. Ultrafiltration equipment connected with collective batch.

3.3 S1 (PEG_{6000} -PVCL), S2 (PEG_{6000} -PVAc-PVCL), S3 (PEG_{6000} -PVAc-PVCL), S4 (PEG_{1000} -PVCL), S6 (PEG $_{20000}$ -PVCL) graft(ss)- copolymers and Soluplus® labelling procedure

Fluorescent labelling is the process of covalently binding fluorescent dyes to a substance so that it can be visualized by fluorescence imaging. Fluorescent labelling also allows to visualize copolymer microcapsules in water and commercial formulation. The involved chemistry should be efficient and should not require harsh conditions (high temperature, presence of strong acids or bases) that could be detrimental to the fluorophore itself but could also lead to partial destruction of the polymer.[175] To a solution of the selected copolymer S1, S2, S3, S4, S6 and Soluplus® in dry Tetrahydrofuran (around 50 mg/mL), under ultra-dry atmosphere, rhodamine-b-isothiocyante, around 0.15 equivalents with respect to PEG chains is added to reaction flask (**Scheme 6**). When complete dissolution occurs, the mixture is heated up to 40 °C and stirred for four days. The solvent was then removed under vacuum affording the desired pink/violet material (**Fig. 17**). No free rhodamine should be present with these conditions. The presence of free rhodamine was tested through thin-layer chromatography (TLC) using TLC Silica gel 60 F_{254}.

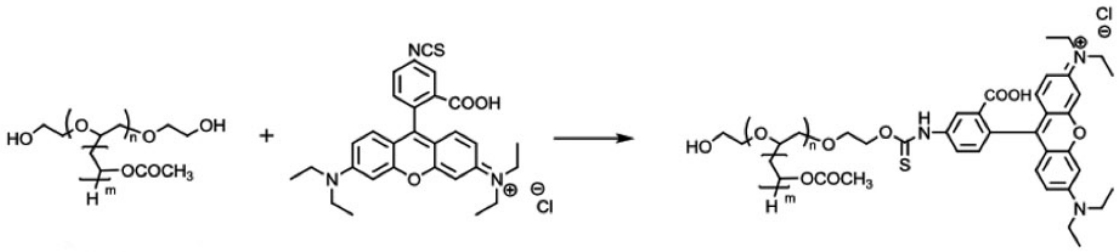

Scheme 6. Labeling procedure of copolymer S1, S2, S3, S4, S6 and Soluplus® with rhodamine B isothiocyanate.

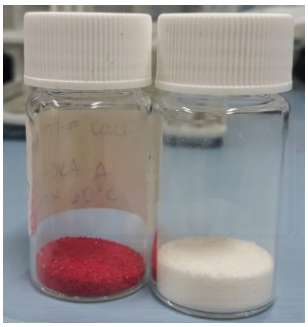

Figure 17. Copolymer S2 labelled with rhodamine B isothiocyanate (left) and copolymer S2 before labelling procedure.

3.4 Synthesis procedure of self-assembly microcapsules of S1 (PEG_{6000} -PVCL), S2 (PEG_{6000} -PVAc-PVCL), S3 (PEG_{6000} -PVAc-PVCL), S4 (PEG_{1000} -PVCL), S6 (PEG $_{20000}$ -PVCL) graft(ss)- copolymers and Soluplus®.

For the preparation of samples containing selected single components of perfume composition (PRMs) or total perfume, 50 mg of each copolymer were mixed with 900 mg of water and 900 mg of SLFE (water solution of cationic surfactant) and then vortexed for few seconds until fully dissolved. Following, 50 mg of one of the PRMs (L-Carvone, Methyl anthranilate) or perfume BZ were added, and the solution was vortexed for few seconds until homogenisation. The samples were stored at 25 °C in an incubator, in sealed vials.

3.5 Characterization methods of synthetized copolymers and supramolecular self-assembly microcapsules.

3.5.1 Fourier transform infrared spectroscopy (FTIR)

All the samples were analyzed by FTIR using a Nicolet IS50 FTIR spectrophotometer (Thermo Nicolet Corp., Madison, WI), equipped with single-reflection germanium ATR crystal (Pike Technologies) and a deuterated-triglycine sulfate (DTGS) detector. For all the samples, a drop of the sample was spread onto the germanium ATR crystal

cell covering the whole crystal surface. Typically, 64 scans at a resolution of 4 cm^{-1} in the range of 4000-800 cm^{-1} were recorded. The frequency scale was internally calibrated with a helium-neon reference laser to an accuracy of 0.01 cm^{-1}. OMNIC software (OMNIC software system Version 9.8 Thermo Nicolet) was used for spectra manipulation.

3.5.2 Nuclear magnetic resonance spectroscopy (NMR)

^{1}H-NMR and 2D-NMR spectra were recorded using a multinuclear Bruker AVANCHE spectrometer operating at the frequency of 400 MHz, at 25°C. Experiments were carried out in DCL3-d6 using the peaks of the residual solvent protons as internal reference. The ^{1}H-NMR spectrum of the synthetized copolymers was compared with the reference spectrum of a structurally related commercial polymer, Soluplus®.

3.5.3 Diffusion ordered spectroscopy (DOSY)

Samples of 20 mg of copolymer S1, S2A, S2B, S3, S4, S6 and Soluplus® in deuterated chloroform were prepared for analysis. All DOSY experiments were performed using the bipolar pulse longitudinal eddy current delay pulse sequence (BPPLED). Typically, a value of 1 ms was used for the gradient puls length (20 ms for the diffusion delay (A), and the gradient power (g) was 128.12 G/cm. Each parameter was chosen to obtain ∼95% signal attenuation for the slowest diffusion species at the last step experiment. Data acquisition and analysis were performed using NMR Machine: 400MHz AVANCE III, BBO Diffusion Probe.

3.5.4 Gel Permeation Chromatography (GPC)

Gel Permeation Chromatography (GPC) is a commonly used method for separation and determination of molecular weight distribution of a polymer. Recent technological advancements have allowed the coupling of GPC systems with multiangle light scattering (MALS) detectors to form a powerful platform capable of determining the

absolute molecular weights. First, the method eliminates assumptions and the use of reference standards, and second, it measures the concentration of the polymer solution using either an on-line UV absorption detector or a differential refractive index (dRI) detector. Using multiangle detection enables detailed statements on physicochemical properties of the dissolved polymer, such as shape in solution, cross-linking, branching, and substitution effects. Refractive index (RI) detectors are generally used for determining the concentration of the employed analyte. An additional UV signal can be used, for example, to detect UV or fluorescence residual or chromophores in material or to monitor UV- or fluorescence-active derivative or labels.[176] Samples were analyzed in term of estimation of average molecular weight, number average molecular weight, and polydispersity to determine compositional differences in various modification of synthetized copolymers. GPC was performed on Agilent HPLC-Wyatt MALS/RI equipment, equipped with a series of two PLgel Mixed C columns (5um particle size), each column 300 x 7.5mm Agilent part# PL1110-6500. The columns were eluted with THF and calibrated using dn/dc value = 0.101 mL/g determined for Soluplus®. A 30 kDa Polystyrene standard was used as a GPC system check. THF was used as the mobile phase at flow rate of 1 mL/min at 40 ^{o}C for both measurements and calibration. Samples of copolymer S1, S2, S3, S4, S6, Soluplus® and PEG 6000 were weighed (~50 mg) in a vial and THF with 12 mM TBAB added to each vial to get a concentration of approximately 5 mg/mL. Samples were filtered through a 0.8 um Vesapor syringe filter into a clean injection vial. Equal volumes (100 uL) of each sample were then injected on to the GPC-MALS for analysis.

3.5.5 Matrix-assisted laser desorption/ionization-time of flight (MALDI-TOF) mass spectrometry (MS).

Samples were weighed and dissolved in water (1%). Each sample was passed through pre-rinsed with water 10KDa MWCO filters (regenerated cellulose membrane filter, 15ml tube). Filtrate was analyzed by MALDI-TOF-MS. Each water filtrate was mixed 1:1 w/ CHCA Matrix (10mg/mL in 80%ACN/H2O/0.1%TFA), 0.6µl of each sample were spotted onto the MALDI plate for analysis using AB-Sciex MALDI-TOF/TOF.

3.5.6 Differential scanning calorimetry (DSC)

To understand the stability mechanism, DSC tests were performed on starting components, synthetized copolymers and Soluplus® used as a reference.A DSC Q1000 (TA Instruments Leatherhead, United Kingdom) was used to investigate the thermal transitions of the copolymer. The DSC measurements were carried out at the temperature range of -90°C to 150°C at the heating rate of 10°C/min under a nitrogen atmosphere (50 mL/min). The melting point was reported as the temperature of the midpoint of the heat capacity change determined from the baseline tangents Omni.

3.5.7 Thermogravimetric analysis (TGA)

TGA experiment was aimed at quantifying the total water content in the selected synthetized copolymers and Soluplus®. The thermal stability of the graft copolymers was examined using SDT-Q600 (TA Instruments Leatherhead, United Kingdom). Briefly, 10-15 mg of sample were placed on platinum pans before equilibrating at 30° C. The temperature was then ramped to 900 ° C at 10 ° C / min. All TGA measurements was done under a nitrogen atmosphere (100mL/min.).

3.5.8 Thermo-responsive properties - cloud point temperature study (C_{TP})

The cloud point of the aqueous polymer was measured by visual observation of the cloudiness of copolymer solution in water in response to the temperature. For this study 1% solution of the selected copolymer in water was prepared and placed in the transparent glass vessel immersed in an ice bath, slowly heated on a magnetic plate equipped with the automatic temperature controller. The copolymer sample was stirred at 300 rpm. The bath temperature was increased at a rate of 1° C per 2 minutes and the polymer solution clarity was observing. The temperature at which the solution of copolymer changed from transparent to turbid was considered as a cloud point.

3.5.9 Optical and fluorescence Electron Microscopy

Optical and fluorescence electron microscopy has been used to directly visualize the formation of microcapsule structures by synthetized graft copolymers and commercial

Soluplus® and to test them as possible microcarriers for fragrance molecules in water-based matrices. The formed microparticles of copolymer's solutions in water and SLFE with selected PRM (L-Carvone or Methyl anthranilate) or Perfume BZ prepared according to the procedure described in Chapter II 3.4 were observed using a Zeiss Axio Imager A1 upright microscope (Zeiss Ltd., Germany) equipped with an Axiocam 305 color camera. All observations were carried out with objective magnification ×40 at 25° C. The excitation wavelength for the rhodamine-b labelled copolymers was around 560 (± 40) nm, and the emission wavelength was around 640 (± 75) nm using a Zeiss 45 Filter Set. For tracking of methyl anthranilate, the Zeiss Filter Set 02 has been used, with excitation wavelength around 300-400 nm, and a long-pass emission filter of 420 nm. For image acquisition, the software AxioVision SE64 has been used. This allows for direct visual inspection of the formed microcapsules their morphologies control. Microscopy analysis confirms also the real existence, including shape, size of different types of copolymers-based micromolecular aggregates and encapsulation of fragrance or particular fragrance molecules.

3.6 OECD 301B biodegradability carbon dioxide evolution test

For three, selected synthetized copolymers S2A, S2C, S4 the standardized OECD 301B biodegradability test approach was applied. In this test method, the amount of CO_2 produced over time (captured and quantified using a sodium hydroxide trap) is expressed as a percentage of the theoretical maximum based on the total organic carbon analysis of the sample and is monitored as a measure of biodegradation.[177]

3.6.1 Description of the standard methodology of the laboratory

Biodegradability of organic compounds by micro-organisms in an aquatic medium is determined using a static test system. The test blend contains an inorganic medium, the organic compound as the only nominal source of carbon and energy with a theoretical content of 10 to 20 mg/L in carbon, and a mixed inoculation from an urban wastewater treatment plant (amount of suspended matter inferior to 30 mg/L in the final blend). The blend is stirred in test vessels exposed to a CO_2-free air flow for about

28 days at temperature of 22°C +/- 2°C (the test length can be increased for two weeks if the degradation has evidently started but has not yet reached a plateau). CO_2 created during the microbial degradation is trapped in external vessels containing a solution of barium hydroxide and measured by titrimetric determination. Released CO_2 is compared to the theoretical released quantity (CO_2Th) and given in percentage. The test normally lasts 28 days but can be extended if the biodegradation curve does not reach a plateau on the 28th day. In this study test has been extended to 60 days.

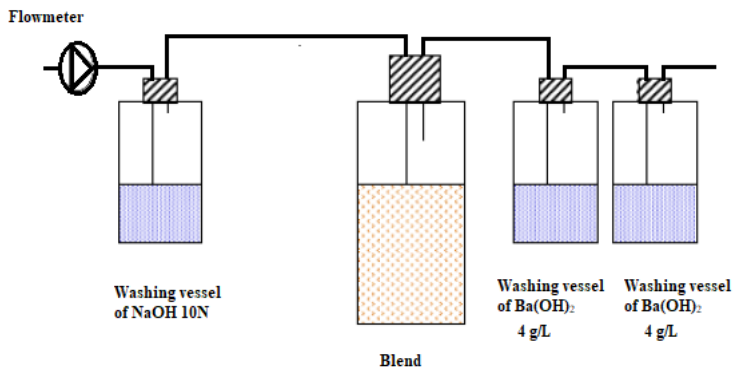

Figure 18. OECD 301b experimental design scheme (EUROFINS Ecotoxicologie France).

The captured CO_2 is determined in the first vessel containing the barium hydroxide solution close to the blend test. The remaining vessel is shifted instead and replaced by a vessel containing a freshly prepared barium hydroxide solution. The volume of barium hydroxide in the vessels varies from 250 to 300 mL, depending on the effective interval time between two measures. The degradation rate at a given time is determined using the following equation:

$$\%\ Degradation = \frac{CO_2\ \text{cumulated}\ (mg/xmL)}{CO_2Th\ (mg/xmL)}\ x\ 100$$

Equation 1. The degradation rate.

CO_2Th is theoretical carbon dioxide. Quantity of carbon dioxide of the test sample calculated from the known or measured organic compound content, which should be released during its complete mineralization. The CO_2Th in mg is calculated using the following equation[178] :

$$CO_2Th = \frac{44}{12} x V_L x \rho c$$

Equation 2. CO_2Th, theoretical carbon dioxide.

where,

- 44 and 12 are respectively the CO_2 relative molecular mass and the carbon atomic weight, intended to calculate the quantity of CO_2 from the test product organic carbon.
- V_L is the volume of the test solution contained on the test vessel, in litres.
- *P*c is the organic carbon concentration of the product analyzed in the test vessel in mg/L. The CO_2Th can also be expressed in mg/mg of substance.

3.6.2 Definitions

Lag phase: period between the sowing moment and the moment when the percentage of degradation has reached around 10 %.

Degradation period: period which begins at the end of the lag phase and ends when 90% of the degradation maximal rate is reached.

10-days window: 10 days which directly follow the moment when the biodegradation rate has reached 10 %.

Readily biodegradable: a product is considered as readily biodegradable if the biodegradation rate has reached at least 60% in the 10-day interval which has to fall within the 28 (first) days of the test.

Readily biodegradable without respecting the 10-day interval: a product is considered as readily biodegradable without respecting the 10-day interval if the biodegradation rate has at least reached 60% within the 28 (first) days of the test without having reached that limit in the 10-day interval.[179]

CHAPTER FOUR
4. RESULTS AND DISCUSSION

The data relevant to synthesis and characterization of amphiphilic graft copolymers, as well as the characterization of membranes were presented with a detailed discussion in this part.

4.1 Synthesis of PEG-g-(PVAc-*co*-PVCL) and PEG-g-PVCL graft copolymers

4.1.1 Morphological observation of PEG-g-(PVAc-*co*-PVCL) and PEG-g-PVCL graft copolymers

PEG based graft copolymers were synthesized via Free radical polymerization using the 'grafting from' method, which has been widely used to obtain various industrial graft copolymers of PEG, such poly(ethylene glycol)-graft-poly(vinyl alcohol), PEG-g-PVA (Kollicoat® IR) comprised of 25% PEG and 75% PVA, and poly(ethylene glycol)-graft-poly(vinyl acetate)-poly(vinyl caprolactam), PEG-g-(PVA-co-PVCL) (Soluplus®) comprised of 13% PEG, 30% PVA and 57% PVCL. Obviously, this polymerization progressed at the vinyl group of N-VCL and/or of VAc monomers. The obtained copolymers were a white/yellowish powder soluble in both water and organic solvents, resulting from its amphiphilic character. As shown in **Figure 1**, the appearance of synthetized copolymers differed from each other due to the change in conformation of molecules and composition.

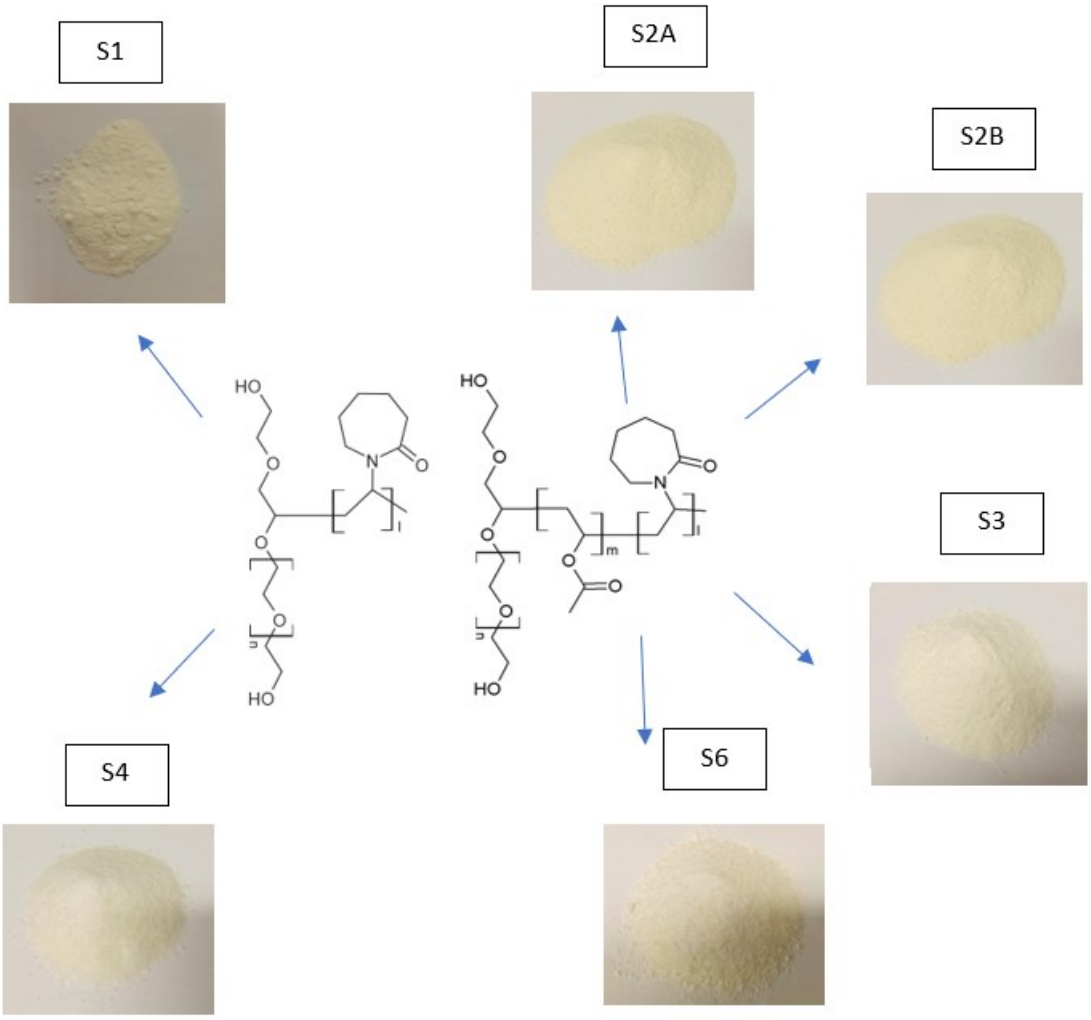

Figure 19. Morphology of synthetized copolymers S1, S2A, S2B, S3, S4, S6.

4.2 Chemical structure and characteristics of PEG-g-(PVAc-*co*-PVCL) and PEG-g-PVCL graft copolymers.

4.2.1 FTIR investigation

The structure of the PEG-g-PVCL and PEG-g-(PVAc-*co*-PVCL) graft copolymers and the absence of impurities were confirmed with FTIR. Infrared spectroscopy is crucial method to elucidate the structure of matter at the molecular scale. The chemical composition and the bonding arrangement of constituents in a homopolymer, copolymer, polymer composite and polymeric materials can be obtained using

Infrared (IR) spectroscopy. The infrared spectra of synthetized copolymer S1, S2A, S2B, S3, S4, S6 and Soluplus® are shown in **Fig. 21-26**. Additional, to confirm structural changes of the obtained copolymers, FTIR analysis was also performed on PEG, VCL and Vac components used into synthesis reaction. Their spectra are presented in **Fig. 20**. Synthetized copolymers were identified by major vibration bands associated with functional groups of all components of the resulting copolymer and compared with Soluplus®. The band assignments are tabulated in **Table 7**. The FT-IR spectrum of samples, as demonstrated in **Figs. 21-26,** showed the characteristic absorptions of PEG, PVCL and/or PVAc domains. In the IR spectrum of components **(Fig. 20),** a characteristic Amide I carbonyl peak C=O of VCL monomer was at 1624 cm^{-1}, and O-C(O)-CH3 stretching vibration characteristic for VAc at 1777 cm^{-1}, 1372 cm^{-1}. The peak for the C=C was observed at 1654 cm^{-1}in VCL and at 1790 cm^{-1}, 1761 cm^{-1} in VAc. The peaks at 2932 cm^{-1}, 2851 cm^{-1}, 2924 cm-1, 2851 cm^{-1}, 2885 cm^{-1} correspond to the aliphatic C-H stretching of VCL, VAc and PEG. The $-CH_2-$ peak was detected at 1452 cm^{-1} in VCL, at 2878 cm^{-1}, 962 cm^{-1}, 843 cm^{-1} in PEG and at 720 cm^{-1} in VAc. The characteristic vinyl peaks, (=CH and =CH2) were located at 3110 cm^{-1} and 933 cm^{-1} in VCL and at 3110 cm^{-1}. The characteristic -C-O-C=(O) stretching vibration of VAc falls at 1294 cm^{-1}, 1020 cm^{-1}. The peak of C-N stretching vibration was observed at 1486 cm^{-1} and 1186 cm^{-1}. Furthermore, the peak at 3274 cm^{-1} was assigned to N-H stretching vibration of VCL. Peaks of $-O-CH_2CH_2$ observed at 1100 cm^{-1} and O-H at 3466 cm^{-1}, 1284 cm^{-1}, 1242 cm^{-1} correspond to PEG.

From **Figures 23-26** it can be observed typical absorption bands corresponding to the polyvinyl acetate block (C=O stretching vibration at 1734 cm^{-1}, 1370 cm-1 in S2A/S2B 1734 cm^{-1}, 1370 cm^{-1} in S3, 1736 cm^{-1} in S6 and 1734 cm^{-1}, 1372 cm^{-1} in Soluplus® 1734 cm^{-1} ,-C-O-C=(O) stretching vibration at 1241 cm^{-1}, 1026 cm^{-1} in S2A/S2B, 1241 cm^{-1},1030 cm^{-1} in S3, 1241 cm^{-1} in S6 and 1240 cm^{-1}, 1024 cm^{-1} in Soluplus®). Those signals were not detected in the spectra of PEG-g-PVCL copolymers (**Figs. 21-22)**. In all of the presented spectra (**Figs. 21-26)** polyvinyl caprolactam absorption bands are identified (C= O stretching, Amide I band at 1617 cm^{-1} in S1, 1632 cm^{-1} in S4, 1633 cm^{-1} in S2A/S2B, 1631 cm^{-1} in S3, 1635 cm^{-1} in S6 and 1633 cm^{-1} in Soluplus®, C-N stretching vibration at 1480 cm^{-1}, 1198 cm^{-1} in S1, 1477 cm^{-1}, 1196 cm-1 in S4, 1477 cm^{-1}, 1196 cm^{-1} in S2A/S2B, S3, S6, Soluplus® and aliphatic C-H stretching peaks located at 2921 cm^{-1} in S1, 2926 cm^{-1} in S4, 2932 cm-

^{1} in S2A/S2B, 2932 cm^{-1} in S3, 2921 cm^{-1} in S6, 2926 cm^{-1} in Soluplus®. Besides, C-H stretching absorption at 2856 cm^{-1} in S1, S4, S2A/S2B, S3, S6, Soluplus®,[180–185] –OCH_2CH_2 unit at 1101 cm^{-1} in S2A/S2B, 1101 cm^{-1} in S3, 1110 cm^{-1} in S6, 1103 cm^{-1} in Soluplus® and C–O–C stretching at 1065 cm^{-1} and and O-H stretching band at 3466 cm^{-1} prove the existence of PEG.[186–190]

Confirmation of the successful polymerization of synthetized PEG-g-PVCL and PEG-g-(PVAc-co-PVCL) graft copolymer was fact that the peak of double bond observed in the spectrum of VCL monomer at 1654 cm^{-1},1624 cm^{-1}, and VAc monomer at 1790 cm^{-1}, 1777 cm^{-1}, the vinyl peaks, (CH and CH2) located in the spectrum of VCL monomer at 3110 cm^{-1} and 993 cm^{-1} and in VAc monomer at 3110 cm^{-1}, disappeared in the spectrum of synthetized copolymer (**Figs. 21-26**), (**Tables 7-8**).[190] The polymerization was achieved without any change in the caprolactam ring (**Figs. 21-26**). Copolymers S2A and S2B spectra (**Fig. 23**) maintained the same absorption pattern and band intensity, confirming reproducibility of the polymer. The most similar spectra to Soluplus® are spectra of copolymers S2A and S2B. All peaks detected in copolymer S2 were present in Soluplus®, although there was increase of C=O signal strength at 1734 cm^{-1} and 1240 cm^{-1} in the Soluplus® system compared to the copolymer S2, what can be attributed to greater content of grafted PVAc unit. These data only confirm the successful polymerization and the presence of all components in copolymer structure, but whether it is a mixture, or a graft remains unanswered.

Table 7. FTIR wavenumbers (cm^{-1}) characteristic for components, PEG. Vac, VCL and copolymer S1 and S4.

Functional group	PEG	VAc	VCL	S1	S4
O-H	3466, 1284, 1242	-	-	3447	3463
C-H	2885	2924, 2851	2932, 2851	2921,2856	2926,2856
=CH, =CH_2	-	3110	3110, 933	-	-
C=C	-	1790, 1761	1654	-	-

O-C(O)-CH3	-	1777, 1372	-	-	-
C(O)N	-	-	1624, 1394	1617	1632
C-N	-	-	1486, 1186	1480, 1198	1477, 1196
CH_2	2878, 962, 843	720 [12]	1452	1444, 964,843	1441,973
-C-O-C=(O)	-	1294, 1020	-	1241	1242
-O-CH_2CH_2	1100	-	-	1112	1113

Table 8. FTIR wavenumbers (cm^{-1}) characteristic for copolymer S2A, S2B, S3, S6 and Soluplus®.

Functional group	S2A/S2B	S3	S6	Soluplus®
O-H	3466	3440	3455	3458
C-H	2932,2856	2932,2856	2921,2856	2926, 2856
=CH, =CH_2	-	-	-	-
C=C	-	-	-	-
O-C(O)-CH3	1734, 1370	1734, 1370	1736	1734, 1372
C(O)N	1633	1631	1635	1633
C-N	1477, 1196	1477, 1196	1477, 1196	1477, 1196
CH_2	1441	1442	1442	1441
-C-O-C=(O)	1241,1026	1241,1030	1241	1240, 1024
-O-CH_2CH_2	1101	1101	1110	1103

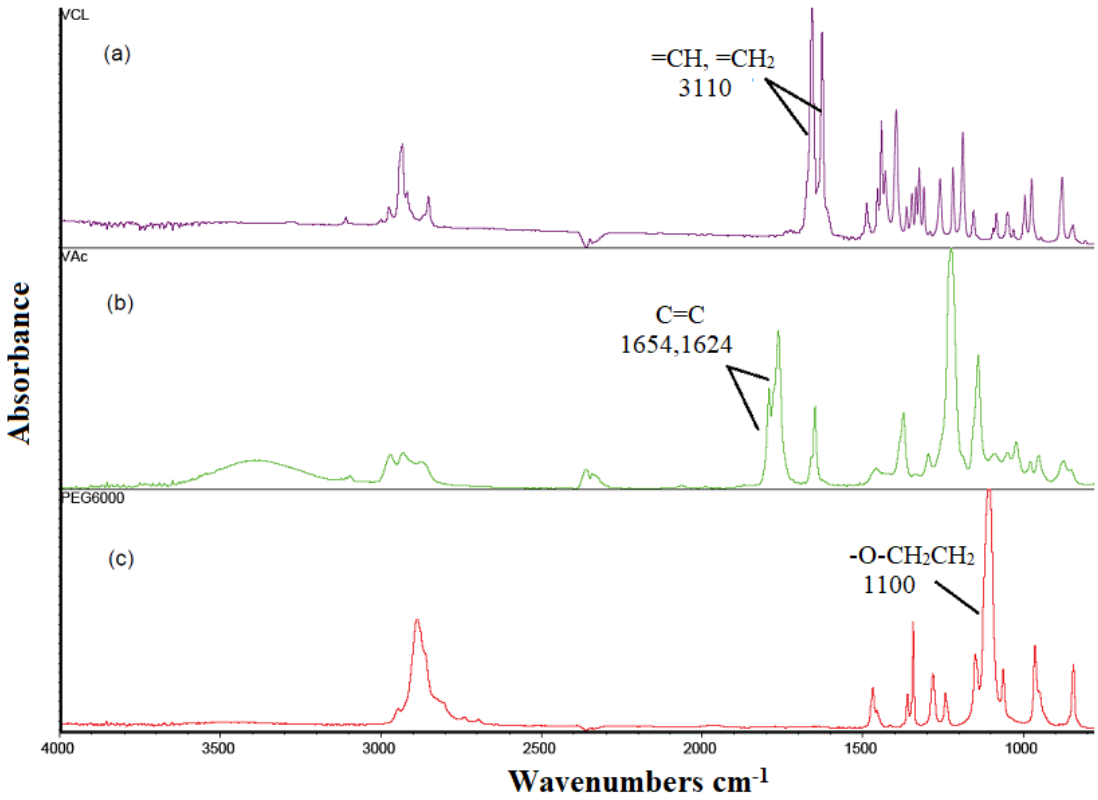

Figure 20. FTIR spectra of (**a**) VCL, (**b**) VAc, and (**c**) PEG-6000.

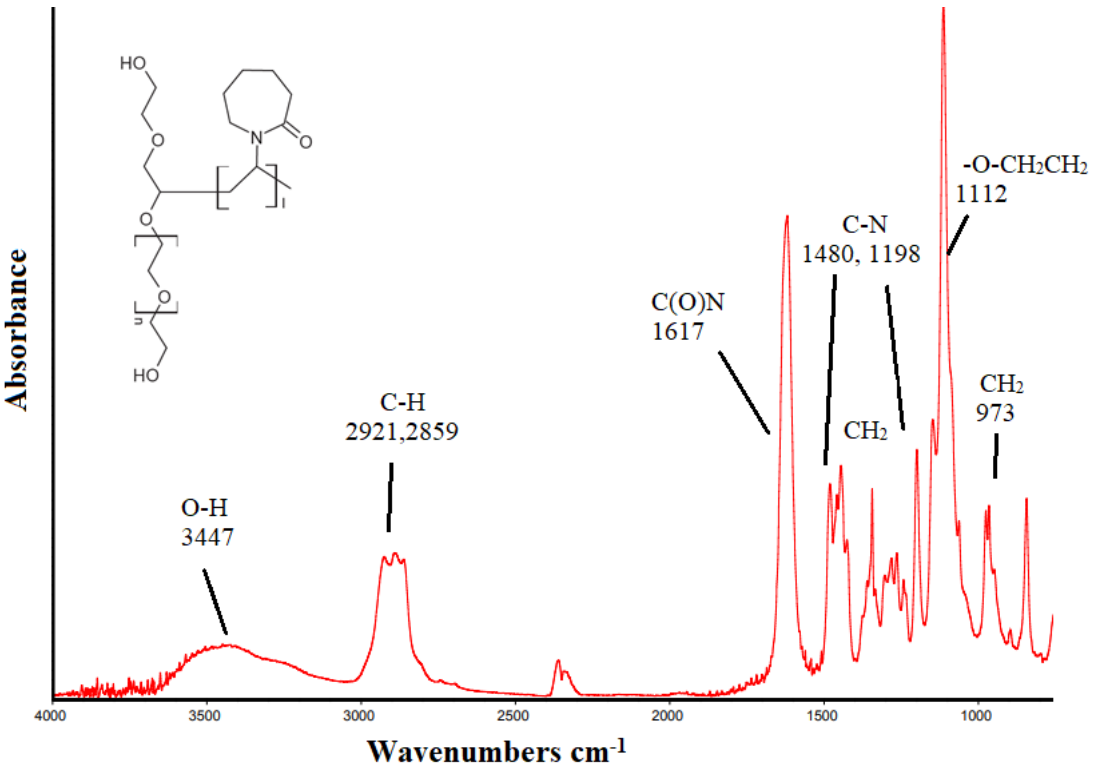

Figure 21. FTIR spectra of copolymer S1 PEG-g-PVCL.

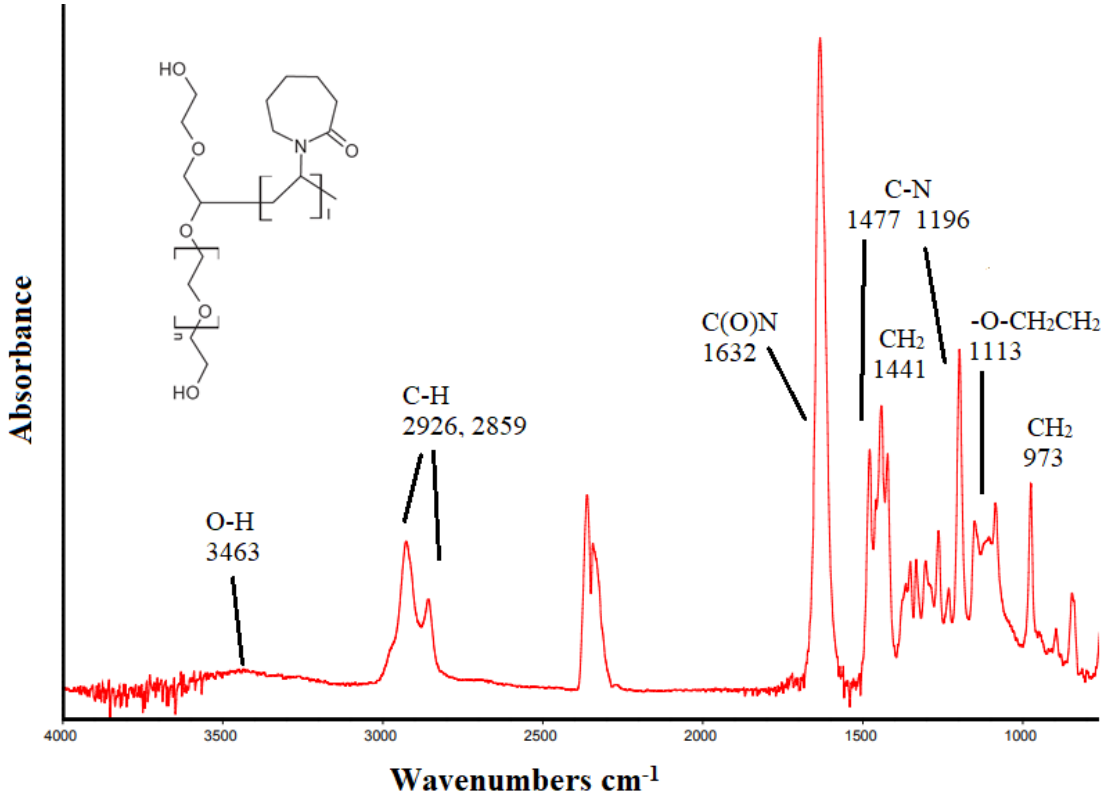

Figure 22. FTIR spectra of copolymer S4 PEG-g-PVCL.

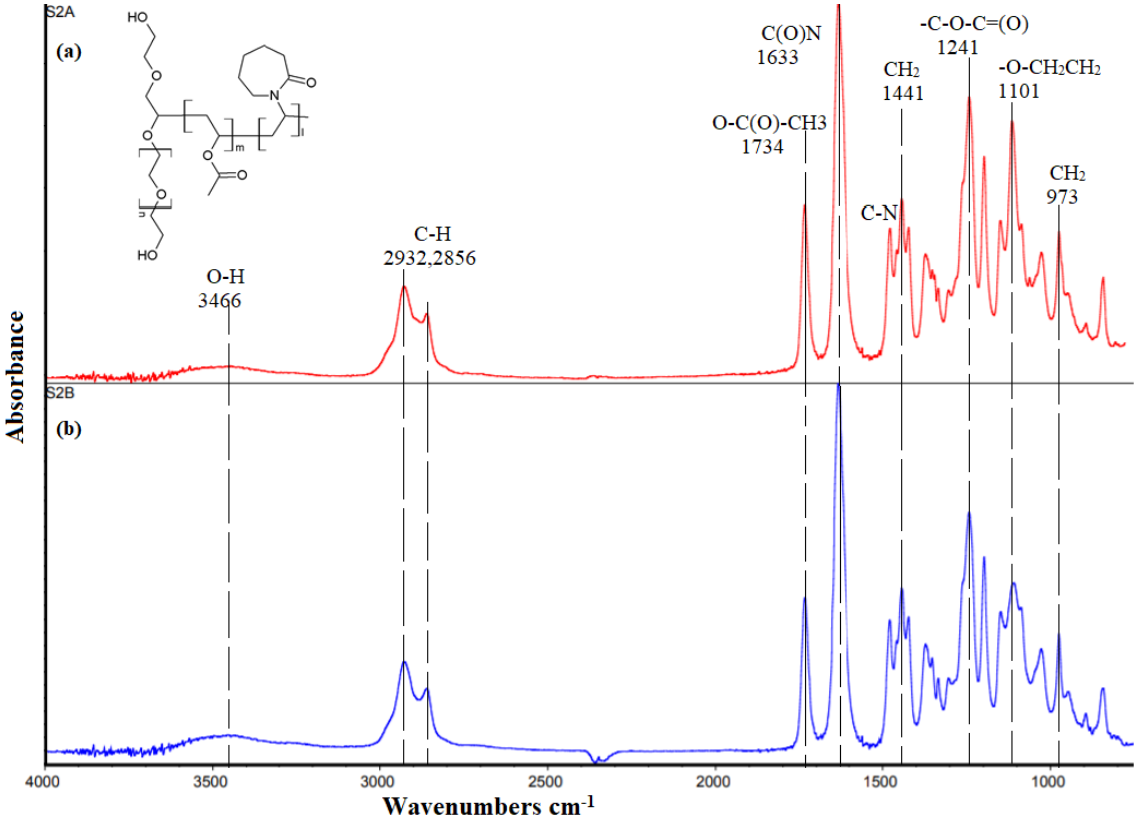

Figure 23. FTIR spectra of copolymer (a) S2A and (b) S2B.

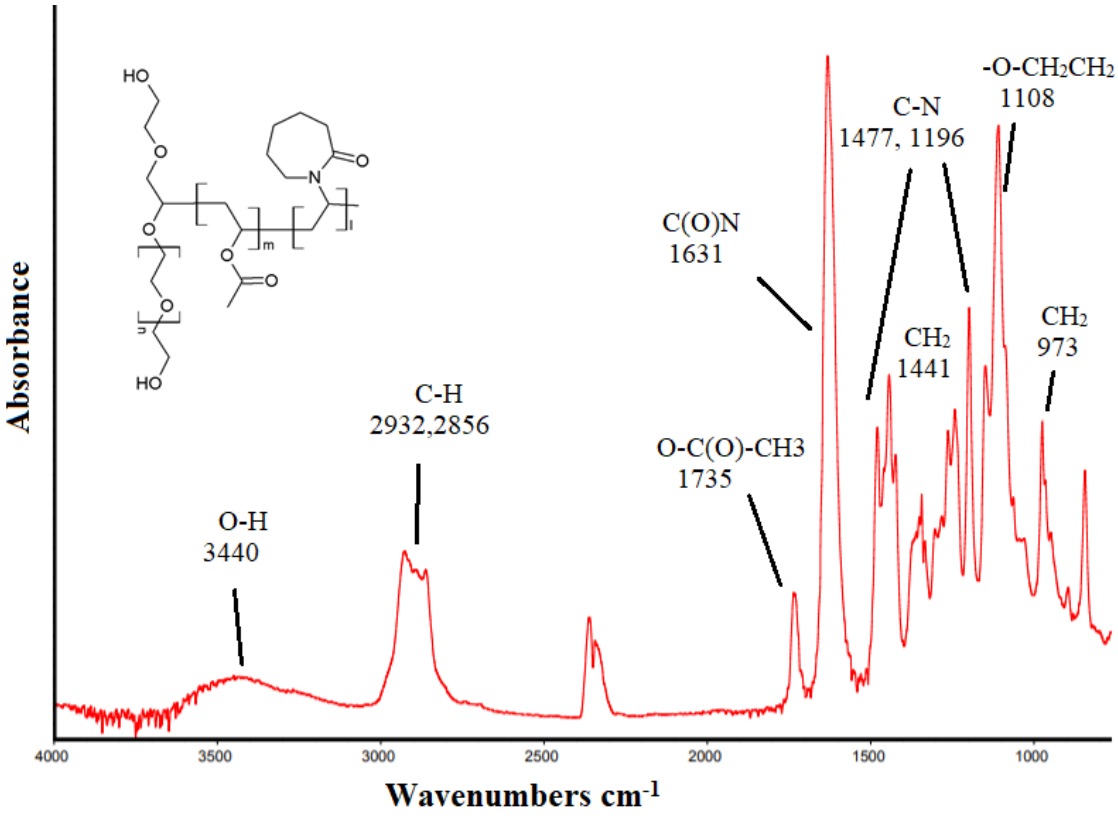

Figure 24. FTIR spectra of copolymer S3.

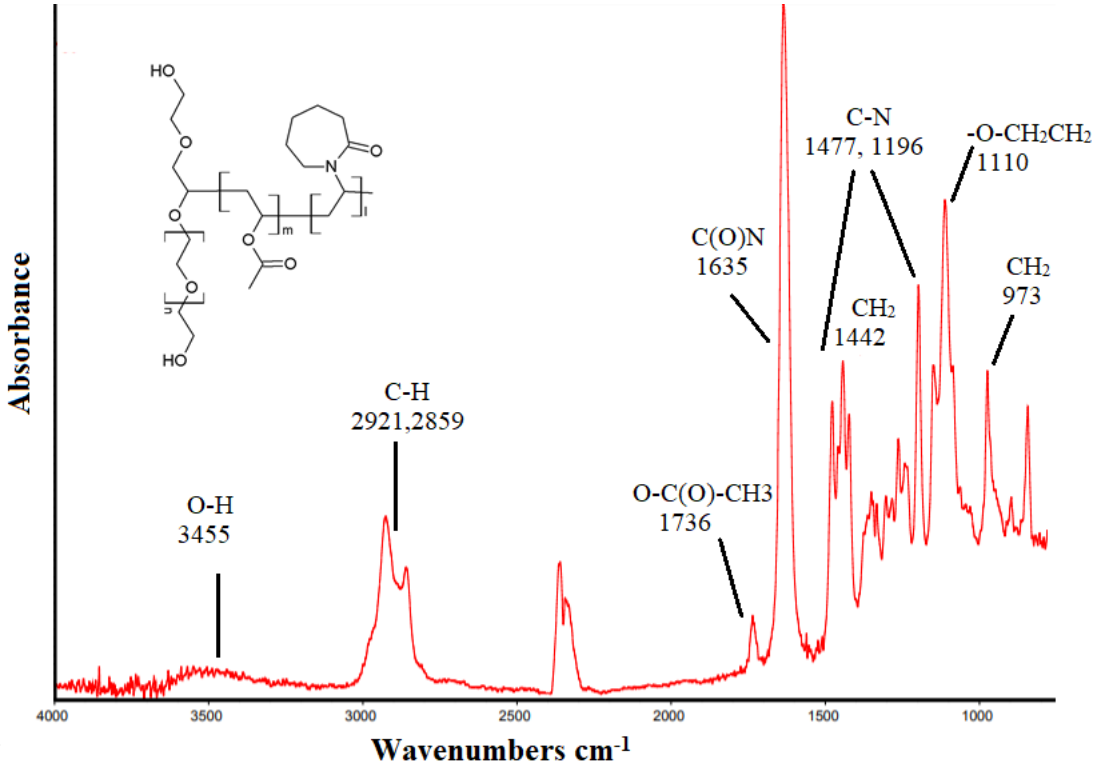

Figure 25. FTIR spectra of copolymer S6.

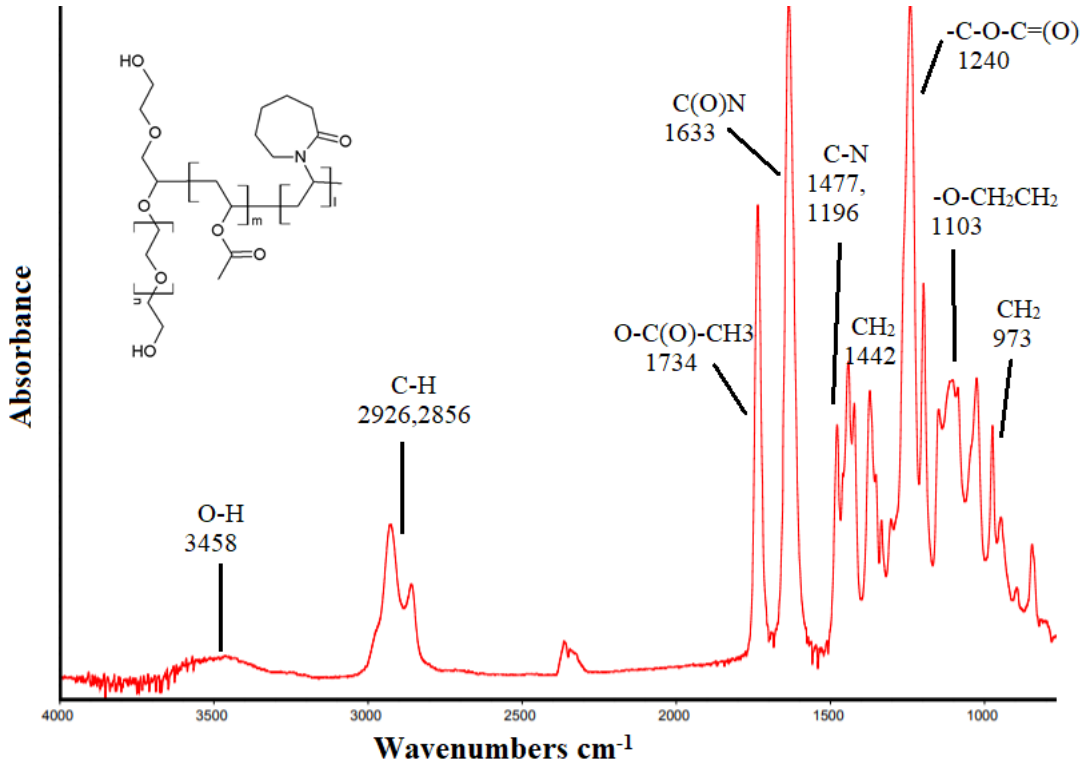

Figure 26. FTIR spectra of copolymer Soluplus®.

4.2.2 NMR investigation

Nuclear magnetic resonance (NMR) spectroscopy it is an important materials characterisation method for controlling polymerization reaction, polymer purity and to study of polymer structure-property relationships. The importance of NMR as a technique arises in part because the signals can be assigned to specific atoms along the polymer backbone and side chains. Since the NMR spectrum is determined by local forces, this method provides valuable and unique information about polymers on an atomic-length scale. [191]

^{1}H-NMR (Proton nuclear magnetic resonance*)* due to its high sensitivity, is one of the most important techniques for copolymer compositions characterization. In this study this technic confirmed structure of synthetized material by proton ^{1}H-NMR analysis of reagents and final products. By comparing the spectra of the substrates and the final copolymer control of the synthesis reactions and changes that occurred during the synthesis can be observed. As the synthesis product is a copolymer with a high molecular weight, the signals for the subsequent bonds are expected to be wide and might overlap that is make analysis complex.

The ^{1}H-NMR technique was applied to further detect the chemical structure of synthetized grafted materials. Soluplus® that is a commercially available polymer based on the same structure is used here for comparison reasons. ^{1}H-NMR spectra of PEG-g-PVCL and PEG-g-(PVAc-*co*-PVCL) copolymers are given in: **Fig. 28**, copolymer S1; **Fig. 29**, copolymer S2A; **Fig. 30**, copolymer S2B; **Fig. 31**, copolymer S3; **Fig. 32**, copolymer S4, **Fig. 33**, copolymer S6 and **Fig. 34**, Soluplus®. The ^{1}H-NMR spectra expressed a broad spectrum consisting of five peaks for PEG-g-PVCL copolymers and six pics for PEG-g-(PVAc-*co*-PVCL) copolymers that influenced by the change after polymerization. Characteristic signals of PVCL, PVAc and PEG remained the different intensity in all copolymer's spectra. The assigned protons are shown in the formula of PEG-g-PVCL (**Fig. 27a**) and PEG-g-(PVAc-*co*-PVCL) (**Fig.27b**) copolymers, the peak assignments are tabulated in **Table 9**.

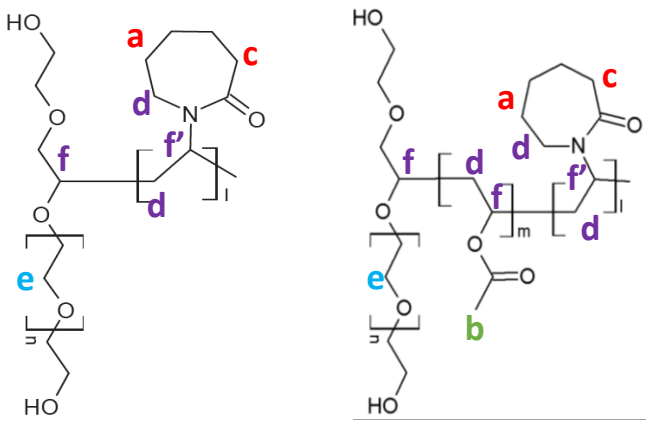

Figure 27. Structure of a) PEG-g-PVCL graft copolymer S1 and S4 and b) PEG-g-(PVAc-co-PVCL) graft copolymer S2, S2C, S3, S6 and Soluplus® with assigned protons.

Furthermore, copolymer S1 spectrum (**Fig. 28**) exhibited essential signals at 4.5, 4.37, 3.62, 3.23, 2.49 and 1.73 ppm, which corresponded to the protons in, –CH–O [H_f], –CH–N [$H_{f'}$], –CH2–CH2– [H_e], –CH2–N [H_d], –CH2–CH [H_d], –CH2–CO [H_c], and –CH2 [H_a], groups, respectively. Spectrum of copolymer S4 (**Fig. 32**) showed the presence of the same 5 peaks with little shift to a smaller value of some the protons. The following peaks occurred at 4.49, 4.37, 3.62, 3.23, 2.49 ppm corresponding to the same protons presented in copolymer S1 [1-3]. However, it can be noticed that the signals coming from the protons in the groups CH_2–N [H_d], –CH_2–CH [H_d], –CH2–CO [H_c], belonging to vinyl caprolactam are more intense and wider in the case of the copolymer S4 with PEG 1000 Mw than copolymer S1 with PEG 6000 Mw, which may indicate PVCL greater content in copolymer S4 composition.

In the ^{1}H-NMR spectra of copolymer S2A, S2B, S3, S6 and Soluplus® as displayed in **Figures 29-31, 33-34** six different peaks of the protons were observed, some of them also detected in copolymer S1 and S4 (**Tab. 9**). It can be observed in three components copolymers spectra signals of the protons [$H_{f'}$], [H_f] in –CH–N and –CH–O groups overlapped and dependently of the PVAc and PVCL content in copolymer structure remind different intensity. Moreover, there is a shift of the position of the protons [$H_{f'}$] and [H_f] in –CH–N and –CH–O groups of PEG-g-(PVAc-*co*-PVCL) copolymers spectra compared to the S1 and S4 copolymers spectra consist of two components. This may be attributed to the appearance of a new proton [H_f] of –CH–O group derived from the grafted PVAc. The difference between the proton arrangement for copolymers S2A, S2B, S3 and Soluplus® consisting of three

components is insignificant. The shifts of the protons of copolymer S6 deviate slightly from the rest of the copolymer. This may be due to its different composition than the rest of the three-component copolymers, such as significantly higher PEG Mw 20000, very low PVAc content (**Tab. 9**) and the lowest grafting degree (**Tab. 10**) of all tested polymers. The spectrum of S6 (**Fig. 33**) showed resonance signals at 1.74, 1.99, 2.48, 3.20, 3.62, 4.45. ppm which were assigned to the CH_2 [H_a], –C–CH_3 [H_b], –CH_2–CO [H_c], CH_2–N [H_d], –CH_2–CH [H_d], –CH_2–CH_2– [H_e], –CH–N [$H_{f'}$]. The signal from the proton [Hf] group –CH–O at 4.70-4.71 ppm present in other PEG-g-(PVAc-*co*-PVCL) copolymers has not been isolated in copolymer S6, which may be caused by a small amount of grafted PVAc and the overlay of the stronger signal of [$H_{f'}$] from –CH–N group.

In copolymer S2 (S2A, S2B), S3 and Soluplus® spectra the chemical shifts of protons in –CH2 [H_a] group were observed at 1.69-1.71 ppm, –C–CH_3 [H_b] at 1.99-2.00, –CH_2–CO [H_c] at 2.48-2.49 ppm, CH_2–N [H_d], –CH_2–CH [H_d] at 3.22-3.23 ppm, –CH_2–CH_2– [H_e] at 6.62-6.64 ppm, –CH–N [$H_{f'}$] at 4.45-4.50 ppm and –CH–O [H_f] at 4.70-4.71 ppm, respectively.[182–184,191,192] Additionally, in spectra the Soluplus® (**Fig. 34**), which has the highest content of PVAc in the structure, clearer signal from [H_f] at 4.85 ppm probably coming from the other –CH–O was detected. Presence of the small pick at 7.26 ppm in the spectrum of the PEG-b-(VAc-*co*-VCL) corresponds to the solvent, deuterated chloroform. However, the characteristic peaks corresponded to vinyl group of vinyl acetate and vinyl caprolactam vanished.[193,194] According to the FT-IR, ^{1}H-NMR results certainly confirmed the polymerization of VAc and PVCL and purity of the samples. Moreover, ^{1}H NMR spectrum shows not sharp peaks but wide peaks because of molecular chains of various lengths. It is proved further that synthetized materials and commercial Soluplus® are random copolymers.[195]

COSY (correlation spectroscopy), NOESY (nuclear Overhauser effect spectroscopy)

Two-dimensional nuclear magnetic resonance spectroscopy (2D NMR) provides more information about a molecule than one-dimensional NMR spectra and are especially useful in determining the structure of a molecule, particularly for molecules that are too complicated to work with using one-dimensional NMR. NOESY is often used in

NMR to obtain information on the distance between nuclei through space and COSY through bonds.[196–198] Based on the study of these correlations, it is possible to analyse the repeatability of the polymer structure units, whether the polymer has a block or graft structure with random distribution of the two components on the main polymer chain

Fact of the random distribution of PVAc and PVCL on PEG backbone confirmed the ^{1}H-^{1}H NOESY and ^{1}H-^{1}H COSY spectra of copolymer S2 presented in **Figures 35-36**. From the interpretation of the two 2D NMR spectra, copolymer S2 is a random copolymer and PVAc and PVCL are randomly distributed on the PEG backbone. This resulted from the fact that all CHs (both from VAc and VCL monomers, orange and blue circles in the structures) couple with CH_2s (between 1.25 and 2.00 ppm) regardless of the specific monomeric unit to which these latter are related. This phenomenon describes a structure in which all VAc units are very proximate (in space) to at least one VCL, and this is not possible for a block configuration.[199,200]

Based on the integrals of the protons of each copolymer unit present at 3.60-3.63, 3.19-3.24, 2.01 ppm of ^{1}H NMR spectra of copolymer S1, S2A, S2B, S3, S4, S6, Soluplus® (**Figs. 28-34**) the ratio was calculated between monomers of copolymer blocks (EO/VAc/VCL), results can be seen in **Table 9.** The copolymers showed different contents of hydrophobic and hydrophilic components in the structure. As the main driving force of self-assembly is the hydrophobic force, the copolymer composition has a significant impact on the study of encapsulating properties. The highest content of the most hydrophobic component of PVAc exhibited by Soluplus®, decreased as follows: copolymer S2A > S2B > S3 > S6. Lactam seven-membered-ring of NVCL is hydrophobic, while –OH of PEG is hydrophilic. Therefore, increasing of hydrophobic PVCL leads to increasing of hydrophobicity of PEG-g-PVCL graft copolymers. Copolymer S1 with PEG Mw 6000 resulted in higher content of PEG (PEG 31%/ PVCL 69%) comparing to similar structured copolymer S4 (PEG 10% /PVCL 90%) with Mw 1000. PEG-b-(VAc-*co*-VCL) S2A, S2B, S3 and Soluplus® copolymers showed similar PEG content, 14%, 15%, 18%, 16% then their different properties might be driven by different value of PVAc-PVCL hydrophobic part. Composition of copolymer S6 with PEG Mw 200000 differ from the other polymers with PEG Mw 6000, expressing the lowest content of hydrophobic component PVAc and highest value of hydrophilic PEG (**Tab. 10**). This value might indicate that the

increase of PEG Mw and subsequently sample viscosity might have important effects on the grafted PVAc content. Composition of copolymer S2A and S2B remains extremely close, confirming the reproducibility of the material.

^{1}H NMR was also used to determine the degree of the grafting of VCL and/or VAc units onto PEG backbone by calculating the pick area of PEG and PVCL signals at 3.62-3.64 and at 3.20-3.23 ppm of ^{1}H-NMR spectra of copolymer S1, S2A, S2B, S3, S6, and Soluplus® (**Figs. 28-34**), assuming PVCL and PVAc diffusing together according to **Figure 39-41, Figure 43-44** (Grafting investigation by diffusion ordered spectroscopy)

Consider two components' copolymers, copolymer S4 had higher degree of grafting (300 PVCL units grafted at every 100 units of PEG Mw 1000) than copolymer S1 (65 PVCL units grafted at every 100 units of PEG Mw 6000) which has the highest degree of grafting among all analysed copolymers. The degree of grafting of three components copolymers increased as follows, S2A (155 u), S2B (145 u), Soluplus® (112 u), S3 (100 u), S6 (52 u). A trend can be seen, regardless of the number of components in the structure, as the Mw of PEG decreases, the grafting degree increases.

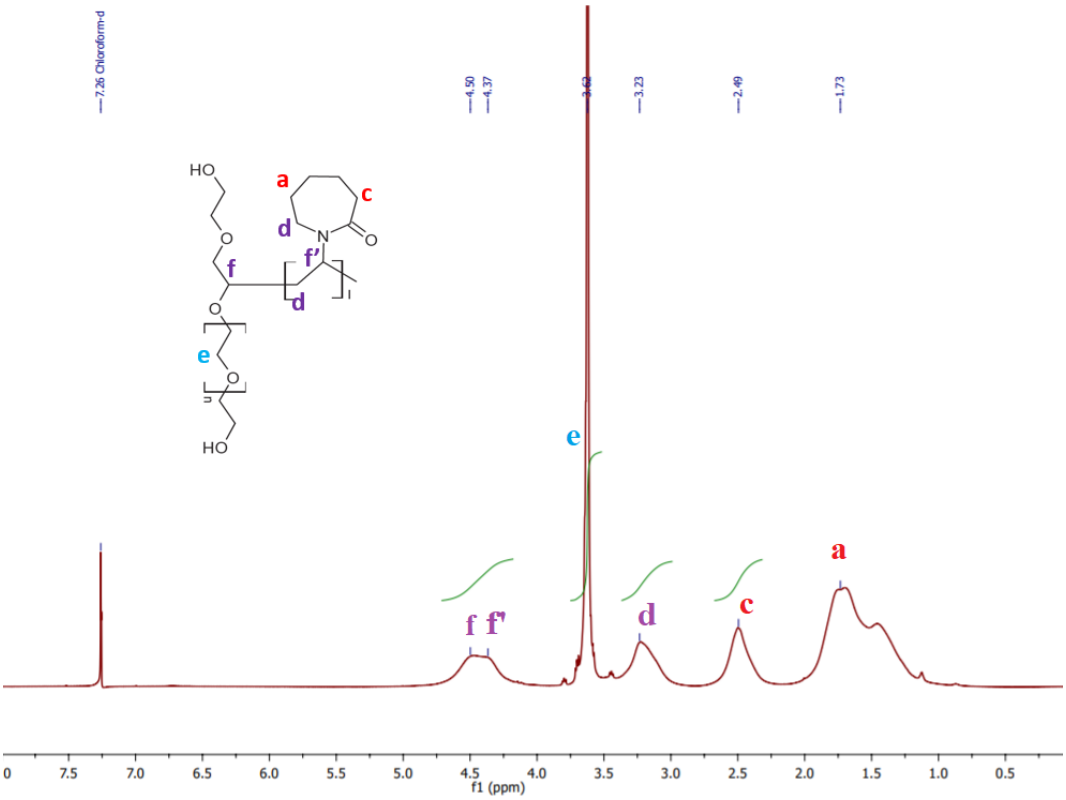

Figure 28. The ^{1}H-NMR Spectrum of PEG-g-PVCL; S1.

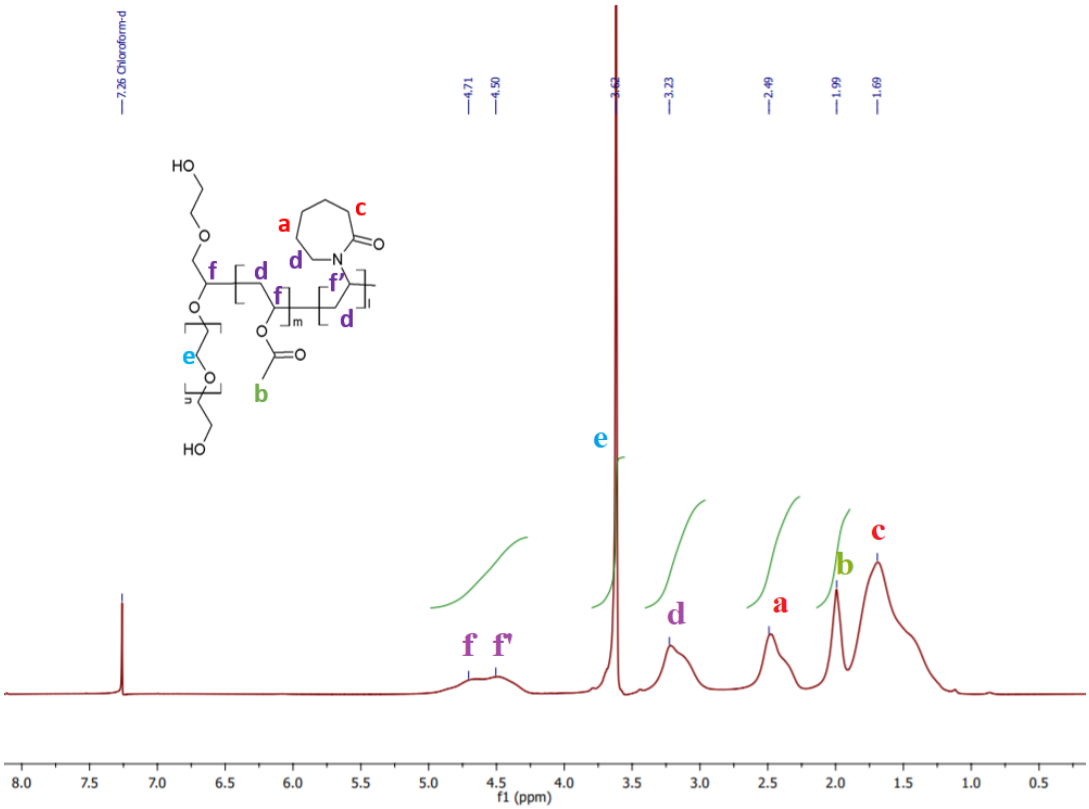

Figure 29. The ^{1}H-NMR Spectrum of PEG-g-(PVAc-co-PVCL); S2A.

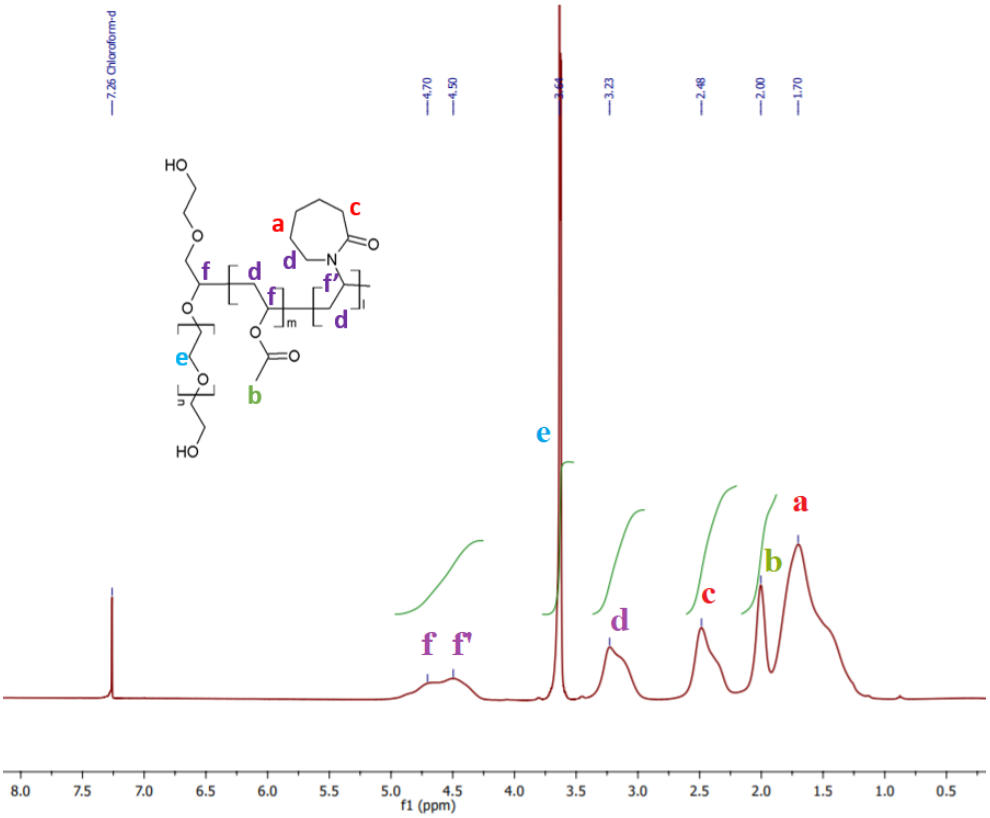

Figure 30. The ^{1}H-NMR Spectrum of PEG-g-(PVAc-co-PVCL); S2B.

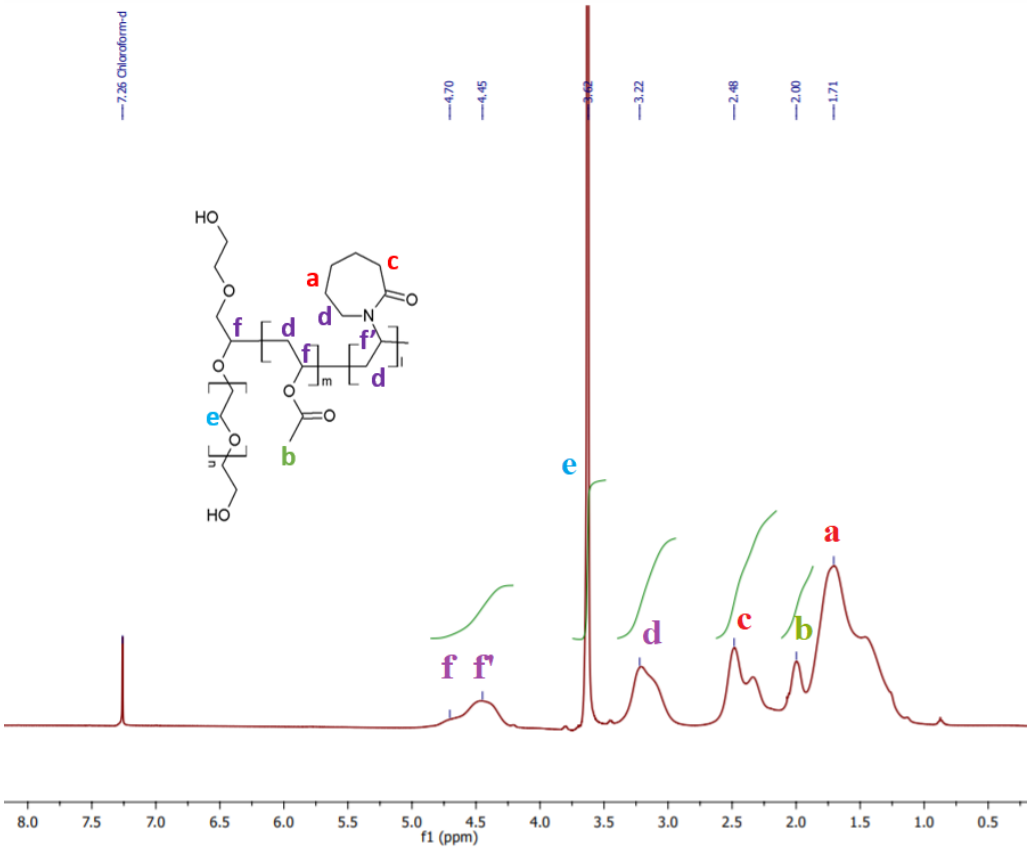

Figure 31. The ^{1}H-NMR Spectrum of PEG-g-(PVAc-co-PVCL); S3.

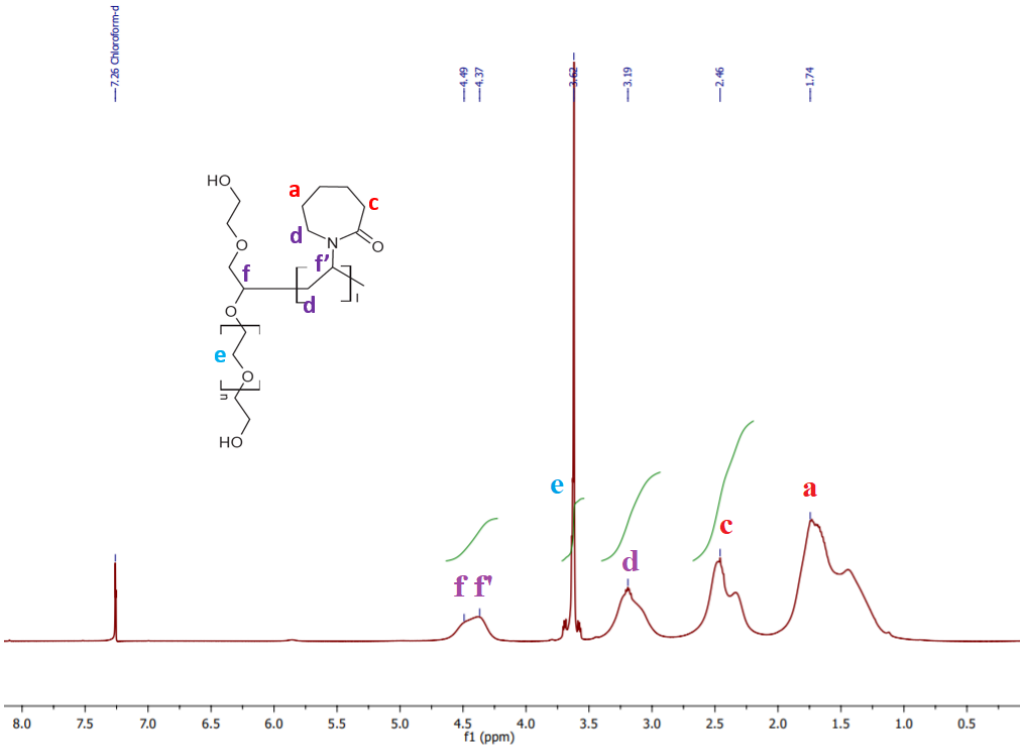

Figure 32. The ^{1}H-NMR Spectrum of PEG-g-PVCL; S4.

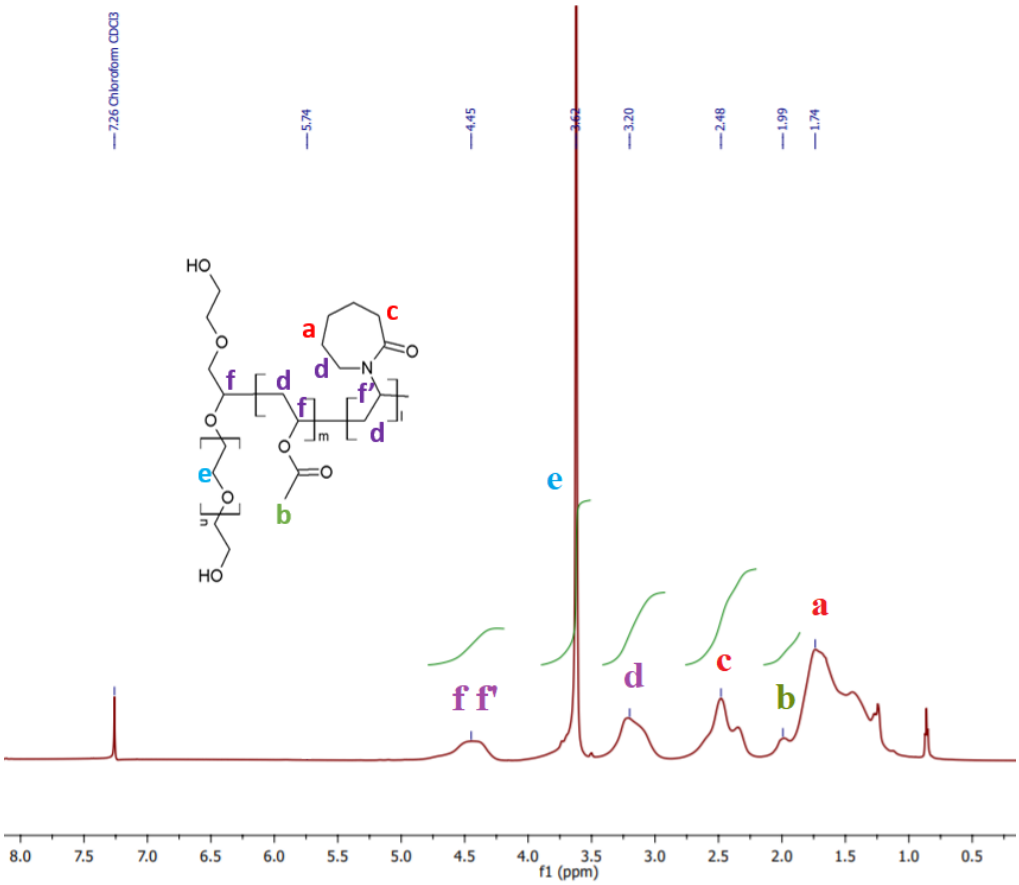

Figure 33. The ^{1}H-NMR Spectrum of PEG-g-(PVAc-co-PVCL); S6.

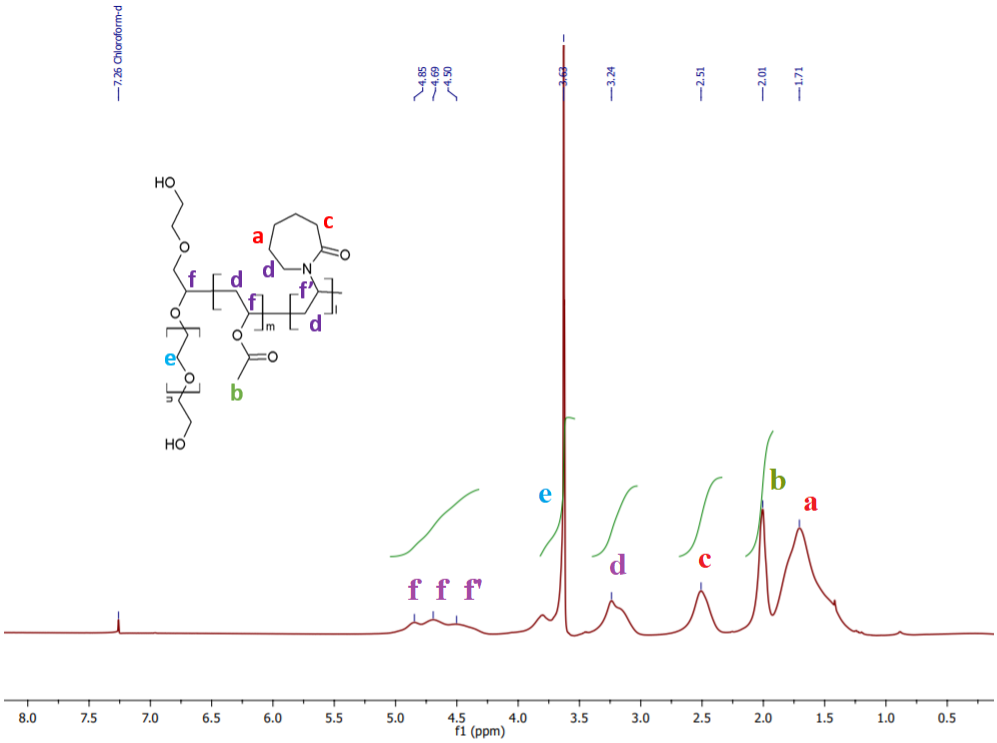

Figure 34. The ^{1}H-NMR Spectrum of Soluplus®.

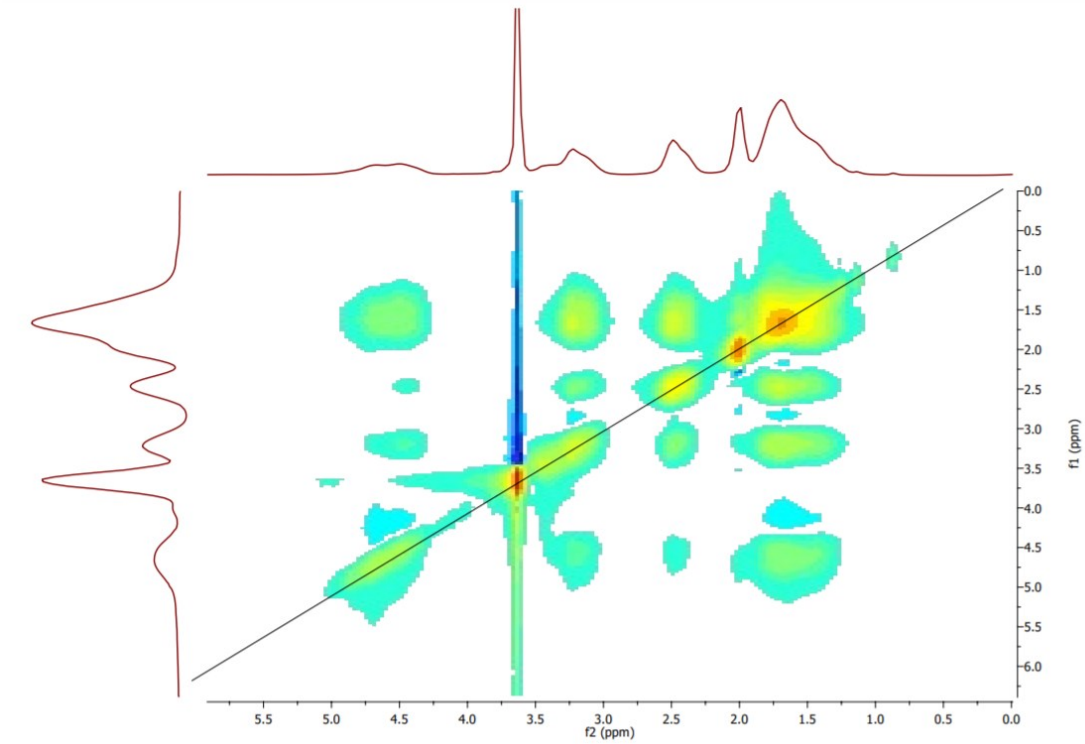

Figure 35. ^{1}H-$_{1}H$ NOESY map of copolymer S2A.

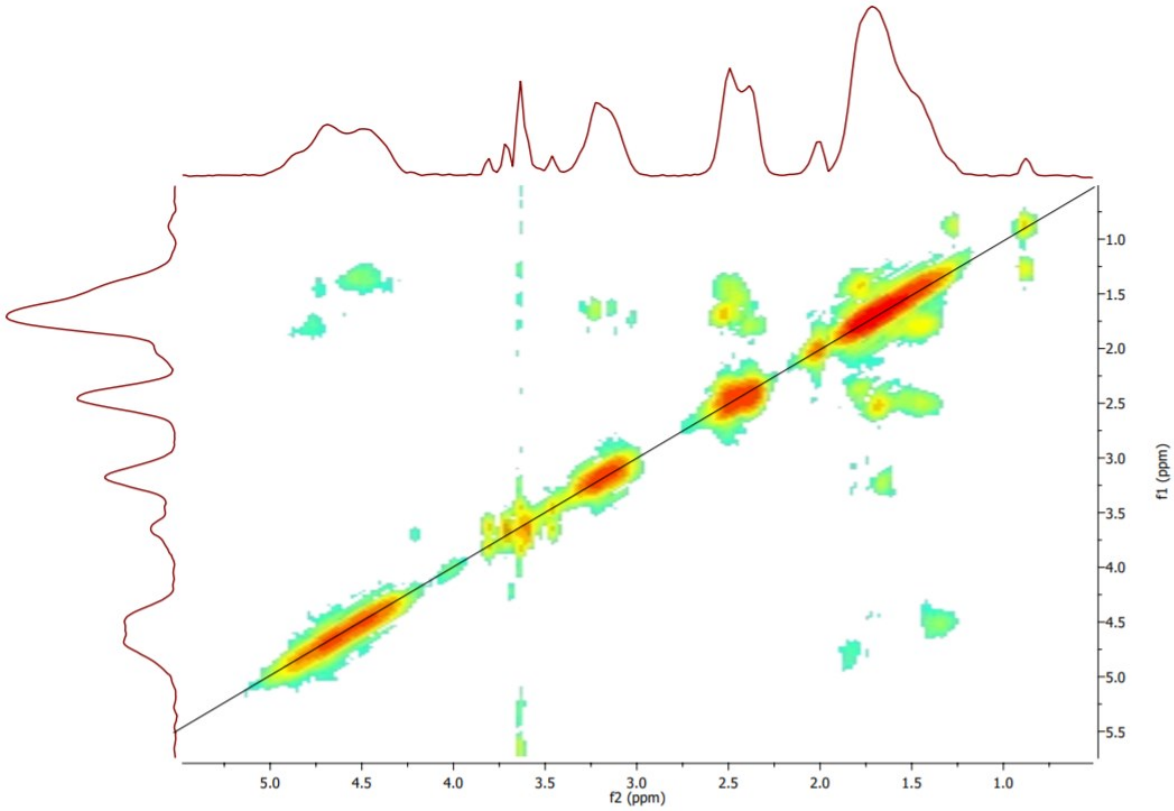

Figure 36. ^{1}H-^{1}H COSY map of copolymer S2A.

Table 9. Assignment of corresponding ^{1}H-NMR spectra for copolymer S1, S2, S3, S4, S6 and Soluplus®.

Proton position	Chemical shift [ppm]	Functional group
(a) Copolymer S1		
Ha	1.73	–CH2
Hb		
Hc	2.49	–CH2–CO
Hd	3.23	–CH2–N/–CH2–CH
He	3.62	–CH2–CH2–
Hf’	4.37	–CH–N
Hf	4.50	–CH–O
(b) Copolymer S2A		
Ha	1.69	–CH2
Hb	1.99	C–CH_3
Hc	2.49	–CH2–CO
Hd	3.23	–CH2–N/–CH2–CH
He	3.62	–CH2–CH2–
Hf’	4.5	–CH–N
Hf	4.71	–CH–O
(c) Copolymer S2B		
Ha	1.70	–CH2
Hb	2.00	C–CH_3
Hc	2.48	–CH2–CO
Hd	3.23	–CH2–N/–CH2–CH
He	3.64	–CH2–CH2–
Hf’	4.45	–CH–N
Hf	4.70	–CH–O
(d) Copolymer S3		
Ha	1.71	–CH2
Hb	2.00	C–CH_3
Hc	2.48	–CH2–CO
Hd	3.22	–CH2–N/–CH2–CH
He	3.62	–CH2–CH2–
Hf’	4.3	–CH–N
Hf	4.49	–CH–O
(d) Copolymer S4		
Ha	1.74	–CH2
Hb		
Hc	2.49	–CH2–CO
Hd	3.19	–CH2–N/–CH2–CH
He	3.62	–CH2–CH2–
Hf’	4.37	–CH–N
Hf	4.49	–CH–O
(d) Copolymer S6		
Ha	1.74	–CH2
Hb	1.99	C–CH_3
Hc	2.48	–CH2–CO
Hd	3.20	–CH2–N/–CH2–CH
He	3.62	–CH2–CH2–
Hf’		–CH–N
Hf	4.45	–CH–O

(d) Soluplus®		
Ha	1.71	–CH2
Hb	2.01	C–CH_3
Hc	2.51	–CH2–CO
Hd	3.24	–CH2–N/–CH2–CH
He	3.63	–CH2–CH2–
Hf'	4.50	–CH–N
Hf	4.69, 4.85	–CH–O

Table 10. Composition and degree of grafting of copolymer S1, S2, S3, S4, S6, Soluplus®.

Polymer name	Ratio [%] PEG/PVAc/PVCL	Degree of grafting PVCL u/ 100 PEG u
S1 PEG_{6000}-g-PVCL	31/-/69	65
S2A PEG_{6000}-g-(PVAc-co-PVCL)	15/25/60	155
S2B PEG_{6000}-g-(PVAc-co-PVCL)	14/25/61	145
S3 PEG_{6000}-g-(PVAc-co-PVCL	18/14/68	100
S4 PEG_{1000}-g-PVCL	10/-/90	300
S6 PEG_{20000}-g-(PVAc-co-PVCL)	24/9/67	52
Soluplus® (refernce)	16/32/51	112

4.2.3 Grafting investigation by diffusion ordered spectroscopy (DOSY 2D NMR)

In general, the formation of the graft copolymer can be confirmed with NMR, IR spectroscopy, and size-exclusion chromatography. In NMR spectroscopy, however, frequently it is very difficult to distinguish grafted polymers from polymer blends due to the similarity of their NMR spectra. In viewpoint of this, 2D-DOSY NMR could be a valuable and potential technique to distinguish between graft copolymers and the polymer blends of their constituents since the translational diffusion coefficients reflect the changes in the shape and/or size of polymers.[201]

DOSY NMR demonstrated the potential of the method for unravelling the character of complex matrices such as the graft-copolymers synthetized in this study PEG-g-PVCL (**Fig. 37a**) and PEG-g-(PVAc-*co*-PVCL) (**Fig. 37b**). 2D-DOSY experiments were performed on copolymers S1, S2A, S2B, S3, S4, S6, and Soluplus® and the output of the diffusion data had been displayed as several 2D NMR maps.

Results presented on **Figures 38-44** showed all NMR peaks corresponding to the protons of each S1, S2A, S2B, S3, S4, S6 graft copolymer and Soluplus® components appeared parallel to the x-axis with similar diffusion coefficients values listed in **Table 11** confirming grafting character of analysed materials.[201–203] Additional DOSY correlations from the homopolymers residuals, small chain copolymers or not bound PEG contaminants that could formed during the free radical polymerization reaction can also be observed with very larger diffusion coefficients values listed in **Table 11**. Those slow diffusing components signals appeared parallel to the x-axis on **Figure 38-44** on the first paraller red line.[18,201,204] By products can be observed in all the copolymer samples except for copolymer S4 where only picks corresponding to graft copolymer can be seen parallel to the x-axis (**Fig. 42**). The absence of additional products in copolymer S4 can be explained by the fact that the reaction time of the synthesis of this copolymer was much shorter compared to the rest of the copolymers. The 20 hours synthesis of the copolymer S4 compared to the 67 hours synthesis of the S1, S2A, S3, S6 copolymer showed no formation of side products of the free radical polymerization reaction. It can be assumed that the same factor contributed to the highest degree of the grafting of copolymer S4 among all tested copolymers (**Tab. 10**). It should be admitted that the commercial version of the PEG-g-(PVAc-*co*-PVCL) copolymers, Soluplus®, also showed the presence of additional signals of by components diffusing much faster than the ones related to the main copolymer chain (**Fig. 44**). Therefore, by comparing the diffusion coefficient values of all synthetized copolymers (**Tab. 11**) it can be concluded that the most grafted material is the copolymer S4 where all the components diffused together with the same rate (**Fig. 42**). Sample S6 seems to be the worse grafted sample as there is more variation in the diffusion coefficient values (**Fig. 43**, **Tab. 11**). These data further establish that peaks arising from components of S1, S2A, S2B, S3, S4, S6 and Soluplus® copolymer are covalently linked together.

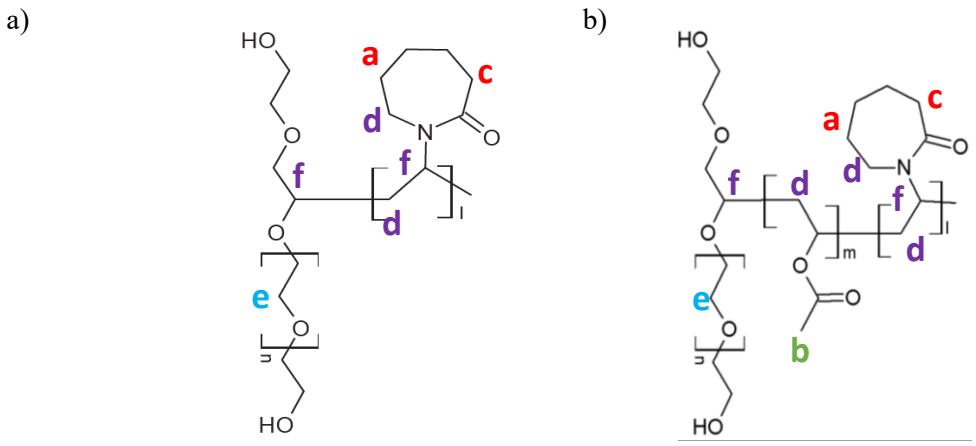

Figure 37. Structure of a) PEG-g-PVCL graft copolymer S1 and S4 and b) PEG-g-(PVAc-co-PVCL) graft copolymer S2, S2C, S3, S6 and Soluplus® with assigned protons.

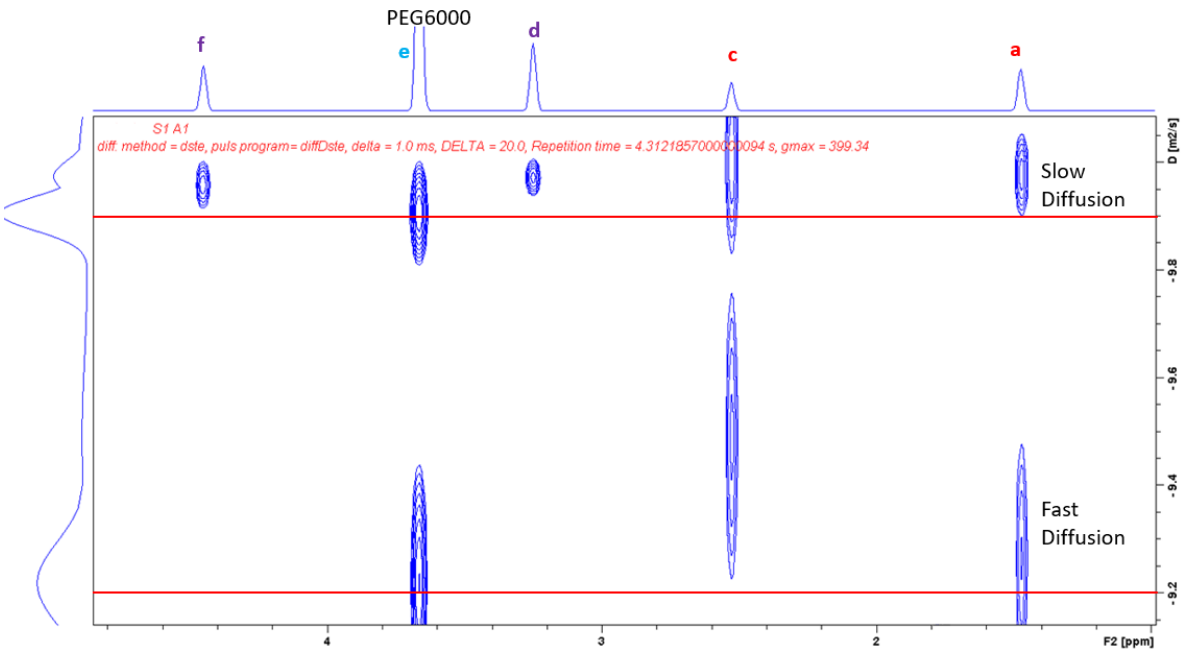

Figure 38. Representative DOSY NMR spectra of copolymer S1 in $CDCl_3$. The horizontal axis represents chemical shifts, whereas the vertical axis is the diffusion coefficient.

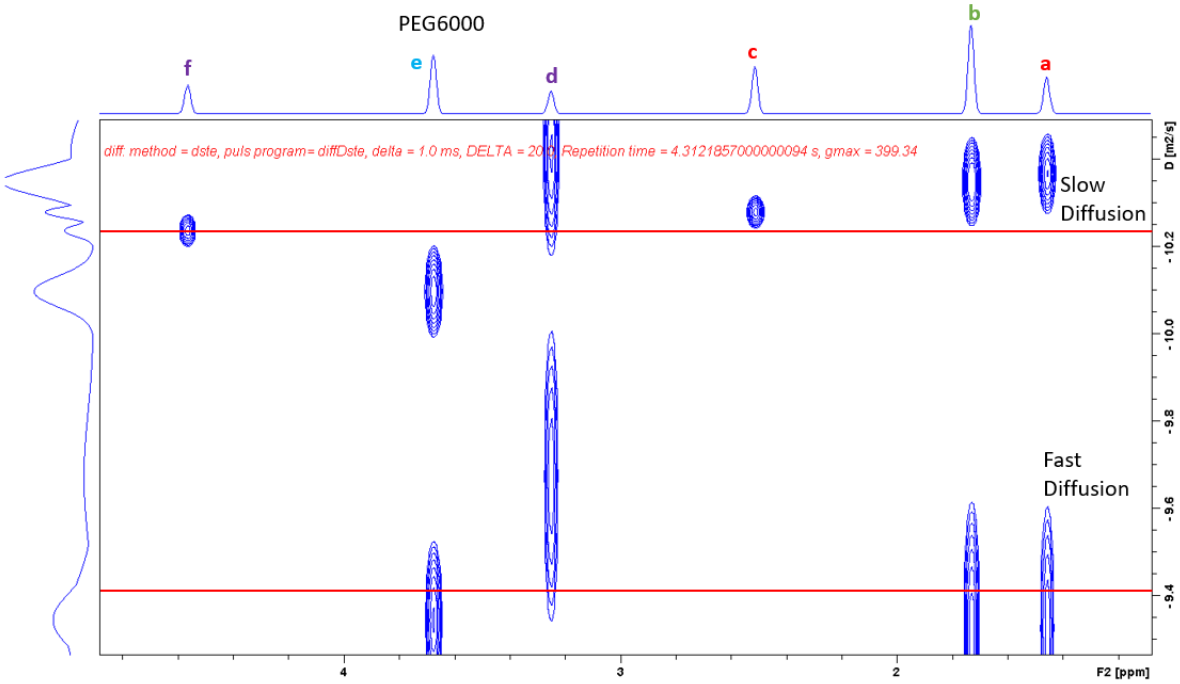

Figure 39. Representative DOSY NMR spectra of copolymer S2A in $CDCl_3$. The horizontal axis represents chemical shifts, whereas the vertical axis is the diffusion coefficient.

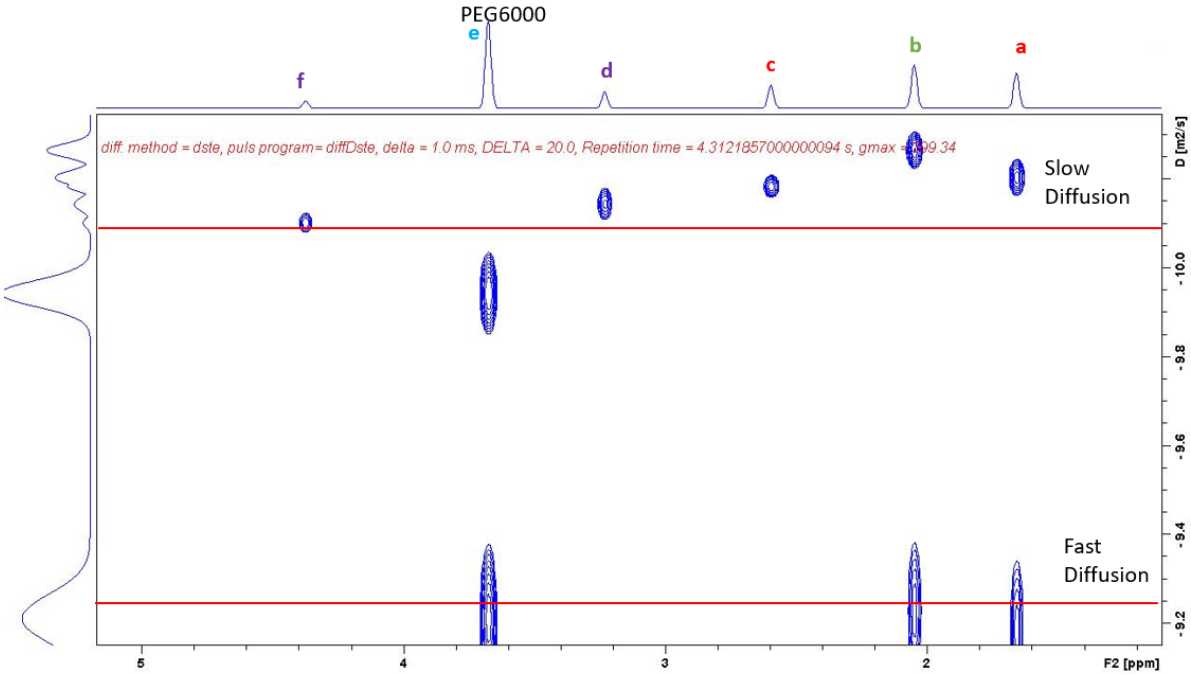

Figure 40. Representative DOSY NMR spectra of copolymer S2B in $CDCl_3$. The horizontal axis represents chemical shifts, whereas the vertical axis is the diffusion coefficient.

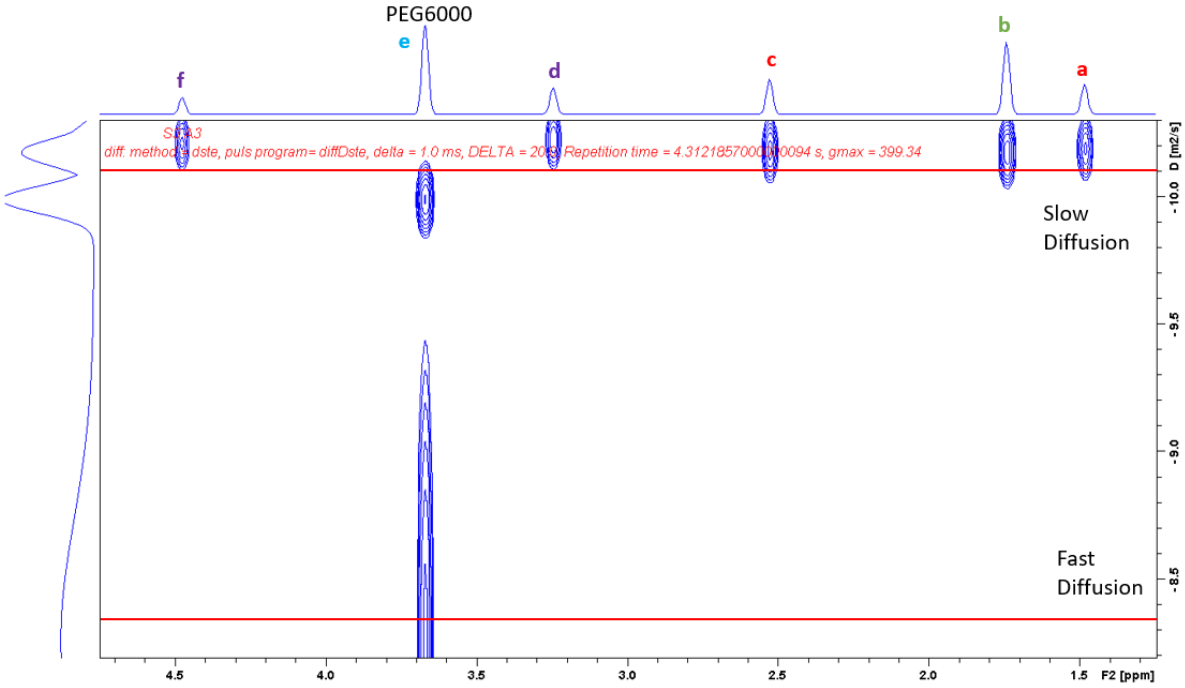

Figure 41. Representative DOSY NMR spectra of copolymer S3 in $CDCl_3$. The horizontal axis represents chemical shifts, whereas the vertical axis is the diffusion coefficient.

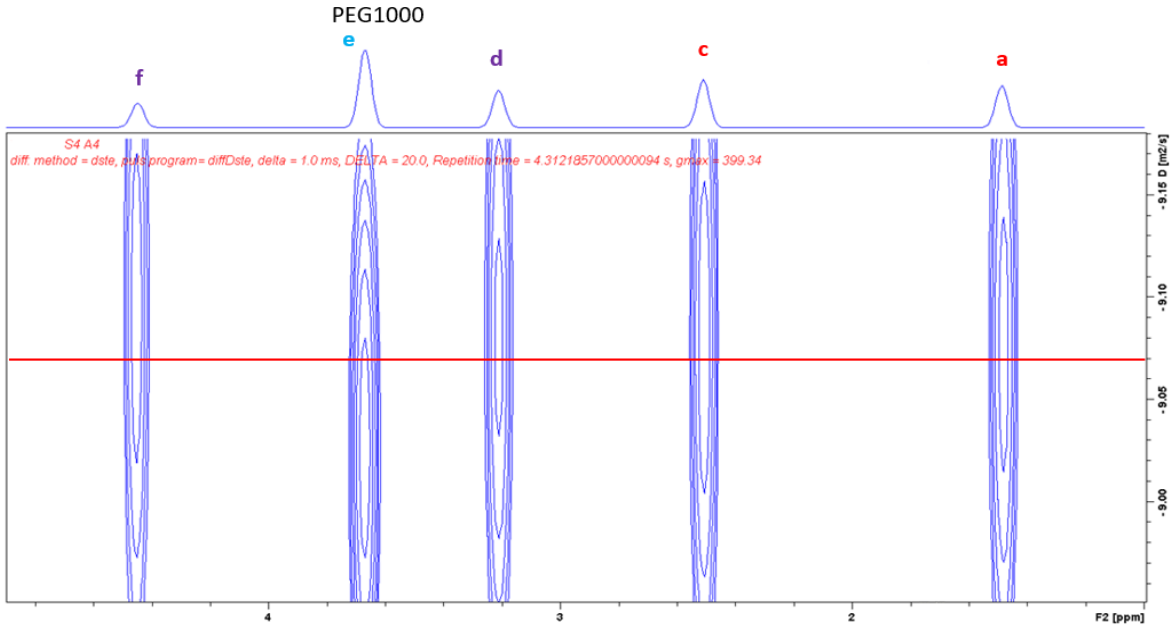

Figure 42. Representative DOSY NMR spectra of copolymer S4 in $CDCl_3$. The horizontal axis represents chemical shifts, whereas the vertical axis is the diffusion coefficient.

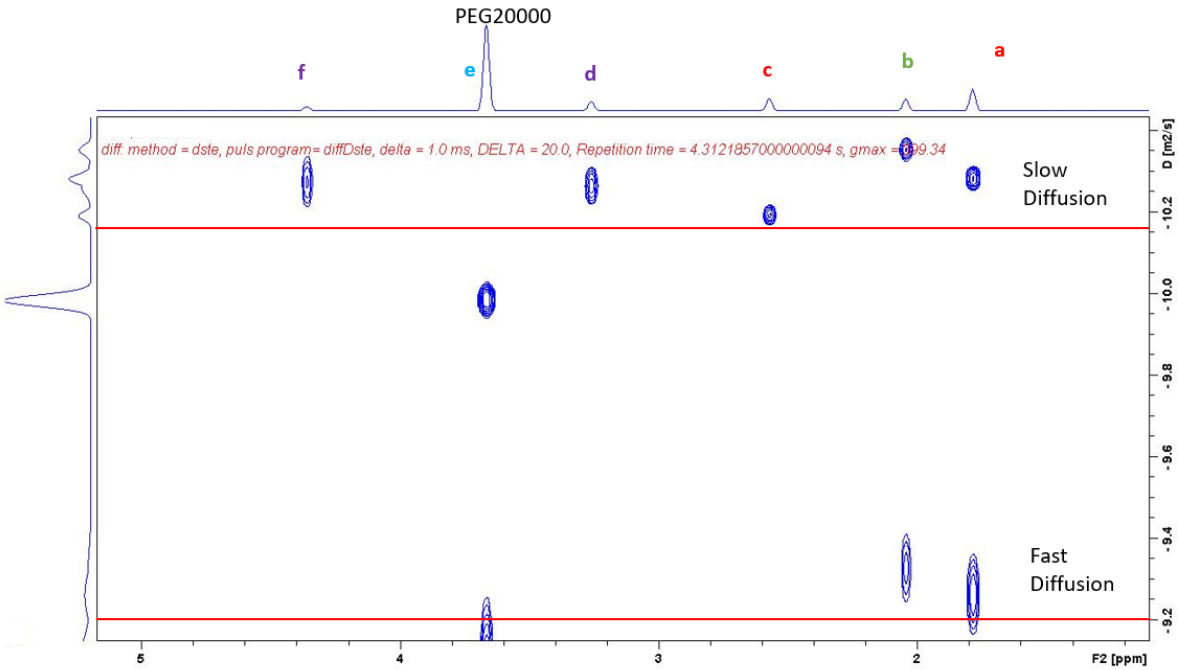

Figure 43. Representative DOSY NMR spectra of copolymer S6 in $CDCl_3$. The horizontal axis represents chemical shifts, whereas the vertical axis is the diffusion coefficient.

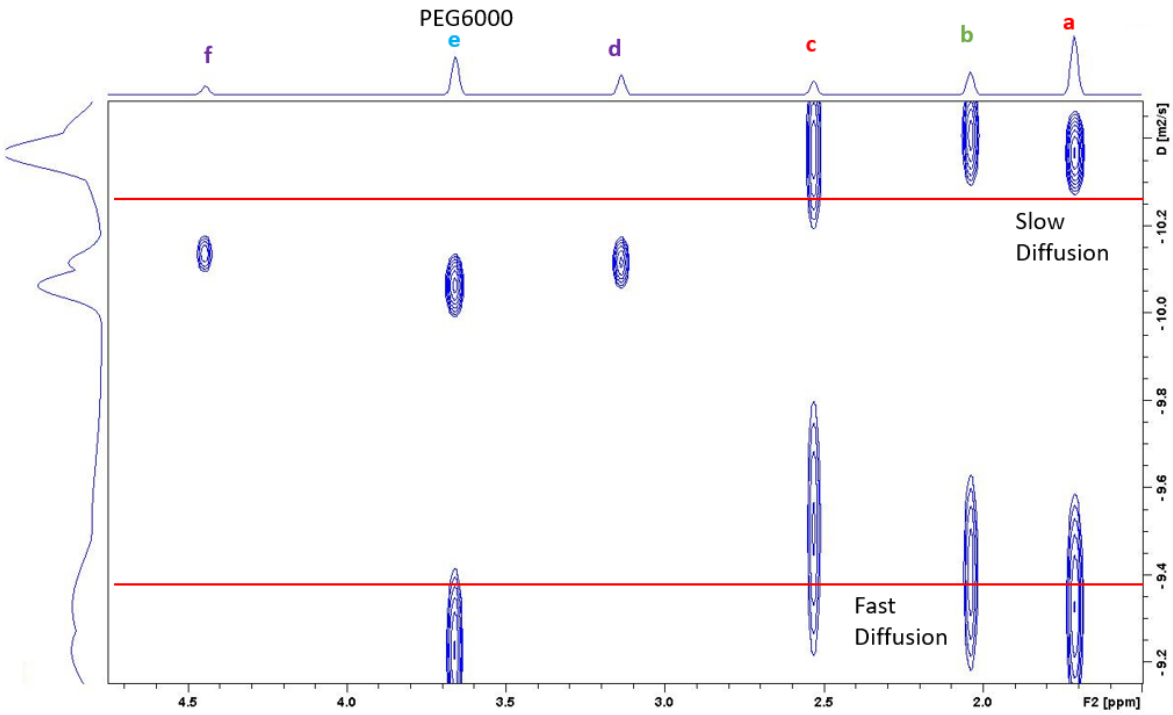

Figure 44. Representative DOSY NMR spectra of copolymer Soluplus® in $CDCl_3$. The horizontal axis represents chemical shifts, whereas the vertical axis is the diffusion coefficient.

Table 11. Diffusion coefficient values of assigned protons of copolymer S1, S2, S2C, S3, S4, S6 and Soluplus® components.

SAMPLE NAME	SIGNAL	PEAK A	PEAK B	PEAK C	PEAK D	PEAK E PEG	PEAK F
Copolymer S1	Copolymer Residual	1.05e-10 5.41e-10		3.22e-10 9.77e-11	1.06e-10	1.24e-10 6.02e-10	1.10e-10
Copolymer S2	Copolymer Residual	4.31e-11 4.79e-10	4.44e-11 4.63e-10	5.29e-11	3.30e-11 1.57e-10	8.10e-11 5.02e-10	5.76e-11
Copolymer S2C	Copolymer Residual	6.22e-11 6.46e-10	5.40e-11 5.88e-10	6.51e-11	7.14e-11	1.13e-10 6.13e-10	7.87e-11
Copolymer S3	Copolymer Residual	6.44e-11	6.79e-11	6.79e-11	6.03e-11	1.03e-10 5.50e-09	6.29e-11
Copolymer S4	Copolymer Residual	8.30e-10		8.17e-10	8.22e-10	9.32e-10	7.91e-10
Copolymer S6	Copolymer Residual	5.19e-11 5.43e-10	4.40e-11 4.68e-10	6.39e-11	5.40e-11	1.03e-10 9.44e-10	5.30e-11
Soluplus®	Copolymer Residual	4.26e-11 4.68e-10	3.89e-11 3.91e-10	4.19e-11 3.10e-10	7.61e-11	8.58e-11 5.88e-10	7.26e-11

4.2.4 Molecular weight investigation by GPC

The average molecular weight of copolymer is a very important parameter that characterizes a certain copolymer sample, and it is strongly related with the properties of the polymeric material. Therefore, its determination and knowledge is imperative in the study of these materials.[18,204] The determination of the number-average molecular weight (Mn), weight average molecular weight (Mw), and the polydispersity of all synthetized copolymer S1, S2A, S2B, S3, S4, S6, and Soluplus® were carried out by GPC. Results are presented in **Table 12**. As seen in chromatograms reported in **Figs. 46-51,** the GPC light scattering (LS) traces of copolymers S2A, S2B, S3, S4, S6 and Soluplus® were found to be unimodal. LS chromatogram of copolymer S1 (**Fig. 45**) showed the main product peak unimodal accompanied by a side peak of lower molecular weight. The origin of the low-molecular-weight fraction can be attributed to rest of the impurities present in the columns seeing in **Figure 53** as the traces of blank sample, detected also in PEG 6000 (**Fig. 53**). Chromatograms exhibits relatively high molecular weight distribution, which can be attributed to the formation of chain coupling product occurred due to a side reaction of free radical polymerization.[205] This is reflected in the polydispersity values of copolymers which are in the range 1.6-3.6. Based on the results presented in **Table 12**, the lowest polydispersity (PDI 1.6) is achieved for copolymer S1 that at the

same time shows the lowest Mw among all polymers, 42kDa. Copolymer S2A and S2B showed the same Mw range 195kDa-193kDa and close polydispersity 3.6-3.3 suggesting formation of material with controllable molecular weight and PDI prepared by free radical polymerization using time, temperature and number of added monomers by the time as a control parameter.[206] The value of Mw and PDI increases as follows, Mw S1<Soluplus®<S4<S6<S3<S2B<S2A and PDI S1< Soluplus®<S6<S2B<S4<S3<S2A. It can be noticed that polydispersity is difficult to control for polymers with MW higher than 42kDa. Moreover, an increase in PDI can be observed with increasing Mw.

Table 12 Non-Aqueous GPC Results Using dn/dc value.

Polymer name	Mw [kDa]	Mn[kDa]	PDI
S1 PEG_{6000}-g-PVCL	42.0	26.2	1.6
S2A PEG_{6000}-g-(PVAc-co-PVCL)	195.0	55.3	3.6
S2B PEG_{6000}-g-(PVAc-co-PVCL)	193.0	59.1	3.3
S3 PEG_{6000}-g-(PVAc-co-PVCL	128.9	37.1	3.5
S4 PEG_{1000}-g-PVCL	107.0	31.2	3.4
S6 PEG_{20000}-g-(PVAc-co-PVCL)	125.2	46.2	2.7
Soluplus®	98.0	45.3	2.2

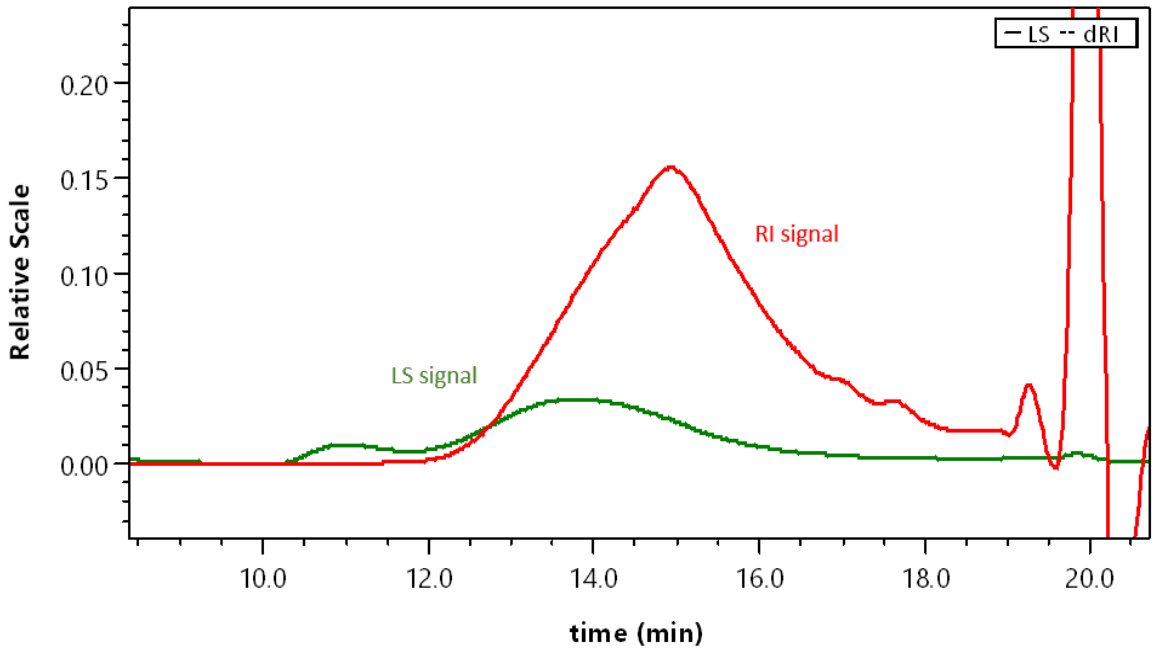

Figure 45. Light scattering and reflective index chromatogram of copolymer S1.

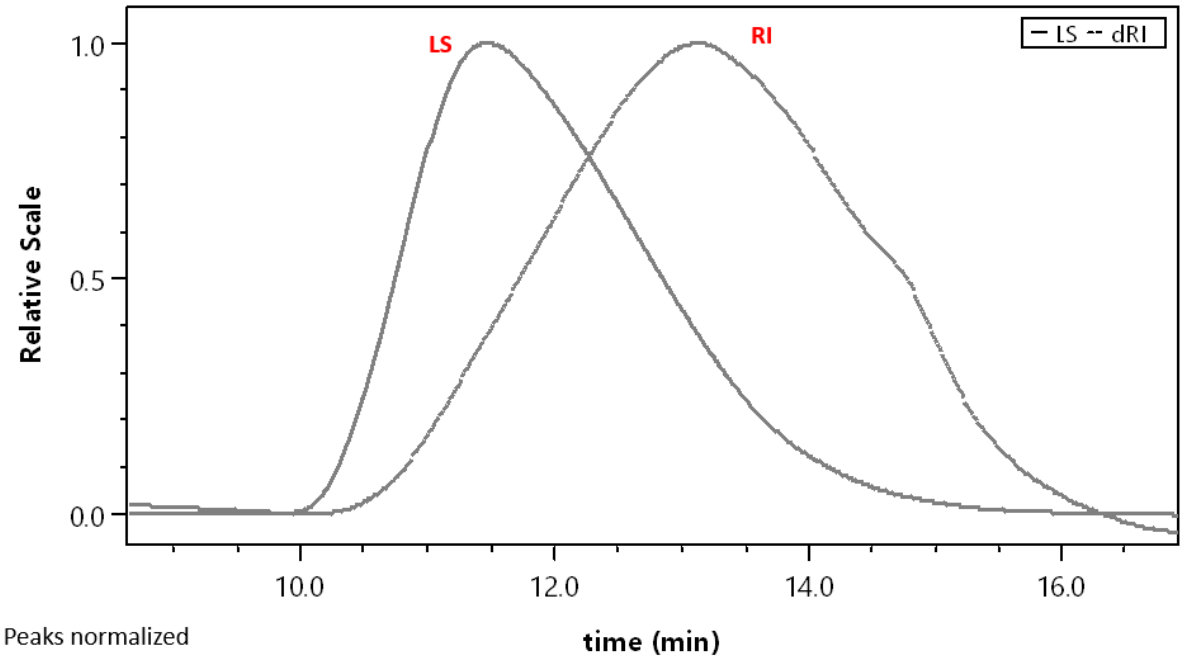

Figure 46. Light scattering and reflective index chromatogram of copolymer S2A.

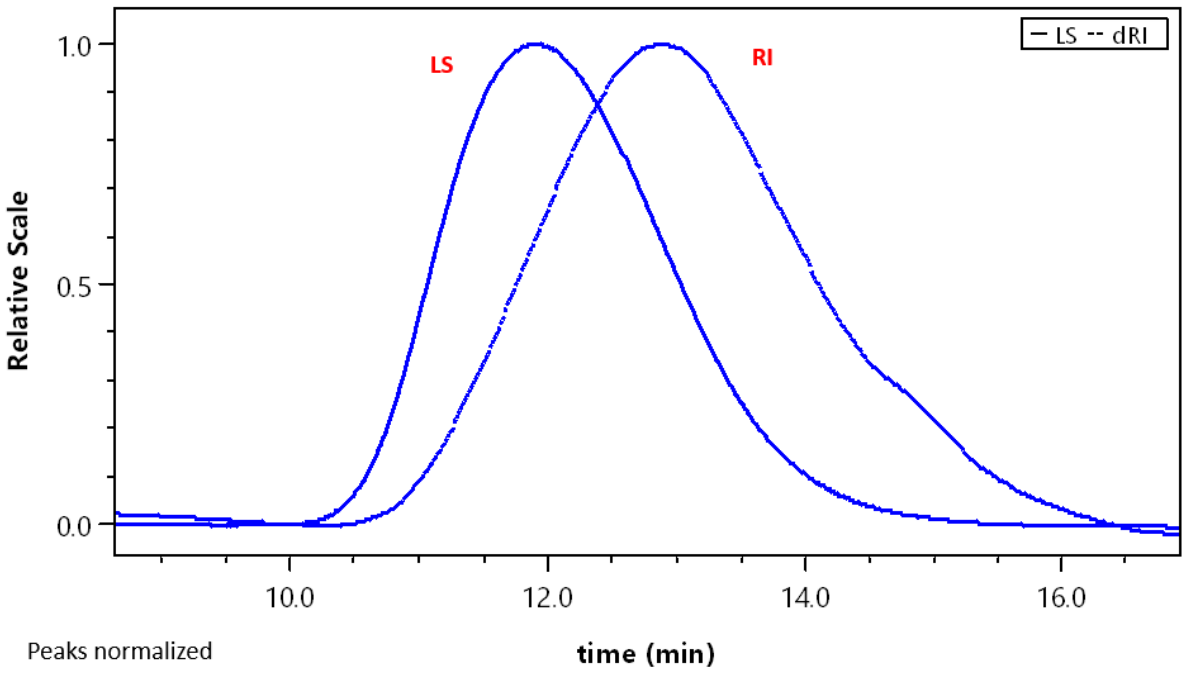

Figure 47. Light scattering and reflective index chromatogram of copolymer S2B.

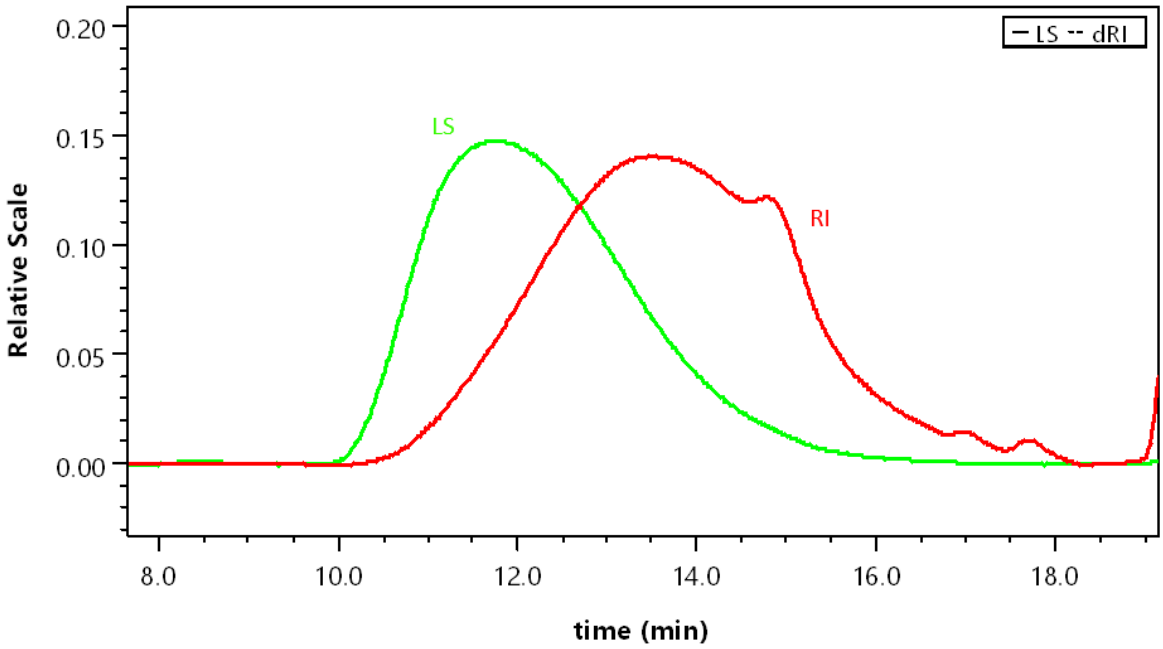

Figure 48. Light scattering and reflective index chromatogram of copolymer S3.

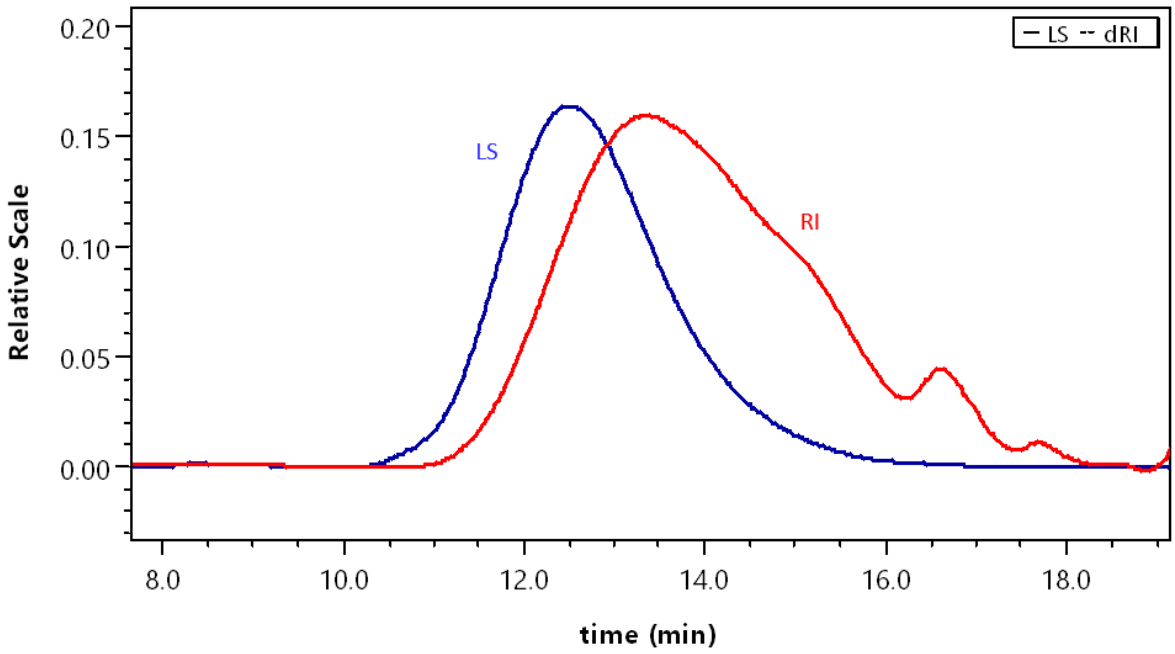

Figure 49. Light scattering and reflective index chromatogram of copolymer S4.

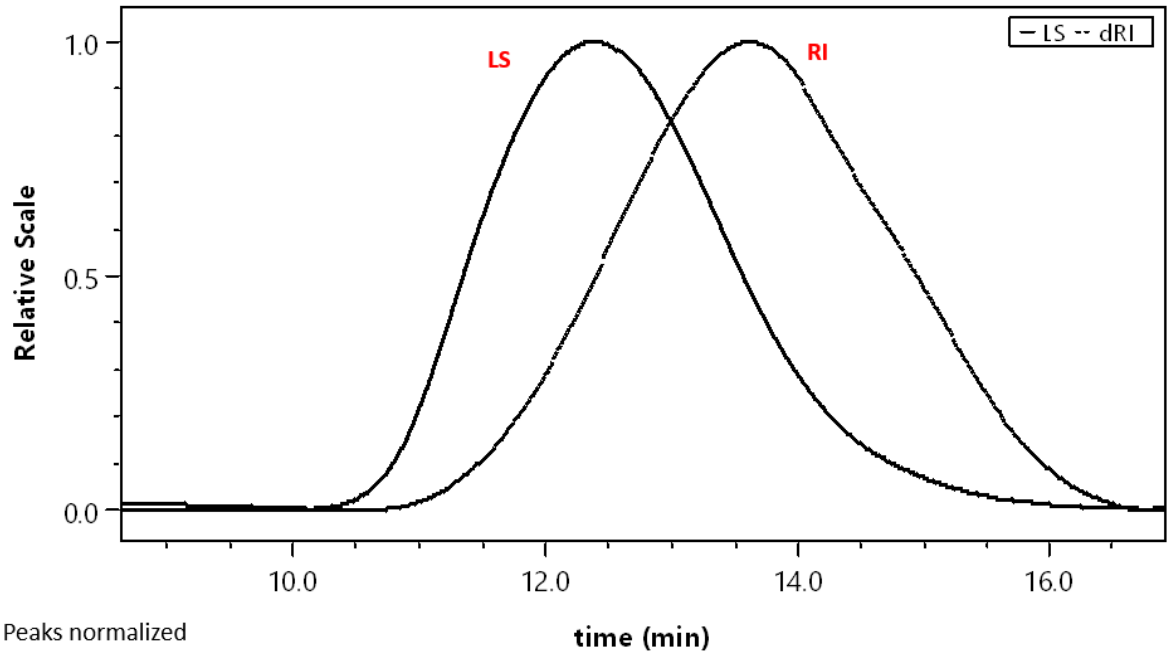

Figure 50. Light scattering and reflective index chromatogram of copolymer S6.

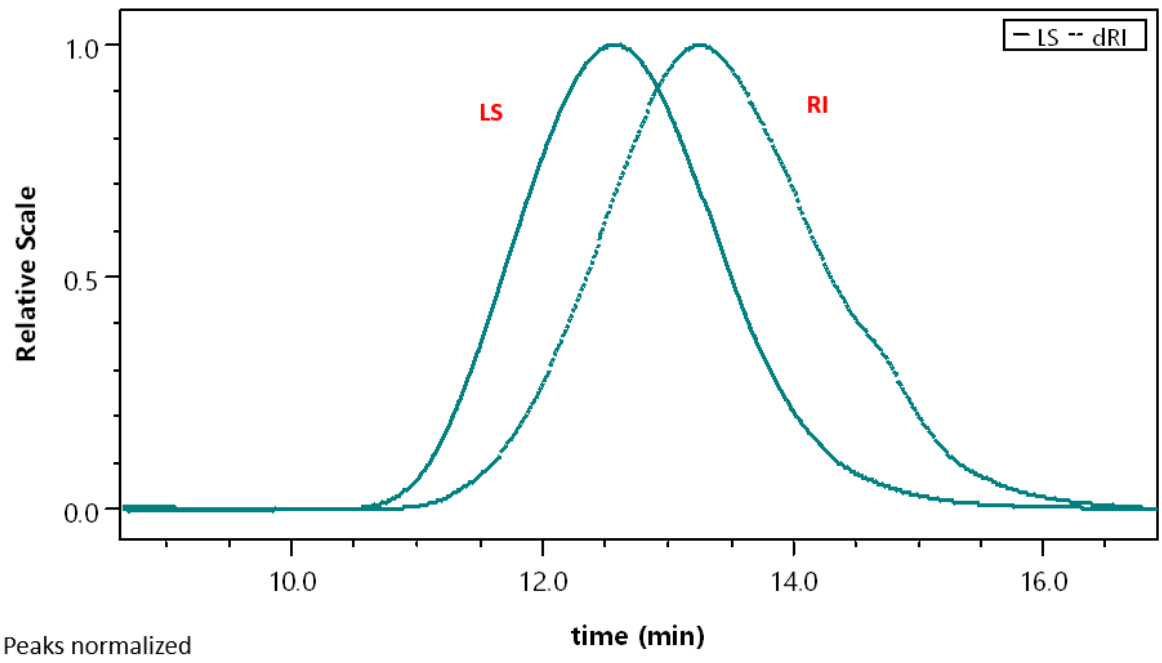

Figure 51. Light scattering and reflective index chromatogram of copolymer Soluplus®.

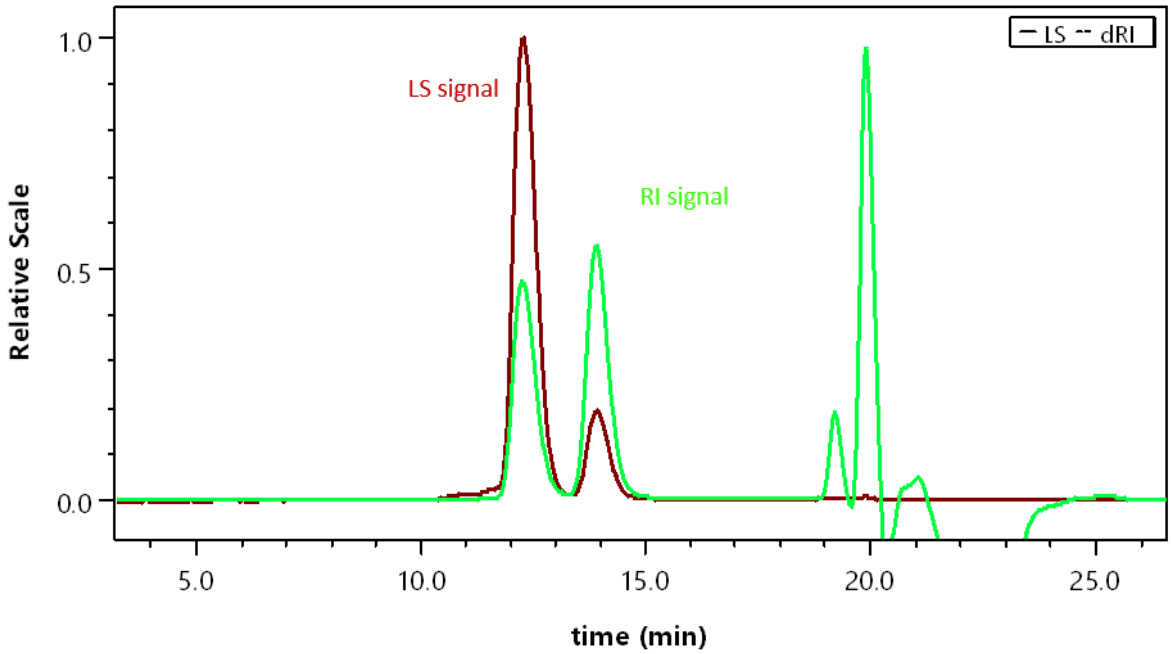

Figure 52. Light scattering and Refractive index chromatograms of Polystyrene Standards.

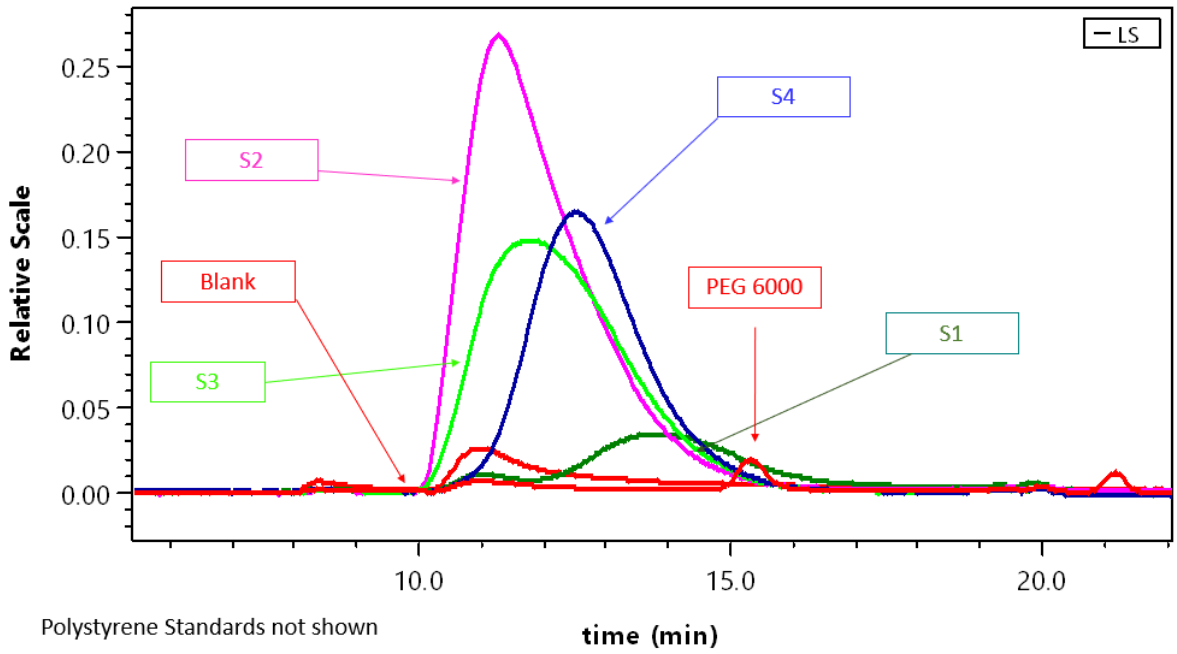

Figure 53. Light Scattering Chromatogram of blank sample, PEG 6000, copolymer S1, S2, S3, S4.

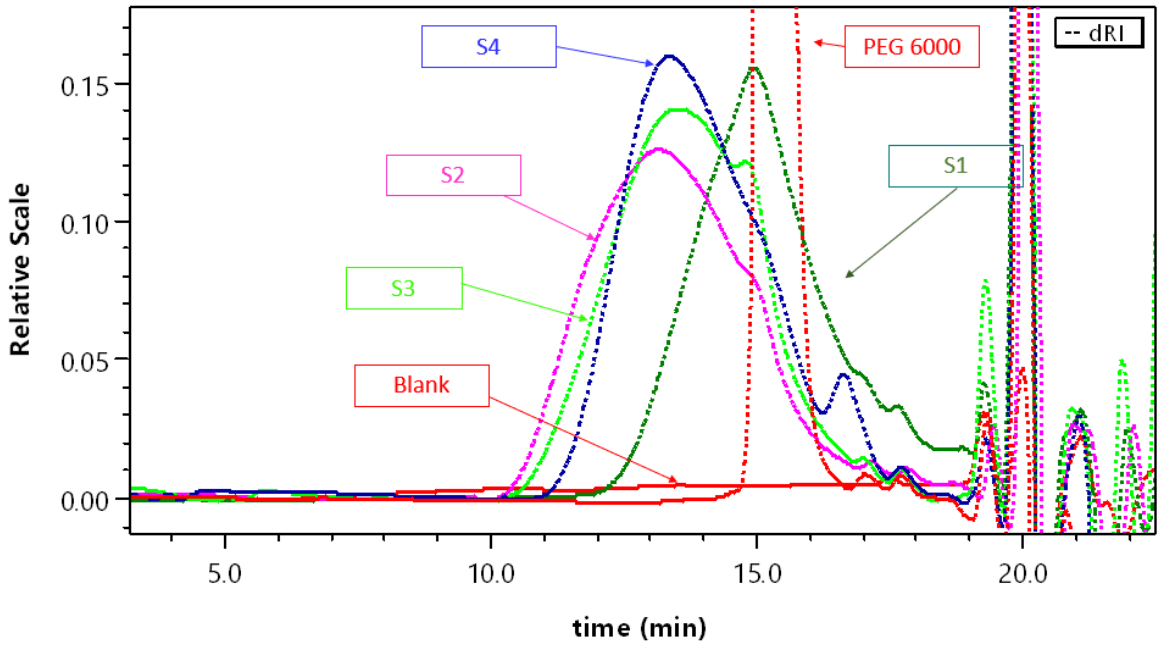

Figure 54 Refractive Index Chromatogram with PEG 6000 Standard, blank sample, copolymer S1, S2, S3, S4.

4.2.5 Composition investigation by MALDI-TOF mass spectroscopy

MALDI-TOF-MS has an advantage in the high-speed determination of structural information and purity of macromolecules as it allows for an absolute measurement of the molecular weight of each individual polymer chain in a sample.[207] In this regard, MALDI-TOF/MS has been used to clarify structure of the most promising graft copolymers (copolymer S2A, S2B) and compare them with commercial version, Soluplus®. This experiment was performed to check if the PEG Mw 6000 used into synthesis reaction of copolymer S2 has been bound to the other components and not remained free in the sample. For this reason, the molecular weight-based separation of copolymer S2A and S2B low concertation solution in water (7%) was first performed using 10kDa molecular weight cut off cellulose membrane. Filtrate of molecular weight lower than 10kDa was analyzed by MALDI-TOF mass spectroscopy. We assumed the PEG with Mw 6000 should be detected in analyte of 10 MW, if not bound to PVAc-co-PVCL part of copolymer. For comparison, the same procedure has been applied to Soluplus®. All MALDI mass spectra illustrated on **Figs. 55**, **56**, **57** display the absence of a characteristic strong single peak of PEG 6000 molecular weight, that implies no evidence of the presence of free PEG in the samples. On the other hand, the MALDI spectra of the copolymer S2A, S2B and Soluplus® filtrates showed mass-resolved peaks in the 602–7000 Da region (**Figs. 55-57**), indicating presence of by-products of free radical polymerization reaction, possibly small molecular weight copolymers or homopolymers[170] of 500- 3000 Da, also detected in DOSY experiment (**Figs. 21, 22, 26**). These results are in line with relatively broad polydispersity indices (**Table 6**) of the three investigated copolymers.

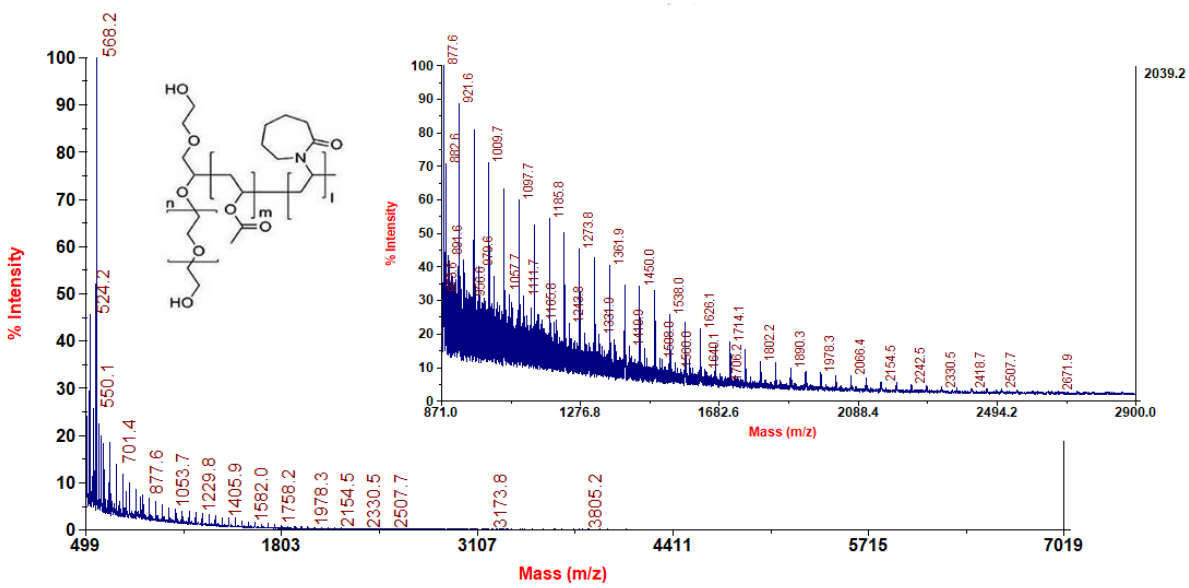

Figure 55. MALDI-TOF mass spectra of copolymer S2A filtrate.

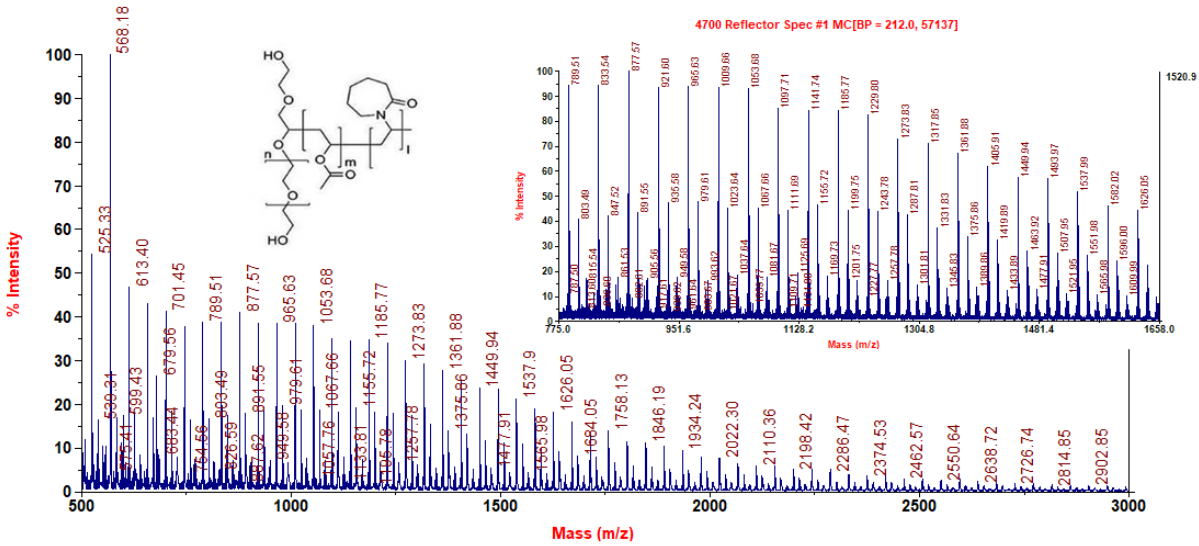

Figure 56. MALDI-TOF mass spectra of copolymer S2B filtrate.

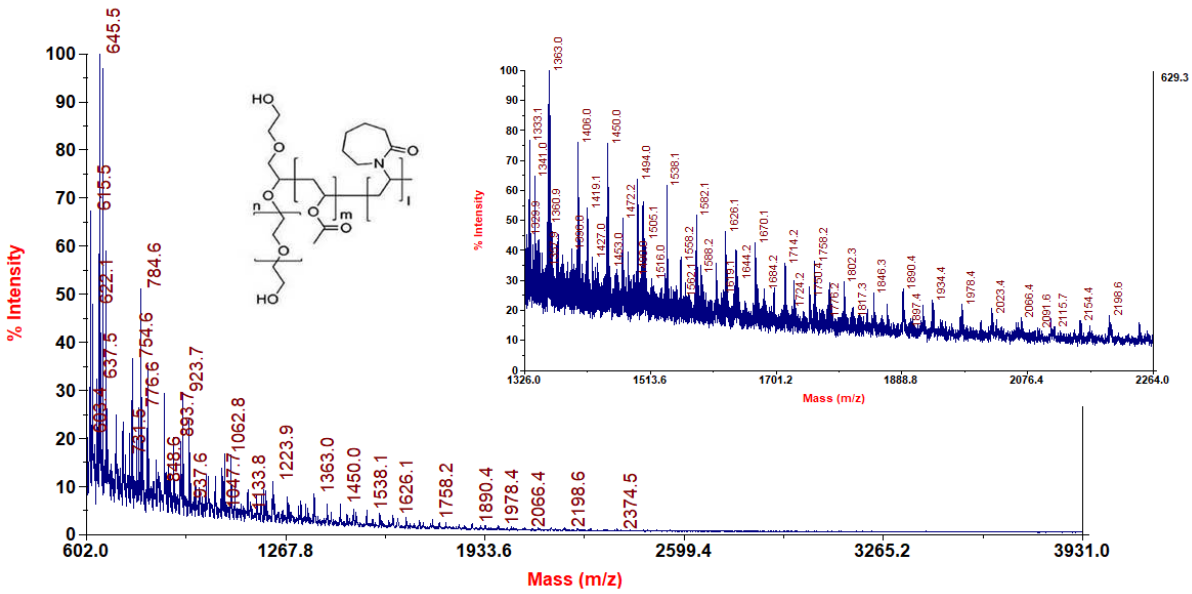

Figure 57. MALDI-TOF mass spectra of Soluplus® filtrate.

4.2.6 Thermal properties investigation by TGA and DSC

Thermogravimetric analysis (TGA) is conducted to measure weight changes as a function of temperature and time. The weight changes of polymeric materials can be caused by decomposition and oxidation reactions as well as physical processes such as sublimation, vaporization, and desorption. TGA measurements provide valuable information that can be used to select materials for certain end-use applications,

predict product performance, and improve product quality. The technique was particularly useful for the compositional analysis of synthetized multicomponent copolymers. TGA was used for precise and accurate analysis of composition and for the identification of polymers from their decomposition pattern and therefore, for quality and purity of copolymers and synthesis process control.[208] TGA measurements were also carried out to explore thermal stability of the synthetized S1, S2A, S2b, S3, S4, S6 graft copolymers and commercial copolymer Soluplus®, used as a reference. In our work, the thermal decomposition stability of the amphiphilic graft copolymers was investigated by taking mass loss into account, arising from volatile substances generated because of increasing temperature. The thermal decomposition temperature, and the temperature at the maximum decomposition rate for each S1, S2, S2C, S3, S4, S6, and Soluplus® amphiphilic graft copolymer obtained from the TGA curves are shown in **Figures 44-50.** To confirm the sample purity and formation of the new grafted copolymer material, thermal degradation curves of PEG Mw 6000 (**Fig. 58**), PEG Mw 1000 (**Fig. 59**), VCL (**Fig. 60**), PVAc (**Fig. 61**) were recorded. According to the thermograms of copolymer S1 and S4 (**Fig. 62, 64**), the decomposition occurs in one stage. Above about 428°C for copolymer S1 and 433°C for copolymer S4, the weight decrease is very sharp reaching the zero percent. Differently, for copolymers containing three components like copolymer S2A, S2B, S3, S6 and Soluplus® decomposition occurs in two stages. In the first stage at 305°C in S2A, at 312°C in S2B, at 300°C in S3, at 305°C in S6, at 324°C in Soluplus® weight loss was observed corresponding to the first degradation step of polyvinyl acetate portion of the copolymer due to the polyester chain scission.[209] It can be observed that temperature of degradation in first step increased with content of PVAc. The main weight loss for the copolymers S2A, S2B, S3, S6, Soluplus®, revealed in the second stage of the thermograms (**Figs. 63-67, 69-68**) was detected at 429°C in S2A, at 429°C in S2B, at 432°C in S3, at 429°C in S6 and at 435°C in Soluplus®. These temperatures were very close to each other, indicating similar composition of the two investigated polymers. The initial weight loss noticed on the thermograms resulted from absorbed moisture. The shifts to higher temperature of thermal degradation of S1, S2A, S2B, S3, S4, S6 and Soluplus® compared to the temperature of thermal degradation of analysed PEG, VCL, and PVAc components confirmed the formation of the new grafted copolymer materials.

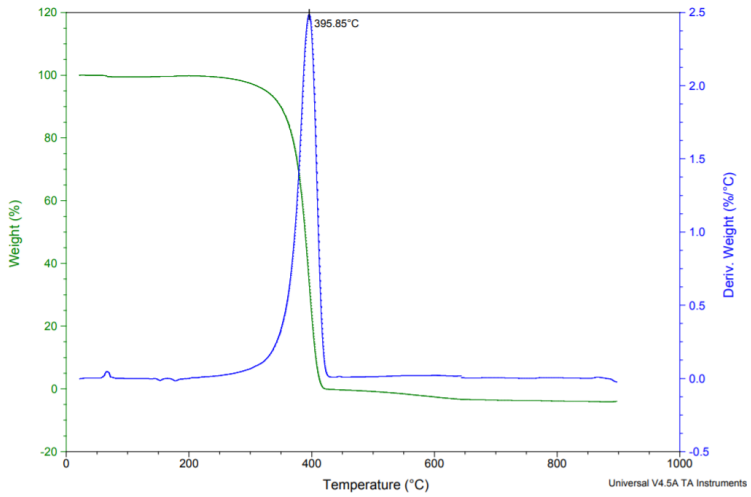

Figure 58. TGA thermogram of PEG 6000.

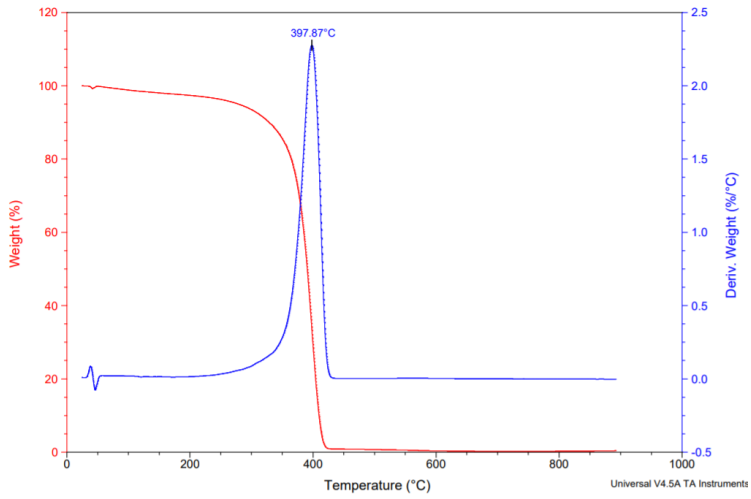

Figure 59. TGA thermogram of PEG 1000.

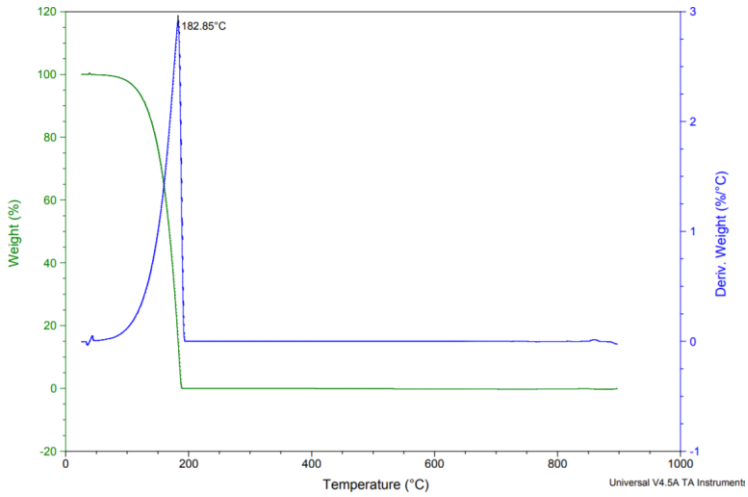

Figure 60. TGA thermogram of VCL.

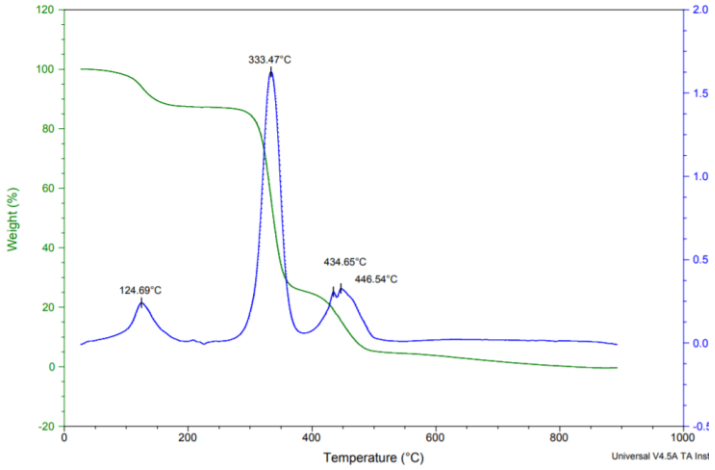

Figure 61. TGA thermogram of PVAc.

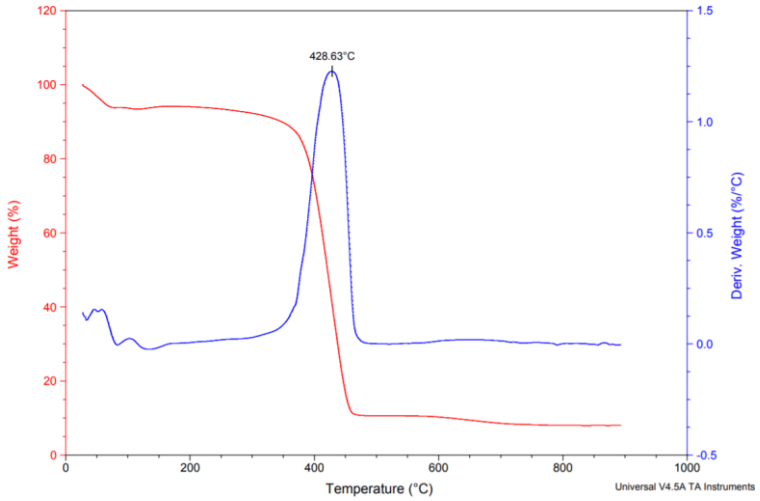

Figure 62. TGA thermogram of copolymer S1.

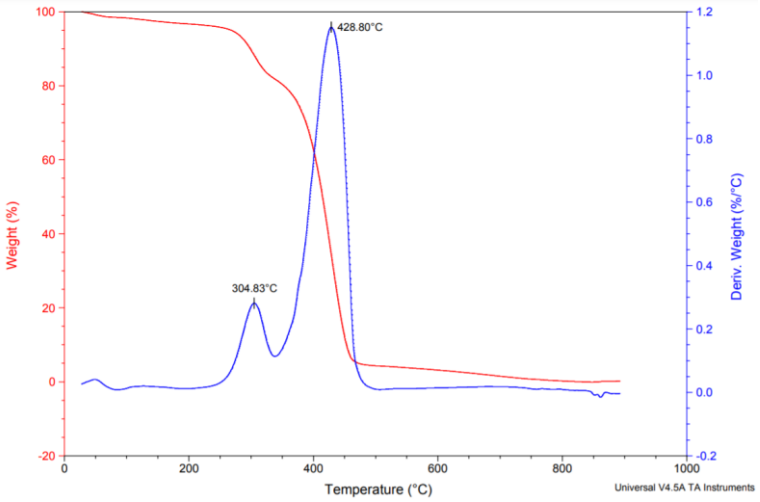

Figure 63. TGA thermogram of S2A

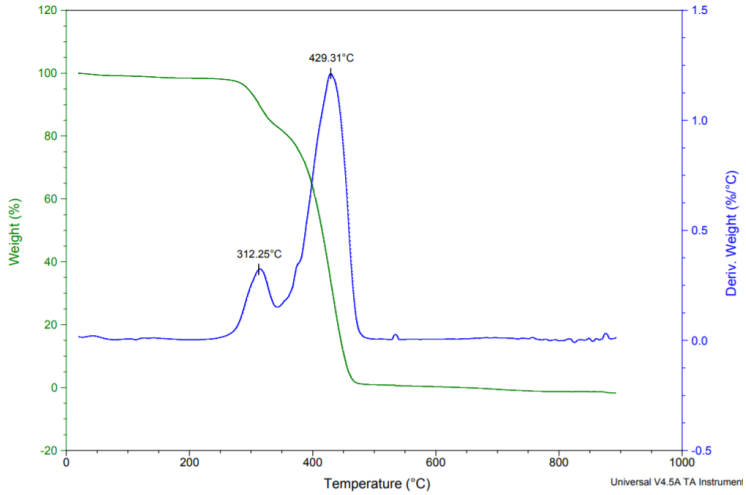

Figure 64. TGA thermogram of S2B

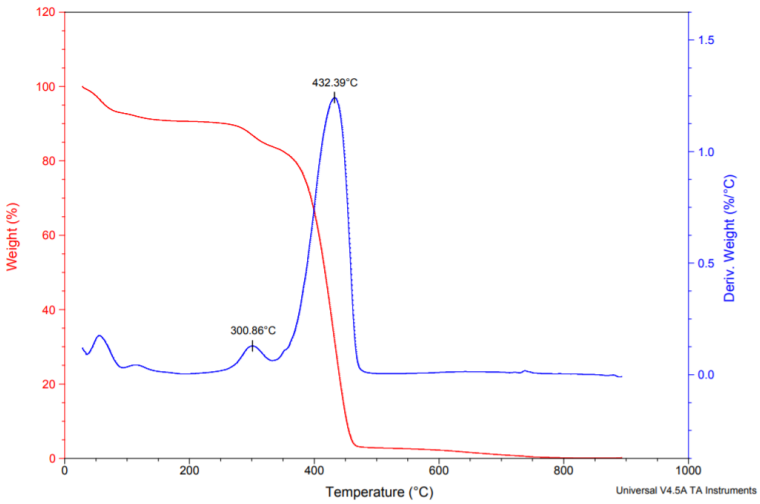

Figure 65. TGA thermogram of copolymer S3.

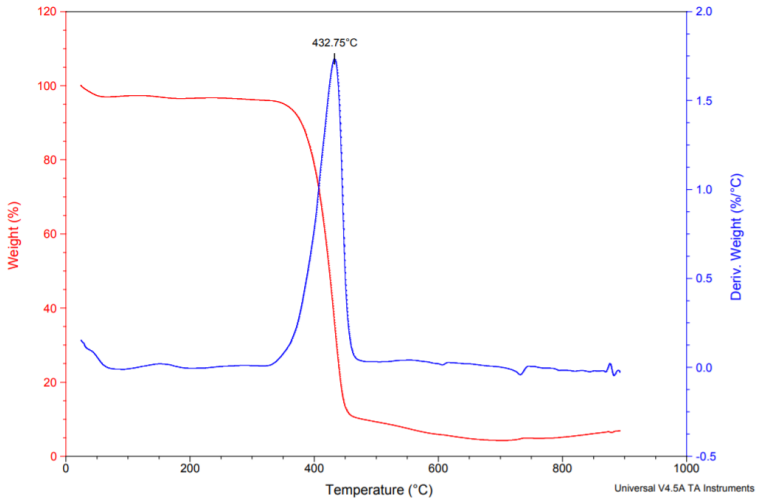

Figure 66. TGA thermogram of S4.

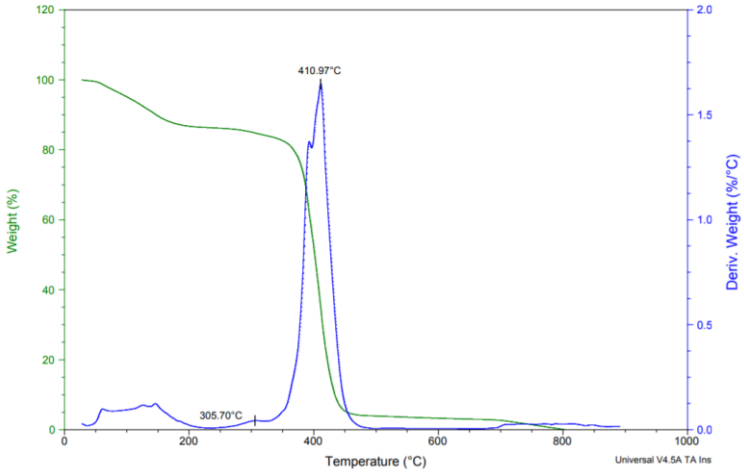

Figure 67. TGA thermogram of S6.

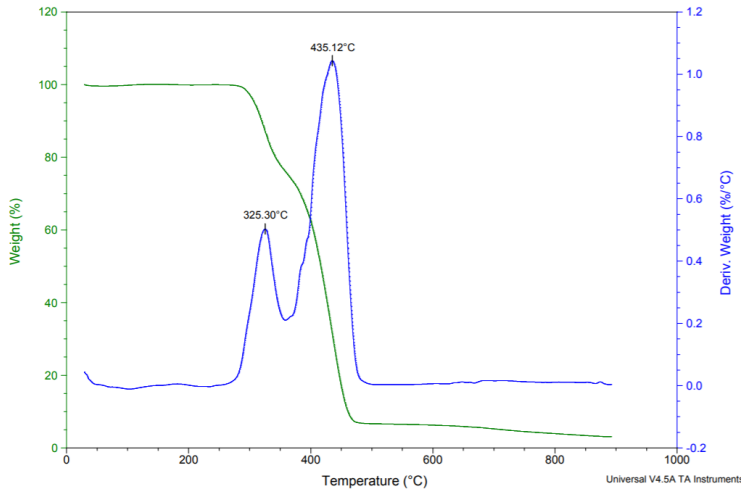

Figure 68. TGA thermogram of Soluplus®.

Differential scanning calorimetry (DSC) is a thermal analysis technique in which the difference in the amount of heat needed to increase the temperature of a sample and an empty reference is measured as a function of temperature providing quantitative and qualitative information about physicochemical changes in the materials. Properties that are mostly measured and studied using the DSC technique are decomposition behaviour, thermal/oxidation stability, boiling points, sample purity, glass transition and melting temperature etc. which depend on the chemical structure of the polymer and can therefore be used to identify polymers. With a DSC experiment it is possible to measure the amount of energy absorbed or released by a sample while it is heated or cooled.[210,211] Knowledge of thermal properties of polymer systems

provides basic information about chemical structure which is an important parameter for the polymer biodegradability study.[167]

To better understand thermal stability mechanism and to confirm, whether the synthetized copolymer is a polymers blend or a new single material, DSC analysis was performed on native components used into synthesis, copolymer S1, S2A, S2B, S3, S4, S6 and Soluplus® used as a reference. Measuring stability of VAc was impossible to handle and for the comparison, we used PVAc homopolymer synthetized by free radical polymerization method and Luperox initiator. The DSC thermograms of monomers and copolymers S1, S2A, S2B, S3, S4, S5, S6, and Soluplus® are given in **Figures 70-72** and components in **Figure 69**, respectively. Melting temperature T_m and glass transition temperature T_g values generated from the DSC curves of the amphiphilic graft copolymers and components are shown in **Tabale 13**. The melting endotherms of PEG Mw 6000 and VCL, copolymer S1, S3, S6 were found in thermograms presented by **Figures 69-70.** PEG Mw 6000 and PEG Mw 1000 showed a main endothermic transformation centred at 60.32°C, 38.59°C and VCL at 37.86°C. Melting transition T_m values of S1 and S3, S6 were very close to each other (approximately 37-54°C). No glass transition was observed in these graft copolymers, which might be linked to their crystallization ability.[170,212,213] The PVAc DSC thermogram showed T_g value at 6.84°C observed by a step in the baseline of the measurement curve. This temperature was no detected in any of synthetized copolymer. Reported on **Figure 71** thermographs of Soluplus and copolymer S2 and S2C were very similar. DSC curves exhibits a small step at a mid-temperature of about 87.19°C in copolymer S2A, 87.51°C in copolymer S2B and of about 52.03°C in Soluplus®, which is due to the glass transition, respectively to their comparable structure. Thermogram of copolymer S4 independently of similar structure to copolymer S1 did not expose softening pick observed in copolymer S1 but glass transition at 68.68°C. DSC thermograms of synthetized copolymers revealed no glass transition characteristic for PVAc and no melting endotherm detected for VCL and PEG, confirming the formation of a completely new material. Reported on S2A, S2B, S4 and thermograms (**Fig. 71**) the only one glass transition T_g and single Tm in copolymer S1, S3, S6 (**Fig. 70**) evidenced the formation of single material. The presence of a glass transition temperature and absence of the melting endotherm in copolymer S2, S2C, S4 and Soluplus® suggest amorphous character of the

copolymers.[213] It has been reported that several factors such as the backbone flexibility, polar/non-polar substituent, side group bulkiness (occupied volume), cross-linking and Mw can influence the T_g of polymers. Towards, the slightly higher glass transition T_g of the copolymer S2 compared to Soluplus® could be related to higher content of incorporated hydrophobic monomer,[214] lower grafting degree and lower molecular weight of commercial copolymer.[215,216] Knowledge of thermal properties of copolymers systems provided basic information about the chemical structure which is an important parameter that can strongly influence the biodegradation rate.[167,217]

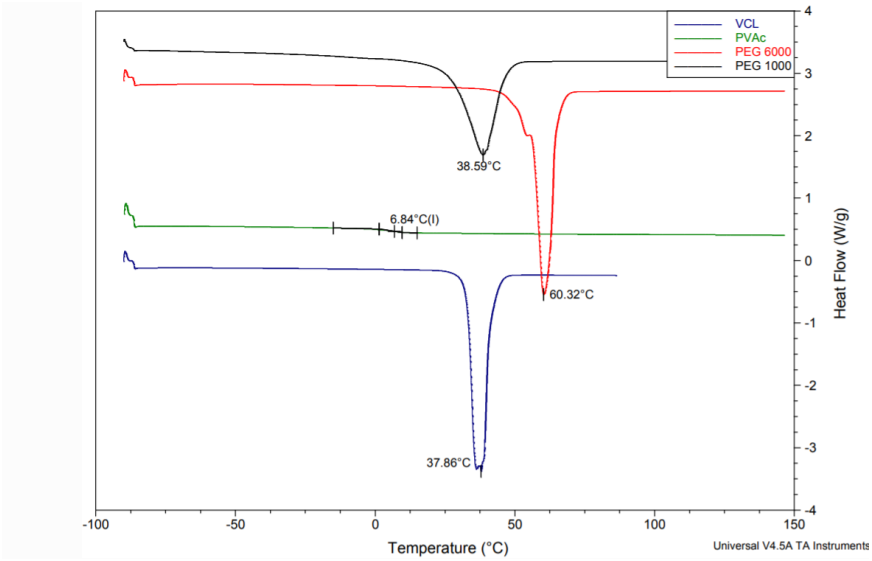

Figure 69. DSC thermogram of PEG 6000, PEG 1000, VCL and PVAc.

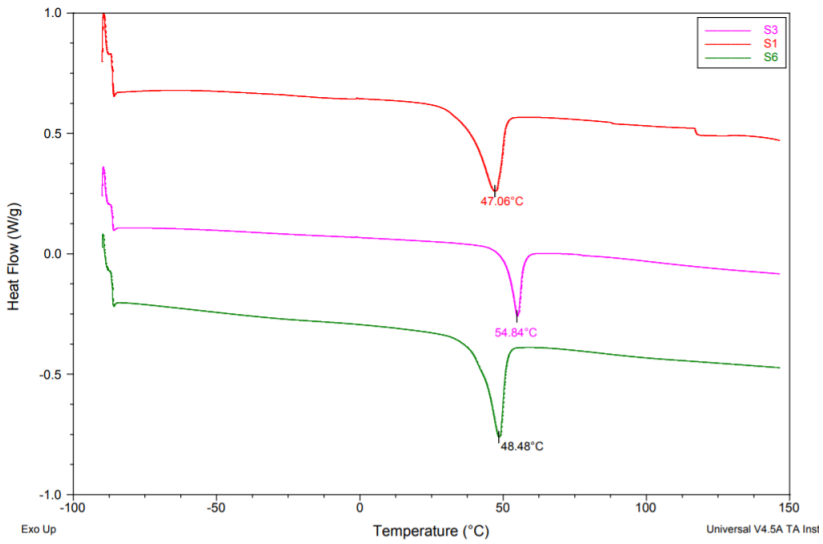

Figure 70. DSC thermogram of copolymer S1, S3, S6.

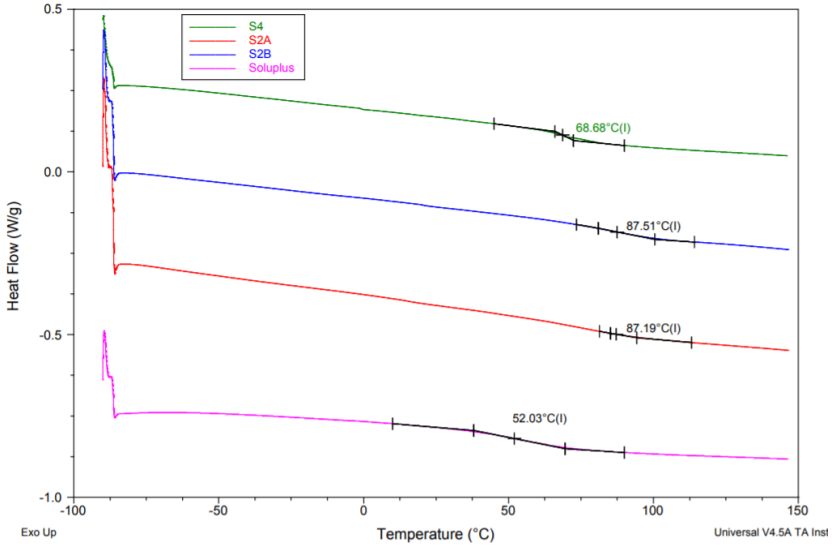

Figure 71. DSC thermogram of copolymer S2A, S2B, S4, and Soluplus®.

Table 13. Thermal properties of the PEG 6000, PEG 1000, VCL, PVAc, copolymer S1, S2A, S2B, S3, S4, S6 and Soluplus®.

Code	DSC (°C)		TGA (°C)		
	T_g	T_m	T_{d1}	T_{d2}	T_{d3}
PEG6000	–	60.32	–	396	–
PEG1000	–	38.59	–	398	–
VCL	–	37.86	183	–	–
PVAc	6.84	–	125	333	435-446
S1	–	47.06	–	429	–
S2A	87.19	–	305	429	–
S2B	87.51	–	312	429	–
S3	–	54.84	300	432	–
S4	68.68	–	–	433	–
S6	–	47.96	305	411	–
Soluplus®	52.03	–	325	435	–

4.2.7 Thermo-Responsive Properties - Cloud Point Study

Below the critical temperature, often referred to as the cloud point temperature T_{CP}, PEG-g-PVCL and PEG-g-(PVAc-co-PVCL) (**Fig. 19**) copolymers are amphiphilic, consisting of a hydrophilic backbone (PEG) and grafted hydrophobic side chains (PVAc-co-PVCL). Above the cloud point temperature (T_{CP}) a transparent solution can undergo either a liquid-liquid phase separation (LLPS) to form a stable colloidal suspension or a liquid-solid phase transition to form a suspension that tends to precipitate. Above this critical temperature point, the solution develops turbidity and becomes cloudy. The phase separation occurred during heating, showing a cloud point as a formation of the cloudy solution, because of the disruption of hydrogen bonds between the polymer and water, the hydrophobic aggregation and the hydrogen bonding between the polymer chains.[218]

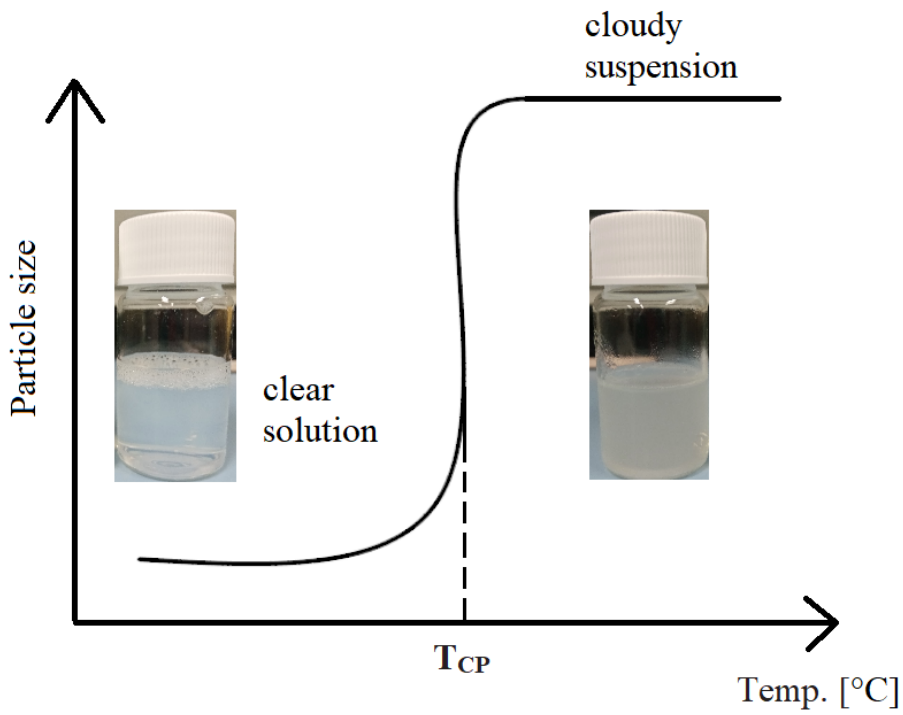

Figure 72. Cloud point.

In the present study, the cloud points of synthetized copolymers S1, S2A, S2B S3, S4, S6 and Soluplus® were measured on 1wt% copolymer aqueous solution. All obtained copolymers were completely soluble in cold water below their T_{CP} (**Fig. 73a**) and their solutions remained transparent. **Figure 73b** showed an optical micrograph of S1, S2A, S2B, S3, S4, and S6 1% aqueous solutions at 25 ° C, where LLPS occurs and coacervate droplets are observed upon heating above their T_{CP}.[219–222] All copolymers consist of a hydrophilic PEG backbone and hydrophobic/PVAc-*co*-PVCL graft chains.

The copolymers show amphiphilic behaviour below their T_{CP}, but they become hydrophobic above their T_{CP}, and tend to precipitate out of the water phase. This transition of 1% copolymer solution in water from transparent to cloudy as a reaction on the certain temperature was considered as a cloud point temperature. All T_{CP} transitions from the experiment are summarized in **Table 14** together with molecular weight (Mw), ratio between PEG/PVAc/PVCL components and degree of grafting, to provide a complete overview. It can be observed that cloud point decreases as follows: S1> Soluplus®>S4>S6>S3>S2A>S2B. From the numerous studies on synthetic nonionic amphiphilic solutions that undergo T_{CP} induced LLPS, it is evident that this parameter is affected by several properties of the amphiphile, including its Mw, graft length, grafting degree and the ratio between its components.[223] Among all synthetized copolymers the lowest cloud point temperatures are showed by copolymers S2A (21.6°C) and copolymer S2B (20.8 °C) [**Fig. 73b**]. The T_{CP} of all PEG-g-PVCL and PEG-g-(PVAc-co-PVCL) amphiphilic graft copolymers solution showed a reverse relation with the polymer's Mw[224–227] (Table 8). A longer hydrophobic chain, and, as a consequence higher Mw, likely exhibits increase in the hydrophobic polymer–polymer interactions, resulting in a decreased T_{CP}. **Table 14** also indicates that the T_{CP} decreases for higher degree of grafting of PVAc-*co*-PVCL or PVCL relative to the PEG backbone. It has been established from previous studies that incorporation of hydrophobic comonomers leads to a lower LCST whereas hydrophilic comonomers to a higher LCST.[228] In the present case, copolymers S2, S3 and Soluplus® displayed similar content (14-18%) and the same length of PEG 6000 that is the most hydrophilic part of copolymers. Thus, the different thermal response of investigated copolymers can apparently be influenced by the differences in total molecular weight more than in amount and distribution of hydrophobic PVAc-*co*-PVCL grafts. However, increasing the degree of branching, the competition between the hydrophilic segments of the copolymer (EO and VCL units) to interact with water is diminished by weakening the interactions of VCL with water in the vicinity of EO, promoting LLPS. In a similar way, the T_{CP} was found to decrease with increasing the grafting degree of the polymer in studies involving a similar graft copolymer, PVCL-*g*-PEO.[56,229] Consequently, as the Mw of those copolymers grows by successive addition of more hydrophobic part of PVAc-*co*-PVCL and the grafting degree of that part is higher, the hydrophobic composition of the copolymer is increased. Therefore, the hydrogen bonding between the copolymer chains and water is lowered while hydrophobic interactions are

enhanced, thus lowering the required energy for the copolymer to collapse and experiences phase separation at relatively lower temperatures.[219] Since the molecular weight of Soluplus® was the lowest among three components copolymers, the commercial copolymer showed the lowest cloud point temperature at about 37-38°C (**Tab. 14**). Compared to the other PEG-g-(PVAc-*co*-PVCL) copolymers, copolymer S6 exhibits similar molecular weight to the copolymer S3 but about 6% higher content of hydrophilic PEG Mw 20000 and about half lower degree of grafting (**Tab. 14**). For the copolymer S6, the difference observed in the cloud point temperatures can be attributed to both the higher Mw and the higher amount of PVCL block, when compared to Soluplus®. It should be noted that by increasing the content of the hydrophobic poly (N-vinyl caprolactam) that is a thermoresponsive polymer with a cloud point of about 30–40°C depending on the molecular weight and method of polymerization, the cloud point temperature decreased. The same phenomenon was observed in PEG-g-PVCL copolymers. The higher Mw (**Tab. 14**) in copolymer S4 shifted the cloud point significantly to lower temperatures (33°C) in comparison to the cloud point of copolymer S1 (39.5-40°C). In this trend there is a small deviation for copolymer S3 and Soluplus probably due to the presence of different driving forces of the T_{CP} such as a higher content of thermoresponsive PVCL and higher MW having stronger impact on T_{CP}. This explained the fact that the cloud point temperature is influenced by many different factors such as Mw[226], the type of components and their thermosensitive properties[230] as well as by grafting degree. Complex structural and dynamic features as well as collective phenomena involving many macromolecules are the main factors influencing amphiphile systems near the cloud point.[28]

Table 14. Cloud point temperatures T_{CP} for copolymer S1, S2A, S2B, S3, S4, S6 and Soluplus® aqueous solutions, their compositions, and molecular weights.

Polymer name	Cloud point temp. [°C]	Mw [kDa]	Ratio [%] PEG/PVAc/PVCL	Degree of grafting [PVCL u/100 PEG u]
S1 PEG_{6000}-g-PVCL	39.5-40	42.0	31/-/69	65
S2A PEG_{6000}-g-(PVAc-co-PVCL)	21.6	195.0	15/25/60	155
S2B PEG_{6000}-g-(PVAc-co-PVCL)	20.8	193.0	14/25/61	145
S3 PEG_{6000}-g-(PVAc-co-PVCL	28.5-29	128.9	18/14/68	100
S4 PEG_{1000}-g-PVCL	33.0	107.0	10/-/90	300

S6 PEG_{20000}-g-(PVAc-co-PVCL)	30.0	125.2	24/09/67	52
Soluplus® (reference)	37-38	98.0	16/32/51	112

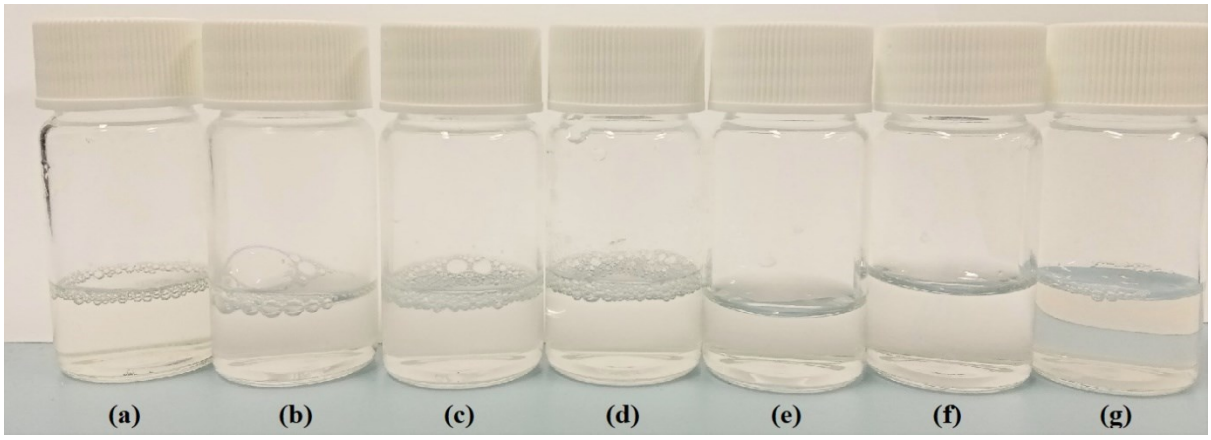

Figure 73a. 1% wt aqueous solutions of copolymer (a) S1, (b) S2A, (c) S2B, (d) S3, (e) S4, (f) S6 and (g) Soluplus® at 15 °C.

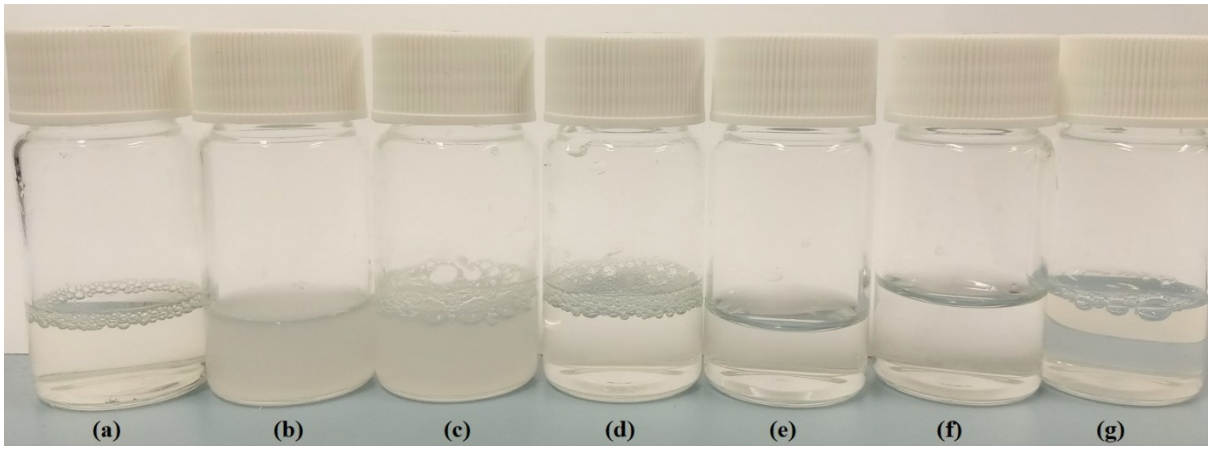

Figure 73b. 1% wt aqueous solutions of copolymer (a) S1, (b) S2A, (c) S2B, (d) S3, (e) S4, (f) S6 and (g) Soluplus® at 23 °C.

4.3 Application of copolymers S1 (PEG_{6000}-g-PVCL), S2 (PEG_{6000}-g-(PVAc-*co*-PVCL)), S3 (PEG_{6000}-g-(PVAc-*co*-PVCL)), S4 (PEG_{1000}-g-PVCL), S6 (PEG_{20000}-g-(PVAc- *co*-PVCL)) as perfume carriers - microscope observation.

4.3.1 Effect of the different polymer architecture and properties on capsules formation process and encapsulation of volatile compounds.

This part of the work relies on the study of capsules formation and encapsulation of benefit agents like perfumes and/or perfume single components (PRMs) of Poly(Ethylene Glycol)-graft-[Poly(Vinyl Acetate)-*co*-Poly(vinyl Caprolactam)] and of Poly(Ethylene Glycol)-graft-Poly(Vinyl Caprolactam) copolymers [PEG-g-(PVAc-*co*-PVCL)] (PEG-g-PVCL) in water and liquid detergent formulation. The original idea focused on using new synthetized copolymers as a microcarriers for fragrance control delivery in home and personal care products. Complex liquid matrices used in household products are composed mainly on a mixture of surfactants and perfume in water. Industrial perfume usually consists in a mixture of many fragrances or perfume raw materials (PRMs) (sometimes 50 – 100 difference PRMs). To understand better how capsules are formed in those matrices, self-assembly copolymers behaviour in water in the presence of a single perfume molecules or perfume and/or surfactant was investigated. A liquid fabric enhancer (LSFE) product works by depositing lubricating ingredients on the fabric, aiming to make it feel softer, to reduce static cling, and to impart a fresh fragrance. LSFE containing 90% water and catanionic surfactant have been selected since in the market today many fabric enhancer products contain perfume microcapsules.[6,231] Commercial perfume BZ and PRMs with different hydrophobicity [expressed by the water/octanol partition coefficient, logKow: Carvone (CA, logKow= 2.74), Methyl anthranilate (MA, logKow=1.9)] were used in the encapsulation studies, to investigate the effect of the nature of the perfume on the phase behaviour and capsule formation ability of the system.[232,233] The morphologies of microcapsules were examined by regular fluorescence microscopy. As a first step, PEG-g-(PVAc-co-PVCL)] (PEG-g-PVCL) has been labeled with a red fluorescent probe (Rhodamine B isothiocyanate (RBITC, ex=400 nm), (see **Scheme 6**) to investigate a possible relation between the polymer and the before mentioned microstructures (see Chapter III 2.4.2.1.). MA has been used to confirm encapsulation of PRM thanks to its light blue-violet fluorescence signal at 589 nm of wavelength. Typical observation under the optical and fluorescence microscope for each sample of synthetized copolymers and comparison with the commercial polymer Soluplus® in water and LSFE with two PRMs CA and MA are presented in **Figure 74** and **Figure 75.** Samples prepared in the LSFE with the CA and MA can be seen in **Figure 76** and **Figure 77,** copolymer S2 in LSFE with presence of commercial perfume BZ is present at **Figure 78.** Self-assembly studies in water medium with L-carvone showed that all copolymers form capsules in 0.5% concertation of copolymer (**Fig.74A, 74B, 74C,**

74D, 74E, 74G). In all the cases, different size distribution of the polymeric micron-sized spherical objects (micro-capsules) can be observed and copolymer S6 led to smaller in size capsules than rest of analysed materials (**Fig.74F**). In **Fig.74A-G** the formation of polymeric micro-capsules is confirmed, via the red signal coming from the rhodamine-b labelled polymer. Different self-assembly behaviour of investigated copolymers has been detected in water in presence of more hydrophilic PRM, Methyl anthranilate. Only copolymer S2 (S2A, S2C) and S1 confirmed capsules formation and encapsulation of MA in water as the fluorescence signal of labelled copolymer coincides with the signal of MA (**Fig. 75A, 75B, 75C**). Commercial Soluplus® and copolymer S3, S4 and S6 were not able to form micro-capsules with low logKow PRMs like methyl anthranilate. **Figure 75D, 75E, 75F, 75G).** Samples of the synthetized copolymers and Soluplus® prepared in the LSFE with CA showed capsules formation only in case of copolymer S2 (S2A and S2B) (**Fig. 76A, 76B**). No micro-capsules but the red background (**Fig. 76C**) was observed under the microscope when the rest of analysed copolymers were used. The same copolymers (S2) self-assembled into microcapsules and encapsulated MA in LSFE base (**Fig.77D-E**). Microscope images of copolymer S3 and S6 in LSFE with MA, differently to formulation with CA, showed spherical shape polymer aggregation (**Fig.77B-C**). Soluplus® did not lead to the formation of micro-capsules, as evident by a red fluorescent background, suggesting a polymer-rich solution, and a blue-fluorescent background, suggesting the diffusion of the perfume in the solution. By mixing copolymers with commercial perfume BZ in LSFE, microcapsules were observed only with polymer S2. Micro-capsules were not observed in the reference LSFE solution (without the addition of polymer) or in the product with the polymer Soluplus®. Micrographs with the capsules with copolymer S2 and Perfume BZ can be seen in **Figure 78.**

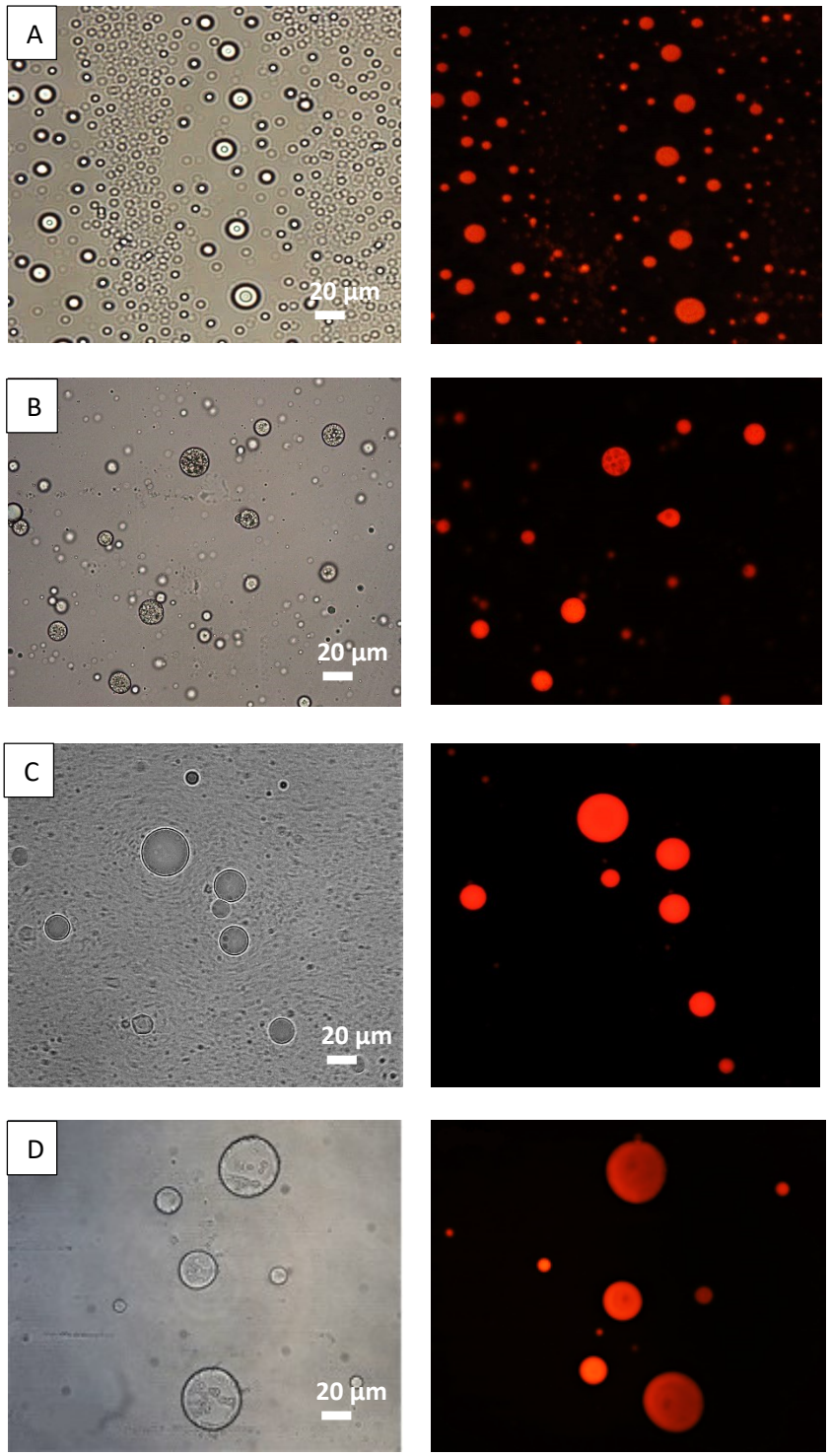
A
20 µm
B
20 µm
C
20 µm
D
20 µm

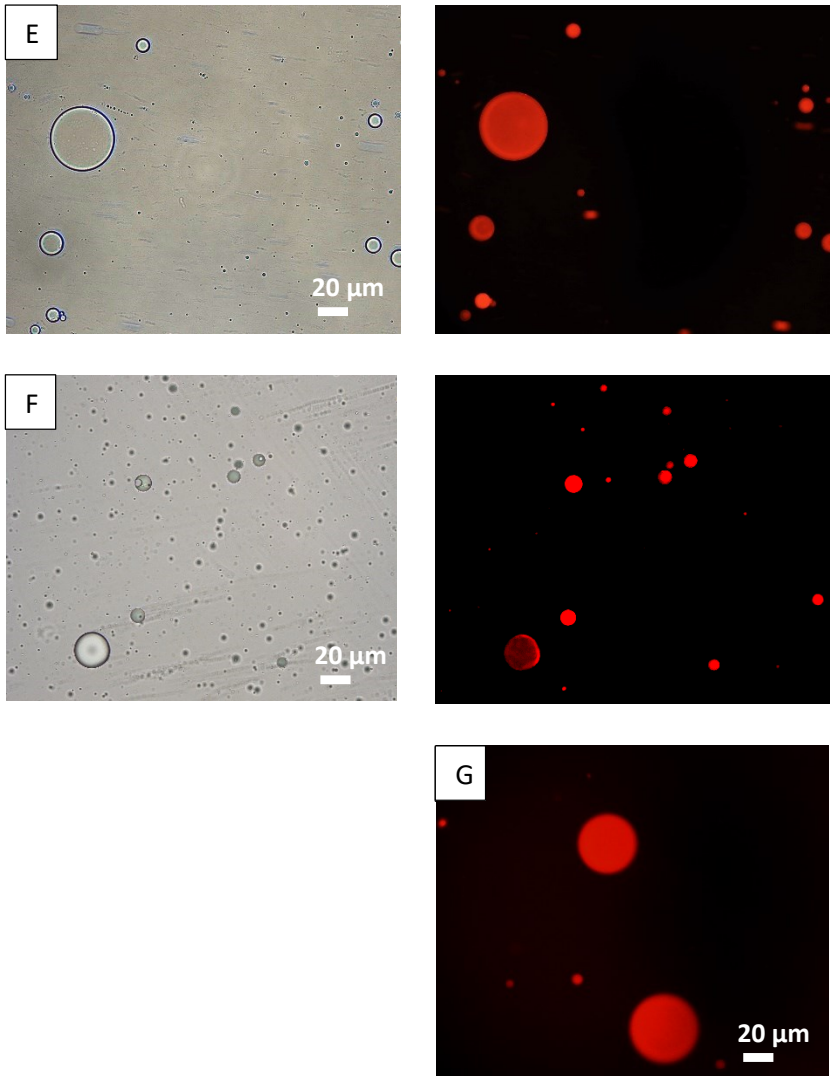

Figure 74: Microscope images of 0.5% copolymer (A) S1, (B) S2A, (C) S2B, (D) S3, (E) S4, (F) S6, (G) Soluplus®, and 0.5 Carvone in water. Left: Tracking of polymer by optical microscope and Right: Tracking of the labelled polymer using the appropriate filters as mentioned in the main text.

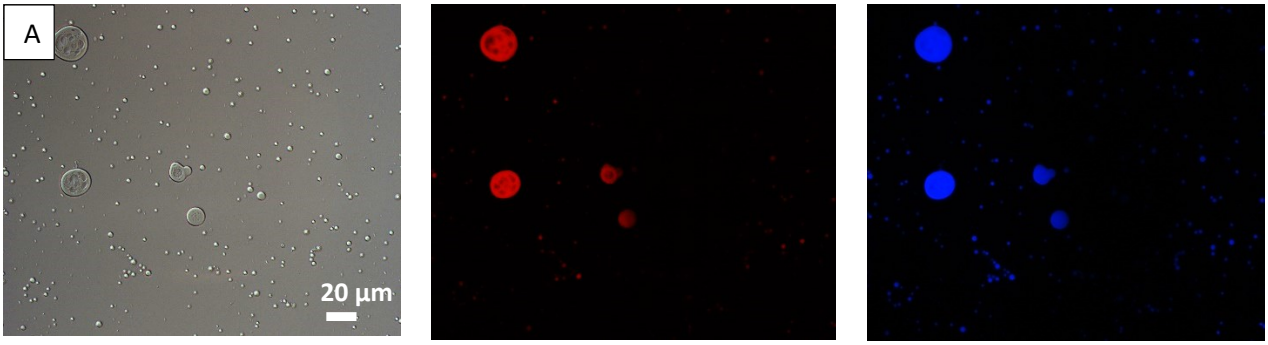

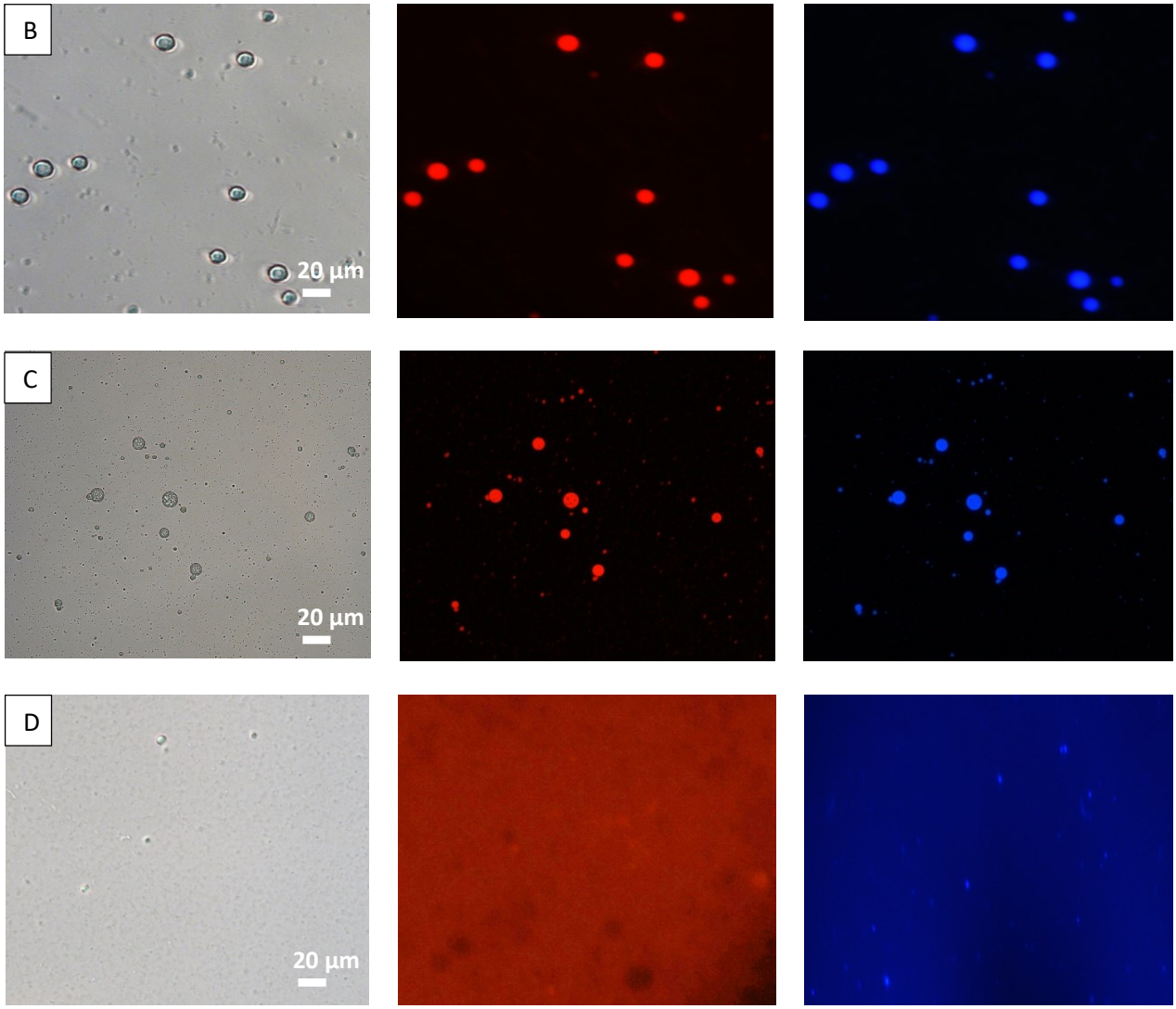

Figure 75: Microscope images of 0.5% copolymer (A) S1, (B) S2A, (C) S2B, (D) S3, S4, S6, Soluplus®, and 0.5 % Methyl anthranilate in water. Left: Tracking of polymer by optical microscope, Middle: Tracking of the labelled polymer and Right: Tracking of Methyl anthranilate using the appropriate filters as mentioned in the main text.

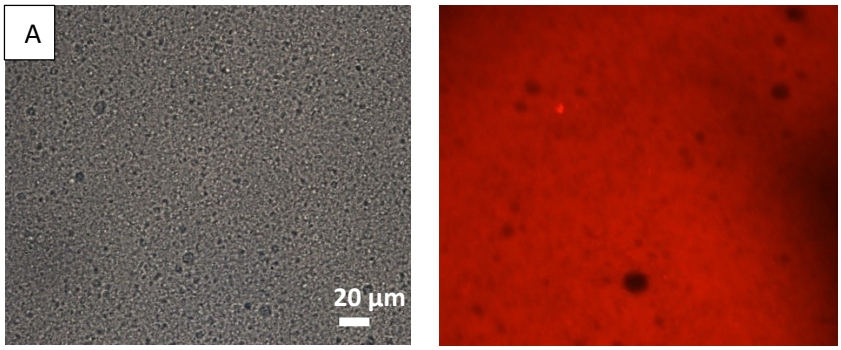

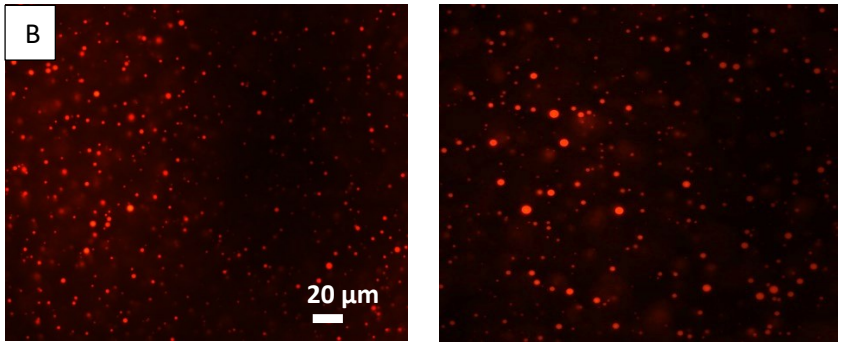

Figure 76: Microscope images of 0.5% copolymer (A) S1, S3, S4, S6, Soluplus® and 0.5 Carvone in LSFE. Left: Tracking of polymer by optical microscope and Right: Tracking of the labelled polymer using the appropriate filters as mentioned in the main text. Microscope images of 0.5% copolymer (B) S2A, S2B, and 0.5 Carvone in LFE. Tracking of the labelled polymer using the appropriate filters as mentioned in the main text.

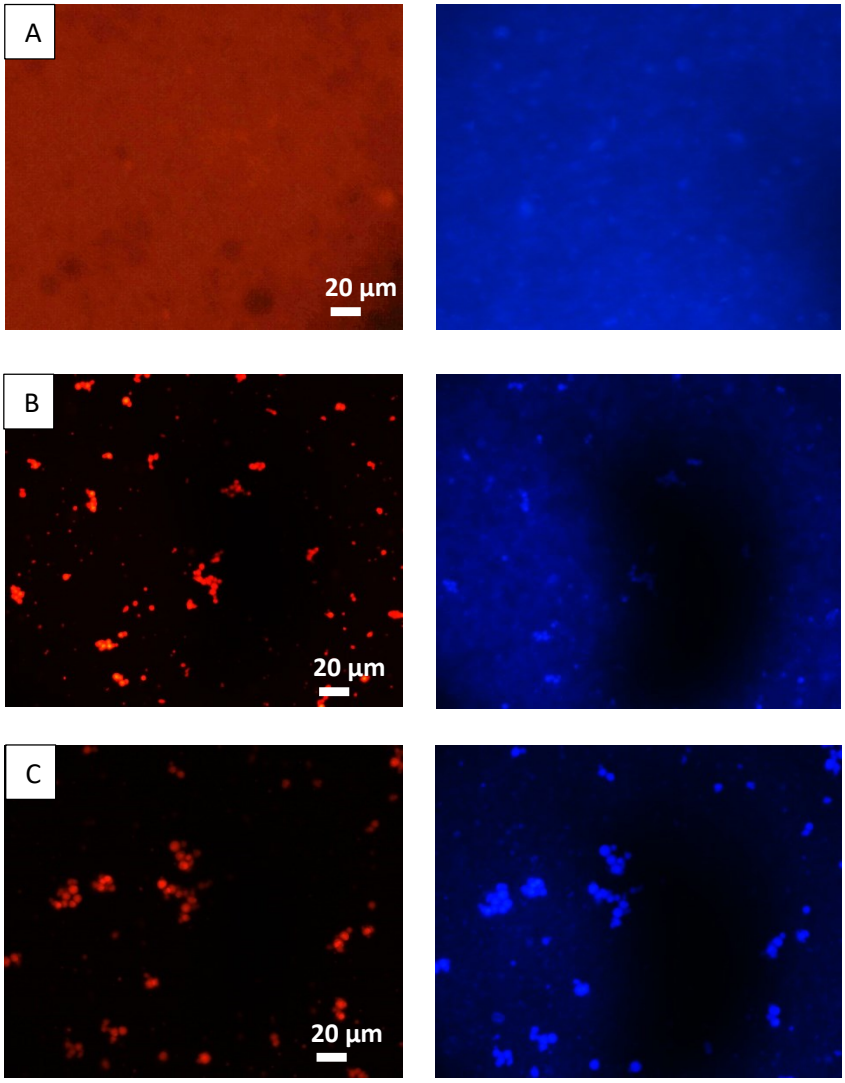

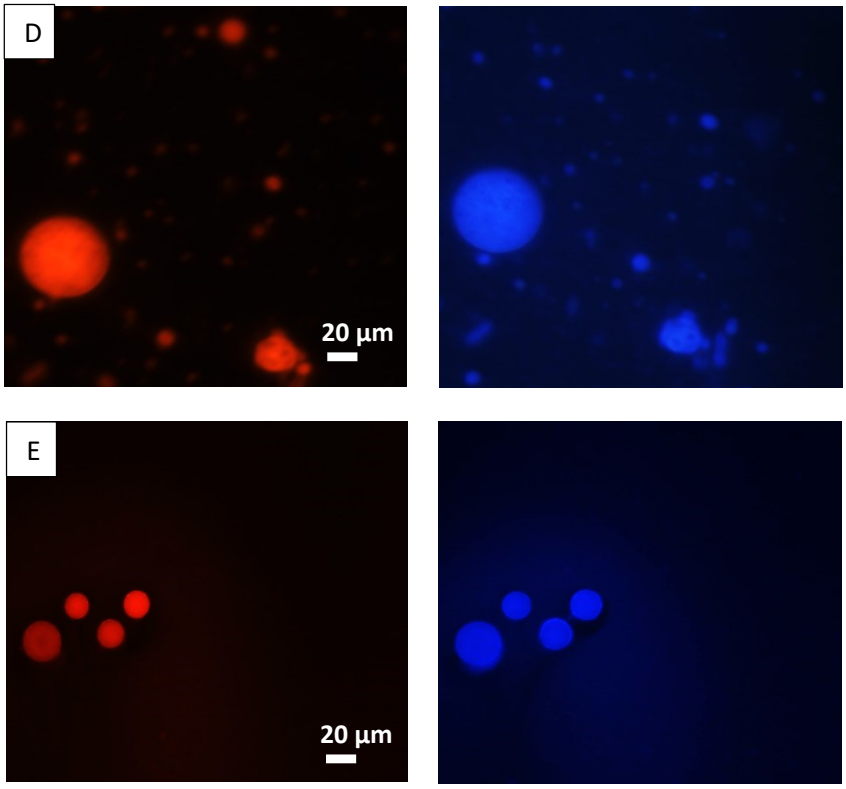

Figure 77: Microscope images of 0.5% copolymer (A) S1, S4, (B) S3, (C) S6, (D) S2A, (E) S2B and 0.5 Methyl anthranilate in LFE. Left: Tracking of the labelled polymer and Right: Tracking of Methyl anthranilate using the appropriate filters as mentioned in the main text.

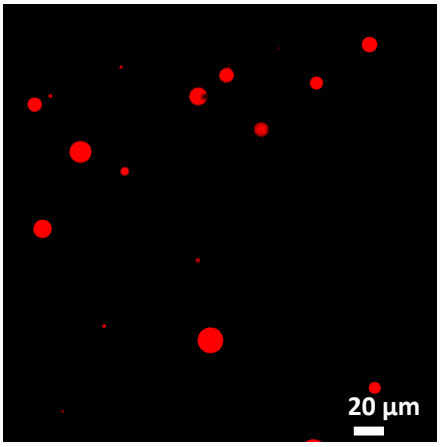

Figure 78: Fluorescence microscope image of copolymer S2 in LFE in presence of commercial perfume BZ.

The micro-capsules formed with the copolymer S2 (S2A, S2B) in LSFE are the result of different phenomena affecting the self-assembly of the species present in the solution. These include the LLPS driven by the cloud point behaviour of the

copolymer, the interactions arising between the copolymer and the fragrance molecules, or the interactions with the cationic surfactant present in the solution.[223] Ionic surfactants (anionic or cationic) are known to increase dramatically the T_{CP}, and as a consequence, the appearance of LLPS coacervate droplets is observed at higher temperatures. This increase of T_{CP} is attributed to the induced polymer-surfactant interactions, leading to the formation of charged polymer chains, and thus to inter-chain repulsion.[234–236] On the other hand, attractive forces (e.g. hydrophobic forces, hydrogen bonding) are induced between the perfume molecules and the polymer, promoting the self-assembly. In this case, the repulsive forces induced from the cationic surfactants are in competition with the polymer-polymer and the polymer-fragrance attractive forces.[237] The formation of micro-capsules with the copolymer S2 (S2A, S2B) can be attributed to the attractive forces in the solution, overcoming the repulsive ones. On the contrary, in the case of the copolymer S1, S3, S4, S6 and Soluplus® in LSFE, an opposite effect is observed, and no micro-capsules are formed. A possible explanation for the above observations could be that the higher Mw of copolymer S2 in conjunction with a higher degree of grafting of hydrophobic (PVAc -co-PVCL) lowers the cloud point temperature and that lower cloud point (20.8-21.6 °C) induces the self-assembly permitting the formation of micro-capsules at room temperature. On the other hand, in water, when the hydrophobic PRM (L-Carvone) is present, there are no repulsive forces of the surfactant and attractive forces (eg hydrophobic forces, hydrogen bonding) are induced between the perfume molecules and the polymer, promoting the self-assembly of all copolymers (**Fig. 1A-G**). Using the same matrix but in the presence of a more hydrophilic PRM (MA), the formation of microcapsules is only possible with polymer S2.

4.4 OECD 301b biodegradability test

Biodegradability OECD 301B test was applied to assess the inherent biodegradability of selected synthetized copolymers and compared to biodegradability of similar structural reference, Soluplus®. OECD 301B biodegradability test allows for direct, explicit certification of a material's biodegradability. The methods establish threshold criteria for the direct classification and marketing of materials under the term of Ready Biodegradability. A product is considered as readily

biodegradable if the biodegradation rate has reached at least 60% within the 28 days of the test. Reference substance (sodium acetate) degradation percentage was superior to 60% (79%) on day 14 (**Fig.79**). The quantity of CO_2 released by the blank control was satisfactory: 28.2 mg/L after 28 days (limit value: 40). The toxicity assay (with tested product and reference substance) highlighted a degradation superior to 25% (40% S2B and 45% S4) after 14 days (**Fig. 80, Fig. 81**).

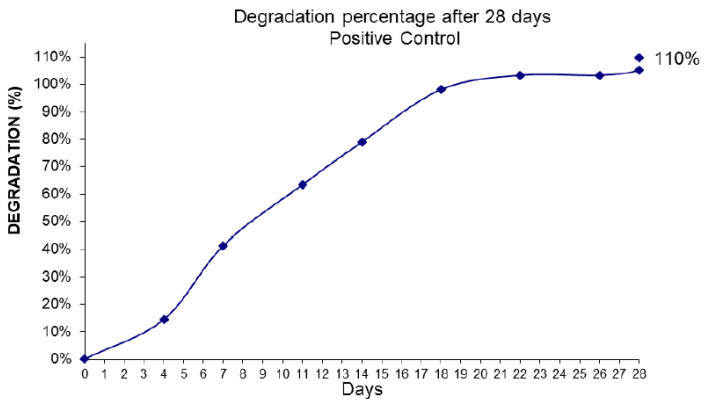

Figure 79. OECD 301B test results of reference substance (sodium acetate), (EUROFINS Ecotoxicologie France).

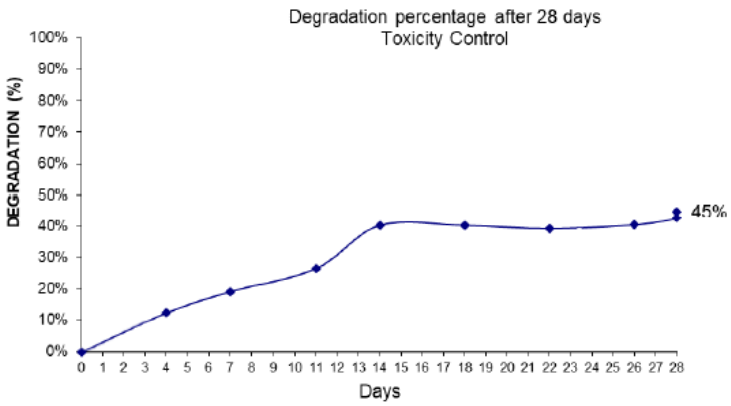

Figure 80. OECD 301B toxicity test results of the copolymer S2Bfor 60 days (EUROFINS Ecotoxicologie France)

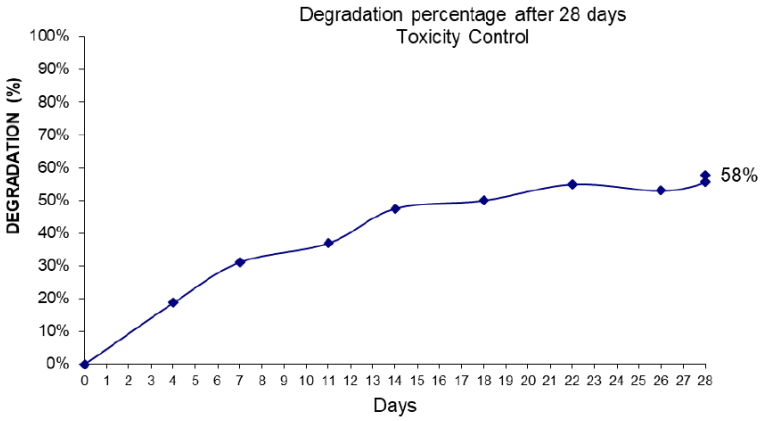

Figure 81. OECD 301B toxicity test results of the copolymer S4 for 60 days (EUROFINS Ecotoxicologie France).

The three synthetized materials exhibited different degradation pattern. The aggregated data for copolymer S2A, S2B and S4 are presented in Figure 4, Figure 5, Figure 6. The information about biodegradability profile of Soluplus® has been reported by BASF and resulted in less than 10% CO_2 formation in OECD 301B test, relative to the theoretical value (28 days) and has been considered as a not readily biodegradable material. For all analyzed materials, the 60% threshold was not reached within 28 days. However, for these specific film materials, the enhanced OECD 301B protocol is applied. It consists in monitoring the biodegradation up to 60 days. As shown in **Figures 82** and **83**, S2A (48%) and S2B (58%) a biodegradation extent well close to the 60% threshold was reached demonstrating that the result below 60% on day 28 did not imply a lack of biodegradability. Despite the extension of the test after 28 days of incubation, Copolymer S4 did not show a significant increase in biodegradability and remained at the same level until the end of the 60-day test (**Fig 84**). The above results showed that none of the analyzed substances can be considered a readily biodegradable polymer as they did not reach the expected target of 60% biodegradability during the OECD 301B test. Nevertheless, it should be noted that all the synthesized polymers showed a greater biodegradability than the commercial copolymer Soluplus®, which biodegradability ends at 10%. In addition, the biodegradability of copolymer S2 and especially S2B almost achieved 60% target. Such divergent biodegradability results of four structurally similar copolymers prove that even a slight difference in structure has a significant impact on the biodegradability of the material.[141–145]

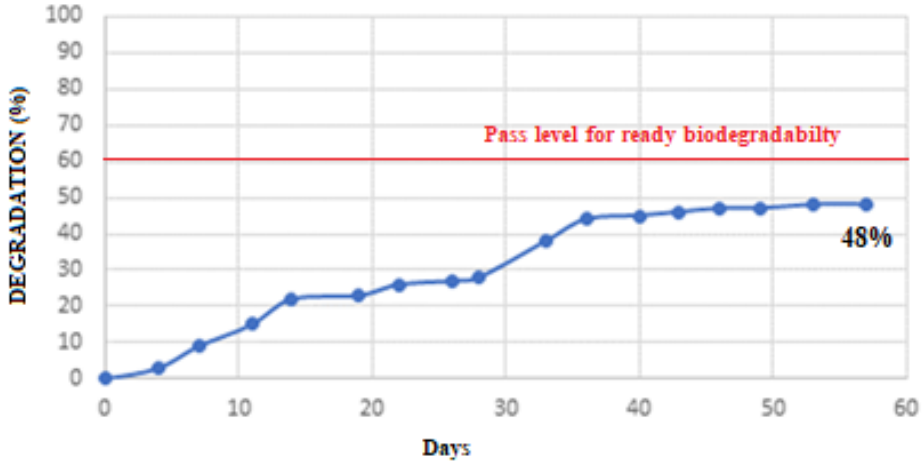

Figure 82. OECD 301B test results of the copolymer S2A for 60 days.

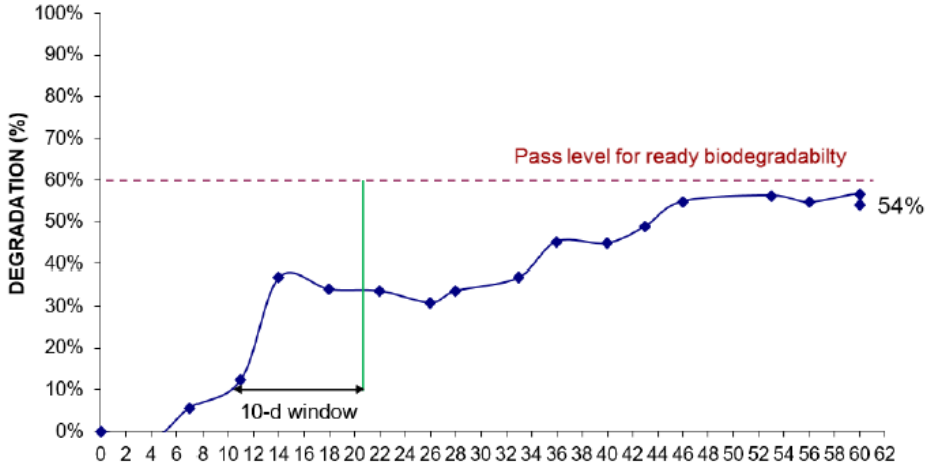

Figure 83. OECD 301B test results of the copolymer S2B for 60 days (EUROFINS Ecotoxicologie France).

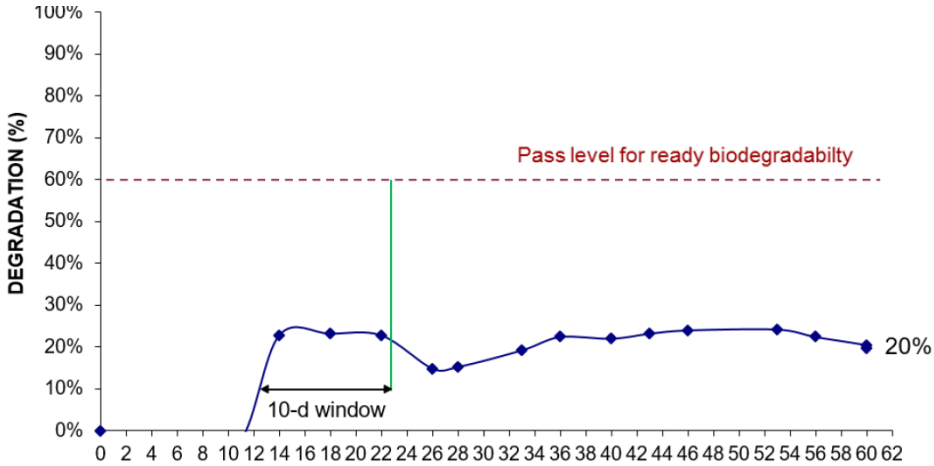

Figure 84. OECD 301B test results of the copolymer S4 for 60 days (EUROFINS Ecotoxicologie France).

4.4.1 Possible relationship between the structure, architecture, composition of copolymer and biodegradability rate.

Biodegradability depends not only on the origin of the polymer but also on its chemical structure and the environmental degrading conditions.[217] The relationship between the chemical structure of selected PEG-g-PVCL and PEG-g-(PVAc-*co*-PVCL) graft copolymers and their biodegradability were studied. To better understand this relation **Table 15** represents the summary of biodegradation and the main different physico-chemical properties of copolymer S2A, S2B and S4. For comparison of biodegradability, properties such as molecular weight of the hydrophilic PEG backbone, composition (ratio between EO/VAc/VCL), average molecular weight (Mw), glass transition and degree of grafting were taken into account. The rate of enzymatic degradation was found to partially depend on the ratio of EO/VAc/VCL in composition of four analyzed copolymers.

Table 15. Summary of biodegradation and the main different physico-chemical properties of Soluplus®, copolymer S2A, S2B and S4.

Copolymer	Biodegradation [%]		PEG Mw [kDa]	Mw copolymer [kDa]	Weight ratio EO/VAc/VCL [%]	Degree of grafting PVCL u/100 PEG u	Glass transition T. [°C]
	28 days	60 days					
Soluplus®	<10		6000	98.0	16/32/51	112	52.03
S2A		48	6000	195	15/25/60	155	87.19
S2B		54	6000	193	14/25/61	145	87.51
S4		24	1000	107	10/-/90	300	68.68

Copolymers with more PVAc content were less susceptible to enzymatic attack due to the high hydrophobicity of component that affects copolymer water solubility.[238] Solubility behaviour in aqueous solutions is a crucial factor in many aspects of biodegradation because almost all living organisms are dependent on the availability of sufficient water phase.[239] However, the biodegradation of the S4 copolymer is significantly lower than that of the S2 even though copolymer does not possess PVCL in its structure. This can be explained by the higher degree of grafting of copolymer S4 comparing to Soluplus® and copolymers S2A and S2B. Indeed, copolymer architecture seems to have greater impact on biodegradability rate than the ratio between analyzed composites. The copolymer architecture affects the polymer chains flexibility. An adequate chain flexibility is crucial to fit into the active site of the enzyme to guarantee a synthetic polymer is degraded by enzymes.[148] Copolymers with PEG Mw values ranging between 6000 and 1000 Da are not readily biodegradable, but higher the Mw higher the biodegradation extent. In terms of copolymer molecular weight, in analyzed copolymers no influence of Mw was observed in biodegradation rate. Finally, all copolymers are amorphous. This is an important aspect since amorphous regions are degraded prior than crystalline ones and copolymers giving the lowest melting point are most susceptible to quick degradation.[239] Consequently, an appropriate manipulation of the characteristics of copolymers, such as their composition and architecture in polymer engineering, can lead to the formation of new, more environmentally friendly copolymers.

CHAPTER FIVE

5. CONCLUTIONS

This thesis reported the synthesis and characterization of different amphiphilic graft copolymers. In particular, the research focused on the development of amphiphilic polymers with improved biodegradability in comparison with polymers actually employed as wall materials for delivery of hydrophobic biologically active substances. This is of paramount applicative relevance since there is a strong attention towards new sustainable and sophisticated materials for delivery systems, especially in food, cosmetic, pharmaceutical, and liquid detergent industry. Amphiphilic copolymers, containing both hydrophilic and hydrophobic parts in their structure, possess unique properties due to the distinct chemical nature of building blocks. Incompatibility of the chemically linked segments may induce the liquid- liquid phase separation (LLPS) and solid- liquid phase separation (SLPS) which make them attractive for numerous industrial applications. Five different PEG-g-(PVAc-*co*-PVCL) and PEG-g-PVCL amphiphilic graft copolymers were synthesized via free radical polymerization method using peroxide as an initiator. All polymers possessed a graft structure based on PEG backbone, where the properties of these graft copolymers were tailored via the systematic variation of the polymers molecular weights (length of PEG chain), grafting densities, and chemical moieties leading to an extremely versatile range of self-assembling structures. The effect of different structural characteristics on capsules formation, encapsulation of fragrance molecules and biodegradability rate was analyzed.

To evaluate the hydrophobic effect on self-assembly properties, two copolymers PEG_{6000}-g- (PVAc-*co*-PVCL) were synthetized, i.e. S2 and S3. The two copolymers showed two different hydrophilic-hydrophobic profiles, being characterized by the same length of the PEG chain and moieties but a different ratio between hydrophobic and hydrophilic blocks. Copolymer S2 composition was richer in PVAc monomers, thus increasing its hydrophobic part in comparison with copolymer S3. The purpose of this manipulation was to find the optimal ratio between components to obtain the best self-forming system and to study the effect of the hydrophobic part on the encapsulation process and polymer properties. This aspect is very important because

the hydrophobic effect is one on the main driving force of amphiphilic copolymers self-assembly into various supramolecular structures. The compositions of the copolymers (EO/VAc/VCL) were calculated on the basis of the integrals of the protons of each copolymers unit of ^{1}H-NMR spectra and resulted for copolymer S2 (15%EO/25%VAc/60%VCL) and copolymer S3 (18%EO/14%VAc/68%VCL). As a consequence of that, Mw of copolymer S2 resulted significantly higher than that of S3 copolymer. The different hydrophilic/hydrophobic balance between those two copolymers resulted in a different cloud point temperature, that decreased as a function of molecular weight of copolymer. The two copolymers showed a different thermal profile, obtained by DSC. A glass transition temperature (Tg) was found for copolymer S2 at about 87 °C whereas an endothermic transformation at 54°C was observed in copolymer S3.

To investigate the effect of molecular weight of PEG backbone on the formation and properties of the graft copolymers, a further copolymer was synthesized, PEG_{20000}-g-(PVAc-*co*-PVCL) (S6). Copolymer S6 contained 20000 molecular weight alkyl chain comparing to 6000 molecular weight of PEG in copolymer S2 and S3, thus increasing the hydrophilic component of the copolymer. Different architecture and properties were reported by employing the same procedure as for the synthesis of copolymer S2 but with PEG molecular weight 20000. The analysis of copolymer S6 showed that a lower grafted content of VAc is obtained on PEG backbone when using higher molecular weight PEG. This result was fully consistent with the hydrophilicity observed for the graft copolymers, which increases with the molecular weight of the PEG chain. The reduction of the hydrophobic fraction of the copolymer affects the self-assembly process but results in increased rate of hydrolytic degradation of encapsulation material.

Two new copolymers (S1 and S4) based on PEG, as a backbone, and PVCL as branched arm were synthetized with the aim of increasing the biodegradability of the copolymer by reducing the complex system to a more water soluble one. For this purpose, polymer hydrophilicity was varied by copolymerizing PVCL containing amide groups with PEG. The introduction of amide group was expected to improve biodegradability through easier accessibility of water molecules as well as to enhance durability by making hydrogen bonding possible. In copolymers S1 and S4 PEG acted as hydrophilic part and PVCL as the hydrophobic motor. Different PEG chain lengths

and different ratio of hydrophilic/hydrophobic segments have been used to prepare these two copolymers, i.e. PEG_{6000}-g-PVCL (S1) and PEG_{1000}-g-PVCL (S4) copolymers. For copolymer S1, where PEG 6000 was used, the obtained composition was found to be more hydrophilic (31% EO/69%VCL) compared to S4 copolymer where PEG 1000 was used. PEG short hydrophilic chain (10%EO/90%VCL) was sufficient to form an amphiphilic compound. The exclusion of PVAc from the polymer composition resulted in an increase in cloud point temperature for both systems compared to copolymers based on the PEG, PVAc, PVCL structure. Copolymer S4 backbone was found to have the highest degree of grafting comparing to all analysed materials. This can be attributed to shorter polymerization time and resulted in less flexible architecture of copolymer S4.

All PEG-g-(PVAc-*co*-PVCL) and PEG-g-PVCL amphiphilic graft copolymers were evaluated for the ability to undergo self-folding in water and liquid detergent formulations resulting in the formation of micron-sized spherical objects (called micro-capsules) and encapsulation of commercial perfume BZ and selected perfumery raw materials such (PRMs) as L-carvone CA, Methyl anthranilate MA. Effects of hydrophilic content, molecular weight, architecture and cloud point temperature were investigated. The studies reported in this work demonstrated that the capsules formation by synthetized copolymers in liquid detergent formulations strongly depend on the molecular weight of hydrophobic content and the degree of grafting of hydrophobic graft chains. Among all synthetized copolymers and commercial copolymer Soluplus® only copolymer S2, which has the highest molecular weight of hydrophobic PVAc-*co*-PVCL part and higher grafting degree, showed capsules formation and encapsulation of perfume and PRMs in both SLFE liquid detergent formulations and water matrix. With respect to conventional chemically cross-linked microcapsules, the encapsulation technology based on the spontaneous self-assembly of amphiphilic copolymers in aqueous solution simples the production of capsules, avoiding the need of high reaction energy and additional steps often required for the removal of unreacted monomers after synthesis. Self-assembled amphiphilic copolymers result to be a growing and promising field in view of the fact that this class of material allows for the sustainable production of capsules using facile, cost- and time-saving methods.

Finally, results showed that the biodegradability rate strongly depends on architecture and composition of copolymer. The copolymer architecture affects the polymer chains flexibility and hydrophobic content influence the solubility. An adequate chain flexibility is crucial to fit into the active site of the enzyme to guarantee a synthetic polymer is degraded. All synthesized copolymers are 4 -5 folds more biodegradable than commercial Soluplus®.

REFERENCES

(1) Https://Www.Livescience.Com/60682-Polymers.Html (Website 28/11/2021).

(2) Zhu, Y.; Romain, C.; Williams, C. K. Sustainable Polymers from Renewable Resources. *Nature* **2016**, *540* (7633), 354–362. https://doi.org/10.1038/nature21001.

(3) Bashir, S. M.; Kimiko, S.; Mak, C.-W.; Fang, J. K.-H.; Gonçalves, D. Personal Care and Cosmetic Products as a Potential Source of Environmental Contamination by Microplastics in a Densely Populated Asian City. *Frontiers in Marine Science* **2021**, *8*. https://doi.org/10.3389/fmars.2021.683482.

(4) Martins, I. M.; Barreiro, M. F.; Coelho, M.; Rodrigues, A. E. Microencapsulation of Essential Oils with Biodegradable Polymeric Carriers for Cosmetic Applications. *Chemical Engineering Journal* **2014**, *245*, 191–200. https://doi.org/10.1016/j.cej.2014.02.024.

(5) Carvalho, I. T.; Estevinho, B. N.; Santos, L. Application of Microencapsulated Essential Oils in Cosmetic and Personal Healthcare Products - a Review. *International Journal of Cosmetic Science* **2016**, *38* (2), 109–119. https://doi.org/10.1111/ics.12232.

(6) Bruyninckx, K.; Dusselier, M. Sustainable Chemistry Considerations for the Encapsulation of Volatile Compounds in Laundry-Type Applications. *ACS Sustainable Chemistry & Engineering* **2019**, *7* (9), 8041–8054. https://doi.org/10.1021/acssuschemeng.9b00677.

(7) C. Ngwuluka, N.; Y. Abu-Thabit, N.; J. Uwaezuoke, O.; O. Erebor, J.; O. Ilomuanya, M.; R. Mohamed, R.; M.A. Soliman, S.; H. Abu Elella, M.; A.A. Ebrahim, N. Natural Polymers in Micro- and Nanoencapsulation for Therapeutic and Diagnostic Applications: Part I: Lipids and Fabrication Techniques. In *Nano- and Microencapsulation - Techniques and Applications*; IntechOpen, 2021. https://doi.org/10.5772/intechopen.94856.

(8) León, G.; Paret, N.; Fankhauser, P.; Grenno, D.; Erni, P.; Ouali, L.; Berthier, D. L. Formaldehyde-Free Melamine Microcapsules as Core/Shell Delivery Systems for Encapsulation of Volatile Active Ingredients. *RSC Advances* **2017**, *7* (31), 18962–18975. https://doi.org/10.1039/C7RA01413A.

(9) Merline, D. J.; Vukusic, S.; Abdala, A. A. Melamine Formaldehyde: Curing Studies and Reaction Mechanism. *Polymer Journal* **2013**, *45* (4), 413–419. https://doi.org/10.1038/pj.2012.162.

(10) Mülhaupt, R. Green Polymer Chemistry and Bio-Based Plastics: Dreams and Reality. *Macromolecular Chemistry and Physics* **2013**, *214* (2), 159–174. https://doi.org/10.1002/macp.201200439.

(11) Leopércio, B. C.; Michelon, M.; Carvalho, M. S. Deformation and Rupture of Microcapsules Flowing through Constricted Capillary. *Scientific Reports* **2021**, *11* (1), 7707. https://doi.org/10.1038/s41598-021-86833-8.

(12) Esser-Kahn, A. P.; Odom, S. A.; Sottos, N. R.; White, S. R.; Moore, J. S. Triggered Release from Polymer Capsules. *Macromolecules* **2011**, *44* (14), 5539–5553. https://doi.org/10.1021/ma201014n.

(13) Perinelli, D. R.; Palmieri, G. F.; Cespi, M.; Bonacucina, G. Encapsulation of Flavours and Fragrances into Polymeric Capsules and Cyclodextrins Inclusion Complexes: An Update. *Molecules* **2020**, *25* (24), 5878. https://doi.org/10.3390/molecules25245878.

(14) Grand View Research. *Microencapsulation Market Size, Share & Trends Analysis Report By Technology (Emulsion, Spray), By Application (Pharmaceutical, Home & Personal Care), By Coating Material, And Segment Forecasts, 2019 - 2025*; 2019.

(15) Hagiopol, C. Copolymers. In *Reference Module in Materials Science and Materials Engineering*; Elsevier, 2016. https://doi.org/10.1016/B978-0-12-803581-8.01126-7.

(16) Stannett, V. T.; Fanta, G. F.; Doane, W. M.; Chatterjee, P. K. Polymer Grafted Cellulose and Starch; 2002; pp 323–347. https://doi.org/10.1016/S0920-4083(02)80012-3.

(17) Jarosz, T.; Gebka, K.; Stolarczyk, A. Recent Advances in Conjugated Graft Copolymers: Approaches and Applications. *Molecules* **2019**, *24* (16), 3019. https://doi.org/10.3390/molecules24163019.

(18) Hadjichristidis, N.; Pitsikalis, M.; Iatrou, H.; Driva, P.; Chatzichristidi, M.; Sakellariou, G.; Lohse, D. Graft Copolymers. In *Encyclopedia of Polymer Science and Technology*; John Wiley & Sons, Inc.: Hoboken, NJ, USA, 2010. https://doi.org/10.1002/0471440264.pst150.pub2.

(19) Santappa, M. Graft Copolymers. *Journal of Macromolecular Science: Part A - Chemistry* **1981**, *16* (8), 1493–1508. https://doi.org/10.1080/00222338108063250.

(20) Choudhary, S.; Sharma, K.; Sharma, V.; Kumar, V. Grafting Polymers. In *Reactive and Functional Polymers Volume Two*; Springer International Publishing: Cham, 2020; pp 199–243. https://doi.org/10.1007/978-3-030-45135-6_8.

(21) Zhang, C.-L.; Feng, L.-F.; Gu, X.-P.; Hoppe, S.; Hu, G.-H. Blend Composition Dependence of the Compatibilizing Efficiency of Graft Copolymers for Immiscible Polymer Blends. *Polymer Engineering & Science* **2010**, *50* (11), 2243–2251. https://doi.org/10.1002/pen.21715.

(22) Maji, B.; Maiti, S. Chemical Modification of Xanthan Gum through Graft Copolymerization: Tailored Properties and Potential Applications in Drug Delivery and Wastewater Treatment. *Carbohydrate Polymers* **2021**, *251*, 117095. https://doi.org/10.1016/j.carbpol.2020.117095.

(23) Pearce, E. M. New Commercial Polymers 2, by Hans-George Elias and Friedrich Vohwinkel, Gordon and Breach, New York, 1986, 508 Pp. Price: $90.00. *Journal of Polymer Science Part C: Polymer Letters* **1987**, *25* (5), 233–234. https://doi.org/10.1002/pol.1987.140250509.

(24) Determan, M. D. Synthesis and Characterization of Stimuli Responsive Block Copolymers, Self-Assembly Behavior and Applications, Ames, 2006. https://doi.org/10.31274/rtd-180813-15427.

(25) Breitenkamp, K.; Emrick, T. Novel Polymer Capsules from Amphiphilic Graft Copolymers and Cross-Metathesis. *Journal of the American Chemical Society* **2003**, *125* (40), 12070–12071. https://doi.org/10.1021/ja036561i.

(26) Chavan, S. N.; Padhan, A. K.; Mandal, D. Self-Assembly of Fluorous Amphiphilic Copolymers with Ionogels and Surface Switchable Wettability. *Polymer Chemistry* **2018**, *9* (17), 2258–2270. https://doi.org/10.1039/C8PY00273H.

(27) Kanapathipillai, M. Synthesis and Characterization of Smart Block Copolymers for Biomineralization and Biomedical Applications, Ames, 2008. https://doi.org/10.31274/rtd-180813-16951.

(28) Lombardo, D.; Kiselev, M. A.; Magazù, S.; Calandra, P. Amphiphiles Self-Assembly: Basic Concepts and Future Perspectives of Supramolecular Approaches. *Advances in Condensed Matter Physics* **2015**, *2015*, 1–22. https://doi.org/10.1155/2015/151683.

(29) Kizil, S.; Bulbul Sonmez, H. Star PEG-Based Amphiphilic Polymers: Synthesis, Characterization and Swelling Behaviors. *Polymer Bulletin* **2019**, *76* (4), 2081–2096. https://doi.org/10.1007/s00289-018-2476-x.

(30) Mendes, A. C.; Baran, E. T.; Reis, R. L.; Azevedo, H. S. Self-Assembly in Nature: Using the Principles of Nature to Create Complex Nanobiomaterials. *Wiley Interdisciplinary Reviews: Nanomedicine and Nanobiotechnology* **2013**, *5* (6), 582–612. https://doi.org/10.1002/wnan.1238.

(31) Paaver, U.; Tamm, I.; Laidmäe, I.; Lust, A.; Kirsimäe, K.; Veski, P.; Kogermann, K.; Heinämäki, J. Soluplus Graft Copolymer: Potential Novel Carrier Polymer in Electrospinning of Nanofibrous Drug Delivery Systems for Wound Therapy. *BioMed Research International* **2014**, *2014*, 1–7. https://doi.org/10.1155/2014/789765.

(32) Lee, Y.-C.; Moon, J.-Y. Bionanotechnology: Biological Self-Assembly. In *Introduction to Bionanotechnology*; Springer Singapore: Singapore, 2020; pp 79–92. https://doi.org/10.1007/978-981-15-1293-3_5.

(33) ’Williams, R. J. ’. Williams R.J., Synthesis and Self-Assembly of Linear and Cyclic Degradable Graft Copolymers. PhD Thesis, University of Warwick, 2014. , Department of Chemistry, 2014.

(34) Khalatur, P. G.; Khokhlov, A. R. Self-Organization of Amphiphilic Polymers. *Polimery* **2014**, *59* (01), 74–79. https://doi.org/10.14314/polimery.2014.074.

(35) Yongmei Zheng. *Bioinspired Design of Materials Surfaces*, Elsevier.; Yongmei Zheng, Ed.; 2019.

(36) Dhotel, A.; Chen, Z.; Delbreilh, L.; Youssef, B.; Saiter, J.-M.; Tan, L. Molecular Motions in Functional Self-Assembled Nanostructures. *International Journal of Molecular Sciences* **2013**, *14* (2), 2303–2333. https://doi.org/10.3390/ijms14022303.

(37) Williams, R. J.; Dove, A. P.; O’Reilly, R. K. Self-Assembly of Cyclic Polymers. *Polymer Chemistry* **2015**, *6* (16), 2998–3008. https://doi.org/10.1039/C5PY00081E.

(38) Subramani, K.; Ahmed, W. Self-Assembly of Proteins and Peptides and Their Applications in Bionanotechnology and Dentistry. In *Emerging Nanotechnologies in Dentistry*; Elsevier, 2012; pp 209–224. https://doi.org/10.1016/B978-1-4557-7862-1.00013-4.

(39) Mishra, P. K.; Ekielski, A. The Self-Assembly of Lignin and Its Application in Nanoparticle Synthesis: A Short Review. *Nanomaterials* **2019**, *9* (2), 243. https://doi.org/10.3390/nano9020243.

(40) Yadav, S.; Sharma, A. K.; Kumar, P. Nanoscale Self-Assembly for Therapeutic Delivery. *Frontiers in Bioengineering and Biotechnology* **2020**, *8*. https://doi.org/10.3389/fbioe.2020.00127.

(41) Ansari Asl, A.; Rahmani, S. Synthesis, Characterization and Self-Assembly Investigation of Novel PEG-g-PCL Copolymers by Combination of ROP and '"Click"' Chemistry Method as a Sustained Release Formulation for Hydrophobic Drug. *International Journal of Polymeric Materials and Polymeric Biomaterials* **2019**, *68* (9), 540–550. https://doi.org/10.1080/00914037.2018.1466140.

(42) Nishimura, T.; Fujii, S.; Sakurai, K.; Sasaki, Y.; Akiyoshi, K. Manipulating the Morphology of Amphiphilic Graft-Copolymer Assemblies by Adjusting the Flexibility of the Main Chain. *Macromolecules* **2021**, *54* (14), 7003–7009. https://doi.org/10.1021/acs.macromol.1c01030.

(43) Williams, R. J.; Pitto-Barry, A.; Kirby, N.; Dove, A. P.; O'Reilly, R. K. Cyclic Graft Copolymer Unimolecular Micelles: Effects of Cyclization on Particle Morphology and Thermoresponsive Behavior. *Macromolecules* **2016**, *49* (7), 2802–2813. https://doi.org/10.1021/acs.macromol.5b02710.

(44) Hattori, G.; Hirai, Y.; Sawamoto, M.; Terashima, T. Self-Assembly of PEG/Dodecyl-Graft Amphiphilic Copolymers in Water: Consequences of the Monomer Sequence and Chain Flexibility on Uniform Micelles. *Polymer Chemistry* **2017**, *8* (46), 7248–7259. https://doi.org/10.1039/C7PY01719G.

(45) Nagahama, K.; Mori, Y.; Ohya, Y.; Ouchi, T. Biodegradable Nanogel Formation of Polylactide-Grafted Dextran Copolymer in Dilute Aqueous Solution and Enhancement of Its Stability by Stereocomplexation. *Biomacromolecules* **2007**, *8* (7), 2135–2141. https://doi.org/10.1021/bm070206t.

(46) Jiang, N.; Chen, J.; Yu, T.; Chao, A.; Kang, L.; Wu, Y.; Niu, K.; Li, R.; Fukuto, M.; Zhang, D. Cyclic Topology Enhancing Structural Ordering and Stability of Comb-Shaped Polypeptoid Thin Films against Melt-Induced Dewetting. *Macromolecules* **2020**, *53* (17), 7601–7612. https://doi.org/10.1021/acs.macromol.0c01205.

(47) Zhang, S.; Tezuka, Y.; Zhang, Z.; Li, N.; Zhang, W.; Zhu, X. Recent Advances in the Construction of Cyclic Grafted Polymers and Their Potential Applications. *Polymer Chemistry* **2018**, *9* (6), 677–686. https://doi.org/10.1039/C7PY01544E.

(48) Xu, J.; Wen, L.; Zhang, F.; Lin, W.; Zhang, L. Self-Assembly of Cyclic Grafted Copolymers with Rigid Rings and Their Potential as Drug Nanocarriers. *Journal of Colloid and Interface Science* **2021**, *597*, 114–125. https://doi.org/10.1016/j.jcis.2021.03.139.

(49) Arno, M. C.; Williams, R. J.; Bexis, P.; Pitto-Barry, A.; Kirby, N.; Dove, A. P.; O'Reilly, R. K. Exploiting Topology-Directed Nanoparticle Disassembly for Triggered Drug Delivery. *Biomaterials* **2018**, *180*, 184–192. https://doi.org/10.1016/j.biomaterials.2018.07.019.

(50) Cabane, E.; Zhang, X.; Langowska, K.; Palivan, C. G.; Meier, W. Stimuli-Responsive Polymers and Their Applications in Nanomedicine. *Biointerphases* **2012**, *7* (1), 9. https://doi.org/10.1007/s13758-011-0009-3.

(51) Shibata, M.; Terashima, T.; Koga, T. Thermoresponsive Gelation of Amphiphilic Random Copolymer Micelles in Water. *Macromolecules* **2021**, *54* (11), 5241–5248. https://doi.org/10.1021/acs.macromol.1c00406.

(52) Stuart, M. A. C.; Huck, W. T. S.; Genzer, J.; Müller, M.; Ober, C.; Stamm, M.; Sukhorukov, G. B.; Szleifer, I.; Tsukruk, V. v.; Urban, M.; Winnik, F.; Zauscher, S.; Luzinov, I.; Minko, S. Emerging Applications of Stimuli-Responsive Polymer Materials. *Nature Materials* **2010**, *9* (2), 101–113. https://doi.org/10.1038/nmat2614.

(53) van Gheluwe, L.; Chourpa, I.; Gaigne, C.; Munnier, E. Polymer-Based Smart Drug Delivery Systems for Skin Application and Demonstration of Stimuli-Responsiveness. *Polymers* **2021**, *13* (8), 1285. https://doi.org/10.3390/polym13081285.

(54) Adeleni Adebola M. Characterization of a Thermoresponsive Water-Soluble Polymer: Block-Copoly [Ethylene Glycol/Graft-Co (Vinyl Alcohol/Vinyl Caprolactam)], 2017.

(55) Biswas, S.; Kumari, P.; Lakhani, P. M.; Ghosh, B. Recent Advances in Polymeric Micelles for Anti-Cancer Drug Delivery. *European Journal of Pharmaceutical Sciences* **2016**, *83*, 184–202. https://doi.org/10.1016/j.ejps.2015.12.031.

(56) Verbrugghe, S.; Bernaerts, K.; du Prez, F. E. Thermo-Responsive and Emulsifying Properties of Poly(N-Vinylcaprolactam) Based Graft Copolymers. *Macromolecular Chemistry and Physics* **2003**, *204* (9), 1217–1225. https://doi.org/10.1002/macp.200390098.

(57) Gandhi, A.; Paul, A.; Sen, S. O.; Sen, K. K. Studies on Thermoresponsive Polymers: Phase Behaviour, Drug Delivery and Biomedical Applications. *Asian Journal of Pharmaceutical Sciences* **2015**, *10* (2), 99–107. https://doi.org/10.1016/j.ajps.2014.08.010.

(58) Zhang, Q.; Weber, C.; Schubert, U. S.; Hoogenboom, R. Thermoresponsive Polymers with Lower Critical Solution Temperature: From Fundamental Aspects and Measuring Techniques to Recommended Turbidimetry Conditions. *Materials Horizons* **2017**, *4* (2), 109–116. https://doi.org/10.1039/C7MH00016B.

(59) Wu, G.; Chen, S.-C.; Zhan, Q.; Wang, Y.-Z. Well-Defined Amphiphilic Biodegradable Comb-Like Graft Copolymers: Their Unique Architecture-Determined LCST and UCST Thermoresponsivity. *Macromolecules* **2011**, *44* (4), 999–1008. https://doi.org/10.1021/ma102588k.

(60) Hoogenboom, R.; Schlaad, H. Thermoresponsive Poly(2-Oxazoline)s, Polypeptoids, and Polypeptides. *Polymer Chemistry* **2017**, *8* (1), 24–40. https://doi.org/10.1039/C6PY01320A.

(61) Zhang, Q.; Weber, C.; Schubert, U. S.; Hoogenboom, R. Thermoresponsive Polymers with Lower Critical Solution Temperature: From Fundamental Aspects and Measuring Techniques to Recommended Turbidimetry Conditions. *Materials Horizons* **2017**, *4* (2), 109–116. https://doi.org/10.1039/C7MH00016B.

(62) Seuring, J.; Agarwal, S. Polymers with Upper Critical Solution Temperature in Aqueous Solution. *Macromolecular Rapid Communications* **2012**, *33* (22), 1898–1920. https://doi.org/10.1002/marc.201200433.

(63) Aijing Lu. Amphiphilic and Thermoresponsive Block Copolymers Based on Hydroxypropyl Methyl Cellulose as Nano-Carrier of Hydrophobic Drugs, 2020.

(64) Cook, M. T.; Haddow, P.; Kirton, S. B.; McAuley, W. J. Polymers Exhibiting Lower Critical Solution Temperatures as a Route to Thermoreversible Gelators for Healthcare. *Advanced Functional Materials* **2021**, *31* (8), 2008123. https://doi.org/10.1002/adfm.202008123.

(65) Laukkanen, A.; Valtola, L.; Winnik, F. M.; Tenhu, H. Thermosensitive Graft Copolymers of an Amphiphilic Macromonomer and N-Vinylcaprolactam: Synthesis and Solution Properties in Dilute Aqueous Solutions below and above the LCST. *Polymer* **2005**, *46* (18), 7055–7065. https://doi.org/10.1016/j.polymer.2005.05.100.

(66) Williams, R. J.; O'Reilly, R. K.; Dove, A. P. Degradable Graft Copolymers by Ring-Opening and Reverse Addition–Fragmentation Chain Transfer Polymerization. *Polymer Chemistry* **2012**, *3* (8), 2156–2164. https://doi.org/10.1039/c2py20213a.

(67) Sand, A.; Vyas, A. Introductory Chapter: Organic Polymer - Graft Copolymers. In *Organic Polymers*; IntechOpen, 2020. https://doi.org/10.5772/intechopen.88037.

(68) Rempp, P. F.; Lutz, P. J. Synthesis of Graft Copolymers. In *Comprehensive Polymer Science and Supplements*; Elsevier, 1989; pp 403–421. https://doi.org/10.1016/B978-0-08-096701-1.00192-0.

(69) Smets, G.; Poot, A.; Mullier, M.; Bex, J. P. Synthesis of Graft Copolymers. *Journal of Polymer Science* **1959**, *34* (127), 287–307. https://doi.org/10.1002/pol.1959.1203412723.

(70) Ejaz, M.; Tsujii, Y.; Fukuda, T. Controlled Grafting of a Well-Defined Polymer on a Porous Glass Filter by Surface-Initiated Atom Transfer Radical Polymerization. *Polymer* **2001**, *42* (16), 6811–6815. https://doi.org/10.1016/S0032-3861(01)00192-6.

(71) Gao, H.; Min, K.; Matyjaszewski, K. Synthesis of 3-Arm Star Block Copolymers by Combination of "Core-First" and "Coupling-Onto" Methods Using ATRP and Click Reactions. *Macromolecular Chemistry and Physics* **2007**, *208* (13), 1370–1378. https://doi.org/10.1002/macp.200600616.

(72) Datta, P.; Genzer, J. "Grafting through" Polymerization Involving Surface-bound Monomers. *Journal of Polymer Science Part A: Polymer Chemistry* **2016**, *54* (2), 263–274. https://doi.org/10.1002/pola.27907.

(73) Matyjaszewski, K. "Graft Copolymers".Carnegie Mellon University, www.cmu.edu. Retrieved 17 March 2022.

(74) Bagheri, A.; Boniface, S.; Fellows, C. M. Reversible-Deactivation Radical Polymerisation: Chain Polymerisation Made Simple. *Chemistry Teacher International* **2021**, *3* (2), 19–32. https://doi.org/10.1515/cti-2020-0025.

(75) Nesvadba, P. Radical Polymerization in Industry. In *Encyclopedia of Radicals in Chemistry, Biology and Materials*; John Wiley & Sons, Ltd: Chichester, UK, 2012. https://doi.org/10.1002/9781119953678.rad080.

(76) Matyjeszewski, K. *Radical Polymerization, In Controlled and Living Polymerizations Methods and Materials*, WILEY-VCH.; Muller, A. H. E., Ed.; 2009.

(77) Braun, D. Origins and Development of Initiation of Free Radical Polymerization Processes. *International Journal of Polymer Science* **2009**, *2009*, 1–10. https://doi.org/10.1155/2009/893234.

(78) Morris, B. A. Commonly Used Resins and Substrates in Flexible Packaging. In *The Science and Technology of Flexible Packaging*; Elsevier, 2017; pp 69–119. https://doi.org/10.1016/B978-0-323-24273-8.00004-6.

(79) BHATTACHARYA, A. Grafting: A Versatile Means to Modify PolymersTechniques, Factors and Applications. *Progress in Polymer Science* **2004**, *29* (8), 767–814. https://doi.org/10.1016/j.progpolymsci.2004.05.002.

(80) Gowda, D. et al. Polymer Grafting-An Overview. *American Journal of PharmTech Research* **2016**, *6* (2).

(81) Odian, G. *Principles of Polymerization (4th Ed.).* ; Wiley-Interscience: New York, 2004.

(82) Shrivastava, A. Polymerization. In *Introduction to Plastics Engineering*; Elsevier, 2018; pp 17–48. https://doi.org/10.1016/B978-0-323-39500-7.00002-2.

(83) Mark R. Leach. Radical chemistry.

(84) Pojman, J. A.; Willis, J.; Fortenberry, D.; Ilyashenko, V.; Khan, A. M. Factors Affecting Propagating Fronts of Addition Polymerization: Velocity, Front Curvature, Temperatue Profile, Conversion, and Molecular Weight Distribution. *Journal of Polymer Science Part A: Polymer Chemistry* **1995**, *33* (4), 643–652. https://doi.org/10.1002/pola.1995.080330406.

(85) McKeen, L. W. Introduction to Plastics and Polymers. In *The Effect of UV Light and Weather on Plastics and Elastomers*; Elsevier, 2019; pp 1–20. https://doi.org/10.1016/B978-0-12-816457-0.00001-0.

(86) Su, W.-F. Radical Chain Polymerization; 2013; pp 137–183. https://doi.org/10.1007/978-3-642-38730-2_7.

(87) Ebewele, R. O. *Polymer Science and Technology*; CRC Press, 2000. https://doi.org/10.1201/9781420057805.

(88) The Open University. Introduction to Polymers:Solutions Manual. The Open University, 1992, http://data.open.ac.uk/openlearn/t838_1. Retrieved 17 March 2022.

(89) Zhu, S.; Hamielec, A. Polymerization Kinetic Modeling and Macromolecular Reaction Engineering. In *Polymer Science: A Comprehensive Reference*; Elsevier, 2012; pp 779–831. https://doi.org/10.1016/B978-0-444-53349-4.00127-8.

(90) McGrath, J. E. Chain Reaction Polymerization. *Journal of Chemical Education* **1981**, *58* (11), 844. https://doi.org/10.1021/ed058p844.

(91) IARC Working Group on the Evaluation of Carcinogenic Risks to Humans. Some Chemicals Present in Industrial and Consumer Products, Food and Drinking-Water.

(92) Cormack, P. A. G.; Elorza, A. Z. Molecularly Imprinted Polymers: Synthesis and Characterisation. *Journal of Chromatography B* **2004**, *804* (1), 173–182. https://doi.org/10.1016/j.jchromb.2004.02.013.

(93) Ensafi, A. A.; Kazemifard, N.; Saberi Dehkordi, Z. Parameters That Affect Molecular Imprinting Polymers. In *Molecularly Imprinted Polymer Composites*; Elsevier, 2021; pp 21–48. https://doi.org/10.1016/B978-0-12-819952-7.00010-X.

(94) Sheppard, C. S.; Kamath, V. R. The Selection and Use of Free Radical Initiators. *Polymer Engineering and Science* **1979**, *19* (9), 597–606. https://doi.org/10.1002/pen.760190902.

(95) Vega-Hernández, M. Á.; Cano-Díaz, G. S.; Vivaldo-Lima, E.; Rosas-Aburto, A.; Hernández-Luna, M. G.; Martinez, A.; Palacios-Alquisira, J.; Mohammadi, Y.; Penlidis, A. A Review on the Synthesis, Characterization, and Modeling of Polymer Grafting. *Processes* **2021**, *9* (2), 375. https://doi.org/10.3390/pr9020375.

(96) Bagheri, A.; Fellows, C. M.; Boyer, C. Reversible Deactivation Radical Polymerization: From Polymer Network Synthesis to 3D Printing. *Advanced Science* **2021**, *8* (5), 2003701. https://doi.org/10.1002/advs.202003701.

(97) Jackson, A. W. Reversible-Deactivation Radical Polymerization of Cyclic Ketene Acetals. *Polymer Chemistry* **2020**, *11* (21), 3525–3545. https://doi.org/10.1039/D0PY00446D.

(98) Matyjaszewski, K.; Xia, J. Atom Transfer Radical Polymerization. *Chemical Reviews* **2001**, *101* (9), 2921–2990. https://doi.org/10.1021/cr940534g.

(99) Matyjaszewski, K. Atom Transfer Radical Polymerization (ATRP): Current Status and Future Perspectives. *Macromolecules* **2012**, *45* (10), 4015–4039. https://doi.org/10.1021/ma3001719.

(100) Sciannamea, V.; Jérôme, R.; Detrembleur, C. In-Situ Nitroxide-Mediated Radical Polymerization (NMP) Processes: Their Understanding and Optimization. *Chemical Reviews* **2008**, *108* (3), 1104–1126. https://doi.org/10.1021/cr0680540.

(101) Lizundia, E.; Meaurio, E.; Vilas, J. L. Grafting of Cellulose Nanocrystals. In *Multifunctional Polymeric Nanocomposites Based on Cellulosic Reinforcements*; Elsevier, 2016; pp 61–113. https://doi.org/10.1016/B978-0-323-44248-0.00003-1.

(102) Crawford, D. E. Extrusion – Back to the Future: Using an Established Technique to Reform Automated Chemical Synthesis. *Beilstein Journal of Organic Chemistry* **2017**, *13*, 65–75. https://doi.org/10.3762/bjoc.13.9.

(103) Raquez, J.-M.; Degée, P.; Nabar, Y.; Narayan, R.; Dubois, P. Biodegradable Materials by Reactive Extrusion: From Catalyzed Polymerization to Functionalization and Blend Compatibilization. *Comptes Rendus Chimie* **2006**, *9* (11–12), 1370–1379. https://doi.org/10.1016/j.crci.2006.09.004.

(104) Chung, T. C. Synthesis of Functional Polyolefin Copolymers with Graft and Block Structures. *Progress in Polymer Science* **2002**, *27* (1), 39–85. https://doi.org/10.1016/S0079-6700(01)00038-7.

(105) Zahran, A. H.; Zohdy, M. H. Effect of Radiation Chemical Treatment on Sisal Fibers I. Radiation Induced Grafting of Ethyl Acrylate. *Journal of Applied Polymer Science* **1986**, *31* (6), 1925–1934. https://doi.org/10.1002/app.1986.070310633.

(106) Ng L-T, G. J. Z. E. N. D. Effect of Monomer Structure on Radiation Grafting of Charge Transfer Complexes to Synthetic and Naturally Occurring Polymers. *Radiat Phy.Chem* **2001**, *62*, 89–98.

(107) *Cellulose-Based Graft Copolymers*; Thakur, V. K., Ed.; CRC Press, 2015. https://doi.org/10.1201/b18390.

(108) Taghizadeh, M. T.; Mehrdad, A. Kinetic Study of Graft Polymerization of Acrylic Acidand Ethyl Methacrylate onto Starch by Ceric Ammonium Nitrate. *Iranian journal of chemistryand chemical engineering* **2006**, *25* (1), 1–12.

(109) Gupta, K. C.; Sahoo, S.; Khandekar, K. Graft Copolymerization of Ethyl Acrylate onto Cellulose Using Ceric Ammonium Nitrate as Initiator in Aqueous Medium. *Biomacromolecules* **2002**, *3* (5), 1087–1094. https://doi.org/10.1021/bm020060s.

(110) Nishioka, N.; Matsumoto, Y.; Yumen, T.; Monmae, K.; Kosai, K. Homogeneous Graft Copolymerization of Vinyl Monomers onto Cellulose in a Dimethyl Sulfoxide–Paraformaldehyde Solvent System IV. 2-Hydroxyethyl Methacrylate. *Polymer Journal* **1986**, *18* (4), 323–330. https://doi.org/10.1295/polymj.18.323.

(111) Patil, D. R.; Fanta, G. F. Graft Copolymerization of Starch with Methyl Acrylate: An Examination of Reaction Variables. *Journal of applied polymer science,* **1993**, *47* (10), 1765–1772. https://doi.org/10.1007/978-3-642-36566-9_3.

(112) Pandey, P. K.; Banerjee, J.; Taunk, K.; Behari, K. Graft Copolymerization of Acrylic Acid onto Xanthum Gum Using a Potassium Monopersulfate/Fe2+ Redox Pair. *Journal of Applied Polymer Science* **2003**, *89* (5), 1341–1346. https://doi.org/10.1002/app.12302.

(113) Deng, J.-P.; Yang, W.-T.; Rånby, B. Surface Photograft Polymerization of Vinyl Acetate on Low Density Polyethylene Film. Effects of Solvent. *Polymer Journal* **2000**, *32* (10), 834–837. https://doi.org/10.1295/polymj.32.834.

(114) Jun, L.; Jun, L.; Min, Y.; Hongfei, H. Solvent Effect on Grafting Polymerization of NIPAAm onto Cotton Cellulose via γ-Preirradiation Method. *Radiation Physics and Chemistry* **2001**, *60* (6), 625–628. https://doi.org/10.1016/S0969-806X(00)00375-3.

(115) Arayapranee, W.; Prasassarakich, P.; Rempel, G. L. Process Variables and Their Effects on Grafting Reactions of Styrene and Methyl Methacrylate onto Natural Rubber. *Journal of Applied Polymer Science* **2003**, *89* (1), 63–74. https://doi.org/10.1002/app.11999.

(116) Joshi, J. M.; Sinha, V. K. Study of the Effect of Reaction Variables on Grafting of Acrylic Acid onto Carboxymethyl Chitosan. *Designed Monomers and Polymers* **2007**, *10* (3), 207–219. https://doi.org/10.1163/156855507780949182.

(117) Kumar, D.; Pandey, J.; Raj, V.; Kumar, P. A Review on the Modification of Polysaccharide Through Graft Copolymerization for Various Potential Applications. *The Open Medicinal Chemistry Journal* **2017**, *11* (1), 109–126. https://doi.org/10.2174/1874104501711010109.

(118) Pekel Bayramgil, N. Grafting of Hydrophilic Monomers Onto Cellulosic Polymers for Medical Applications. In *Biopolymer Grafting: Applications*; Elsevier, 2018; pp 81–114. https://doi.org/10.1016/B978-0-12-810462-0.00003-X.

(119) Han, T. L.; Kumar, R. N.; Rozman, H. D.; Noor, Mohd. A. M. GMA Grafted Sago Starch as a Reactive Component in Ultra Violet Radiation Curable Coatings. *Carbohydrate Polymers* **2003**, *54* (4), 509–516. https://doi.org/10.1016/j.carbpol.2003.08.001.

(120) Waly, A.; Abdel-Mohdy, F. A.; Aly, A. S.; Hebeish, A. Synthesis and Characterization of Cellulose Ion Exchanger. II. Pilot Scale and Utilization in Dye-Heavy Metal Removal. *Journal of Applied Polymer Science* **1998**, *68* (13), 2151–2157.

https://doi.org/10.1002/(SICI)1097-4628(19980627)68:13<2151::AID-APP11>3.0.CO;2-2.

(121) Xie, J.; Hsieh, Y.-L. Thermosensitive Poly(n-Isopropylacrylamide) Hydrogels Bonded on Cellulose Supports. *Journal of Applied Polymer Science* **2003**, *89* (4), 999–1006. https://doi.org/10.1002/app.12206.

(122) Wan Yunus, W. Md. Z. Chemical Modification of Polymers: Current and Future Routes for Synthesizing New Polymeric Compounds, 2002.

(123) Kumar, B.; Negi, Y. S. Water Absorption and Viscosity Behaviour of Thermally Stable Novel Graft Copolymer of Carboxymethyl Cellulose and Poly(Sodium 1-Hydroxy Acrylate). *Carbohydrate Polymers* **2018**, *181*, 862–870. https://doi.org/10.1016/j.carbpol.2017.11.066.

(124) Yeng, W. S.; Tahir, P. Md.; Chiang, L. K.; Yunus, W. Md. Z. W.; Zakaria, S. Sago Starch and Its Acrylamide Modified Products as Coating Material on Handsheets Made from Recycled Pulp Fibers. *Journal of Applied Polymer Science* **2004**, *94* (1), 154–158. https://doi.org/10.1002/app.20793.

(125) Ramnath, V.; Sekar, S.; Sankar, S.; Sankaranarayanan, C.; Sastry, T. P. Preparation and Evaluation of Biocomposites as Wound Dressing Material. *Journal of Materials Science: Materials in Medicine* **2012**, *23* (12), 3083–3095. https://doi.org/10.1007/s10856-012-4765-5.

(126) Lee, S. B.; Koepsel, R. R.; Morley, S. W.; Matyjaszewski, K.; Sun, Y.; Russell, A. J. Permanent, Nonleaching Antibacterial Surfaces. 1. Synthesis by Atom Transfer Radical Polymerization. *Biomacromolecules* **2004**, *5* (3), 877–882. https://doi.org/10.1021/bm034352k.

(127) Fakhru'L-Razi, A.; Qudsieh, I. Y. M.; Yunus, W. M. Z. W.; Ahmad, M. B.; Rahman, M. Z. Ab. Graft Copolymerization of Methyl Methacrylate onto Sago Starch Using Ceric Ammonium Nitrate and Potassium Persulfate as Redox Initiator Systems. *Journal of Applied Polymer Science* **2001**, *82* (6), 1375–1381. https://doi.org/10.1002/app.1974.

(128) Kalia, S.; Sabaa, M. W.; Kango, S. Polymer Grafting: A Versatile Means to Modify the Polysaccharides. In *Polysaccharide Based Graft Copolymers*; Springer Berlin Heidelberg: Berlin, Heidelberg, 2013; pp 1–14. https://doi.org/10.1007/978-3-642-36566-9_1.

(129) Perin, F.; Motta, A.; Maniglio, D. Amphiphilic Copolymers in Biomedical Applications: Synthesis Routes and Property Control. *Materials Science and Engineering: C* **2021**, *123*, 111952. https://doi.org/10.1016/j.msec.2021.111952.

(130) Huang, Z.; Chen, Q.; Wan, Q.; Wang, K.; Yuan, J.; Zhang, X.; Tao, L.; Wei, Y. Synthesis of Amphiphilic Fluorescent Polymers via a One-Pot Combination of Multicomponent Hantzsch Reaction and RAFT Polymerization and Their Cell Imaging Applications. *Polymer Chemistry* **2017**, *8* (33), 4805–4810. https://doi.org/10.1039/C7PY00926G.

(131) Lochhead, R. Y. A Review of Recent Advances in the Polymeric Delivery of Attributes in Cosmetics and Personal Care Products; Polymeric Delivery of Therapeutics, 2010; pp 3–22. https://doi.org/10.1021/bk-2010-1053.ch001.

(132) Zhang, L.; Lin, J.; Lin, S. Aggregate Morphologies of Amphiphilic Graft Copolymers in Dilute Solution Studied by Self-Consistent Field Theory. *The Journal of Physical Chemistry B* **2007**, *111* (31), 9209–9217. https://doi.org/10.1021/jp068429l.

(133) Bláhová, M.; Randárová, E.; Konefał, R.; Nottelet, B.; Etrych, T. Graft Copolymers with Tunable Amphiphilicity Tailored for Efficient Dual Drug Delivery *via* Encapsulation and PH-Sensitive Drug Conjugation. *Polymer Chemistry* **2020**, *11* (27), 4438–4453. https://doi.org/10.1039/D0PY00609B.

(134) Huang, Y.-C.; Jan, J.-S. Carboxylmethyl Chitosan-Graft-Poly(γ-Benzyl-l-Glutamate) Glycopeptides: Synthesis and Particle Formation as Encapsulants. *Polymer* **2014**, *55* (2), 540–549. https://doi.org/10.1016/j.polymer.2013.12.037.

(135) Logie, J.; Owen, S. C.; McLaughlin, C. K.; Shoichet, M. S. PEG-Graft Density Controls Polymeric Nanoparticle Micelle Stability. *Chemistry of Materials* **2014**, *26* (9), 2847–2855. https://doi.org/10.1021/cm500448x.

(136) Nottelet, B.; Darcos, V.; Coudane, J. Polyiodized-PCL as Multisite Transfer Agent: Towards an Enlarged Library of Degradable Graft Copolymers. *Journal of Polymer Science Part A: Polymer Chemistry* **2009**, *47* (19), 5006–5016. https://doi.org/10.1002/pola.23553.

(137) Lin, G.; Cosimbescu, L.; Karin, N. J.; Gutowska, A.; Tarasevich, B. J. Injectable and Thermogelling Hydrogels of PCL-g-PEG: Mechanisms, Rheological and Enzymatic Degradation Properties. *Journal of Materials Chemistry B* **2013**, *1* (9), 1249–1255. https://doi.org/10.1039/c2tb00468b.

(138) Karakasyan, C.; Lack, S.; Brunel, F.; Maingault, P.; Hourdet, D. Synthesis and Rheological Properties of Responsive Thickeners Based on Polysaccharide Architectures. *Biomacromolecules* **2008**, *9* (9), 2419–2429. https://doi.org/10.1021/bm800393s.

(139) Gao, Y.-Z.; Chen, J.-C.; Wu, Y.-X. Amphiphilic Graft Copolymers of Quaternized Alginate- *g* -Polytetrahydrofuran for Anti-Protein Surfaces, Curcumin Carriers, and Antibacterial Materials. *ACS Applied Polymer Materials* **2021**, *3* (7), 3465–3477. https://doi.org/10.1021/acsapm.1c00389.

(140) Patil, A.; Ferritto, M. S. Polymers for Personal Care and Cosmetics: Overview; 2013; pp 3–11. https://doi.org/10.1021/bk-2013-1148.ch001.

(141) Bujak, T.; Nizioł-Łukaszewska, Z.; Ziemlewska, A. Amphiphilic Cationic Polymers as Effective Substances Improving the Safety of Use of Body Wash Gels. *International Journal of Biological Macromolecules* **2020**, *147*, 973–979. https://doi.org/10.1016/j.ijbiomac.2019.10.064.

(142) Ammala, A. Biodegradable Polymers as Encapsulation Materials for Cosmetics and Personal Care Markets. *International Journal of Cosmetic Science* **2013**, *35* (2), 113–124. https://doi.org/10.1111/ics.12017.

(143) Odrobińska, J.; Niesyto, K.; Erfurt, K.; Siewniak, A.; Mielańczyk, A.; Neugebauer, D. Retinol-Containing Graft Copolymers for Delivery of Skin-Curing Agents. *Pharmaceutics* **2019**, *11* (8), 378. https://doi.org/10.3390/pharmaceutics11080378.

(144) Odrobińska, J.; Neugebauer, D. Micellar Carriers Based on Amphiphilic PEG/PCL Graft Copolymers for Delivery of Active Substances. *Polymers* **2020**, *12* (12), 2876. https://doi.org/10.3390/polym12122876.

(145) Mamusa, M.; Mastrangelo, R.; Glen, T.; Murgia, S.; Palazzo, G.; Smets, J.; Baglioni, P. Rational Design of Sustainable Liquid Microcapsules for Spontaneous Fragrance Encapsulation. *Angewandte Chemie International Edition* **2021**, *60* (44), 23849–23857. https://doi.org/10.1002/anie.202110446.

(146) Mamusa, M.; Sofroniou, C.; Resta, C.; Murgia, S.; Fratini, E.; Smets, J.; Baglioni, P. Tuning the Encapsulation of Simple Fragrances with an Amphiphilic Graft Copolymer. *ACS Applied Materials & Interfaces* **2020**, *12* (25), 28808–28818. https://doi.org/10.1021/acsami.0c05892.

(147) Vroman, I.; Tighzert, L. Biodegradable Polymers. *Materials* **2009**, *2* (2), 307–344. https://doi.org/10.3390/ma2020307.

(148) Jiang, L.; Zhang, J. Biodegradable Polymers and Polymer Blends. In *Handbook of Biopolymers and Biodegradable Plastics*; Elsevier, 2013; pp 109–128. https://doi.org/10.1016/B978-1-4557-2834-3.00006-9.

(149) Panchal, S. S.; Vasava, D. v. Biodegradable Polymeric Materials: Synthetic Approach. *ACS Omega* **2020**, *5* (9), 4370–4379. https://doi.org/10.1021/acsomega.9b04422.

(150) Guo, B.; Ma, P. X. Synthetic Biodegradable Functional Polymers for Tissue Engineering: A Brief Review. *Science China Chemistry* **2014**, *57* (4), 490–500. https://doi.org/10.1007/s11426-014-5086-y.

(151) Dhaliwal, K. Biodegradable Polymers and Their Role in Drug Delivery Systems. *Biomedical Journal of Scientific & Technical Research* **2018**, *11* (1). https://doi.org/10.26717/BJSTR.2018.11.002056.

(152) Doppalapudi, S.; Katiyar, S.; Domb, A. J.; Khan, W. Biodegradable Natural Polymers. In *Advanced Polymers in Medicine*; Springer International Publishing: Cham, 2015; pp 33–66. https://doi.org/10.1007/978-3-319-12478-0_2.

(153) Chen, H.; Truckenmüller, R.; van Blitterswijk, C.; Moroni, L. Fabrication of Nanofibrous Scaffolds for Tissue Engineering Applications. In *Nanomaterials in Tissue Engineering*; Elsevier, 2013; pp 158–183. https://doi.org/10.1533/9780857097231.1.158.

(154) Babu, R. P.; O'Connor, K.; Seeram, R. Current Progress on Bio-Based Polymers and Their Future Trends. *Progress in Biomaterials* **2013**, *2* (1), 1–16. https://doi.org/10.1186/2194-0517-2-8.

(155) Chen, G.-Q.; Patel, M. K. Plastics Derived from Biological Sources: Present and Future: A Technical and Environmental Review. *Chemical Reviews* **2012**, *112* (4), 2082–2099. https://doi.org/10.1021/cr200162d.

(156) Abhilash, M.; Thomas, D. Biopolymers for Biocomposites and Chemical Sensor Applications. In *Biopolymer Composites in Electronics*; Elsevier, 2017; pp 405–435. https://doi.org/10.1016/B978-0-12-809261-3.00015-2.

(157) Lucas, N.; Bienaime, C.; Belloy, C.; Queneudec, M.; Silvestre, F.; Nava-Saucedo, J.-E. Polymer Biodegradation: Mechanisms and Estimation Techniques – A Review. *Chemosphere* **2008**, *73* (4), 429–442. https://doi.org/10.1016/j.chemosphere.2008.06.064.

(158) Bastioli, C. Handbook of Biodegradable Polymers; Smithers Rapra , 2005; p 535.

(159) Künkel, A.; Becker, J.; Börger, L.; Hamprecht, J.; Koltzenburg, S.; Loos, R.; Schick, M. B.; Schlegel, K.; Sinkel, C.; Skupin, G.; Yamamoto, M. Polymers, Biodegradable. In *Ullmann's Encyclopedia of Industrial Chemistry*; Wiley-VCH Verlag GmbH & Co. KGaA: Weinheim, Germany, 2016; pp 1–29. https://doi.org/10.1002/14356007.n21_n01.pub2.

(160) Andrej Kržan. Biodegradable polymers and plastics. Innovative Value Chain Development for Sustainable Plastics in Central Europe (PLASTiCE) 2012. https://icmpp.ro/sustainableplastics/files/Biodegradable_plastics_and_polymers.pdf. Retrieved 17 March 2022

(161) Witt, U.; Einig, T.; Yamamoto, M.; Kleeberg, I.; Deckwer, W.-D.; Müller, R.-J. Biodegradation of Aliphatic–Aromatic Copolyesters: Evaluation of the Final Biodegradability and Ecotoxicological Impact of Degradation Intermediates. *Chemosphere* **2001**, *44* (2), 289–299. https://doi.org/10.1016/S0045-6535(00)00162-4.

(162) Elashmawi, I. S.; Hakeem, N. A.; Abdelrazek, E. M. Spectroscopic and Thermal Studies of PS/PVAc Blends. *Physica B: Condensed Matter* **2008**, *403* (19–20), 3547–3552. https://doi.org/10.1016/j.physb.2008.05.024.

(163) Erlandsson, B.; Karlson, S. The Mode of Action of Corn Starch and a Pro-Oxidant System in LDPE: Influence of Thermo-Oxidation and UV-Irradiation on the Molecular Weight Changes. *Polym Degrad Stab* **1997**, *55*, 237-245.

(164) The European Environment Agency. Biodegradable and compostable plastics — challenges and opportunities.

(165) Laycock, B.; Nikolić, M.; Colwell, J. M.; Gauthier, E.; Halley, P.; Bottle, S.; George, G. Lifetime Prediction of Biodegradable Polymers. *Progress in Polymer Science* **2017**, *71*, 144–189. https://doi.org/10.1016/j.progpolymsci.2017.02.004.

(166) Niaounakis, M. Definitions and Assessment of (Bio)Degradation. In *Biopolymers Reuse, Recycling, and Disposal*; Elsevier, 2013; pp 77–94. https://doi.org/10.1016/B978-1-4557-3145-9.00002-6.

(167) Musuc, A. M.; Badea-Doni, M.; Jecu, L.; Rusu, A.; Popa, V. T. FTIR, XRD, and DSC Analysis of the Rosemary Extract Effect on Polyethylene Structure and Biodegradability. *Journal of Thermal Analysis and Calorimetry* **2013**, *114* (1), 169–177. https://doi.org/10.1007/s10973-012-2909-y.

(168) OECD. OECD Test Guidelines for Chemicals.

(169) BASF. Technical Information Soluplus® .

(170) Zhu, X.; Li, B.-G.; Wu, L.; Zheng, Y.; Zhu, S.; Hungenberg, K.-D.; Müssig, S.; Reinhard, B. Kinetics and Modeling of Vinyl Acetate Graft Polymerization from Poly(Ethylene Glycol). *Macromolecular Reaction Engineering* **2008**, *2* (4), 321–333. https://doi.org/10.1002/mren.200800011.

(171) WO2007/051743.

(172) WO2009/013202.

(173) US8158686B2.

(174) Wang, W.; Wang, W.; Li, H.; Lu, X.; Chen, J.; Kang, N.-G.; Zhang, Q.; Mays, J. Synthesis and Characterization of Graft Copolymers Poly(Isoprene- *g* -Styrene) of High Molecular Weight by a Combination of Anionic Polymerization and Emulsion Polymerization. *Industrial & Engineering Chemistry Research* **2015**, *54* (4), 1292–1300. https://doi.org/10.1021/ie504457e.

(175) Bou, S.; Klymchenko, A. S.; Collot, M. Fluorescent Labeling of Biocompatible Block Copolymers: Synthetic Strategies and Applications in Bioimaging. *Materials Advances* **2021**, *2* (10), 3213–3233. https://doi.org/10.1039/D1MA00110H.

(176) Potthast, A.; Radosta, S.; Saake, B.; Lebioda, S.; Heinze, T.; Henniges, U.; Isogai, A.; Koschella, A.; Kosma, P.; Rosenau, T.; Schiehser, S.; Sixta, H.; Strlič, M.; Strobin, G.; Vorwerg, W.; Wetzel, H. Comparison Testing of Methods for Gel Permeation Chromatography of Cellulose: Coming Closer to a Standard Protocol. *Cellulose* **2015**, *22* (3), 1591–1613. https://doi.org/10.1007/s10570-015-0586-2.

(177) Byrne, D. et. al. Biodegradability of Poly Vinyl Alcohol Based Film Used for Liquid Detergent Capsules. *Tenside Surf. Det.* **2021**, *58* (2), 88–96.

(178) OECD Guidelines for the Testing of Chemicals the Testing of Chemicals, S. 3. OCDE Test No. 301: Ready Biodegradability, .

(179) EUROFINS. *EUROFINS Test Report N°19FYBA1144*; 2019.

(180) Kavitha, T.; Kang, I.-K.; Park, S.-Y. Poly(N-Vinyl Caprolactam) Grown on Nanographene Oxide as an Effective Nanocargo for Drug Delivery. *Colloids and Surfaces B: Biointerfaces* **2014**, *115*, 37–45. https://doi.org/10.1016/j.colsurfb.2013.11.022.

(181) Halligan, S. C.; Dalton, M. B.; Murray, K. A.; Dong, Y.; Wang, W.; Lyons, J. G.; Geever, L. M. Synthesis, Characterisation and Phase Transition Behaviour of Temperature-Responsive Physically Crosslinked Poly (N-Vinylcaprolactam) Based Polymers for Biomedical Applications. *Materials Science and Engineering: C* **2017**, *79*, 130–139. https://doi.org/10.1016/j.msec.2017.03.241.

(182) Etchenausia, L.; Khoukh, A.; Deniau Lejeune, E.; Save, M. RAFT/MADIX Emulsion Copolymerization of Vinyl Acetate and N-Vinylcaprolactam: Towards Waterborne Physically Crosslinked Thermoresponsive Particles. *Polymer Chemistry* **2017**, *8* (14), 2244–2256. https://doi.org/10.1039/C7PY00221A.

(183) Farjadian, F.; Rezaeifard, S.; Naeimi, M.; Ghasemi, S.; Mohammadi-Samani, S.; Welland, M. E.; Tayebi, L. <p>Temperature and PH-Responsive Nano-Hydrogel Drug Delivery System Based on Lysine-Modified Poly (Vinylcaprolactam)</P>. *International Journal of Nanomedicine* **2019**, *Volume 14*, 6901–6915. https://doi.org/10.2147/IJN.S214467.

(184) Kozanoğlu, S.; Özdemir, T.; Usanmaz, A. Polymerization of N-Vinylcaprolactam and Characterization of Poly(N-Vinylcaprolactam). *Journal of Macromolecular Science, Part A* **2011**, *48* (6), 467–477. https://doi.org/10.1080/10601325.2011.573350.

(185) Niemczyk; Moszyński; Jędrzejewski; Kwiatkowski; Piwowarczyk; Baranowska. Chemical Structure of EVA Films Obtained by Pulsed Electron Beam and Pulse Laser Ablation. *Polymers* **2019**, *11* (9), 1419. https://doi.org/10.3390/polym11091419.

(186) Chao, Y.-C.; Su, S.-K.; Lin, Y.-W.; Hsu, W.-T.; Huang, K.-S. Preparation and Application of PEG/PVP Copolymers. *Journal of Polymers and the Environment* **2013**, *21* (1), 160–165. https://doi.org/10.1007/s10924-012-0450-5.

(187) Patil, M. P.; Gaikwad, N. J. Characterization of Gliclazide-Polyethylene Glycol Solid Dispersion and Its Effect on Dissolution. *Brazilian Journal of Pharmaceutical Sciences* **2011**, *47* (1), 161–166.

(188) Shameli, K.; bin Ahmad, M.; Jazayeri, S. D.; Sedaghat, S.; Shabanzadeh, P.; Jahangirian, H.; Mahdavi, M.; Abdollahi, Y. Synthesis and Characterization of Polyethylene Glycol Mediated Silver Nanoparticles by the Green Method. *International Journal of Molecular Sciences* **2012**, *13* (6), 6639–6650. https://doi.org/10.3390/ijms13066639.

(189) Vrandečić, N. S.; Erceg, M.; Jakić, M.; Klarić, I. Kinetic Analysis of Thermal Degradation of Poly(Ethylene Glycol) and Poly(Ethylene Oxide)s of Different Molecular Weight. *Thermochimica Acta* **2010**, *498* (1–2), 71–80. https://doi.org/10.1016/j.tca.2009.10.005.

(190) Reddy, K. R.; Raghu, A. v.; Jeong, H. M. Synthesis and Characterization of Novel Polyurethanes Based on 4,4'-{1,4-Phenylenebis[Methylylidenenitrilo]}diphenol. *Polymer Bulletin* **2008**, *60* (5), 609–616. https://doi.org/10.1007/s00289-008-0896-8.

(191) INTRODUCTION TO NMR SPECTROSCOPY.

(192) Meszlényi, G.; Körtvélyessy, G. Direct Determination of Vinyl Acetate Content of Ethylene-Vinyl Acetate Copolymers in Thick Films by Infrared Spectroscopy. *Polymer Testing* **1999**, *18* (7), 551–557. https://doi.org/10.1016/S0142-9418(98)00053-1.

(193) Cortez-Lemus, N. A.; Licea-Claverie, A. Preparation of a Mini-Library of Thermo-Responsive Star (NVCL/NVP-VAc) Polymers with Tailored Properties Using a Hexafunctional Xanthate RAFT Agent. *Polymers* **2017**, *10* (1), 20. https://doi.org/10.3390/polym10010020.

(194) Chemical Book. Vinyl acetate(108-05-4) 1H NMR.

(195) Liu, L.; Bai, S.; Yang, H.; Li, S.; Quan, J.; Zhu, L.; Nie, H. Controlled Release from Thermo-Sensitive PNVCL- Co -MAA Electrospun Nanofibers: The Effects of Hydrophilicity/Hydrophobicity of a Drug. *Materials Science and Engineering: C* **2016**, *67*, 581–589. https://doi.org/10.1016/j.msec.2016.05.083.

(196) Bax, A., & Lerner, L. Two-dimensional nuclear magnetic resonance spectroscopy. Science (New York, N.Y.), 1986, 232(4753), 960–967. https://doi.org/10.1126/ science.3518060

(197) Mirau, P. A. 2D NMR Studies of Synthetic Polymers. *Bulletin of Magnetic Resonance* **1992**, *13*.

(198) Moreira, G.; Fedeli, E.; Ziarelli, F.; Capitani, D.; Mannina, L.; Charles, L.; Viel, S.; Gigmes, D.; Lefay, C. Synthesis of Polystyrene-Grafted Cellulose Acetate Copolymers via Nitroxide-Mediated Polymerization. *Polymer Chemistry* **2015**, *6* (29), 5244–5253. https://doi.org/10.1039/C5PY00752F.

(199) Chroni, A.; Mavromoustakos, T.; Pispas, S. Poly(2-Oxazoline)-Based Amphiphilic Gradient Copolymers as Nanocarriers for Losartan: Insights into Drug–Polymer

Interactions. *Macromol* **2021**, *1* (3), 177–200. https://doi.org/10.3390/macromol1030014.

(200) Brar, A. S.; Goyal, A. K.; Hooda, S. Two-Dimensional NMR Studies of Acrylate Copolymers. *Pure and Applied Chemistry* **2009**, *81* (3), 389–415. https://doi.org/10.1351/PAC-CON-08-06-01.

(201) Sang Doo, A.; Eun Hee, K.; Chul Hyun, L. Diffusion-Ordered NMR Spectroscopy of Poly([Ethylene-Co-Vinyl Acetate]-Graft-Vinyl Chloride) in Solution. *Bulletin of the Korean Chemical Society* **2005**, *26* (2), 331–333.

(202) Yu, W.; Inam, M.; Jones, J. R.; Dove, A. P.; O'Reilly, R. K. Understanding the CDSA of Poly(Lactide) Containing Triblock Copolymers. *Polymer Chemistry* **2017**, *8* (36), 5504–5512. https://doi.org/10.1039/C7PY01056G.

(203) Zhang, Y.; Fry, C. G.; Pedersen, J. A.; Hamers, R. J. Dynamics and Morphology of Nanoparticle-Linked Polymers Elucidated by Nuclear Magnetic Resonance. *Analytical Chemistry* **2017**, *89* (22), 12399–12407. https://doi.org/10.1021/acs.analchem.7b03489.

(204) BOVEY, F. A.; MIRAU, P. A. THE MICROSTRUCTURE OF POLYMER CHAINS. In *NMR of Polymers*; Elsevier, 1996; pp 117–154. https://doi.org/10.1016/B978-012119765-0/50002-0.

(205) Masař, B.; Janata, M.; Látalová, P.; Netopilík, M.; Vlček, P.; Toman, L. Graft Copolymers and High-Molecular-Weight Star-like Polymers by Atom Transfer Radical Polymerization. *Journal of Applied Polymer Science* **2006**, *100* (5), 3662–3672. https://doi.org/10.1002/app.23196.

(206) Celebi, O.; Barnes, S. R.; Narang, G. S.; Kellogg, D.; Mecham, S. J.; Riffle, J. S. Molecular Weight Distribution and Endgroup Functionality of Poly(2-Ethyl-2-Oxazoline) Prepolymers. *Polymer* **2015**, *56*, 147–156. https://doi.org/10.1016/j.polymer.2014.11.005.

(207) Chen, Z.; Geng, Z.; Shao, D.; Mei, Y.; Wang, Z. Single-Crystalline EuF_3 Hollow Hexagonal Microdisks: Synthesis and Application as a Background-Free Matrix for MALDI-TOF-MS Analysis of Small Molecules and Polyethylene Glycols. *Analytical Chemistry* **2009**, *81* (18), 7625–7631. https://doi.org/10.1021/ac901010p.

(208) Ng, H. M.; Saidi, N. M.; Omar, F. S.; Ramesh, K.; Ramesh, S.; Bashir, S. Thermogravimetric Analysis of Polymers. In *Encyclopedia of Polymer Science and Technology*; John Wiley & Sons, Inc.: Hoboken, NJ, USA, 2018; pp 1–29. https://doi.org/10.1002/0471440264.pst667.

(209) Rimez, B.; Rahier, H.; van Assche, G.; Artoos, T.; van Mele, B. The Thermal Degradation of Poly(Vinyl Acetate) and Poly(Ethylene-Co-Vinyl Acetate), Part II: Modelling the Degradation Kinetics. *Polymer Degradation and Stability* **2008**, *93* (6), 1222–1230. https://doi.org/10.1016/j.polymdegradstab.2008.01.021.

(210) Gill, P.; Moghadam, T. T.; Ranjbar, B. Differential Scanning Calorimetry Techniques: Applications in Biology and Nanoscience. *Journal of biomolecular techniques : JBT* **2010**, *21* (4), 167–193.

(211) Halligan, S. C.; Dalton, M. B.; Murray, K. A.; Dong, Y.; Wang, W.; Lyons, J. G.; Geever, L. M. Synthesis, Characterisation and Phase Transition Behaviour of Temperature-Responsive Physically Crosslinked Poly (N-Vinylcaprolactam) Based

Polymers for Biomedical Applications. *Materials Science and Engineering: C* **2017**, *79*, 130–139. https://doi.org/10.1016/j.msec.2017.03.241.

(212) Inomata, K.; Nakanishi, E.; Sakane, Y.; Koike, M.; Nose, T. Side-Chain Crystallization Behavior of Graft Copolymers Consisting of Amorphous Main Chain and Crystalline Side Chains: Poly(Methyl Methacrylate)-Graft-Poly(Ethylene Glycol) and Poly(Methyl Acrylate)-Graft-Poly(Ethylene Glycol). *Journal of Polymer Science Part B: Polymer Physics* **2005**, *43* (1), 79–86. https://doi.org/10.1002/polb.20311.

(213) Altamimi, M. A.; Neau, S. H. Investigation of the in Vitro Performance Difference of Drug-Soluplus® and Drug-PEG 6000 Dispersions When Prepared Using Spray Drying or Lyophilization. *Saudi Pharmaceutical Journal* **2017**, *25* (3), 419–439. https://doi.org/10.1016/j.jsps.2016.09.013.

(214) Rueda, J.; Zschoche, S.; Komber, H.; Schmaljohann, D.; Voit, B. Synthesis and Characterization of Thermoresponsive Graft Copolymers of NIPAAm and 2-Alkyl-2-Oxazolines by the "Grafting from" Method. *Macromolecules* **2005**, *38* (17), 7330–7336. https://doi.org/10.1021/ma050570p.

(215) Zhang, N.; Wang, S.; Gibril, M. E.; Kong, F. The Copolymer of Polyvinyl Acetate Containing Lignin-Vinyl Acetate Monomer: Synthesis and Characterization. *European Polymer Journal* **2020**, *123*, 109411. https://doi.org/10.1016/j.eurpolymj.2019.109411.

(216) Gupta, S. S.; Solanki, N.; Serajuddin, A. T. M. Investigation of Thermal and Viscoelastic Properties of Polymers Relevant to Hot Melt Extrusion, IV: Affinisol™ HPMC HME Polymers. *AAPS PharmSciTech* **2016**, *17* (1), 148–157. https://doi.org/10.1208/s12249-015-0426-6.

(217) Zambrano, M. C.; Pawlak, J. J.; Venditti, R. A. Effects of Chemical and Morphological Structure on Biodegradability of Fibers, Fabrics, and Other Polymeric Materials. *BioResources* **2020**, *15* (4), 9786–9833. https://doi.org/10.15376/biores.15.4.Zambrano.

(218) Zhang, M.; Jia, Y.-G.; Liu, L.; Li, J.; Zhu, X. X. Soluble–Insoluble–Soluble Transitions of Thermoresponsive Cryptand-Containing Graft Copolymers. *ACS Omega* **2018**, *3* (8), 10172–10179. https://doi.org/10.1021/acsomega.8b01308.

(219) Etchenausia, L.; Rodrigues, A. M.; Harrisson, S.; Deniau Lejeune, E.; Save, M. RAFT Copolymerization of Vinyl Acetate and *N* -Vinylcaprolactam: Kinetics, Control, Copolymer Composition, and Thermoresponsive Self-Assembly. *Macromolecules* **2016**, *49* (18), 6799–6809. https://doi.org/10.1021/acs.macromol.6b01451.

(220) Shibanuma, T.; Aoki, T.; Sanui, K.; Ogata, N.; Kikuchi, A.; Sakurai, Y.; Okano, T. Thermosensitive Phase-Separation Behavior of Poly(Acrylic Acid)- *g Raft* -Poly(*N,N* -Dimethylacrylamide) Aqueous Solution. *Macromolecules* **2000**, *33* (2), 444–450. https://doi.org/10.1021/ma9915374.

(221) Yin, X.; Stöver, H. D. H. Hydrogel Microspheres by Thermally Induced Coacervation of Poly(*N,N* -Dimethylacrylamide- *c o* -Glycidyl Methacrylate) Aqueous Solutions. *Macromolecules* **2003**, *36* (26), 9817–9822. https://doi.org/10.1021/ma034809i.

(222) Yin, X.; Stöver, H. D. H. Probing the Influence of Polymer Architecture on Liquid−Liquid Phase Transitions of Aqueous Poly(*N,N* -Dimethylacrylamide)

Copolymer Solutions. *Macromolecules* **2005**, *38* (6), 2109–2115. https://doi.org/10.1021/ma048853p.

(223) Bartolini, A.; Tempesti, P.; Ghobadi, A. F.; Berti, D.; Smets, J.; Aouad, Y. G.; Baglioni, P. Liquid-Liquid Phase Separation of Polymeric Microdomains with Tunable Inner Morphology: Mechanistic Insights and Applications. *Journal of Colloid and Interface Science* **2019**, *556*, 74–82. https://doi.org/10.1016/j.jcis.2019.08.015.

(224) Yin, X.; Stöver, H. D. H. Temperature-Sensitive Hydrogel Microspheres Formed by Liquid-Liquid Phase Transitions of Aqueous Solutions of Poly(*N* , *N* -Dimethylacrylamide- *Co* -Allyl Methacrylate). *Journal of Polymer Science Part A: Polymer Chemistry* **2005**, *43* (8), 1641–1648. https://doi.org/10.1002/pola.20523.

(225) Ieong, N. S.; Hasan, M.; Phillips, D. J.; Saaka, Y.; O'Reilly, R. K.; Gibson, M. I. Polymers with Molecular Weight Dependent LCSTs Are Essential for Cooperative Behaviour. *Polymer Chemistry* **2012**, *3* (3), 794. https://doi.org/10.1039/c2py00604a.

(226) Horiuchi, T.; Rikiyama, K.; Sakanaya, K.; Sanada, Y.; Watanabe, K.; Aida, M.; Katsumoto, Y. Effect of Molecular Weight on Cloud Point of Aqueous Solution of Poly (Ethylene Oxide)–Poly (Propylene Oxide) Alternating Multiblock Copolymer. *Journal of Oleo Science* **2020**, *69* (5), 449–453. https://doi.org/10.5650/jos.ess20026.

(227) Tong, Z.; Zeng, F.; Zheng, X.; Sato, T. Inverse Molecular Weight Dependence of Cloud Points for Aqueous Poly(*N* -Isopropylacrylamide) Solutions. *Macromolecules* **1999**, *32* (13), 4488–4490. https://doi.org/10.1021/ma990062d.

(228) Feil, H.; Bae, Y. H.; Feijen, J.; Kim, S. W. Effect of Comonomer Hydrophilicity and Ionization on the Lower Critical Solution Temperature of N-Isopropylacrylamide Copolymers. *Macromolecules* **1993**, *26* (10), 2496–2500. https://doi.org/10.1021/ma00062a016.

(229) Verbrugghe, S.; Laukkanen, A.; Aseyev, V.; Tenhu, H.; Winnik, F. M.; du Prez, F. E. Light Scattering and Microcalorimetry Studies on Aqueous Solutions of Thermo-Responsive PVCL-g-PEO Copolymers. *Polymer* **2003**, *44* (22), 6807–6814. https://doi.org/10.1016/j.polymer.2003.07.003.

(230) Verbrugghe, S.; Bernaerts, K.; du Prez, F. E. Thermo-Responsive and Emulsifying Properties of Poly(N-Vinylcaprolactam) Based Graft Copolymers. *Macromolecular Chemistry and Physics* **2003**, *204* (9), 1217–1225. https://doi.org/10.1002/macp.200390098.

(231) Smets, J.; Pintens, A.; Orlandini, L.; Sands, D. P. Benefit Agent Delivery Particle. US10092485B2, 2018.

(232) National Center for Biotechnology Information PubChem. Compound Summary for CID 7439, Carvone.

(233) National Center for Biotechnology Information PubChem. Compound Summary for CID 8635, Methyl anthranilate.

(234) Goel, S. K. Critical Phenomena in the Clouding Behavior of Nonionic Surfactants Induced by Additives. *Journal of Colloid and Interface Science* **1999**, *212* (2), 604–606. https://doi.org/10.1006/jcis.1998.6079.

(235) Manohar, C.; Kelkar, V. K. Model for the Cloud Point of Mixed Surfactant Systems. *Journal of Colloid and Interface Science* **1990**, *137* (2), 604–606. https://doi.org/10.1016/0021-9797(90)90436-R.

(236) Carlsson, A.; Karlstroem, G.; Lindman, B. Characterization of the Interaction between a Nonionic Polymer and a Cationic Surfactant by the Fourier Transform NMR Self-Diffusion Technique. *The Journal of Physical Chemistry* **1989**, *93* (9), 3673–3677. https://doi.org/10.1021/j100346a060.

(237) Thomas, S.; Rane, A. V.; Kanny, Krishnan. Recycling of Polyurethane Foams, Technology & Engineering . In *Google Books* ; 2018; p 39.

(238) Amann, M.; Minge, O. Biodegradability of Poly(Vinyl Acetate) and Related Polymers; 2011; pp 137–172. https://doi.org/10.1007/12_2011_153.

(239) Ghanbarzadeh, B.; Almasi, H. Biodegradable Polymers. In *Biodegradation - Life of Science*; InTech, 2013; p 171. https://doi.org/10.5772/56230.

APPENDICES

APPENDIX A. UV-Vis of 0.5 % solution of filtrated copolymer S2.

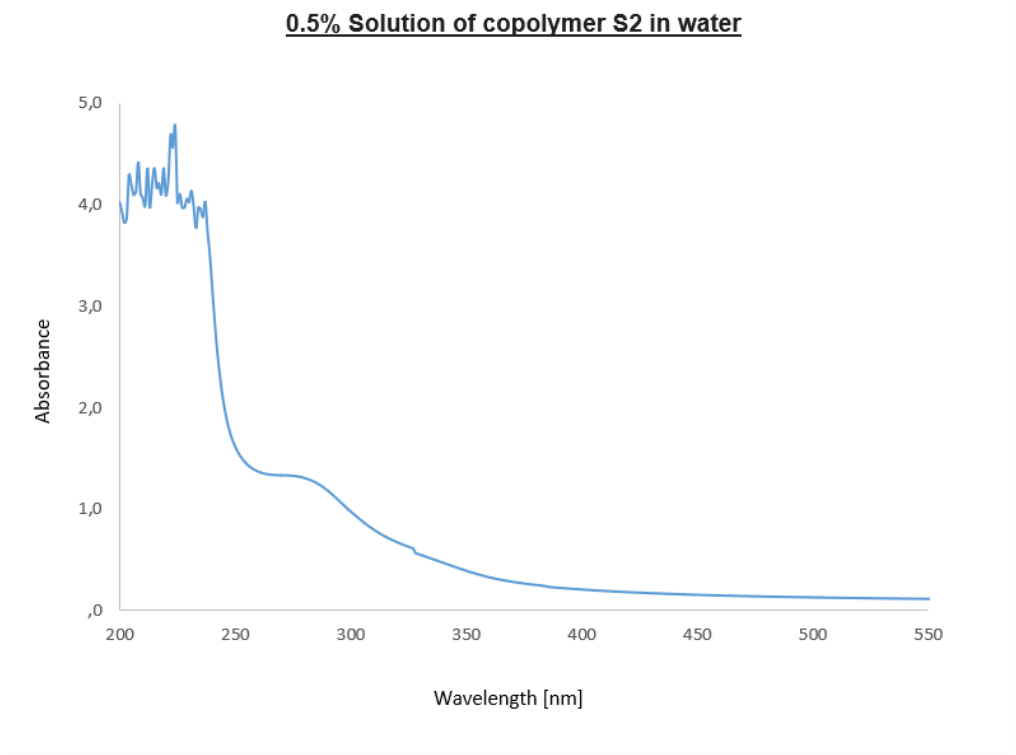

APPENDIX B. First 50 ml of filtrated copolymer S2 solution passed through membrane, 1st collected batch.

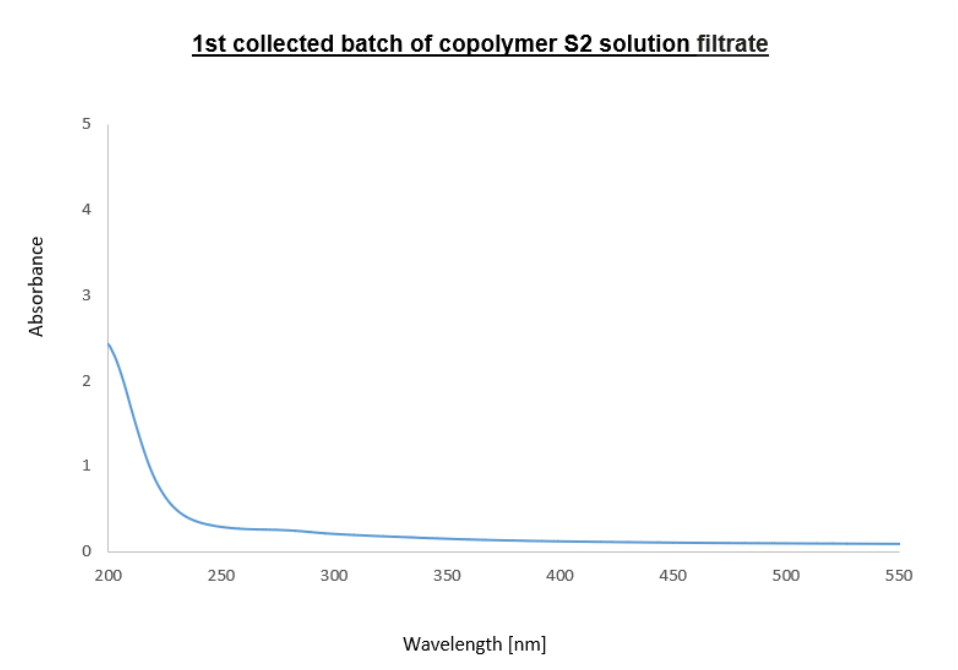

APPENDIX C. UV-Vis of collected 43rd batch (last) of filtrated copolymer S2 solution after one month of ultrafiltration.

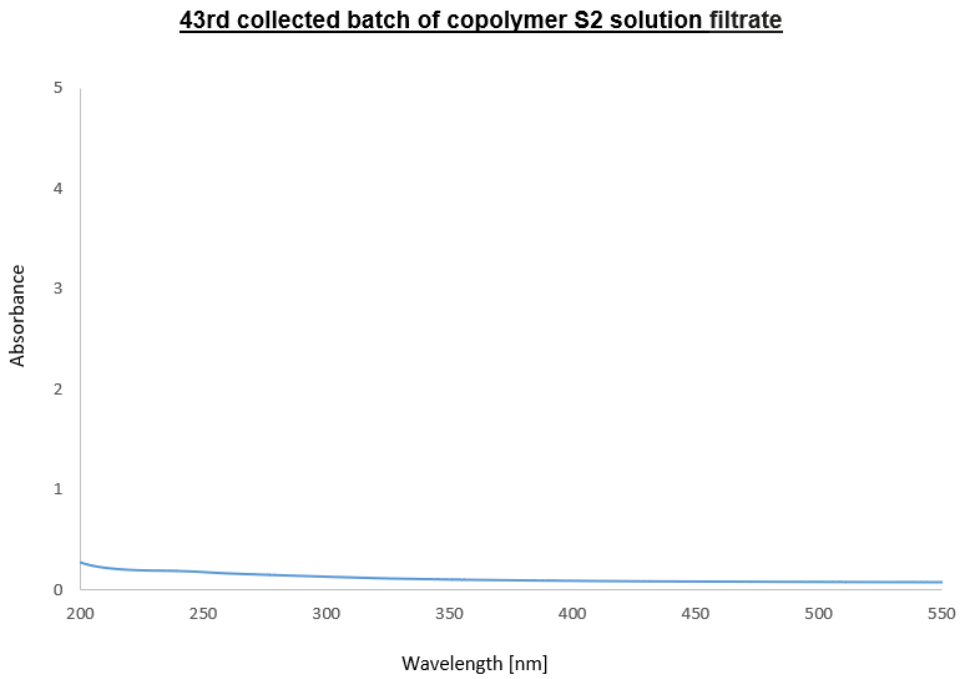

APPENDIX D. Microscope images of (A) 0.5% copolymer S2A before microfiltration and (B) 0.5% copolymer S2A after microfiltration with Methyl anthranilate in water.

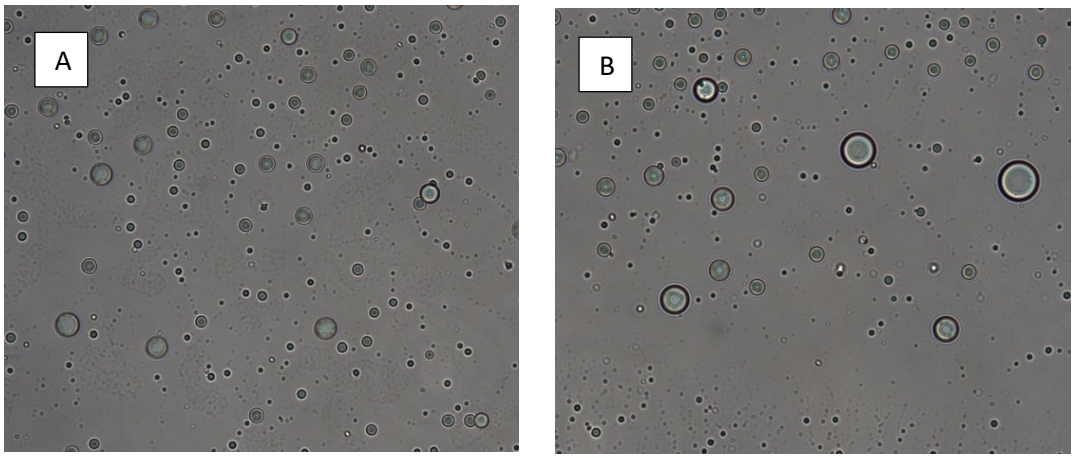

APPENDIC E. FTIR spectra of the first 50 ml of copolymer solution passed through the membrane during ultrafiltration (green) and copolymer S2 before ultrafiltration (red).

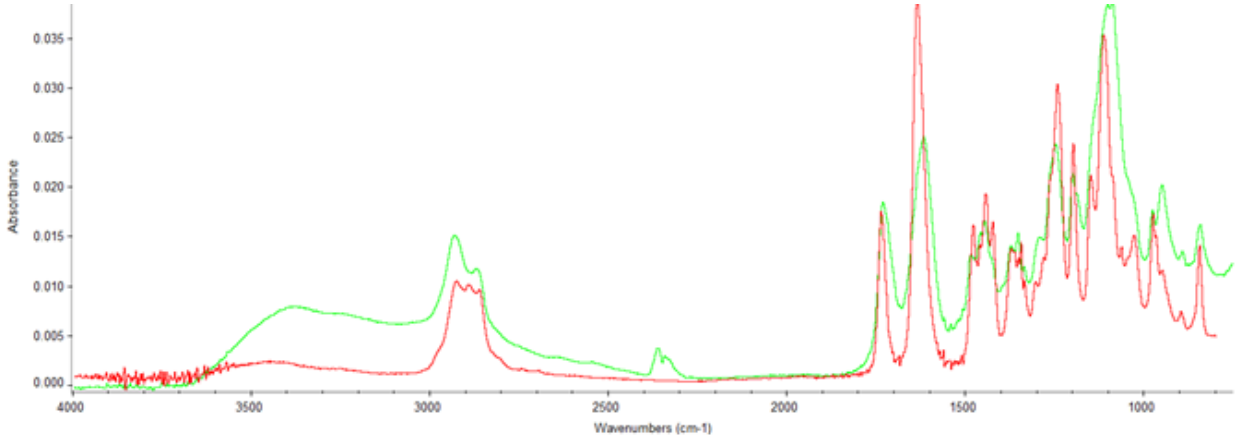
Absorbance
0.035
0.030
0.025
0.020
0.015
0.010
0.005
0.000
4000
3500
3000
2500
2000
1500
1000
Wavenumbers (cm-1)